Statistical approaches of investigating intrinsic mechanisms underlying spike patterning in oxytocin neurones

Arleta Reiff-Marganiec

A dissertation submitted to the University of Edinburgh for the degree of Doctor of Philosophy

Edinburgh

August, 2003

Declaration

The studies outlined in this thesis were undertaken in the School of Biomedical and Clinical Laboratory Sciences, University Medical School, Edinburgh, under the supervision of Professor Gareth Leng. This dissertation has not been submitted for any other qualification at any other university.

All of the work was performed by the author, except where otherwise indicated. Paired cells recording were undertaken by the author in the Laboratoire de Biologie des Neurones Endocrines in Montpellier/ France, under the guidance of Dr Françoise Moos.

Material presented in this thesis has been published as indicated in the appendix. In particular, the analyses and results discussed in Chapters 3 and 4 provided a substantial part of a book chapter co-authored by the author of this thesis (Leng *et al.*, in press).

Arleta Reiff-Marganiec

August, 2003

Acknowledgements

First and foremost my thanks to Professor Gareth Leng for believing in my abilities, for taking upon himself administrative and other duties so that I could concentrate on my studies: I have learned a lot from you, and not only academically.

I would also like to thank David Brown, formerly at the Babraham Institute, for introducing me to computational methods in neuroscience, Dr Françoise Moos at the Laboratoire de Biologie des Neurones Endocrines in Montpellier/ France, for her expert intructions in paired cell recording, and Professor John Russell for guidance throughout the course of my PhD. Thank you to Dr Mike Ludwig and Dr Colin Brown for their expertise and assistance in all things electrophysiological and neuroendocrinological, and thanks to Dr Peter Roper for discussions on computational neuroscience.

Big thank you to all those in the laboratory for their friendship and encouragement, especially during the arduous time of writing up: Celine, Nancy, Ped, Jayne, Sinéad, Jack, Shuaike, Paula, Louise, Val, Duncan, Carol, Simone, Alex, and Morag. Your support has meant a lot to me.

I would like to extend my thanks to my friends, particularly Dani, Christina, Mirjam, Ben and Ivan for reminding me that there is life besides the PhD, and laughing at me when I couldn't quite believe it.

Last but not least many thanks to my family: my parents, my sister, and especially my husband for giving me love, encouragement and strength to see this through. I could not have done it without you.

Table of Contents

Abstract

Information in the brain is carried by the temporal pattern of action potentials generated by neurones. The patterns of spike discharge are determined by intrinsic properties of each neurone and the synaptic inputs it receives. Modulation of either of these parameters changes the output of the neurone and through this the behaviour of physiology of the organism. Computational models of brain function usually focus on how patterns of connectivity contribute to information processing, but fail to take the different intrinsic properties of different neuronal phenotypes into account. Models of single neurones that take into account all intrinsic mechanisms will be extremely complex, and hence building large-scale models of neurone networks will be computationally intense, if not infeasible. In order to develop simple models that still reflect realistically the intrinsic properties of the neurone we first need to know which of the many identified mechanisms are the most important for its function.

Conventionally, intrinsic properties are investigated in detail in isolated cells *in vitro*. Insights gained thereby are taken to speculate how these mechanisms contribute to spike patterning or neuronal responses *in vivo*. However, *in vitro* experiments are performed under artificial circumstances. Besides the relative scarcity of afferent input in dissociated cells, the preparations for the experiments require interventions that fundamentally disturb cell properties. Thus, it is problematic to interpret observations made *in vivo* on the basis of results obtained *in vitro*.

In this thesis a novel, radically different way of investigation is presented. We examine recordings of firing activity of oxytocin neurones using statistical methods. The use of spontaneous, unexceptional activity recorded *in vivo* avoids all the interventions and alterations associated with *in vitro* preparations, also allowing to take the influence of afferent input into account. The main purpose of our work is to determine key features involved in the regulation of discharge patterns, and consider possible explanations in terms of known intrinsic properties. A further objective is to determine whether there are any consistent, characteristic differences in the firing pattern of oxytocin neurones recorded under a variety of physiological conditions (naïve, pregnant, lactating, and hyperosmotic stimulation).

We have found that while firing activity appears to be random (except for the effects of the HAP) on a small time scale (>0.5 s), on a time scale of several seconds it appears to be much more ordered. Also, we found evidence of a 'balancing' mechanism, whereby on a short to medium time scale periods of faster activity are followed by periods of slower activity (and vice versa), thus leading to a rather homogenous and steady activity overall. Of the known intrinsic mechanisms the AHP effects the firing activity in a way compatible with the firing characteristics found. Thus, from the results of the statistical analyses we conclude that the most important parameters to determine the firing of oxytocin neurones are the post-*spike* HAP and the post-*train* AHP.

In addition, the analysis of the activity recorded under different physiological conditions reveal that the firing of pregnant and hyperosmotically stimulated neurones is remarkably similar to the firing in naïve organisms. In contrast, firing activity during lactation shows subtle differences indicating that the AHP decays faster in these circumstances, which is in agreement with results obtained *in vitro*.

CHAPTER ONE

GENERAL INTRODUCTION

Information in the brain is carried by the temporal pattern of action potentials. The patterns of action potential discharge are determined by intrinsic properties of the neurones and the synaptic inputs they receive. Thus, modulation of either of these parameters changes the output of the neurones, and through this the behaviour or physiology of the organism is influenced.

Computational models of brain function have principally focussed on how patterns of connectivity contribute to information processing, but most of the models largely neglect the different intrinsic membrane properties of different neuronal phenotypes. Computational models of single neurones that truthfully reflect intrinsic membrane properties can be extremely complex, and hence building large scale realistic models of neuronal networks is computationally intense. To give an idea of the scale of the problem, a typical neurone in the brain makes 10 000 synaptic contacts with other neurones, and receives a similar number of inputs. Each neurone in turn has a large number of channels that contribute to its membrane excitability – including several different classes of Ca^{2+}, K^+ and Na^+ channels –, and each neuronal phenotype differs in its exact composition of membrane channels.

Neurones differ from each other also morphologically, in the distribution of channel types in different cellular compartments and in intracellular properties that influence channel function. Thus, a realistic model of a single neurone incorporating all these factors will have a very large number of parameters. Their values are either estimated with reasonable precision from experimental observations, or more often have to be guessed for particular cell types as the detailed information is not available. The number of parameters – often measured *in vitro* in conditions that may lead to inaccuracies when extrapolating them to *in vivo* conditions – involved in modelling any single neurone to biophysical accuracy is large, often in the order of 100. All parameters must be set for each cell type within a network in order to build

a realistic network model. Even with the huge computational power available at the present time, this computational task is daunting at least, if not infeasible.

The purpose of computational models – as for any model – is to understand systems by simplifying them to reveal the key variables. It makes little sense to try to build a model of the brain that is as complex as the brain. Clearly, we need to develop computationally simple models of neurones that preserve the essential properties and discard those which have no major impact upon the information processing functions under investigation. However, it is not always clear which properties of a neurone are important and must be included in any model, and which can be neglected for the current purpose.

Conventionally, the approach to understanding the role of intrinsic membrane properties in single neurones has been to study individual channel properties in single cells in great details through experiments on isolated cells *in vitro*, and then to speculate about how these might contribute to spike patterning or neuronal responses *in vivo*. In this thesis, a very different approach was taken. Rather than looking at membrane properties and speculating about how they might influence firing patterns, we have looked at spontaneous firing patterns of neurones in order to determine the key features involved in their regulation and then looked for possible explanations in terms of the known intrinsic properties.

1.1 The Hypothalamo-Hypophysial System

The hypothalamus is located at the base of the brain, divided in two by the third ventricle. It is intimately interconnected with many other brain areas and exerts overall control over the sympathetic nervous system, and over much of the endocrine system. It is connected to the pituitary gland by the hypophysial stalk, through which blood-borne and electrical signals are transmitted (Figure 1.1).

The neurosecretory cells of the hypothalamus can be divided into parvocellular and magnocellular cells. In mammals the somata of magnocellular neurosecretory cells are concentrated in the paired supraoptic and paraventricular nuclei, or SON and PVN (Lincoln & Wakerley, 1974; Sherlock *et al.*, 1975). Here

these neurones synthesise either the peptide hormone oxytocin or vasopressin (Swaab *et al.*, 1975), although it has been reported that in circumstances that demand enhanced hormone secretion a minority can synthesise both (Mezey & Kiss, 1991).

Action potentials that are generated at the soma are conducted along the axons that project through the internal zone of the median eminence to their terminals in the posterior pituitary gland (also known as pars nervosa or neurohypophysis), where the hormones are released into the blood stream (Bargmann & Scharrer, 1951); thus they can be unequivocally identified as they are excited by antidromic stimulation of the stalk (Poulain & Wakerley, 1982).

The soma and axons of the magnocellular neurosecretory cells are easily identifiable and readily accessible for experimental manipulation. Thus, they are one of the few groups of central neurones in which changes in activity pattern can be related to the physiological stimulus and the precise neuronal response to the stimulus, the state of the organism and the hormonal secretion, respectively.

1.1.1 Distribution of Magnocellular Neurosecretory Cells (MNCs)

Magnocellular neurosecretory cells can be identified by the presence of horseradish peroxidase (HRP) retrogradely transported from the injection site in the neurohypophysis into various areas of the rat hypothalamus. Magnocellular neurosecretory cells are concentrated in the medial and lateral portions of the paraventricular nucleus (PVN; Armstrong *et al.*, 1980; Armstrong & Hatton, 1980; Sherlock *et al.*, 1975). A small amount of oxytocin and vasopressin neurones are scattered individually or in small clusters throughout the medial hypothalamus (Fisher *et al.*, 1979; Rho & Swanson, 1989). In the SON, most neurones are labelled following HRP injection to the neurohypophysis (Sherlock *et al.*, 1975) and immunostain for either vasopressin or oxytocin (Sofroniew & Schrell, 1980).

As the SON has been the subject of most experimental investigation due to its homogeneity and ready visual accessibility the following descriptions will focus on neurones in this structure. In the rat, the SON is a sausage-shaped nucleus extending approximately 2 mm in the rostrocaudal direction, lying alongside the dorsal and

lateral edge of the optic tract. From the ventral surface, the nucleus extends up to 500 μm dorsally at the caudal end and about 200 μm at the rostral pole. Neurones staining for vasopressin are more concentrated at the posteroventral end of the nucleus, while those staining for oxytocin tend to be located antero-dorsally (Swaab *et al.*, 1975). Although reports of ratios of vasopressin to oxytocin neurones in the SON differ considerably, vasopressin neurones typically predominate.

1.1.2 Morphology – Naïve Animals

Dyball and Kemplay (1982) investigated the cytoarchitecture of the rat SON using the Golgi-Cox method for staining. Two types of cells were found in the SON: a small minority of cells, which were multipolar with four or more processes, and round (diameter of approx. 20 μm), were interpreted as interneurones. The majority of neurones in the SON were identified as magnocellular neurosecretory cells.

Studies of rat supraoptic magnocellular neurosecretory cells using Golgi impregnation (Armstrong *et al.*, 1982; Dubois-Dauphin *et al.*, 1985), intracellular lucifer yellow injection (Randle *et al.*, 1986), or biocytin injection (Armstrong *et al.*, 1994) show that vasopressin and oxytocin neurones are indistinguishable on the basis of cell morphology alone, since both types are generally oval in shape, with observed diameters ranging from 10 to 40 μm. All neurones studied had at least one dendrite arise from the soma, while 60% had two and 15% had three dendritic processes, featuring small spiny processes up to 15 μm long (Armstrong, 1995). Dendrites are largely confined within the nucleus (Randle *et al.*, 1986). Dendrites project towards and into the ventral glia lamina (Armstrong *et al.*, 1982; Randle *et al.*, 1986), where they form a dense plexus with many synaptic connections with presynaptic elements (Randle *et al.*, 1986), while some continue laterally into the periamygdaloid area (Smithson *et al.*, 1989). Dendrites are capable of releasing sufficient oxytocin or vasopressin to account for the peptide known to be released into the hypothalamus (Morris & Pow, 1991).

In contrast to dendrites, axons are smooth and varicose in appearance, with a smaller diameter and are at most sparsely branched (Tweedle *et al.*, 1989). One axon

arises from either the soma or a primary dendrite (Armstrong *et al.*, 1982; Dyball & Kemplay, 1982; Randle *et al.*, 1986), rather than from a characteristic pyramidally shaped axon hillock as described in other parts of the brain. Axons project dorsomedially over the optic tract, then arch ventrally and project towards the medial basal hypothalamus, through the internal zone of the median eminence and enter the posterior pituitary gland (Dyball & Kemplay, 1982; Randle *et al.*, 1986). Here each axon arborises, branching into thousands of neurosecretory endings abutting fenestrated capillaries (Nordmann, 1977).

1.1.3 Oxytocin Cell Morphology – Lactating Animals

Marked changes occur in the SON of pregnant and lactating animals. Montagnese *et al.* (1987) investigated the structural changes in the rat SON during gestation and lactation. They looked at rats on days 18, 19, 21 (morning and evening) of a first pregnancy, and on days 1 and 51 of lactation. In addition, rats deprived of their litters at parturition were studied on days 2 and 10 post partum, as well as primiparous rats on days 1 and 12 of artificially induced lactation. They found that direct appositions between adjacent neurons (i.e. surface membranes of cell bodies and dendrites are in direct and extensive juxtaposition, without any glial interposition) increased rapidly during the day before parturition: from around 20% on the last days (including day 21 in the morning) of pregnancy to over 40% in the evening of day 21, a few hours before the onset of parturition. It was also found that 'double' synapses, where more than one neurone is contacted by the same presynaptic terminal, develop late in gestation, though more progressively (to around 10% of all neurosecretory profiles). The latter are seen only rarely in male or virgin female rats.

These proportions remained the same throughout lactation. This was found to be true also for artificially induced lactation, i.e. when primiparous rats were continuously exposed to suckling litters (in these cases, lactation started in 16 – 22 days), or when mothers received new suckling litters upon weaning of their own pups. In contrast, when the rats were separated from their own litter following

parturition neuronal appositions and 'double' synapses disappeared within 2 and 10 days, respectively.

Hatton and Tweedle (1982) generally found similar figures (around 45% of SON cells showing direct apposition). Following the suggestion that this change is seen only in oxytocinergic cells reported by earlier studies, they estimated that nearly all of these cells are in direct contact during times of high hormone demand. This of course would suggest far reaching consequences for the speed of transfer of synaptic input, as well as for the spread of electrical activity.

Theodosis, Poulain and Vincent (1981) argue in the same direction, reporting that in the nuclei of lactating rats 34% of neurosecretory cell bodies were in direct contact with each other, and a further 22% were in direct contact with dendrites. This corresponds to around 10% of the total measured soma surface membrane, as compared to approx. 1.5% in control animals. In addition, a significant increase of the frequency of attachment plates, which usually are thought to have a purely adhesive function, between membranes in extensive apposition, was observed.

Closely related to the above findings are the observations made by Hatton and Yang (1994). They investigated neuronal coupling in SON of virgin and lactating rats. Simultaneously, Lucifer Yellow (LY) and neurobiotin (NB) were compared for effectiveness in staining coupled cells. The results were in agreement with previous findings: the amount of coupling was four fold increased in lactating rat SON as compared with virgin rat SON. However, NB stained four times as many cells, widely distributed, as LY. One explanation is that since LY requires relatively large junctional conductances, this extensive NB transfer represents relatively weaker coupling, i.e. below the threshold for LY.

Further changes were reported by Stern and Armstrong (1998). They investigated the reorganisation of dendritic trees in the rat SON during lactation and found that dendritic trees of oxytocin neurones shrunk by approx. 41% of their total length because of decreased dendritic branching concentrated at a distance of 100 – 200 μm from the soma. In contrast, no changes were observed in the maximal extension of the dendrites. The opposite was found to be true for vasopressin cells in

the SON. The dendritic trees elongated (approx. 48% increase in total dendritic length), because of an increase of branching in close proximity to the soma. The consequences of these reconstructions are changes in the availability of postsynaptic space and alterations in the electrotonic properties of the neurones, which could affect the efficacy of synaptic input.

Armstrong (1995) suggested the possibility that differences in the number of dendrites could imply a difference in the amount or variety of synaptic input across neurones, as well as a difference in electrotonic processing of synaptic input. Since increasing the number of dendrites with similar diameters would also mean an increase in the dendritic contribution to the whole cell conductance, the result would be progressively faster rise times and the decay for somatic inputs corresponding to the increased amount of dendritic membrane.

Tweedle, Smithson and Hatton (1989) investigated the formation of additional endings of neurosecretory axons in the posterior pituitary during lactation. In the resting state, axons, endings and swellings occupied 42% of the total volume (Nordmann, 1977). Individual neurosecretory axons frequently entwine around or ran adjacent to blood vessels, a short length of axon forming multiple endings. Tweedle *et al.* demonstrated that the areas of preferential hormone release (indicated by a combination of synaptoid membrane specialisation, dense core vesicles and accumulation of microvesicles) is likely to occur where the axons contact the basal lamina lining the perivascular space. It was hypothesised that increased pituicyte coverage of the basal lamina could mediate reductions in the contact length of individual nerve terminal. Conversely, a reduction of pituicyte coverage along the basal lamina could lead to more areas of axonal contact with the basal lamina inducing or allowing the formation of more endings in situations of increased hormone demand, like for example during lactation.

1.2 Functions of the Hormones

As described above, axons from magnocellular neurosecretory cells project via the neural stalk to the posterior pituitary gland where oxytocin and vasopressin

are released into the circulation, reaching their peripheral target sites transported by the blood. Individual magnocellular neurosecretory cells produce either oxytocin or vasopressin, although it has been reported that a minority of cells can produce both in times of high hormonal demand (Mezey & Kiss, 1991), although usually in very unequal amounts (Xi *et al.*, 1999). Oxytocin and vasopressin are nonapeptides, and indeed are structurally very similar, differing by only two amino acids (Figure 1.2). In mammals they are encoded by separate genes that are believed to be descendants of a common ancestral gene that codes for the peptide vasotocin in lower vertebrates (Acher *et al.*, 1997; Sawyer, 1977). A precursor protein is synthesised in the soma of the magnocellular neurosecretory cell, where it is packaged into secretory granules that are transported along the axon to the terminals in the posterior pituitary gland. During the transport this protein is enzymatically cleaved to produce oxytocin, vasopressin and related neurophysins, respectively (Brownstein *et al.*, 1980).

1.2.1 Vasopressin

Through its role as the antidiuretic hormone, vasopressin is primarily concerned with body fluid homeostasis. Its release is increased in response to increased plasma osmotic pressure, and in response to hypovolaemia (Dunn *et al.*, 1973) and decreases in blood pressure (Harris *et al.*, 1975). Vasopressin acts on the V_2 receptors on the basolateral surface of renal epithelial cells in the kidney collecting tubules (Jard, 1983), where it increases water re-uptake by the insertion of aquaporin protein into the luminal membrane (Ecelbarger *et al.*, 1997). Vasopressin is also involved in cardiovascular regulation through its actions as a vasoconstrictor. This is achieved by the activation of V_1 receptors on vascular smooth muscle cells (Cooke *et al.*, 1992).

1.2.2 Oxytocin

The classical roles of oxytocin are in lactation and parturition. At parturition oxytocin is released (Higuchi *et al.*, 1983) and stimulates uterine contractions through actions on endometiral smooth muscle cells (Cunningham, Jr. & Sawchenko, 1991; Poulain & Wakerley, 1982). Although once thought to be essential for

parturition in mammals it has since been shown that oxytocin knockout mice can give birth normally (Young, III *et al.*, 1996). During lactating oxytocin is released in response to suckling (Higuchi *et al.*, 1983) in a pulsatile manner as opposed to a steady continuous discharge, and promotes milk ejection through its action on oxytocin receptors on the myoepithelium of the milk duct in the breast (Poulain & Wakerley, 1982). Oxytocin is essential in this capacity, and milk ejection does not occur in oxytocin knockout mice (Young, III *et al.*, 1996; for a review of work on essential functions of oxytocin and oxytocin knockout mice see Russell & Leng, 1998).

Oxytocin is also released in response to increased osmotic pressure and hypovolaemia (Stricker & Verbalis, 1986) and gastric distension (Renaud *et al.*, 1987), a response that is associated with the systemic release of the satiety peptide cholecystokinin (CCK; Verbalis *et al.*, 1986). While oxytocin neurones are excited following an i.v. administration of CCK, vasopressin neurones are either unaffected or inhibited. Oxytocin has further been implicated in the regulation of carbohydrate metabolism (Cunningham, Jr. & Sawchenko, 1991), and further diverse roles, such as male sexual behaviour (Arletti *et al.*, 1992), female maternal behaviour (Caldwell *et al.*, 1990), and other behavioural responses (Panksepp, 1992).

The stimuli for oxytocin and vasopressin release are not mutually exclusive, and in fact there is evidence for a beneficial interrelationship between peripheral effects of oxytocin and vasopressin, whereby oxytocin enhances the effect of vasopressin on the kidney (Balment *et al.*, 1986). In turn, vasopressin is released during the normal course of parturition and might assist with uterine contractions acting through oxytocin receptor, although it is not as effective as oxytocin (Chan *et al.*, 1996).

1.3 Afferent Inputs

Magnocellular neurosecretory cells receive direct afferent projection from the forebrain. Direct connections from the olfactory bulb, amygdala, septum,

hypothalamus, the region anteroventral to the third ventricle (including the organum vasculosum of the lamina terminalis and the subfornical organ, which contain some osmosensitive neurones) and the medial preoptic area activate oxytocin and vasopressin cells.

Further projections to these cells come from the brainstem. During parturition, stimulation of the uterus and cervix, via the vagal and pelvic nerves and spinal pathways relay in the brainstem. Cells in the nucleus tractus solitarii receive information about gastrointestinal distension, vascular volume, and from nociceptors, as well as the inputs from the vagina and uterus, and stimulation of this region excites both oxytocin and vasopressin neurones. The SON receives substantial noradrenergic projection from the A1 cell group of the ventral lateral medulla, although they have been mostly implicated to provide excitatory input to vasopressin neurones, while activation of oxytocin neurones is mediated by the A2 noradrenergic cells.

Also, magnocellular neurosecretory cells respond directly to changes in plasma osmolality via mechnosensitive membrane channels (Bourque *et al.*, 1993). A comprehensive discussion of neuronal inputs to magnocellular neurosecretory cells is beyond the scope of this introduction. An exhaustive review can be found in Hatton (1990).

1.4 Firing Patterns

Many stimuli have an excitatory or inhibitory effect on both oxytocin and vasopressin neurones, which correspondingly increase or decrease the release of the associated hormones, such as increases in osmotic pressure (Wakerley *et al.*, 1978). Other stimuli affect the firing activity of either vasopressin or oxytocin neurones selectively, such as haemorrhage increasing the firing rate of vasopressin neurones (Poulain *et al.*, 1977), and systemic administration of CCK having an excitatory effect on oxytocin neurones, but an inhibitory or no effect at all on vasopressin neurones (Renaud *et al.*, 1987). The latter action can be used to distinguish between the two cell types during experiments *in vivo*. Electrical activity of oxytocin neurones

changes with increased stimulation from absence of activity – i.e. electrical silence –, to a slow irregular pattern and then to a fast continuous pattern, while vasopressin neurone activity changes from electrical silence to slow irregular pattern to a kind of 'bursting' which is called *phasic* pattern (Poulain & Wakerley, 1982). Thus, in certain conditions it is difficult if not impossible to distinguish between oxytocin and vasopressin neurones on the grounds of their electrical activity, or their reaction to certain stimuli alone.

1.4.1 Vasopressin

The firing pattern associated with vasopressin neurones consists of alternating periods of activity and silence lasting tens of seconds each (Figure 1.3A), so called *phasic* firing. The duration of silent and active periods is variable for each neurone. The firing within an active period, or 'burst', is faster (10-30 Hz) on the onset (for the first 1-2 s) and then decreases. For the remainder of the burst the neurones fires at a slower rate (5-10 Hz; Poulain & Wakerley, 1982). The firing rate within this burst is also increased by stimuli that increase vasopressin secretion such as during carotid occlusion (Dreifuss *et al.*, 1976) or water deprivation (Wakerley *et al.*, 1978). Although these results suggest that phasic activity can be associated with vasopressin neurones, there is evidence that a small percentage of oxytocin neurones display the ability to fire phasically, at least *in vitro* (Armstrong *et al.*, 1994).

Phasic firing of vasopressin neurones occurs asynchronously. The onset and termination of the bursts can be precipitated by brief trains of antidromic activation of the hypophysial stalk during silent and active periods respectively (Dreifuss *et al.*, 1976). Vasopressin neurones fire phasically when the spontaneous activity exceeds an overall mean firing rate of 3 Hz (Poulain & Wakerley, 1988). These results suggest that the mechanism underlying the generation of the phasic firing pattern is extraordinarily dependent on spike activity, and is not sufficiently activated until a threshold firing frequency is achieved.

1.4.2 Oxytocin

Oxytocin neurones display a wide range of behaviour, ranging from absence of activity, to a slow irregular to a fast continuous pattern in naïve animals. However, their activity changes dramatically during lactation. In response to suckling, in addition to the background activity (Figure 1.3B) that resembles the one seen in non-lactating animals, high frequency discharges of up to 80 Hz lasting 2-4 s occur every 5-10 minutes, for as long as the suckling continues (Lincoln & Wakerley, 1974). During background activity, interspike intervals will seldom be less than 40 ms, but during bursting most intervals are in the range of 8-14 ms (Dyball & Leng, 1986). While the amplitude of these *bursts* is influenced by extrinsic cues (e.g. the number of pups suckling) the profile remains remarkably consistent: within a few initial spikes the peak frequency is reached and maintained for a short period, after which the frequency decreases and is followed by several seconds of electrical quiescence (Leng & Brown, 1997).

Intriguingly, in contrast to the lower rate 'bursts' of phasically firing vasopressin neurones, high frequency bursts in oxytocin neurones are synchronised between all oxytocin neurones, not only within one nucleus, but between all SO and PV nuclei (Belin *et al.*, 1984; Belin & Moos, 1986; Figure 1.4A and B). This synchronisation allows each neurone to contribute to a bolus release of oxytocin, which stimulates the milk letdown from the mammary gland. Similar high frequency discharges are observed in the rat prior to expulsion of pups (Summerlee & Lincoln, 1981).

1.4.3 Importance of Firing Patterns

The different patterns of cell activity have important consequences for hormone release, as they are closely related to the hormonal response required by different stimuli. Lactation and parturition require a short exposure to a large amount of the hormone, and the high frequency burst of activity, synchronised for all oxytocin neurones, causes this required bolus release of oxytocin. There is a period of silence after each burst, and interburst intervals are 5-10 min, allowing for the

clearance of oxytocin from the system and preventing a desensitisation of the target tissue. However, in its other role oxytocin promotes natriuresis, and is released in response to increases of plasma sodium. The kidney does not require a bolus of oxytocin to work efficiently, thus in naïve rats oxytocin neurones are continuously active to provide a constant plasma oxytocin level. The high-frequency discharge of activity in oxytocin neurones is a very specific answer to a particular demand, and not simply a standard response to higher hormonal request, since it is only seen during suckling and parturition. I.v. CCK administration produces only an increase in the firing rate (Renaud *et al.*, 1987), but no bursts.

Similarly, in the dehydrated rat, prolonged asynchronous phasic firing pattern cause a continuous vasopressin release at a sustained high level to promote antidiuresis over the long term. Further experiments studying the relationship between specific activity patterns and hormone output from rat magnocellular neurosecretory cells involved antidromic stimulation mimicking observed firing frequencies and patterns. Increasing the rate of stimulation increases the amount of peptides released per action potential, a phenomenon known as *frequency-dependent facilitation* (Dreifuss *et al.*, 1971; Dutton & Dyball, 1979). Frequency-dependent facilitation is accompanied by a rapid frequency-dependent broadening of the Ca^{2+} component of the action potential (Bourque & Renaud, 1985) and increased Ca^{2+} influx (Jackson *et al.*, 1991).

During sustained high frequency stimulation the release of both hormones decreases progressively, a phenomenon known as *secretory fatigue* (Bicknell *et al.*, 1984), which is particularly rapid in vasopressin neurones. This was demonstrated by Cazalis, Dayanithi and Nordmann (1985), showing that 77% of vasopressin release occurred in the first 9 of a 27 s stimulation of isolated rat neural lobe at 13 Hz. Furthermore, they showed that a single burst with an intraburst mean frequency of 13 Hz led to a greater amount of vasopressin being released than the same number of stimuli delivered at a constant frequency of 13 Hz. This suggests that the emergence of clustered firing represents an important functional response for the enhancement of hormone release by magnocellular neurosecretory cells. Intraburst clustering

seems to be another extremely important factor for enhancing hormone release, as release increased markedly when stimulation was delivered in groups of four stimuli at a rate of about 60 Hz alternating with 920 ms silent periods, rather than given at a constant mean firing rate of 4 Hz. This proves that not only is the basic firing pattern correlated to hormone release, but that the fine temporal structure within this 'coarse' pattern has a further enhancing function. Also, series of 'bursts' of stimulating pulses alternating with silent periods evoked more hormone release than stimulating pulses delivered without silent periods. This is particularly true when the silent periods last more than 21s, revealing that they provide time necessary for recovery from spike failure and secretory fatigue so that efficient hormone secretion can resume with subsequent bursts. This is further supported by experiments showing that with increased osmotic pressure an increasing fraction of vasopressin neurones fires in a phasic manner, responding to the increased demand (Wakerley *et al.*, 1978).

Altogether, these results indicate that the release of oxytocin and vasopressin is regulated so that the optimum pattern for their target is produced, as is the stimulus-secretion coupling within the magnocellular neurosecretory cells. Interspike intervals in a burst and the silent intervals between bursts are two important determinants of the effectiveness of the bursting pattern in promoting neuropeptide release. The ability to regulate the intrinsic membrane properties of magnocellular neurosecretory cells is therefore an important functional feature in the regulation of vasopressin and oxytocin release.

1.5 Intrinsic Cell Properties

Magnocellular neurosecretory cells *in vitro* retain the ability to fire spontaneously as well as displaying some (e.g. phasic bursts) but not all of their firing pattern (e.g. milk-ejection bursts), suggesting that firing patterns are determined by a combination of input to the neurone (cf. section 1.3) and intrinsic properties.

Ca^{2+} is a universal intracellular messenger with enormous versatility, creating a range of spatial and temporal signals to control processes as diverse as fertilisation,

proliferation, development, contraction and secretion (for a general review see Berridge, Bootman & Lipp, 1998; Berridge, Lipp & Bootman, 2000a, 2000b). In the SON magnocellular neurosecretory cells' signalling depends on increased levels of intracellular Ca^{2+}, derived from either internal or external sources.

After an action potential the membrane potential undergoes transient after potentials before returning to its resting potential (Figure 1.5). *In vitro* techniques like hypothalamic slices, explants and acutely isolated cell preparations of oxytocin and vasopressin neurones are particularly useful in investigating electrical membrane properties and a variety of intrinsic conductances that might be involved in regulating the shape, frequency and pattern of action potential.

In the following sections we will discuss the main elements influencing firing activity in magnocellular neurosecretory cells that are most relevant to our work, including membrane properties, intrinsic Ca^{2+} and K^+ currents, as well as internal Ca^{2+} stores and Ca^{2+} buffers.

1.5.1 Passive Membrane Properties of MNCs

In vitro experiments indicate that magnocellular neurosecretory cells have a resting membrane potential of between –55 and –70 mV (Armstrong *et al.*, 1994; Bourque & Renaud, 1985; Stern & Armstrong, 1995), an input resistance of between 50 and 250 MΩ in intracellular recordings (Andrew & Dudek, 1984a; Armstrong *et al.*, 1994; Bourque & Renaud, 1985), and membrane time constants ranging between 9 and 18 ms (Armstrong *et al.*, 1994; Bourque & Renaud, 1985). Intracellular recordings *in vivo* confirm these observations (Bourque & Renaud, 1991), although it appears that the input resistance is in the lower range (about 100 MΩ). This might be because there is more spontaneous synaptic activity converging on magnocellular neurosecretory cells in whole animals. No significant differences could be found between oxytocin and vasopressin neurones – identified by injections of biotinylated markers during intracellular recordings – in resting membrane potential, input resistance, membrane time constants, or spike height and duration (Armstrong *et al.*, 1994; Stern & Armstrong, 1996).

1.5.2 Intrinsic Ionic Conductances in MNCs

Single electrode voltage-clamp recordings in explant preparations measured steady-state current-voltage (I-V) relationships that were nearly linear between –100 and –60 mV when performed from a holding potential of near –60 mV. Varying the holding potential and the application of various channel blockers resulting in changes in the I-V relationship, showing a variety of Ca^{2+} and K^+ currents, the most important of which are discussed below.

Electrophysiologically, oxytocin and vasopressin neurones are characterised by a prominent transient outward rectification, which was identified as an I_a-like current by Bourque (1988). When the membrane potential was hyperpolarised below –80 mV depolarising pulses provoked a strong transient outward rectification which delayed the occurrence of the first spike (Armstrong & Stern, 1998). More specifically, oxytocin neurones are characterised by the presence of a sustained outward rectifier above –50 mV (active below spike threshold), a rebound depolarisation following deactivation of the sustained rectification which can sustain short spike trains, and a smaller transient outward rectification (probably associated with the potassium current I_a). Vasopressin neurones show little of the sustained outward rectification and rebound depolarisation, but have a stronger transient outward rectification. Although both oxytocin and vasopressin neurones exhibit depolarising afterpotentials (DAP), in vasopressin neurones these lead to plateau potentials (see section 1.5.5) underlying prolonged discharges, while in oxytocin neurones they usually sustain a short spike discharge, rather than prolonged bursts (Armstrong & Stern, 1998).

Ca^{2+} channels are performing different function in different parts of a neurone, such as the transfer of charge, the activation of enzymes or ionic channels, and the activation of exocytosis. Fisher and Bourque (1995; 1996) have revealed 6 different components in the voltage-dependent calcium current in whole cell patch

clamp recordings from acutely isolated magnocellular neurosecretory cells. The following Ca^{2+} channels have been identified in their somata: (1) a T-type current was identified by its low threshold of activation (-60 mV), rapid inactivation at peak amplitudes (~40 ms), high sensitivity to Ni^{2+}, and insensitivity to blockers of other types of currents, although others have failed to find this current (Foehring & Armstrong, 1996); (2) a low threshold L-type channel with a threshold of around –50 mV, slowly inactivating (~1300 ms), and sensitive to dihydropyridine-nifedipine; (3) a R?-type (similar but slower inactivation), threshold of –50 mV, inactivation of ~200 ms, and insensitive to toxins; and (4) a P-type current, non-inactivating, and nifedipine and ω -CgTX-insensitive, but blocked by ω -agatoxin IVA. In addition, (5) a slowly inactivating (~1800 ms), N-type-channel selective blocker ω -conotoxin GVIA-sensitive channel, as well as (6) an unidentified inactivating component were identified.

In the axon terminals, by contrast, identified Ca^{2+} current types of magnocellular neurosecretory cells are (1) a high-threshold L-type, (2) a rapidly inactivating high threshold N-type (peak ~100ms), (3) a high threshold Q?-type current blocked by high doses of ω -Aga-IVA, and (4) Ca^{2+} dependent K^+ currents. It has been concluded that differences in biophysical properties of Ca^{2+} channels have important functional implications, and highlight the complex processes regulating Ca^{2+} channel distribution and function in different parts of the neurone. These results indicate that magnocellular neurosecretory cells possess a variety of means to regulate voltage-gated entry of Ca^{2+} into the cell and the subsequent activation of Ca^{2+} and activity-dependent phenomena involved in the modulation of magnocellular neurosecretory cell firing.

The large diversity of K^+ channels in excitable cells fulfils a wide range of roles, chiefly related to the stabilisation of the membrane potential. This is done through actions such as setting the resting potential, keeping fast action potential short, terminating periods of intense activity, timing the interspike intervals during repetitive firing, and generally lowering the effectiveness of excitatory inputs on a cell when they are open (for a comprehensive discussion of all these roles see Hille,

1991). Altogether, this diversity results in the ability of excitable membranes to encode trains of action potentials and to have rhythmic activity. A discussion of the most important K^+ currents in magnocellular neurosecretory cells – as well as their roles – is included in the following sections.

1.5.3 Currents Underlying the Hyperpolarising Afterpotential (HAP)

Each individual action potential is immediately followed by a hyperpolarising afterpotential (HAP), which lasts between 50-100 ms and results from a Ca^{2+}-dependent K^+ conductance (I_{to}) that is rapidly activated during each action potential (Bourque *et al.*, 1985). Voltage-clamp studies indicated that this transient current is similar in characteristics to the current termed I_a, which has been described in other cells (Bourque, 1988). The I_a can be activated when a cell is depolarised following a period of hyperpolarisation. Through complex interactions between its associated channel and other K^+ channels it serves as a constraint of the firing rate to space successive action potentials. The HAP sets an upper limit on the maximal firing rate which can be achieved during a depolarising stimulus by the neurone, by reducing the probability of firing immediately after each action potential (Andrew & Dudek, 1984a). The activity of vasopressin neurones always stays within this limit. Oxytocin neurones adhere to it under all circumstances but one: during milk-ejection bursts, where they dramatically escape this limit.

Bourque (1988) studied the current underlying the HAP in perfused explants using the single-electrode voltage-clamp technique. This rapidly activating and inactivating transient outward current is evoked by a depolarising voltage current pulse from a threshold of –75 mV, reaches the peak within 7 ms and subsequently decays monotonically with a time constant of 30 ms. Steady-state inactivation is complete at potentials positive to –55 mV, and the inactivation was removed following tens of milliseconds at hyperpolarised voltages. Further, it was shown that the I_{to} is strongly dependent on extracellular Ca^{2+}, whereby its influx during a spike may contribute to the repolarisation, as well as to the peak and initial phase of the

hyperpolarising afterpotential. Indeed Bourque *et al.* (1985) suggested that its amplitude is directly proportional to the external concentration of Ca^{2+}.

Bourque (1988) concluded that the current is involved in the regulation of spike duration, the post-spike HAP, and influences both the firing rate and pattern, by interacting with other post-spike currents. Thus synaptic modulation of the I_{to} may effectively control the activity pattern or responsiveness to additional synaptic stimuli.

1.5.4 Currents Underlying the Afterhyperpolarisation (AHP)

In contrast to the hyperpolarising afterpotential, which is evoked by *single* action potential, *trains* of action potentials are followed by a prominent AHP. The frequency reported to be necessary to elicit an AHP varies between studies, with a frequency of >20 Hz reported by Bourque *et al.* (1985), a frequency of >10 Hz reported by Andrew and Dudek (1984), and frequencies of only >1 Hz reported by Kirkpatrick and Bourque (1996). The magnitude of the AHP is proportional to the number of spikes elicited during the bursts (Bourque *et al.*, 1985), with an exponentially progressing onset and a maximum after the first fifteen to twenty impulses, regardless of the frequency at which spikes were evoked (Kirkpatrick & Bourque, 1996). The steady-state amplitude increases logarithmically between 1 and 20 Hz.

The AHP lasts hundreds of ms, and its duration also depends on the duration and frequency of the spike train (Andrew & Dudek, 1984a). The dependence of the amplitude on both spike number and firing frequency suggests that it is activated in an activity dependent way. Greffrath *et al.* (1998) reported the existence of two AHPs: in 43% of their neurones only a fast AHP (peak amplitude within 10-30 ms, decay with a time constant of 256±118 ms, resting membrane potential reached within 2 s) was elicited by spike trains following an injection of depolarising current, while 26% of studied neurones additionally displayed a slow AHP (time constant of decay 1010±311 ms and a duration of up to 6 s). The remaining 31% displayed a sequence of a fast AHP and a depolarising afterpotential (DAP).

The AHP is associated with a 20-60% decrease in input resistance and shows little voltage dependence in the range of –70 to –120 mV. Also, AHP evoked by the same length spike train recorded at a given membrane potential is proportional to the extracellular concentration of Ca^{2+} and can be reduced or abolished by adding Ca^{2+} channel blockers or by exchanging Ca^{2+} with ethyleneglycol-bis(ß-aminoethylether)-*N,N'*-tetraacetic acid (EGTA; Bourque *et al.*, 1985). Incidentally, replacing Ca^{2+} with Mn^{2+}, Mg^{2+} or Co^{2+} *in vitro* increases the firing rate of magnocellular neurosecretory cells. These observations led to the conclusion that the AHP results from the activation of a slow, voltage-independent Ca^{2+} -dependent K^+ conductance, the I_{AHP}.

The distinction between the I_{AHP} and the I_{to}, and correspondingly between the post-*train* AHP and the post-*spike* HAP, is made since the ionic currents are pharmacologically distinct. The I_{to} is less sensitive to effects of tetraethylammonium, but was reduced by 4-aminopyridine and dendrotoxin (Bourque, 1988). By contrast, I_{AHP} is blocked by the bee venom apamin, with the effect of a threefold increase in the mean firing rate of spontaneously active neurones (Kirkpatrick & Bourque, 1996). Greffrath *et al.* (1998) further suggest that the fast AHP is blocked by apamin, while the slow AHP is blocked by charybdotoxin (ChTX), and is affected by low concentrations of tetraethylammonium, although Kirkpatrick and Bourque (1996) could not find the latter effect. It has been suggested that apamin generally blocks the small (SK) Ca^{2+} dependent K^+ channels (Hugues *et al.*, 1982), while charybdotoxin blocks some large Ca^{2+} dependent K^+ channels (Miller *et al.*, 1985), as well as some other K^+ channels.

The AHP is important for the firing frequency, as it functions as a direct feedback inhibitor of activity and so stabilises the steady-state firing activity of continuously active cells. Also, it is thought to be involved in the generation of bursting activity in magnocellular neurosecretory cells by its interactions with the DAP (see below section 1.5.5). Finally, it has been suggested that through temporary inhibition of the I_{AHP} by either modulation of apamin sensitive K^+ channels, or channels regulation spike dependent Ca^{2+} influx there exists a mechanism by which oxytocin neurones could fire at the high frequencies seen during the milk ejection

bursts (Kirkpatrick & Bourque, 1996). Hence the AHP may have pronounced effects on the activity of magnocellular neurosecretory cells and consequently for the neurosecretion of their hormones.

1.5.5 Currents Underlying the Depolarising Afterpotentials (DAP)

Lincoln & Wakerley (1974) noted that, from 58 antidromically identified magnocellular neurosecretory cells recorded in lactating rats *in vivo*, 28% displayed a phasic pattern of activity. This corroborates with findings that in 31% of magnocellular neurosecretory cells a depolarising afterpotential (DAP) is observed in addition to the AHP (Greffrath *et al.*, 1998). Bourque (1989) argued that the DAP is exclusively displayed by vasopressin neurones, however, (Stern & Armstrong, 1996) report that 57% of oxytocin neurones exhibit a DAP, in both virgin and lactating animals. *In vivo* observations (Dreifuss *et al.*, 1976) provided first clues about the importance of intrinsic mechanisms for the generation of phasic discharge, and *in vitro* studies provided more direct evidence that phasic bursting involves the occurrence of a slow DAP of 1-10 mV, lasting from hundreds of milliseconds to several seconds (Andrew & Dudek, 1983; 1984b).

Bourque (1986), using a procedure that involves switching rapidly between current- and voltage-clamping magnocellular neurosecretory cells in an explant reported aftercurrents including an early outward and a late inward component, termed I_{AHP} and I_{DAP} due to their temporal correlation with the AHP and DAP. As an overlap between these two currents exists, the rate of onset of the I_{DAP} could not be determined, but it was reported to be at least one order of magnitude more prolonged that the I_{AHP} and decayed exponentially with a time constant of approx. 2 s. Also, it was reported that DAPs could still be evoked by Ca^{2+} spikes in the presence of tetrodotoxin (TTX; a Na^{+} channel blocker), but were abolished by adding Cd^{2+} to the perfusate. This indicates that the DAP is carried by or otherwise dependent on Ca^{2+} influx. Further, similarly to the AHP the amplitude of the DAP relies on the influx of Ca^{2+}, and is also influenced by voltage: the amplitude of DAPs decreased as the membrane potential was made more negative, and DAPs were abolished and could

not be reversed by hyperpolarisation beyond –80 mV. Altogether, the I_{DAP} appears to be a voltage- and Ca^{2+} -dependent inward membrane current of unspecified ionic nature.

Li and Hatton (1997a) conducted patch-clamp experiments to investigate the nature of the I_{DAP}. They reported that the I_{DAP} is associated with a decrease in membrane conductance, that it is dependent on K^+ concentration gradients across the membrane, that it is reversibly reduced by low concentrations of K^+ channel blockers and that Ca^{2+} and Na^+ influx cannot induce a slow inward I_{DAP}-like current after K^+ efflux was suppressed. They concluded that the DAP generation in magnocellular neurosecretory cells involves a rapid increase in intracellular Ca^{2+} levels, due to Ca^{2+} influx via high-threshold channels following an action potential and release from internal Ca^{2+} stores which then suppresses K^+ conductance.

The basis of phasic firing pattern in magnocellular neurosecretory cells is the summation of individual DAPs into a so-called *plateau potential*. After each action potential, the I_{DAP}, as an inward membrane current, shifts the membrane potential toward spike threshold and transiently increases the probability that a subsequent excitatory postsynaptic potential (EPSP) will trigger a further action potential. In that case, the DAP following the second action potential can sum up with the first, further depolarising the membrane potential and increasing the probability of a subsequent spike. The process repeats itself and can result in a suprathreshold DAP, allowing repetitive firing independent of the EPSP activity. So the ability of a DAP to produce and sustain a phasic burst depends on the prevailing membrane potential: while the I_{DAP} can depolarise magnocellular neurosecretory cells at all potentials from which it can be activated, it is maximally effective when triggered from potentials near or above –65 mV, where its activation will result in a suprathreshold regenerative depolarisation, ensuring repetitive firing will be sustained (Bourque, 1986).

While the onset and sustenance of phasic bursts can be explained by the properties of the inward spike aftercurrent I_{DAP} the mechanisms leading to the termination of the bursts are less well known. Andrew and Dudek (1984b) observed that the I_{DAP} becomes inactivated with time during a burst, and that recovery occurs

slowly during the interburst interval. The inactivation of prolonged plateau potentials is Ca^{2+} -dependent (Bourque *et al.*, 1986). The activity-dependent inactivation of I_{DAP} progressively appearing during a burst may be mediated by a gradual increase in free internal Ca^{2+}: for each spike the Ca^{2+} ions enter the cell faster than they can be cleared away, which leads to a build up of internal Ca^{2+} until Ca^{2+} dependent channels become activated. The cell is hyperpolarised by a combination of the enhanced Ca^{2+}-dependent K^+ current, and a reduction of Ca^{2+} currents that are weakened as a result of a Ca^{2+}-induced inactivation of Ca^{2+} channels, thus shutting off activity and further Ca^{2+} entry, which allows the clearance of the built-up intracellular $[Ca^{2+}]$. This in turn allows the K^+ channels to close, permitting a new cycle of bursting.

As mentioned before, the DAP is enhanced (or unmasked if previously not present) by ChTX (Ghamari-Langroudi & Bourque, 2000). Also, with increased frequencies at which the impulses are forced during an evoked spike train the amplitude of the AHP increases, but is reduced for the DAP (Andrew & Dudek, 1984a). As the mechanism underlying the AHP – in contrast to the mechanism underlying the DAP – does not become inactive in response to prolonged activity, the outward aftercurrent I_{AHP} can oppose the effects of the inward current responsible for the DAP. This is supported by findings of Ghamari-Langroudi and Bourque (1998), who investigated the effects of Cs^+ on DAP and AHP. They found that Cs^+ acts as a blocker of the DAP through a direct interaction with the channels responsible for its production. Bath application of Cs^+ reversibly inhibits the DAP, but this is associated with an enhancement of the amplitude and duration of the AHP, indicating that the currents underlying the AHP and DAP overlap in time following a train of action potentials.

The presence of a DAP alone cannot account for phasic firing and the difference in firing pattern between oxytocin and vasopressin neurones, as it has been shown that around 57% of oxytocin neurones exhibit the DAP, however, phasic firing in these neurones is seldom seen (Armstrong *et al.*, 1994). Also, discharges

beyond the time course of the DAP were rarely observed after inducing a DAP in oxytocin neurones (Stern & Armstrong, 1996).

Magnocellular neurosecretory cells therefore possess several spike dependent aftercurrents, and interactions of these shape the activity pattern of the neurone. As the amplitude and duration of these conductances affect the probability of the generation of subsequent action potential, the I_{to}, I_{AHP} and I_{DAP} represent autoinhibitory and autoexcitatory mechanisms that are important in the activity-dependent regulation of hormone discharge in magnocellular neurosecretory cells.

1.5.6 Differences Between Oxytocin and Vasopressin Neurones, and Changes in Lactation

Armstrong *et al.* (1994) used a combination of intracellular recordings with dye-labelling and subsequent immunocytochemical identification in explants and conclude that there is no significant differences between oxytocin and vasopressin neurones in neither HAPs nor AHPs. However, later studies showed marked differences between oxytocin and vasopressin neurones in several points. Stern and Armstrong (1995) found that oxytocin, but not vasopressin neurones displayed a sustained outward rectification and an associated rebound depolarisation that follows its deactivation, which they suggested might favour the expression of short bursts of action potentials. Further, while neither incidence nor magnitude of the sustained outward rectification was changed during lactation, the rebound depolarisation peak amplitude was significantly larger in lactating rats (Stern & Armstrong, 1996). Thus, during lactating the expression of further short burst might be further enhanced by the greater rebound depolarisation

In oxytocin neurones action potentials were significantly wider, and slower rising and decay times were reported (Stern & Armstrong, 1996). These effects were linked to an enhanced Ca^{2+} influx per spike in lactation. Further, spike height was always significantly lower in oxytocin than in vasopressin neurones. While no significant differences could be found in the incidence nor mean amplitude of the

DAP in oxytocin and vasopressin neurones in lactating and non-lactating animals, the AHP was shown to have a larger mean peak amplitude and a larger per spike area in oxytocin neurones from lactating in comparison to non-lactating animals. The time constant of the decay of the AHP was smaller in oxytocin neurones. Stern & Armstrong (1996) argue that the time course of the AHP and its peak amplitude influence the time course of spike frequency adaptation and the initial spike frequency during trains of action potentials. Because of the role as an intrinsic inhibitor, strong depolarisation during lactation would result in a stronger stabilising effect on spike firing. The conclusion from these results is that, during lactation, the spike-induced Ca^{2+} influx is selectively increased.

1.5.7 Internal Calcium Stores and Autoregulatory Mechanisms

Intracellular free Ca^{2+} is an important contributor to neuronal excitability and firing pattern in magnocellular neurosecretory cells. There are two sources for Ca^{2+}, external Ca^{2+} – which can enter the cell via voltage-gated or receptor-coupled channels (discussed above) – or internal Ca^{2+} stores. The release of Ca^{2+} can be stimulated through channels in the endoplasmic reticulum by a variety of substances. Thapsigargin depletes Ca^{2+} release by specifically inhibiting the endoplasmic reticulum Ca^{2+}-ATPase, thus reducing Ca^{2+} uptake into internal stores. Thapsigargin-releasable stores include the stores sensitive to inositol 1,4,5-triphosphate. Also known to release Ca^{2+} from internal stores are caffeine and ryanodine (Berridge *et al.*, 1998; Lambert *et al.*, 1994).

In a process called Ca^{2+}-induced Ca^{2+} release (CICR), Ca^{2+} influx can evoke Ca^{2+} release from internal stores and thus prolong high levels of intracellular Ca^{2+}. This has been suggested to be of importance for the generation of DAPs (Li & Hatton, 1997b). Intracellular Ca^{2+} levels due to influx during action potentials peak much more quickly than the DAP, and lasts much shorter. CICR was hypothesised to be another source of Ca^{2+}, which could slow down the decline in Ca^{2+} levels following a spike and thus allowing the long duration of DAPs and promoting phasic firing. This was supported by findings that perfusions of slices of the SON with

internal Ca^{2+} release channels blockers (such as ryanodine) reduces DAP amplitudes and shortens its duration by 50%, and depletion of internal stores by thapsigargin also reduces DAP amplitude by 50% and eliminates phasic firing.

In rabbit otic ganglion cells and in guinea pig vagal neurones, application of ryanodine abolished the slow component of the AHP (Yoshizaki *et al.*, 1995; Sah & McLachlan, 1991), thus implicating a participation of CICR in the formation of the AHP.

Ludwig *et al.* (2002) have shown the importance of internal Ca^{2+} in magnocellular neurosecretory cell autoregulation. While thapsigargin application – via a microdialysis probe implanted into the SON *in vivo* – had no effect on hormone secretion into the circulation following systemic osmotic stimulation, oxytocin release in the SON was significantly increased. From these results and the results of thapsigargin application during constant collision stimulation it was suggested that the mobilisation of Ca^{2+} from thapsigargin sensitive stores evoke oxytocin release from dendrites, but not from axon terminals, without an increase in the firing rate. Further, thapsigargin application causes subtle differences in the activity patterning: very short interspike intervals were followed by intervals that were also very short, suggesting that the AHP my have been overridden by post-spike depolarisation. Incidentally, this clustering in the electrical activity has been shown to be of importance in the generation of milk-ejection bursts (Brown *et al.*, 2000; discussed in section 1.6.2). Thus the activity dependent exocytosis from the dendrites may have a positive feedback effect on electrical activity, as oxytocin itself has been shown to have an important effect on internal Ca^{2+} stores. In approx. 50% of freshly dissociated magnocellular neurosecretory cells the addition of 100nM oxytocin induced a 5 to 6 fold rise in intracellular Ca^{2+} levels that was not affected by the removal of extracellular Ca^{2+}, and was mimicked by application of thapsigargin but not other internal Ca^{2+} store mobilisers (Lambert *et al.*, 1994). This indicates that oxytocin mobilises intracellular Ca^{2+} from thapsigargin sensitive stores in oxytocin neurones. So, once internal Ca^{2+} from the thapsigargin sensitive stores in oxytocin cells has been mobilised, somato-dendritic oxytocin release might be triggered,

leading to further involvement of internal Ca^{2+} stores: oxytocin release may be self-sustained and very long-lasting. As dendritic release evoked by depolarisation seems to facilitate clustering in the activity pattern, oxytocin itself in its autoregulatory role seems to underlay the generation of milk-ejection bursts by this mechanism.

In this context, Moos *et al.* (1989) reported that oxytocin release within the SON is significantly increased during suckling, even before the first milk-ejection burst, and also during burst-like electrical stimulation of the posterior pituitary. Also, application of oxytocin into the 3rd ventricle dramatically enhances milk-ejection bursts during suckling, increasing both the amplitude and frequency in a dose dependent manner, and even triggering bursts when none had appeared an hour after suckling started (Freund-Mercier & Richard, 1984).

Vasopressin also exerts autoregulatory effects via intracellular Ca^{2+} levels, but this is mediated by an influx of Ca^{2+} through L-, N- and T-type channels (discussed above), involving phospholipase C and adenylate cyclase intracellular pathways (Sabatier *et al.*, 1998) which are activated by V_1 (V_{1a} and V_{1b})- and V_2-type receptors, respectively (for a review see Dayanithi *et al.*, 2000).

Leng (1981) has speculated as far back as 1981 that vasopressin could modulate the phasic firing pattern of vasopressin neurones, however, the nature of the autoregulatory effect of vasopressin on vasopressin neurones have variously been reported as inhibitory (Leng & Mason, 1982), excitatory (Inenaga & Yamashita, 1986) or non-existent. More recently a unifying hypothesis based on the initial level of activity has been proposed: for highly active neurones the effect appears to be inhibitory, for faintly active neurones excitatory, while the activity of moderately active neurones seems not to be affected (Moos *et al.*, 1998). Thus it appears that vasopressin considerably narrows the range of possible firing activity, regularising it around an intermediate level that is known to optimise systemic vasopressin release (Gouzenes *et al.*, 1998). Summarising, both oxytocin and vasopressin facilitate the expression of activity pattern of their respective neurones so as to optimise neurosecretion by autoregulary mechanisms involving intracellular Ca^{2+}.

Another neurotransmitter which is important in the autoregulation of firing activity in magnocellular neurosecretory cells is nitric oxide (NO). NO synthase (NOS) has been shown to be abundant in the dendrites, somata, and axon terminals of magnocellular neurosecretory cells (Bredt *et al*,. 1990). The expression of NOS mRNA is increased in circumstances known to induce high-frequency discharge of activity (e.g. osmotic stimulation (Kadowaki *et al.*, 1994), or hypovolaemia (Ueta *et al.*, 1998)) suggests that NO may be expressed in an activity dependent manner. NO release it also stimulated in response to elevations in intracellular Ca^{2+} levels, which are increased in response to action potentials. Thus, NO within the SON may work as an inhibitory feedback regulator, protecting neurones from excessive excitation. This is supported by reports that NO is inhibitory to both oxytocin and vasopressin neurones, and by findings that NO inhibits oxytocin secretion in both rats (Kadekaro *et al.*, 1997) and humans (Chiodera *et al.*, 1994). Furthermore, Srisawat *et al.* (2000) report a dramatic downregulation of NO in late pregnancy, shown by a reduced expression of NOS mRNA and a loss of efficacy of NOS inhibitors on stimulation evoked oxytocin release. This may allow the oxytocin system to become more excitable at term, thus potentially allowing greater neurosecretion during parturition.

1.5.8 Calcium Buffering

As discussed in the previous sections, the adequate elevation of intracellular Ca^{2+} levels – whether originating from internal or external sources – is vitally important in the regulation of the activity of oxytocin and vasopressin neurones. The peak and time course of the increase in intracellular Ca^{2+} are controlled by two major cellular mechanisms, namely Ca^{2+} pumps which transport Ca^{2+} into the interstitial space and refill internal stores and Ca^{2+} chelators, such as Ca^{2+} binding proteins.

As mentioned previously (cf. section 1.5.5), while vasopressin neurones exhibit the Ca^{2+} dependent DAP, oxytocin neurones generally do not. The differences in Ca^{2+} buffering and its role for the activity pattern in these neurones was investigated. Li *et al.* (1995) injected calbindin-D_{28k} – a Ca^{2+} binding protein that acts to passively buffer intracellular Ca^{2+} – directly into phasically firing

magnocellular neurosecretory cells. This resulted in a suppression of the DAP and changed the activity from phasic to continuous. Conversely, introducing an anti-calbindin antiserum into continuously firing and so putatively identified oxytocin neurones unmasked a DAP and induced phasic firing. Thus, it appears that oxytocin neurones express calbindin, which helps to determine the firing pattern. Immuno-fluorescence studies confirm that while around 80% of oxytocin neurones were positively labelled for calbindin, only around 25% of vasopressin neurones were (Miyata *et al.*, 1998).

Li *et al.* (1995) suggest that the difference in firing pattern of OT and VP cells can be explained by the amount of endogenous calbindin present: in cells with more calbindin the rise of Ca^{2+} is buffered rapidly and DAPs cannot be generated, hence they would fire continuously. Cells with less calbindin would be unable to buffer the Ca^{2+} rise fast enough so that DAPs emerge and the firing activity becomes phasic. This leads to the conclusion that OT and VP cells both posses membrane channels and intracellular components essential to generate phasic firing patterns, as indeed was observed in early *in vivo* work by Brimble and Dyball (1977). There is no obvious correlation between the presence of calbindin and cellular properties, and it is present in a wide range of neurones (Baimbridge *et al.*, 1992). From this distribution pattern it seems likely that calbindin is not essential for basic cellular functions, but rather that it might modulate existing properties. The high frequencies achieved during the milk-ejection burst are associated with a large influx of Ca^{2+}. The importance of buffering to protect against the neuro-toxic levels of Ca^{2+} that would ensue has been suggested as one role for Ca^{2+} binding proteins (Miyata *et al.*, 1998). Another important role might be to promote bursting by the inhibition of outward Ca^{2+} dependent K^{+} currents.

1.6 Spike Discharge

1.6.1 Spike Duration

Action potentials in rat magnocellular neurosecretory cells are carried by Na^+ and Ca^{2+} ions, with the Ca^{2+} component contribution to a shoulder on the falling phase of the spike.

Bourque and Renaud (1991) looked at spike duration recorded *in vivo* in rat magnocellular neurosecretory cells. Action potentials evoked at frequencies <1 Hz had a duration of 1.11±0.08 ms when measured at half amplitude, whereas action potentials evoked at frequencies >5 Hz had a duration of 1.56±0.4 ms. Spike duration was proportional to the firing rate when measured at steady-state. Spike broadening developed progressively at the onset of a spike train until the new duration was reached and were not seen in adjacent non-neuroendocrine neurones.

Spike duration ranging between 1.2 and 3.9 ms (measured at one-third amplitude) were recorded *in vitro*, depending on frequency. In phasically firing neurones, spike broadening at the beginning of the burst developed during the first 5 – 10 spikes, whereafter it remained the same duration for the rest of the burst, despite a reduction in firing frequency. The broadening was reversed during the following silent periods, with a time constant of 4.9 s. In addition, Bourque & Renaud (1985) concluded that a Ca^{2+} conductance contributes to frequency- and firing pattern-dependent changes in spike duration.

Another study reported spike duration of 1.0 to 2.1 ms for the first spike of a phasic burst, increasing by up to 87% for spikes in the second half of the burst (Andrew & Dudek, 1985). While the degree of the broadening was variable between magnocellular neurosecretory cells, spike broadening was seen to be a direct result of an increase in spike frequency, either during burst initiation or during transition to fast firing. It was also suggested that although spikes involve Ca^{2+} influx in or near the soma it is not facilitated by spike broadening, but rather by a slow accumulation of residual Ca^{2+} which is freed from intracellular Ca^{2+} stores during previous spikes.

However, broadening in itself cannot readily explain why bursts evoke maximal hormone release from terminals, since the broadening – even if it would reflect an increased Ca^{2+} influx at the terminals – develops faster than the maximal secretion rate, and also during continuous firing the broadening is maintained, but this activity pattern is not as effective for hormone secretion as phasic firing (Andrew & Dudek, 1985). Nonetheless, spike broadening is expected to have an indirect effect on voltage and Ca^{2+} dependent currents, such as in oxytocin neurones of female rats where longer spikes are associated with an enhancement of Ca^{2+} dependent AHPs and spike frequency adaptation (Stern & Armstrong, 1996).

Magnocellular neurosecretory cells change their firing pattern with increased osmotic stimulation from electrical silence, to a slow irregular firing and a fast continuous pattern, with firing frequencies between <1 Hz to 15 Hz (e.g. Lincoln & Wakerley, 1974). This upper limit is only exceeded at the onset of a phasic burst and during the milk-ejection burst. Dyball and Leng (1986) investigated the regulation of the milk ejection burst in rats under urethane anaesthesia. The similarity between firing pattern in non-lactating and background activity in lactating animals, and the observation that antidromic pulse trains did not trigger bursts (although they significantly increased the chance of a burst occurring within 2.5 min) led them to conclude that there is a temporary inhibition of an intrinsic membrane conductance which normally slows firing in these cells, and so may enable the cells to fire at the high frequencies observed.

Also, it has been argued that since it is possible to drive magnocellular neurosecretory cells antidromically to fire at frequencies >100 Hz, it is not post-spike refractoriness that limits firing rate and that Ca^{2+} is a necessary factor in the mechanism that normally prevents high frequency discharge (Thomson, 1984). As mentioned above, K^+ channels throughout excitable membranes and the associated currents have been implicated in the regulation of firing frequencies. Specifically, the HAP functions as an inhibition in the interspike interval to space successive action potentials, setting an upper limit on the maximal firing rate which can be achieved during a depolarising stimulus by the neurone (Andrew & Dudek, 1984a), and thus

contributing to the regulation of firing frequency. Further, synaptic modulation of the underlying Ca^{2+} dependent K^+ current may be involved in the control of activity pattern, responsiveness to additional synaptic stimuli, and in the regulation of spike duration (Bourque, 1988).

Of further importance for the firing frequency is the AHP, as it functions as a direct feedback inhibitor of activity and so stabilises the steady-state firing activity of continuously active cells. Through its interactions with the DAP it probably contributes to the generation of bursting activity in magnocellular neurosecretory cells. A temporary inhibition of the I_{AHP} by either modulation of apamin sensitive K^+ channels, or channels regulation spike dependent Ca^{2+} influx has been postulated as a likely mechanism by which oxytocin neurones could fire at the high frequencies seen during the milk ejection bursts (Kirkpatrick & Bourque, 1996).

Summarising, currents underlying the HAP, the AHP, and other Ca^{2+} dependent K^+ currents are likely to have pronounced effects on the spontaneous electrical activity of magnocellular neurosecretory cells and hence on their neurosecretion.

1.6.2 Spike Clustering

As described in previous sections 'long-term' firing patterns have an important role in the regulation of hormone secretion (section 1.4.3). However, the fine temporal structure during firing activity may also be of importance.

Cazalis *et al.* (1985) report that not only does stimulation of isolated rat neural lobes mimicking a burst leads to a release of a larger amount of vasopressin than a constant stimulus with the same mean frequency, but that the efficiency of the burst stimulus can be further enhanced by delivering pulses in groups of four at a rate of about 60 Hz alternating with 920 ms silent periods, rather than giving it at a constant mean firing rate of 4 Hz.

Poulain and colleagues (1988) statistically analysed spontaneous firing patterns from *in vivo* recordings of oxytocin and vasopressin neurones during progressive dehydration. Firing in both oxytocin and vasopressin neurones is far

from random: there is a greater number of runs of short interspike intervals than would be expected if firing would follow a Poisson process. Further, clustering is independent of the firing pattern, as it is not only seen during the initial peak of activity, but also during the stationary periods within phasic bursts, and even in slow irregular firing patterns. Therefore, clustering of action potentials may not only play a role under conditions requiring enhanced hormone release, but also at low levels of electrical activity, thus contributing to basal neurosecretion.

Further evidence for the importance of fine temporal structure comes from analyses of oxytocin electrical activity before milk-ejection bursts, performed by Brown *et al.* (2000). They report that variability of basal firing prior to high frequency discharges appears to be an essential accompaniment of a marked bursting pattern. Treatment which facilitates bursting, like oxytocin application had the effect of increases in irregularity of the basal activity. By contrast, treatment that inhibited bursting, such as hypertonic saline application induced faster, but more regular firing. The one measure strongly related to burst amplitude was the standard deviation of the firing rate: the higher the standard deviation the higher the burst amplitude, indicating again the importance of spike clustering.

1.7 Summary and Aim of the Dissertation

Magnocellular neurosecretory cells in the hypothalamo-hypophysial systems offer an excellent model to study neuronal behaviour. In response to a variety of physiological stimuli their somata initiate well characterised activity patterns which regulate hormone release from their axon terminals in the posterior pituitary. Magnocellular neurosecretory cells display an array of intrinsic mechanisms, such as several different classes of Ca^{2+} and K^{+} currents, internal Ca^{2+} stores and Ca^{2+} buffers which are all involved in the regulation of intracellular Ca^{2+} levels. These, in interaction with synaptic input, govern the firing patterns, and thus the secretion of the peptides.

Computational models of neural networks taking into account all intrinsic properties are overwhelmingly complex and computationally intense, and hence are

in practise infeasible. Thus, in order to build a realistic model of neuronal behaviour, parameters that are of vital importance for the system need to be distinguished from parameters with a more subtle role.

In this thesis, we use statistical methods to look at spontaneous firing activity of oxytocin neurones to determine the most important parameters governing their neuronal excitability. Analyses of the firing rates and the fine temporal structure between individual action potentials lead to the hypothesis that the two main parameters governing neuronal activity in oxytocin neurones *in vivo* are the hyperpolarising afterpotential (HAP) and the afterhyperpolarisation (AHP).

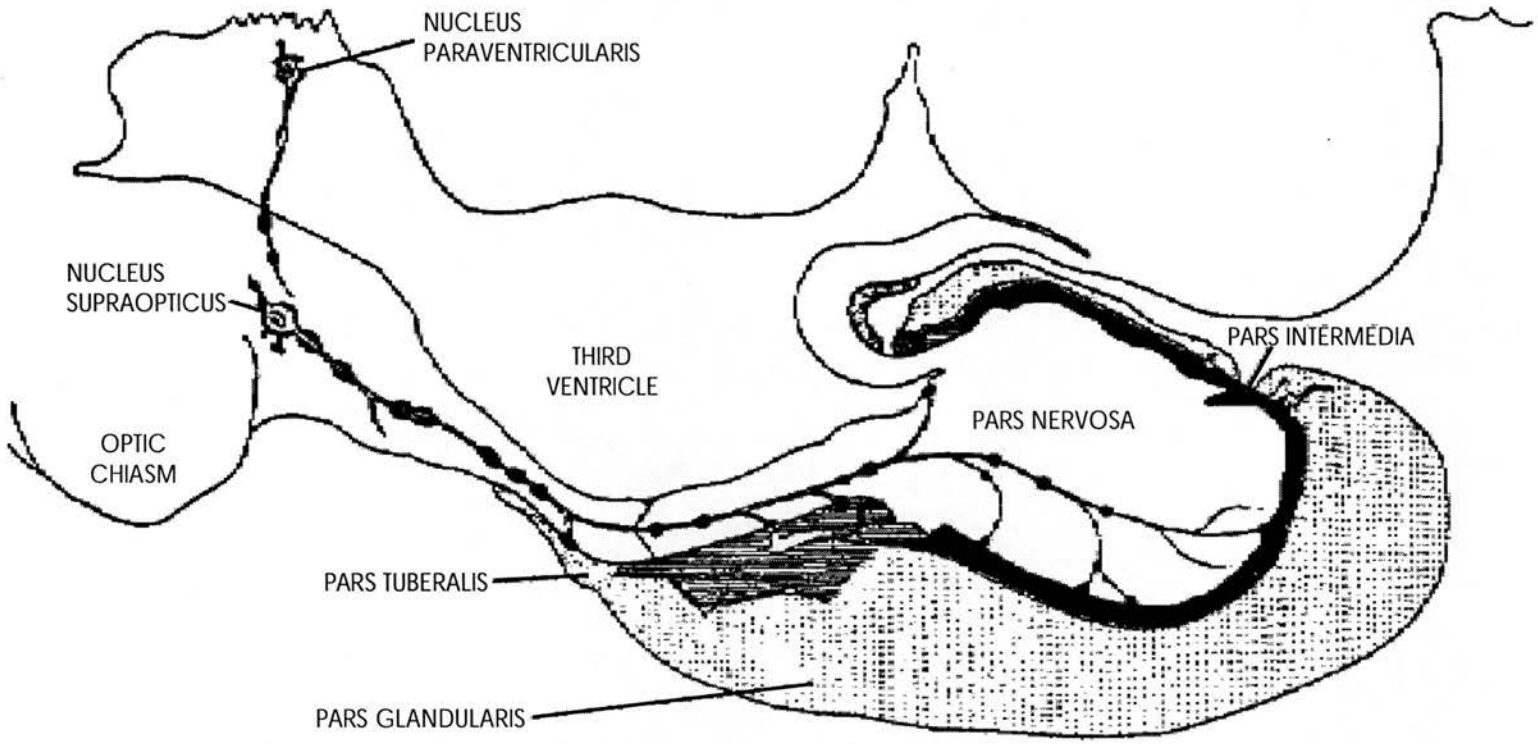

Figure 1.1 Diagram of the mammalian hypothalamic-hypophysial system.
The product of the secretory activity of nerve cells in the hypothalamus are transferred to the neurohypophysis by way of the tractus supraoptico-hypophyseus.
(Bargmann & Scharrer, 1951)

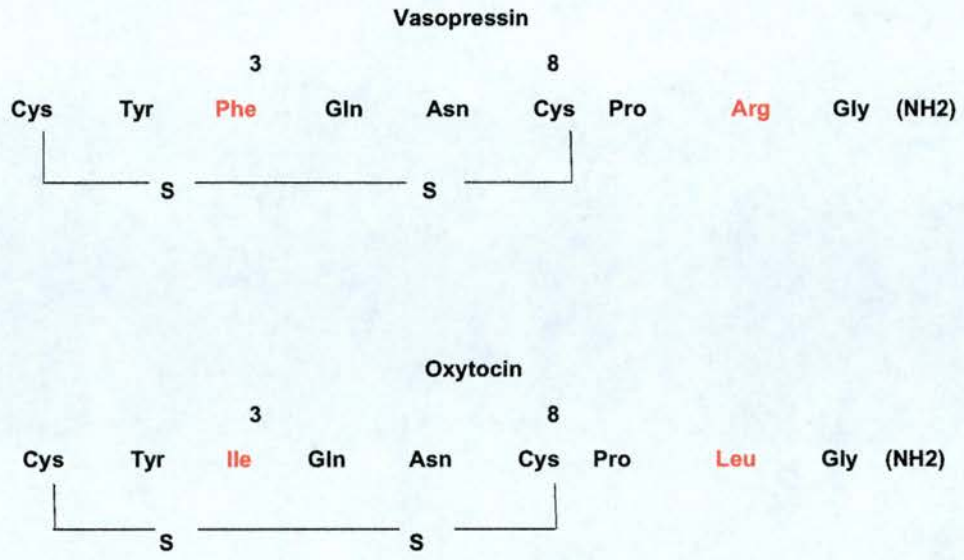

Figure 1.2 Structures of vasopressin and oxytocin.

The nonapeptides are structurally very similar, differing by only two amino acids.

Figure 1.3 Examples of patterns of activity of a vasopressin neurone (A), an oxytocin neurone (B), and a non-SON neurone (C).

Each of these cells displays a different firing pattern, which results in a different interspike interval distribution (Figure 1.4).
(A) This *in vivo* recording of a vasopressin neurone shows the typical 'phasic' pattern associated with this kind of cells, whereby periods of activity are interspersed with periods of silence.
(B) Oxytocin cells fire in general continuously at between 2 to 6 Hz, with a dramatically different firing pattern during lactation (Figure 1.4).
(C) The firing pattern of a cell recorded dorsally of the SON.

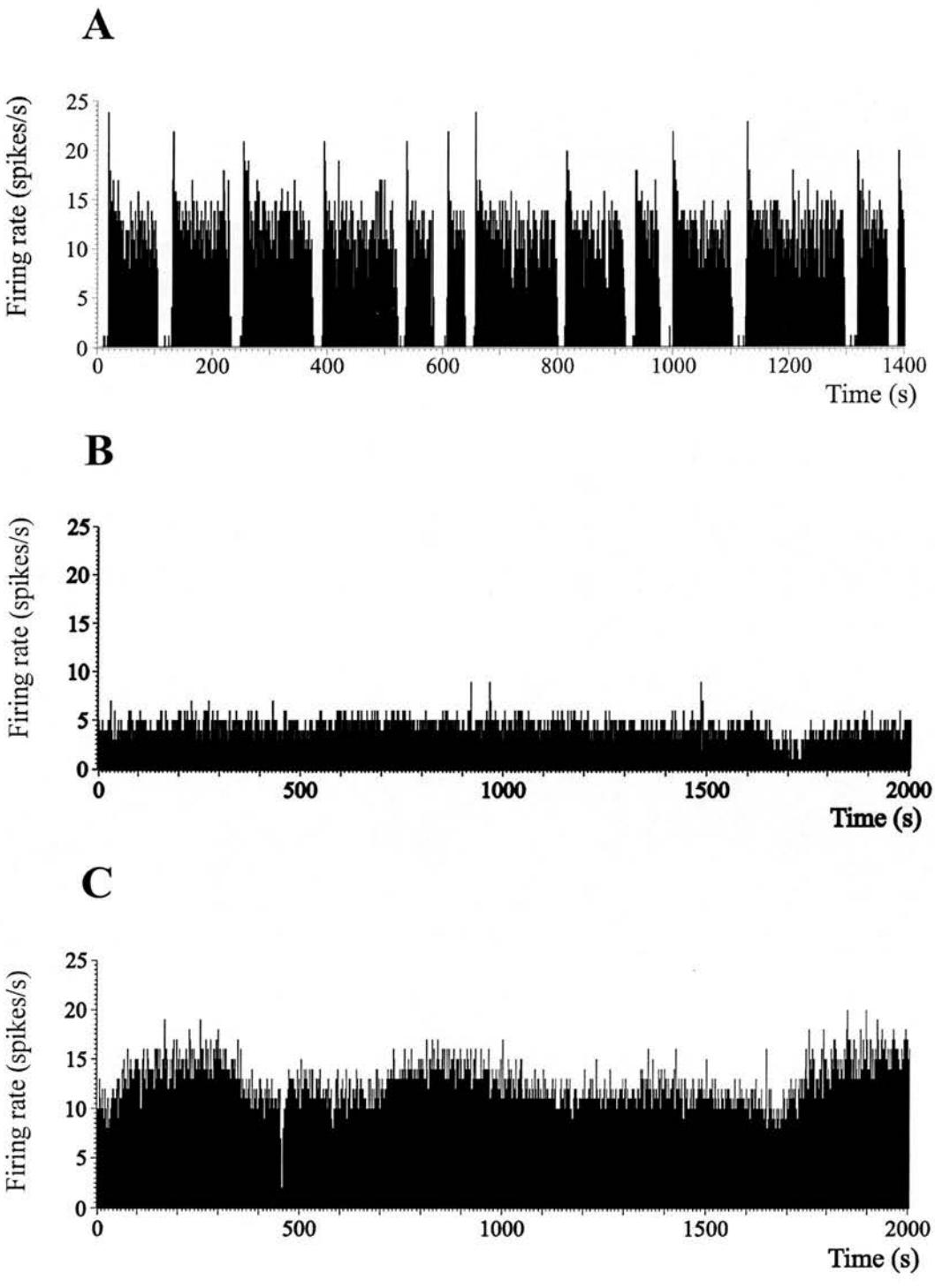
A
Firing rate (spikes/s)
0
5
10
15
20
25
0
200
400
600
800
1000
1200
1400
Time (s)
B
Firing rate (spikes/s)
0
5
10
15
20
25
0
500
1000
1500
2000
Time (s)
C
Firing rate (spikes/s)
0
5
10
15
20
25
0
500
1000
1500
2000
Time (s)

Figure 1.4 A double recording of two vasopressin cells displaying phasic 'bursts' (A), and a double recording of two oxytocin cells displaying milk-ejection bursts (B).

The vasopressin cells in this simultaneous recording show the typical phasic firing pattern, whereby 'bursts' of activity are interspersed with periods of silence (A). The bursts - which typically last 20-40 s but can last up to 80 s - consist of quite high activity on the onset which then slows down for the remainder. The cell then falls silent for 10 to 20 s. Vasopressin cells 'burst' independently of each other. In contrast, the milk-ejection bursts displayed by oxytocin cells are synchronised as seen in the simultaneous recording of these two oxytocin cells (B). While the background activity is independent between cells, the oxytocin cells across all four nuclei start the milk-ejection burst (marked with 'b') within 400 ms of each other.

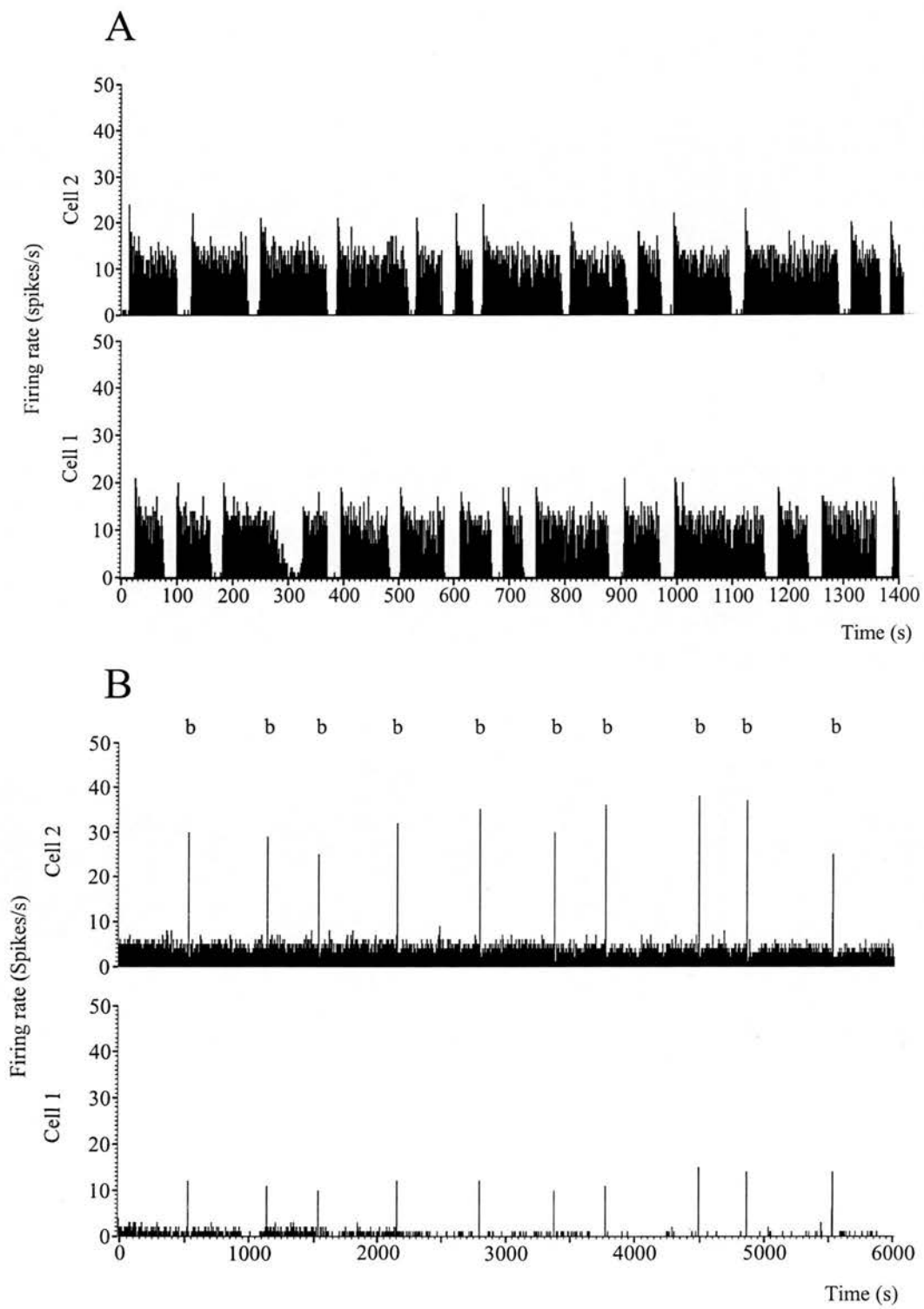
A
Firing rate (spikes/s)
Cell 2
Cell 1
0
10
20
30
40
50
0 100 200 300 400 500 600 700 800 900 1000 1100 1200 1300 1400
Time (s)
B
b b b b b b b b b b
Firing rate (Spikes/s)
Cell 2
Cell 1
0
10
20
30
40
50
0 1000 2000 3000 4000 5000 6000
Time (s)

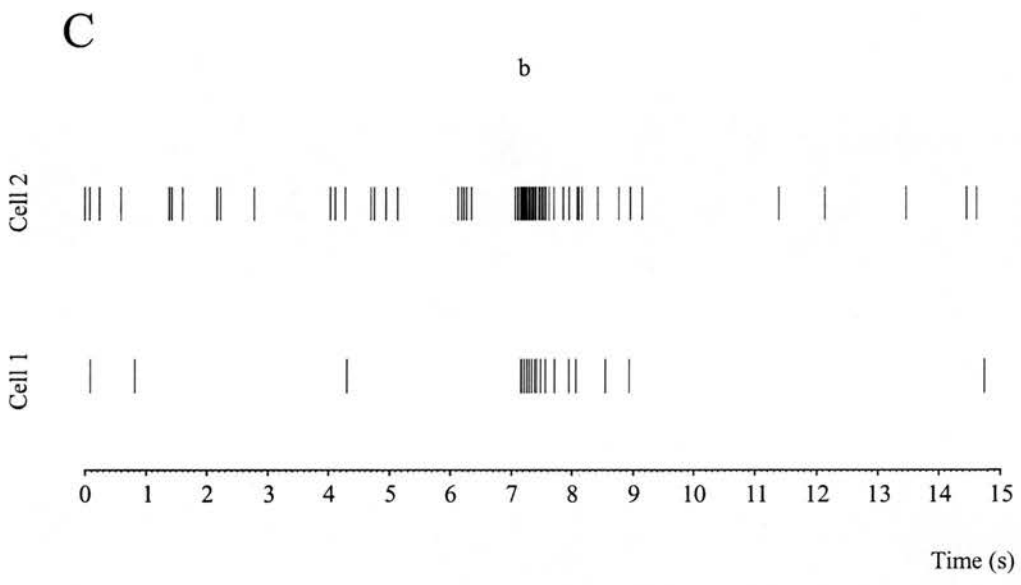

Figure 1.4C Spike by spike display of a milk-ejection burst in simultaneously recorded oxytocin cells.

Extract of the double recording shown in Figure 1.5B of a milk-ejection burst (marked by the 'b'). The burst starts synchronously in both cells (which in this case have been recorded from different nuclei), and the firing rate is very fast for the first spikes, slowing down for the remainder. The burst lasts around 2 s and is followed by a period of no activity before firing resumes again. Note that the spikes themselves are not in synchrony, it is only the start of the milk-ejection burst which is.

Figure 1.5 Action potential and post-spike membrane afterpotentials.

Magnocellular neurosecretory cells have a resting membrane potential between -55 mV and -70 mV. When the cell is sufficiently depolarised to reach the threshold an action potential is generated. Following each action potential the hyperpolarising afterpotential (HAP) - short lasting but strong - prevents further action potentials being triggered by a drastic reduction in excitability, and thus sets a firm upper limit on the firing rate.
The weaker but longer lasting afterpolarisation (AHP) follows a train of action potentials, its amplitude proportional to the number of spikes evoking it. Thus, the AHP 'smoothes' the firing activity, aiding in maintaining a steady long-term output in oxytocin neurones..
The depolarising afterpotential (DAP) overlaps in its time course with the AHP, and has been found to be of particular importance for vasopressin neurones, where it has been implicated in contributing to the phasic pattern which is important for the efficient release of its hormone.

(diagrammatic representation after C.H. Brown, personal communication)

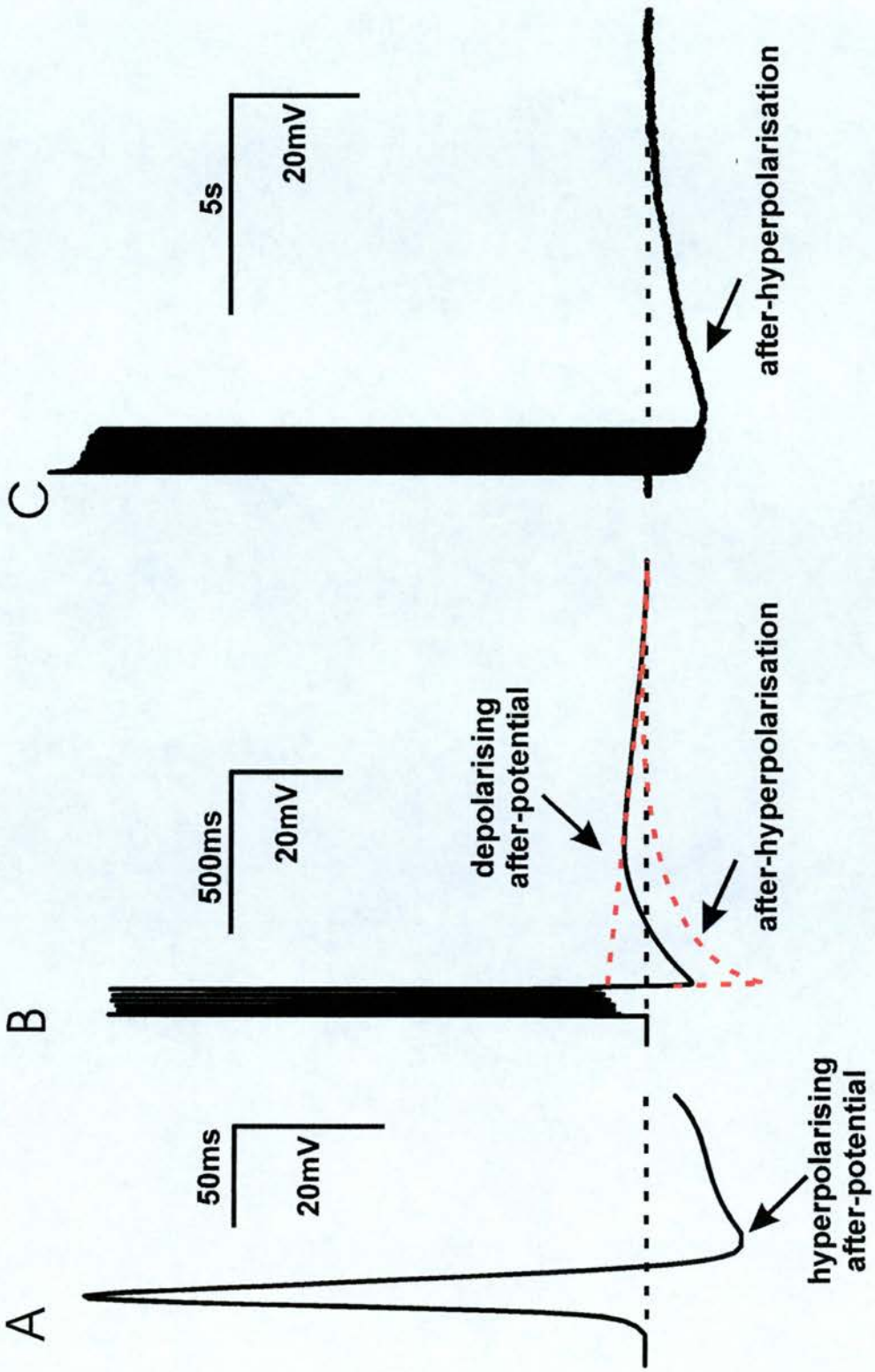
A
50ms
20mV
hyperpolarising
after-potential
B
500ms
20mV
depolarising
after-potential
after-hyperpolarisation
C
5s
20mV
after-hyperpolarisation

CHAPTER TWO

DATA COLLECTION: METHODS AND DATA SAMPLE DESCRIPTIONS

All the analyses described in the following chapters of this thesis are based on the spontaneous electrical activity of oxytocin neurones, recorded extracellularly from rats *in vivo*. The data pool for the different analyses is the same, so rather than describing the methods and basic descriptive statistics repeatedly, the intention of this chapter is to describe the methods used to gather the data. Afterwards the data is summarised and descriptive statistics for it presented. This chapter is intended as an introduction of the main characteristics of importance for our analyses and as a reference point for later chapters.

2.1 Single Cell Recordings

Female Sprague-Dawley rats (200-250 g) were mated in house and kept in single cages until the experiment. Between the fifth and the eleventh day of lactation the rats were separated from their pups in the late afternoon. The following morning the rat was anaesthetised by a 1.25 mg/ kg dose of 25% urethane solution given intraperitonealy. If necessary, further injections of small doses of urethane were given after a minimum of 30 min. In addition, local anaesthetic (xylocaine) was applied to all surgical sites. A jugular vein was cannulated for the intravenous delivery of quantifiable doses of oxytocin. For a number of experiments one thoracic mammary gland was cannulated to record intramammary pressure as an index of oxytocin release. If the mammary cannulation failed, or in the cases were no cannulation was made, the stretch response of the pups – a characteristic, stereotyped behavioural reaction involving the extension of limbs – was used for this purpose.

The rat was then placed in the stereotaxic frame. A cannula was inserted into the left third ventricle for intracerebroventricular drug injections. The position was determined as 1.6 mm lateral of the central suture, 0.6 mm posterior of bregma and 8 mm deep measured from the brain surface, and confirmed by sucking up some

cerebrospinal fluid. A syringe containing oxytocin (Sandoz; at a dose of 1 ng) was connected to the cannula ready for administration. The contralateral side of the brain was exposed, leaving the central suture intact. A bipolar stainless steel electrode was inserted into the neurohypophysis and its exact position was attested by the abrupt increase in intramammary pressure following repetitive electrical stimulations (40 Hz, 15 V, 1 ms pulses for 4 s).

A glass micro-electrode was prepared and filled with 0.9% NaCl solution. It was lowered into the supraoptic nucleus. The extracellular electrical activity of oxytocin cell was recorded using Spike2 laboratory software (Cambridge Electronic Design Ltd). The oxytocin cells were identified by means of their antidromic response to electrical stimulation of the neurohypophysis (1 ms single pulses of 15 V every 4 s) and distinguished from vasopressin cells by their firing patterns, i.e. continuous rather than phasic. After a control period of 15 minutes the pups were allowed to suckle. If after one hour of suckling no bursting activity was observed 0.2 ml of i.c.v. oxytocin (at a dose of 1 ng) was administered. If this proved to be unsuccessful in inducing the milk-ejection reflex, a further dose of i.c.v. oxytocin was given. If this too was unsuccessful the experiment was abandoned and the rat killed with a urethane overdose.

For hyperosmotic stimulation experiments the jugular vein was cannulated under urethane anaesthesia, the rat was placed in the stereotaxic frame and the brain was exposed and prepared for electrophysiology according to the same protocol as used above. Once the recording electrode was lowered into the SON, an oxytocin neurone was identified by its response to antidromic activation of the axons in the neurohypophysis and by its firing pattern, i.e. continuous rather than phasic. After a control period (~30 min) of spontaneous, i.e. non-manipulated background activity was recorded, a continuous 2M NaCl i.v. infusion was given at a rate of 1.56 ml/ h, for the remainder of the recording. The extracellular electrical activity of the oxytocin neurone was recorded for as long as possible during the infusion.

2.2 Paired Cell Recordings

Lactating Wistar rats were taken between the seventh and eleventh day postpartum and separated from all but one pup no more than 15 h before the beginning of the experiment. On the morning of the experiment the rat was anaesthetised with a single i.p. injection of a 1.2 mg/kg dose of 25% urethane solution. The pups were allowed to suckle for 15 min. If more anaesthetic was required chloroform was used while the jugular vein was cannulated, in preparation for i.v. drug administration. Thereafter, if the need for deeper levels of surgical anaesthesia arose 0.01 ml doses of pentobarbital were given i.v. Local anaesthetic (xylocaine) was applied to all surgical sites.

The rat was placed in the stereotaxic frame, and the brain was exposed. A microsyringe was inserted into the third ventricle for i.c.v. oxytocin (Sandoz, 1 μl of a 10-6 M solution in isotonic saline) administration, used to facilitate milk-ejection bursts. The correct position was attested by sucking up some cerebrospinal fluid. A bipolar stainless steel electrode slanted from back to front was lowered into the neurohypophysis. A few pups were allowed to suckle, and the exact position of the stimulating electrode was determined using the stretch response following repetitive electrical stimulation (40 Hz, 15 V, 1 ms for 4 s) as an indicator of increased intramammary pressure. The pups were removed once more.

Two recording electrodes were prepared and filled with 0.5 M sodium acetate solution. One microelectrode was lowered into the supraoptic nucleus on each side to record the extracellular electrical activity of two oxytocin neurones. Oxytocin neurones were identified by their antidromic response to electrical stimulation of the neurohypophysis and were distinguished from vasopressin neurones by their firing pattern: continuous firing and – in response to suckling – short high-frequency bursts of spikes followed by electric quiescence. The activity was recorded using Spike2.

After recording a control period of 15 min at least 8 pups were allowed to suckle. If after one hour of suckling no milk-ejection burst was seen, a 40 Hz 15 V current was injected into the neurohypophysis for 4 s to simulate a milk-ejection

burst and induce the system to start an bursting pattern. If this failed to induce the milk-ejection bursts within 20 min, a 0.2 ml i.c.v. injection of oxytocin was given. If this failed another high frequency stimulation was attempted, and again a further dose of oxytocin was given. After this the experiment was terminated and the rat was killed with a urethane overdose.

2.3 Data Samples

The sample of recordings gained with the above described procedures were supplemented by further recordings from virgin and pregnant rats kindly given by other researchers (M. Ludwig, P. Bull, C. Brown, S. Scullion), recorded using essentially similar experimental protocols. From this pool of data stretches of recording were chosen for analysis according to criteria presented next.

2.3.1 Stationarity

A time series is *stationary* if there are no systematic trends or "rhythmic" variations (cf. Brown & Rothery, 1993). More formally, a time-series is stationary if the mean and the variance of the series are constant over time, and the autocorrelation function (ACF) depends on the length of the lag but on no other variable.

Stationarity of the activity is an essential requirement for further analysis, as even short periods displaying a trend in the activity – whether random or real – can mask the long term but weak effects that we are interested in. To establish that the activity conforms to the assumption of no systematic trends or rhythmic variations we have different possibilities:

"The first and easiest test is to visually examine the data. For many time series, a quick glance at the data (or diagram of the data) will tell you that the mean of a variable is increasing dramatically over time and that the series is non-stationary.

A second, more careful, test is to see if the ACFs for a variable tend to zero as k (the length of the lag) increases [...] to see if the AHF is significantly different from 0. If the ACFs tend to zero fairly quickly, the variable is stationary, but if they don't, the variable if non-stationary." *(Studenmund, 2001, page 426)*

In order to aid visual examination, i.e. to see any trends more clearly and to emphasise trends, a smoothing technique was used. The activity of each cell was plotted as the average firing rate over time (Figure 2.1), and *bicubic splines* (a series of smooth cubic curves fitted over short stretches of activity, then joined with the same slope at the joints to form one continuous curve) were fitted to the averaged firing rate. In addition, the overall mean of the activity was plotted, thus the overall and the acute mean of the activity can be compared easily, and divergence between the two detected reliably. This technique has the advantage, compared to fitting with a single curve, that it is more sensitive and more precise on a short time scale, and the curve does not need to be updated when new observations are added. In the first instance, data is regarded as stationary if the bicubic splines fluctuate around the overall mean at most for short stretches during the recording (further examination of stationarity – whether the ACFs for a variable tend to zero as the length of the lag increases – is described in chapter 3, section 3.4). If this is not the case for the whole recording, then only a single continuous stretch of stationary activity was extracted for analysis, discarding the remainder of the recording. For the analysis of activity recorded in osmotically stimulated cells two stationary stretches were chosen, one before the stimulation and another once the cell has settled on the higher plateau of activity, again establishing stationarity. If no stationary periods of sufficient length for the analysis could be extracted the whole recording was excluded.

After testing for stationarity, rejecting some recordings because of noise or other difficulties, and choosing stretches appropriate for analysis from recordings of neurones that received osmotic stimulation – both control period and period after stimulation –, a total of 75 stretches remain for analysis. This figure include stretches used only for the analyses presented in Chapter 4. Of these stretches, 13 are from naïve animals, 13 from pregnant animals, 23 from lactating (of which 9 were suckled but non milk-ejecting) animals, 8 from animals displaying milk-ejection bursts, and 8 before and 10 after hyperosmotic stimulation. The discrepancy in the last numbers is due to two neurones firing too slowly before the stimulation, so that not enough

material is available for analysis. The firing of the neurones from milk-ejecting animals is of course inherently non-stationary and thus is unsuitable and disregarded for some of the analyses, such as those described in Chapter 3.

Please note that for the sake of simplicity and readability, throughout the remainder of this thesis we will refer to the stretches of recordings from naïve animals as "naïve neurones" or collectively as "naïve group", stretches of recordings from pregnant animals as "pregnant neurones" or collectively as "pregnant group", stretches of recordings from animals before excitatory stimulation as "before neurones" or collectively as "before group", stretches of recordings from animals after excitatory stimulation as "after neurones" or collectively as "after group", and stretches of recordings from suckled or non-suckled animals as "suckled" and "non-suckled neurones", unless otherwise stated. Please also note that when speaking about lactating or suckled neurones, these neurones did not display milk-ejection burst. In this context, "non-lactating group" refers to all naïve, pregnant and stimulated neurones, while "lactating group" refers to both suckled (but not milk-ejecting) and non-suckled neurones. Stretches of recordings from neurones displaying milk-ejection bursts will be referred to as "milk-ejecting" or "burst" neurones, and "milk-ejecting" or "burst" group.

2.3.2 Descriptive Statistics for Samples

Having identified stationary stretches of recordings suitable for analysis, we will now describe their most important firing characteristics. Since the analyses based on these recordings are performed on interspike intervals (ISIs) the summary statistics is also given for the ISIs derived from this data pool.

The naïve group (n=13) has a mean firing rate of 7.06±1.03 Hz (mean±sem). The number of ISIs derived from each recording was 2496±481. The lengths of the ISIs varied from the shortest at 16±2 ms to the longest at 1.18±0.27 s, with a mean length of 190±36 ms and a median of 145±26 ms (Table 2.1).

The pregnant group consists of 13 recordings, with an average of 2042±209 ISIs. The mean firing rate for this group is 6.06±0.41 Hz. The average of the shortest

ISI is 20±2 ms, the longest is 1.2±0.13 s, with a mean length of 176±13ms and a median of 115±6 ms (Table 2.2).

The lactating-suckled group consists of 9 recordings. On averaged, the shortest and longest ISIs are 21±4 ms and 3.74±0.85 s, respectively. The mean length of the ISIs is 563±70 ms, and the median 416±42 ms. The average mean firing rate is 2.07±0.34 Hz (Table 2.3).

Recordings in the non-suckled group (n=14) have an average mean firing rate of 2.7±0.59 Hz. On average, the length of the shortest ISI is 27±3 ms, and the longest ISI is 6.14±1.99 s. The mean ISI length is 827±279 ms, and the median 553±172 ms (Table 2.3).

As the two lactating groups – lactating-suckled and lactating-unsuckled – are rather similar in their firing characteristics they are in some instances combined to form one group and analysed together. This 'lactating' group, therefore, consists of 23 recordings, with an average of 1586±330 ISIs and a mean firing rate of 2.45±0.38 Hz. The averages for the combined group are 25±3 ms for the shortest ISI, 5.2±1.27 s for the longest ISI, a mean length of 724±172 ms and a median of 499±105 ms (Table 2.3).

The hyperosmotic stimulation groups are stretches taken from the same recordings: 'before' is the control period, 'after' is a period following the infusion of 2 M NaCl. The before group consists of 8 stretches, rather than the 10 stretches included in the after group as two of the neurones were firing at very low frequencies, thus not containing enough ISIs for a valid analysis. In this context, the before stretches contain fewer ISIs than the after stretches, 672±125 vs. 2807±449. Also, the mean firing rate – as intended – was much higher after the infusion, 7.61±1.14 Hz vs. 2.36±1.14 Hz before the hyperosmotic stimulation. Consequently, the averaged shortest ISI, longest ISI, mean and median ISI length for the before group are all longer than for the after group: 21±5 ms vs. 14±1 ms, 5.36±1.9 s vs. 1.03±.19 s, 686±191 ms vs. 156±21 ms, and 442±127 ms vs. 107±13 ms, respectively (Table 2.4).

The recordings taken from neurones displaying milk-ejection bursts – forming the burst group – are made up by two essentially separate firing "modes": the background activity and bursts. The characteristics of these two modes are determined separately. The background activity contains 13448±2773 ISIs, where the shortest is 9±1 ms and the longest 54.78 s (this is due to one extremely long interval in one recording; if this is excluded the group average is 6.97±1.34 s). The mean length is 690±289 ms and the median is 340±70 ms. The mean firing rate for the background activity is 2.47±0.52 Hz (Table 2.5). The recordings analysed displayed 4 to 16 bursts, with an average of 9. The samples made up of bursts contain 384±100 ISIs, and the firing frequency for the whole burst sample is 13.85±1.2 Hz. The shortest ISI is 10±1 ms, and the longest 850±90 ms. The mean ISI length is 80±10 ms, and the median 40±4 ms (Table 2.5).

The mean firing rates seem to divide the groups into two clusters: the lower frequency one formed by suckled, lactating and before, and a higher frequency one consisting of pregnant, naïve and after. One way analysis of variance between the mean firing rates shows that there are significant differences between the different groups. Post-hoc Dunn's pairwise tests confirms that there are no significant differences between 'lactating', 'suckled' and 'before' groups, nor between 'naïve', 'pregnant' and 'after' groups, but significant differences between these two clusters ($p<0.05$ taken as significant).

In general, the firing rates seen in all neurones conform to those reported previously (Lincoln & Wakerley, 1974). Brown and Moos (1997) reported that cells displaying milk-ejection bursts were most likely to have a firing rate in the range of 1 to 3 Hz 30 minutes after suckling began, whereas non-bursting cells had a more varied firing rate. The recordings in the lactating group conform to this pattern. Although the mean firing rates for both suckled and non-suckled fall comfortably in this range, all but one recording in the suckled group individually falls into this range, but most (10/ 14) of the recordings in the non-suckled group do not. It should, however, be emphasised that the Brown and Moos base their study on firing rates 30

minutes after the beginning of suckling, while our firing rates are for the whole stretch of recording analysed.

Surprisingly, the firing rate after hyperosmotic stimulation is not significantly different to the naïve group. This is possibly due to choosing particularly slowly firing neurones for this kind of experiment. The lower than usual firing rate for the before group supports this explanation.

In general, the faster the mean firing rate the shorter the ISIs. While the shortest ISI possible is determined by the refractory period and hence should be relatively independent of the mean firing rate, the maximum length of an ISI will be restricted by a fast firing frequency. Consequently, the mean and median ISI length should be shorter for a fast firing neurone, too.

Therefore, the picture that emerges from the examination of the mean ISI length and is confirmed by the one way analysis of variance is the same as for the mean firing rate: no significant differences between naïve, pregnant and after, and also between suckled, lactating and before, but significant differences between these two clusters.

2.4 Summary

This chapter introduced the methods used to gather the data needed for the analyses described in the following chapters. Electrical activity of identified oxytocin neurones was recorded extracellularily in urethane anaesthetised rats. The rats were either naïve, pregnant (day 21), or lactating (days seven to eleven of lactation). An osmotic stimulation was performed in several cases. Also, some of the lactating animals were suckled, and part of these displayed the milk-ejection reflex. 75 stretches of recordings suitable for analysis were thus obtained and categorised into 8 groups: naïve (n=13), pregnant (n=13), lactating-unsuckled (n=9), lactating-suckled (but not displaying milk-ejection bursts; n=14), burst (milk-ejection bursts; n=8), before (n=8) and after (n=10) hyperosmotic stimulation.

Since the main analyses of the firing patterns described throughout this theses are based on interspike intervals (ISIs) their main characteristics were presented in the form of descriptive statistics.

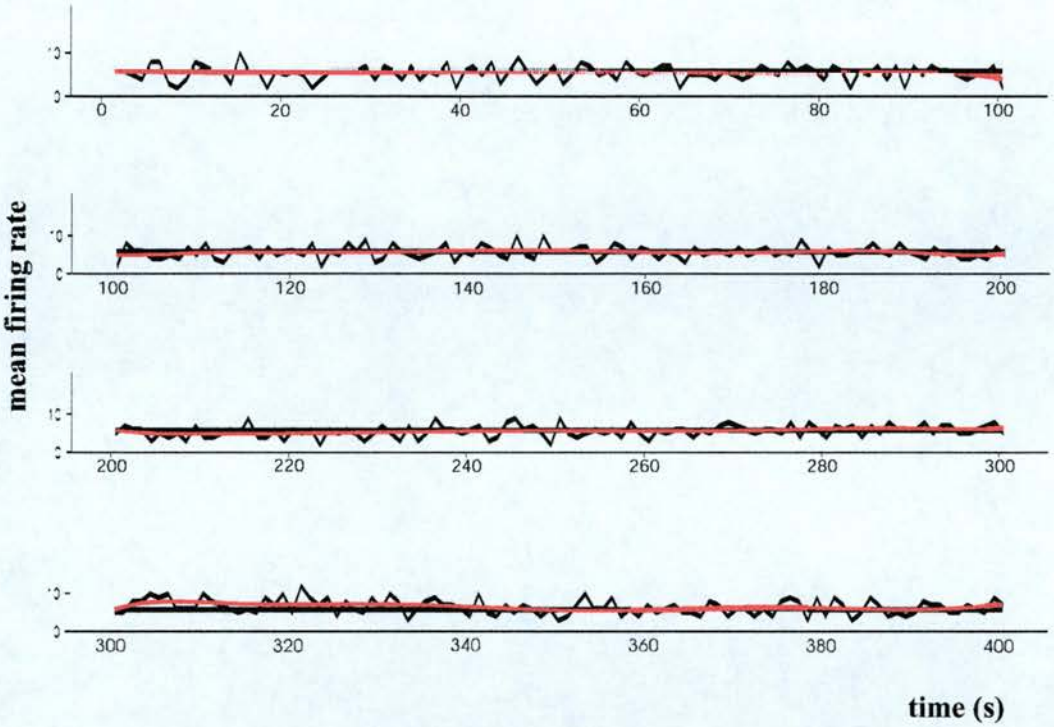

Figure 2.1 Example of stationarity test: Firing rate, overall mean and bicubic splines (red) for one stretch of a recording.

To analyse the spike activity statistically, it is essential first to establish that the data are "stationary" - in other words, that there is no progressive change in behaviour with time. To check this, the activity of each cell was plotted as the firing rate over time, and bicubic splines (cubic curves) were fitted to successive short stretches of activity (red), joined smoothly to form one continuous curve. Stationarity was inferred if the bicubic splines remained close to the overall mean (black) throughout the recording.

Cell	Number of ISIs in recording	Length of shortest ISI in s	Length of longest ISI in s	Mean length of ISI in s	Median length of ISI in s	Mean firing rate in spikes/ s
n1	1663	0.014	1.178	0.180	0.139	5.55
n2	1431	0.025	0.990	0.209	0.176	4.77
n3	1795	0.025	0.860	0.211	0.172	4.73
n4	858	0.020	4.032	0.579	0.424	1.7
n5	1374	0.011	1.346	0.218	0.164	4.58
n6	1347	0.011	1.692	0.222	0.165	4.49
n7	7077	0.025	0.304	0.108	0.103	9.37
n8	2694	0.011	0.856	0.111	0.068	8.99
n9	2199	0.010	0.727	0.136	0.101	7.34
n10	3177	0.015	0.586	0.094	0.078	10.59
n11	2950	0.018	0.850	0.102	0.068	9.83
n12	4713	0.015	0.273	0.064	0.054	15.7
n13	1174	0.014	1.626	0.238	0.172	4.19
mean	2496	0.016	1.178	0.190	0.145	7.06
sem	481	0.002	0.267	0.036	0.026	1.03

Table 2.1 Summary information about ISI lengths, ISI amounts and mean firing rates by recording from naive neurones, as well as mean and standard error of means for the whole group.

Cell	Number of ISIs in recording	Length of shortest ISI in s	Length of longest ISI in s	Mean length of ISI in s	Median length of ISI in s	Mean firing rate in spikes/ s
p1	2931	0.020	0.678	0.135	0.105	7.41
p2	2446	0.021	0.725	0.131	0.091	7.66
p3	1340	0.018	1.205	0.171	0.099	5.85
p4	2387	0.016	1.142	0.188	0.117	5.30
p5	3502	0.014	1.540	0.228	0.138	4.38
p6	2403	0.011	1.574	0.226	0.153	4.43
p7	1975	0.013	1.338	0.207	0.139	4.83
p8	2248	0.028	0.501	0.147	0.135	6.81
p9	1315	0.019	0.845	0.127	0.084	7.88
p10	933	0.034	2.207	0.283	0.140	3.51
p11	1101	0.033	1.476	0.172	0.109	5.82
p12	2367	0.017	1.228	0.146	0.098	6.85
p13	1598	0.014	1.154	0.125	0.090	7.99
mean	2042	0.020	1.201	0.176	0.115	6.06
sem	209	0.002	0.126	0.013	0.006	0.41

Table 2.2 Summary information about ISI lengths, ISI amounts and mean firing rates by recording from pregnant neurones, as well as mean and standard error of means for the whole group.

Cell	Number of ISIs in recording	Length of shortest ISI in s	Length of longest ISI in s	Mean length of ISI in s	Median length of ISI in s	Mean firing rate in spikes/ s
s1	5052	0.011	1.997	0.600	0.466	1.40
s2	585	0.021	3.108	0.649	0.560	1.54
s3	1094	0.013	3.526	0.676	0.482	1.48
s4	1965	0.020	1.138	0.255	0.221	3.93
s5	1397	0.014	1.273	0.304	0.258	3.29
s6	1385	0.011	1.787	0.342	0.291	2.91
s7	671	0.022	6.037	0.803	0.539	1.24
s8	1205	0.029	6.849	0.797	0.500	1.25
s9	1558	0.050	7.898	0.642	0.425	1.56
mean	1657	0.021	3.735	0.563	0.416	2.07
sem	447	0.004	0.853	0.070	0.042	0.34
l1	1836	0.028	4.620	0.533	0.353	1.87
l2	240	0.041	2.247	0.735	0.591	0.79
l3	703	0.026	5.720	0.792	0.536	1.26
l4	93	0.045	25.939	4.179	2.587	0.24
l5	1200	0.028	15.599	0.677	0.380	1.47
l6	6264	0.012	0.744	0.144	0.108	6.86
l7	1395	0.030	2.875	0.308	0.215	3.24
l8	1838	0.018	1.394	0.246	0.187	4.05
l9	1269	0.022	1.286	0.227	0.169	4.41
l10	4478	0.019	0.835	0.160	0.122	6.24
l11	1358	0.018	1.022	0.206	0.166	4.84
l12	494	0.009	6.431	0.931	0.680	1.07
l13	83	0.057	2.600	0.869	0.599	0.80
l14	315	0.026	14.695	1.568	1.045	0.64
mean	1540	0.027	6.143	0.827	0.553	2.70
sem	472	0.003	1.996	0.279	0.172	0.59
summary for lactating-unsuckled and lactating-suckled group together						
mean	1586	0.025	5.201	0.724	0.499	2.45
sem	330	0.003	1.265	0.172	0.105	0.38

Table 2.3 Summary information about ISI lengths, ISI amounts and mean firing rates by recording from lactating-suckled (s1 to s9) and lactating-unsuckled (l1 to l14) neurones. Mean and standard error of means are stated for each group, and also for the two groups combined.

Cell	Number of ISIs in recording	Length of shortest ISI in s	Length of longest ISI in s	Mean length of ISI in s	Median length of ISI in s	Mean firing rate in spikes/ s
l13	83	0.057	2.600	0.869	0.599	0.80
l14	315	0.026	14.695	1.568	1.045	0.64
b1	657	0.012	2.557	0.288	0.088	3.50
b2	640	0.011	1.701	0.470	0.418	2.13
b3	1185	0.012	0.952	0.194	0.136	5.17
b4	669	0.024	14.073	1.422	0.856	0.70
b5	820	0.018	2.297	0.349	0.215	2.85
b6	1004	0.012	3.991	0.330	0.182	3.07
mean	672	0.021	5.358	0.686	0.442	2.36
sem	125	0.005	1.994	0.191	0.127	0.57
a1	2658	0.021	2.223	0.300	0.193	3.32
a2	3557	0.011	1.200	0.179	0.124	5.67
a3	2053	0.012	1.493	0.169	0.067	5.90
a4	3249	0.015	0.718	0.115	0.088	8.71
a5	6272	0.017	0.295	0.067	0.057	15.02
a6	1249	0.021	0.836	0.159	0.128	6.28
a7	1800	0.016	1.116	0.165	0.108	6.09
a8	3000	0.009	0.198	0.070	0.058	12.68
a9	2517	0.007	0.967	0.138	0.102	7.26
a10	1710	0.014	1.273	0.195	0.143	5.12
mean	2807	0.014	1.032	0.156	0.107	7.61
sem	449	0.001	0.186	0.021	0.013	1.14

Table 2.4 Summary information about ISI lengths, ISI amounts and mean firing rates by recording from neurones before (l13 to b6) and after (a1 to a10) hyperosmotic stimulation. Mean and standard error of means are stated for each group.

Cell	Number of ISIs in recording	Length of shortest ISI in s	Length of longest ISI in s	Mean length of ISI in s	Median length of ISI in s	Mean firing rate in spikes/ s	Number of bursts in recording
me1	4115	0.009	389.47	2.62	0.80	0.17	14
me2	19186	0.008	9.29	0.45	0.29	2.17	16
me3	5829	0.008	7.26	0.73	0.48	1.36	9
me4	17175	0.010	6.48	0.41	0.29	2.14	9
me5	10412	0.007	2.29	0.26	0.19	3.80	6
me6	26753	0.006	2.34	0.21	0.16	4.70	6
me7	16977	0.005	9.82	0.28	0.20	3.56	10
me8	7139	0.018	11.28	0.55	0.33	1.83	4
mean	13448	0.009	54.78	0.69	0.34	2.47	9
sem	2773	0.001	47.83	0.28	0.07	0.52	

me1	252	0.012	1.28	0.11	0.06	8.75
me2	866	0.008	0.88	0.06	0.03	17.51
me3	475	0.012	0.77	0.07	0.04	15.13
me4	234	0.012	0.99	0.09	0.05	11.31
me5	132	0.005	0.69	0.09	0.05	10.82
me6	227	0.009	0.88	0.08	0.04	12.85
me7	747	0.010	0.91	0.06	0.03	17.17
me8	142	0.011	0.43	0.06	0.04	17.23
mean	384	0.010	0.85	0.08	0.04	13.85
sem	100	0.001	0.09	0.01	0.004	1.20

Table 2.5 Summary of main ISI characteristics and mean firing rate by recording for the background activity and for only the bursts for 8 neurones displaying milk-ejection bursts.

CHAPTER THREE

FIRING RATE ANALYSES

The milk-ejection reflex is a dramatic, and apparently highly exceptional, event. An oxytocin cell firing typically at just a few spikes/ s will suddenly discharge up to over 100 spikes in 2-3 s, followed by a longer period of relative quiescence. This behaviour is thought to arise from mechanisms that involve feedback from the oxytocin neurones themselves – i.e. activity-dependent mechanisms. If this is so then we might expect to find some signs of the same mechanisms operating at all times – not only during the actual bursts.

In this section, we look at the *structure* of "spontaneous" spike activity in oxytocin neurones. In particular, we ask what activity-dependent influences upon that activity can be inferred from rigorous statistical analyses, and whether consistent differences in spike patterning (in "spontaneous" or "background" activity) characterise different physiological states.

We are interested here particularly in finding the "footprints" of intrinsic mechanisms – in other words, mechanisms that are invariably present, even when there is no overt bursting behaviour. Can we find, in the details of ordinary, apparently unexceptional background activity, subtle signs that mark the presence of intrinsic mechanisms that may underlie the genesis of complex behaviour such as the milk ejection burst? Thus, after identifying stationary recordings (cf. Chapter 2) and selecting sections of spontaneous firing activity we now analyse these for evidence of activity-dependence of the spike pattern.

3.1 Random Processes

We should start by clarifying exactly what features should be expected of random data. If spikes were generated wholly independently of the previous incidence of spikes (by a process analogous to radioactive decay, for instance), then

the statistical features of spike trains would conform to certain well-established laws, and are referred to as "Poisson" processes. Of course spikes are never wholly independent of past activity for *any* neurone – most obviously, in any neurone every spike is followed by an absolute refractory period within which another spike cannot be initiated. We know also that oxytocin neurones possess a prominent post-spike hyperpolarising afterpotential (HAP) that – at least in virgin rats – imposes a long relative refractory period after spikes. Hence, we do not expect the statistics of spike trains to fully adhere to the statistics of Poisson processes. Nevertheless it is worth stating here what is expected of a random process, in order to judge how far and in what way the statistics of spike trains deviate from randomness:

1) *Inter-event distributions.* For a Poisson process, the probability of an event occurring at any particular time is independent of the time of the preceding event. This condition means that the inter-event histogram can be described by a single negative exponential.

2) *Invariant statistical characteristics.* Data that arise as a random process should show invariant statistical characteristics when these data are shuffled randomly.

3) *Index of dispersion.* For a Poison process, the *variance* of the event frequency (σ^2) has a fixed relationship to the *mean* of the event frequency (μ) – in fact $\sigma^2 = \mu$. The "index of dispersion", μ/σ^2, should therefore equal 1 for a random process, should be independent of μ in a sample of data where μ varies, and should be independent of *bin-width* (a chosen range over which the calculations are performed).

We analyse *in vivo* recordings from oxytocin neurones to see exactly how they deviated from randomness as discernible from each of these three criteria.

3.2 Interspike Interval Analysis

3.2.1 Introduction

An *interspike interval* (ISI) is the time between two consecutive spikes. ISIs provide information about the relationship between individual, successive spikes in a way most easily accessible for statistical scrutiny. They also have the added advantage that they are independent of temporal context, which is important for later analyses. The *interspike interval histogram* (ISIH) is a graphical representation of the characteristics of the distribution of the occurrences of ISIs of a certain length. The number of occurrences of ISIs for a given range of lengths is plotted against this range, or "bin". This is a common method to obtain first indications about spike patterning in an individual neurone.

3.2.2 Comparison of ISIH of Oxytocin and Vasopressin Neurones

The ISIH has a characteristic shape for each cell type that reflects interpretable differences in intrinsic membrane properties or the properties of the network of which the neurone is a part. The firing patterns and ISIH derived from different cell types are shown in Figures 3.1 and 3.2 (A-C). The ISIH for both oxytocin and vasopressin neurones is skewed with a single mode (the most frequently occurring value in a set of observations) that is generally between 30 and 80 ms (in the neurones analysed in this thesis, mean mode 54.80 $\pm$ 3.67ms, n=51 out of 65 cells; no modes were available for several neurones, as for these cells there were several peak values occurring with the same frequency) and a long tail. Shorter ISIs, from zero up to the mode, are rare (for our neurones, the average ISI was 235$\pm$24ms long, and 13.74 $\pm$1.06% of all ISIs were shorter than the mode). This is consistent with the effect of a post-spike HAP, which makes the occurrence of further spikes immediately after each spike very unlikely. Electrophysiological studies of the HAP from intracellular recordings of supraoptic neurones *in vitro* estimate the duration of the HAP as being approx. 50 ms (Andrew & Dudek, 1983; Leng *et al.*, 2001).

The effects of spike activity upon neuronal excitability decay with time. Hence, if there were no underlying intrinsic rhythmicity in neuronal excitability (such as a generator potential) then at long enough times since the last spike we would expect the probability of a spike occurring to be constant. If this is true then the tail of the ISIH should take the form of an exponentially decaying curve. The question is, if we fit an exponential to the distant tail of an ISIH, and then extrapolate this back to lower ISI values, at what point does the fit to the observed ISIH cease to be good? This will be a first indication of the time scale over which significant excitability changes follow single spikes.

Rather than fit a negative exponential curve to the tail of the ISIH, it is better to plot the ISIH after log-transformation. This converts a negative exponential into a straight line, which can be fitted more robustly. We fitted straight lines to tails of log-transformed ISIHs, although in the description that follows we talk of the equivalent exponential fits.

The ISIs were log transformed and a new ISIH was calculated. Using a built-in function of our statistical package (Genstat, NAG Ltd, Oxford) we then fitted a straight line to the tail of the ISIH. The line was then extrapolated to ISIs smaller than the mode. For our sample of oxytocin neurones the line fitted the ISIH very well from the mode through to the tail, or in other words the tail of the ISIH can be easily fitted well with a single exponential. Before the mode there was a marked lack of ISIs from 0 to the mode, consistent with the effects of an HAP (Figure 3.3).

Our result is in agreement with results published by Leng *et al.* (2001) – and therefore it was deemed unnecessary to apply statistical tests for the goodness of fit other than visual inspection. This study reported that for oxytocin neurones a negative exponential fitted the tail of the ISIH very well, while for vasopressin neurones, exponentials fitted to the tail of the ISIH "undershoot" the observed ISIH. The typical phasic firing pattern of vasopressin neurones is believed to be the result of the activity-dependent expression and deactivation of a post-spike depolarising after-potential (DAP). The ISIH of vasopressin neurones is affected by the DAP, such that the proportion of ISI of a length close to the mode is increased, shown as an

excess of intervals above the curve in the range of 40-100 ms (Figure 3.4). This fits well with data from intracellular recordings of the DAP, that give an estimate of the duration of the DAP as being between ~1 s and 2 s (Andrew & Dudek, 1983; Leng *et al.*, 2001).

By contrast, for oxytocin neurones, exponentials fitted to the tail of the ISIH describe the ISIH very well for all ISI values greater than the mode, indicating that the DAP plays only a minor role in the spontaneous firing of oxytocin neurones *in vivo*, if at all (cf. section 1.1.5). The good fit of the exponential is consistent with the interpretation that the underlying activity with ISIs longer than the mode is effectively random, or rather that the processes underlying the generation of individual spikes are effectively random, and that the occurrence of a single spike does not influence the excitability of an oxytocin cell in any significant way that outlasts the HAP (Figure 3.3).

3.3 Firing Rate Analyses

From the analyses of the ISIH we might conclude that spike occurrence outside the time scale of the post-spike HAP is effectively random. We then asked whether there might be other weaker activity-dependent influences upon the excitability of oxytocin neurones that might not be apparent from the ISIH, but would require the occurrence of several spikes in a short period to become apparent. As stated above, data that arise as a random process should show invariant statistical characteristics when these data are shuffled randomly.

As a first step, in order to see whether there are any reasons for believing that there are any such weak influences on the spontaneous firing patterns of oxytocin neurones, we measured firing rates in second-by-second bins for each recording analysed, and considered the observed distribution of these second-by-second firing rates.

The firing rate (in spikes per unit time) was calculated for each recording (Figure 3.5a). The firing rate distribution was then plotted as the relative frequency of the occurrence of particular firing rates for that recording (Figure 3.6). The

distributions are bell shaped, with the peak around the mean firing rate of the cell (range 0.24 to 15.85 spikes/ s; 4.92±0.413 spikes/ s mean±sem, n=65) and a rather symmetrical spread. For several recordings (n=17) from neurones with a particularly low mean firing rate (1.3±0.15 spikes/ s), the distribution is skewed – as expected since 0 is a minimum value. The mean firing rate for the lactating group (2.45±0.38 spikes/ s; n=23, range 0.24 to 6.86 spikes/ s) is much lower than the mean for either pregnant (6.06±0.41 spikes/ s; n=13; range 3.51 to 7.99 spikes/ s) or naïve neurones (7.06±1.03 spikes/ s; n=13; range 1.7 to 15.7 spikes/ s; cf. Chapter 2). In fact, the difference in the firing rate between the lactating group and the non-lactating group is statistically highly significant ($p<0.001$, Mann-Whitney rank sum test).

We then went back to the *original* ISIs to investigate any non-random ordering. The ISIs were randomly shuffled using the built-in randomisation function of Genstat, creating a new "recording" with the *same* ISIs (Figure 3.5b for further explanation). Now we recalculated second-by-second firing rates, and plotted their new "randomised" firing rate distribution based on this 'recording' (Figure 3.6). Obviously, the ISIH is not affected, since the ISIs used are exactly the same for both the observed and the randomised histograms. We now compared the randomised distribution with the original, the observed distribution.

Out of 65 neurones 17 which show a skewed distribution due to a very slow firing rate (1.3±0.15 spikes/ s mean±sem) are disregarded for this purpose. For a further 8 neurones the results are uncertain, as the observed and the randomised distributions are too similar to allow a reliable judgement. For all but one the remaining 40 neurones –regardless of the physiological state of the animal, i.e. virgin naïve, pregnant, lactating, before or after hyperosmotic stimulation – the randomised distribution is wider and lower than the observed distribution. Only for one neurone is the randomised distribution higher and narrower than the observed distribution.

In other words, for the majority of neurones analysed, the observed distribution of firing rates is *more* uniform than would be expected if there is no serial dependence between ISIs (Figure 3.6a-f).

If randomisation would not consistently affect the shape of the distribution, then we could reasonably conclude that there are no activity-dependent influences that have a significant effect on spike patterning beyond those that influence the ISIH. If randomisation would produce distributions consistently *less* dispersed than the original distributions, we could conclude that the recordings are not in fact stationary, but subject to frequent perturbations in a manner that varied with time, or that there might be significant "rhythmic" influences. In the event, we found that the randomised distributions were consistently more dispersed than the original distributions.

This observation is consistent with the interpretation that there is weak activity-dependent negative feedback in the processes underlying the spontaneous activity of oxytocin neurones. The feedback has to be weak in the sense that it is not readily apparent in the ISIH itself, but its effects are apparent on a time scale of 1s. To paraphrase, variations in average activity of the order observed from second to second are enough to produce discernible feedback effects on spike activity. These effects mean that the average second-by-second firing rate is less variable than would be expected from the instantaneous firing rate (i.e. the variability between ISIs).

Clearly, this observation of greater variability must be dependent upon the time unit by which the firing rate is calculated. The analysis of this will provide information over the time scale in which the underlying activity-dependent influences operate, and thereby give a guide as to the likely underlying mechanisms. This analysis will equally give some indication of the likely physiological implications of the underlying mechanisms.

To analyse the time scale, we might have repeated the above randomisation procedure, using time units different from 1s to calculate firing rates. Instead we looked at certain characteristics of the distributions of firing rates for each recording: how the shape of the distributions changed when they were calculated using different time units for the calculation of firing rate, and in what ways these distributions differed from those expected of a random or Poisson process.

3.3.1 Index of Dispersion

3.3.1.1 Introduction

A distribution cannot be described fully by only the measures of central tendency such as mean, median, or mode. Such averages locate the centre of a distribution, but tell nothing about how the scores are arranged around that centre. The latter is referred to as variability. In some distributions, there is a great deal of variability, while others have less. An index of dispersion is also needed to show how the scores scatter around the mean, is needed as a measure of variability. The index of dispersion for a given time 'window' (bin width or period over which the measurement is taken) is the ratio of the variance of interspike interval to the mean number of interspike intervals, or

$$id = \frac{\frac{\sum(x-\bar{x})^2}{n}}{\bar{x}}$$

The *variance* (σ^2) measures the extent to which the distribution spreads about the mean. With increased mean firing rate the variance increases, but for a Poisson distribution the variance of the event frequency has a fixed relationship to the *mean* of the event frequency (μ) – in fact, $\sigma^2 = \mu$, that is, the variance always equals the mean. Thus, if we assume that spike arrival is governed by a Poisson process then the index of dispersion, μ/σ^2, should be 1. Conversely, the closer to zero the index of dispersion, the more ordered the underlying series. The index of dispersion can take values above one, in which case it would suggest that the series is more irregular than the Poisson process. This could be an indication of heavy clustering, or it could reflect some non-stationarity. As such the index of dispersion is a valuable tool for describing non-random patterns.

Thus for a Poisson process, the index of dispersion should, therefore

(a) equal 1,

(b) should be independent of μ in a sample of data where μ varies, and

(c) should be independent of bin-width.

We therefore investigate how the index of dispersion varies with the time unit over which μ is measured. For each recording, we calculate the index of dispersion for the observed firing rate per window (with window sizes from 0.0625 s, 0.125 s, 0.25 s... up to 16 s).

3.3.1.2 Index of Dispersion Analysis

While the analysis of the ISIH indicates that the firing pattern is governed by essentially random processes, the analysis of observed and randomised firing rate distributions indicate the presence of weak activity-dependent negative feedback influences upon the spontaneous firing activity. In order to investigate the activity-dependent negative feedback influences further we turn to the effects of bin-widths. As stated above (cf. section 3.3.1.1) for Poisson processes the index of dispersion should be independent of bin-width. To determine what effect the change of bin-width has for our data the index of dispersion was calculated for each recording for a window size of 0.0625 s, 0.125 s, 0.25 s, 0.5 s, 1 s, 2 s, 4 s, 8 s, and 16 s. A summary of all the individual indexes of dispersion for each neurone and window can be found in table 3.1. Also, the indexes of dispersion for all the stretches within a group – naïve, stimulated (before and after osmotic stimulation), pregnant, and lactating (suckled, but non milk-ejecting and non-suckled) – were averaged.

Let us consider the results for the naïve group in detail. Figure 3.7 shows a graphic representation of the individual indexes of dispersion of the analysed recordings of the 13 naïve neurones. It also displays the index of dispersion average for that group (red). The averaged index of dispersion for naïve neurones starts at a value of 0.72 ± 0.05 for the 0.0625 s window, followed by 0.68 ± 0.06, 0.63 ± 0.06, 0.55 ± 0.06, 0.45 ± 0.05, 0.34 ± 0.4, 0.29 ± 0.4 for the windows of 0.125 s, 0.25 s, 0.5 s, 1 s, 2 s and 4 s, respectively until reaching its lowest value of 0.27 ± 0.4 for the 8 s window. The biggest window – 16 s – sees a very slight increase to a value of

0.29±0.04. While differences between the indexes of dispersion of different neurones exist, they all follow a very similar pattern to the one presented above: the highest value for the index of dispersion can be found at the smallest time scale, usually 0.0625 s, or 0.125 s. Thereafter, the index of dispersion decreases and reaches its smallest value for one of the biggest time scales. For the majority of the neurones this is at either 4 s, or 8 s. After the lowest point the index of dispersion typically increases slightly.

The averaged indexes of dispersion for each group and their standard errors of means are displayed in figure 3.8. The averaged indexes of dispersion for the groups of naïve (n=13), pregnant (n=13) and osmotically stimulated neurones (whether before or after stimulation, combined n=18) all follow the characteristic pattern described above in detail: generally, for very small window sizes the index of dispersions is high, but becomes lower with increasing window size. This means that for a very small window size of around 0.0625 s the firing appears to be near random. With increased window size – 0.125 s, 0.25 s, 0.5 s, 1 s, 2s – the index of dispersion decreases, i.e. the firing appears to be more and more ordered. The firing seems to be most ordered when looking at a scale of 4 s to 8 s, where the index of dispersion on average is the smallest.

The exceptions from the above described pattern are the lactating groups. Suckled and non-suckled neurones are grouped together for this analysis since they both display the same pattern, and a Tukey's (HSD) test establishes that there is no significant difference between their mean values (p=0.87). For the lactating group the averaged index of dispersion stays at a very high level for window sizes of 0.0625 s to 2 s (mean±sem of 0.89±0.02, 0.87±0.03, 0.85±0.04, 0.8±0.05, 0.72±0.07, and 0.66±0.08, respectively), and increases thereafter (0.7±0.09 for 4 s window and 0.79±0.11 for 8 s window) until at window size of 16 s the index of dispersion is 0.996±0.15 (Figure 3.8). Again, this increase for window size of 4 s and above is true for both suckled and non-suckled neurones (Figure 3.9).

To determine whether there is a statistically significant difference between the lactating and non-lactating (naïve, pregnant and after stimulation neurones) group as well as to see whether the window size has any significant effect on the index of dispersion a 2-way repeated measure analysis of variance (ANOVA) was carried out, and the Bonferroni t-test was used for multiple post hoc comparisons where appropriate ($p<0.05$ was taken as significant). Our data do not fit the assumptions for a parametric test exactly, however, there is no non-parametric alternative. Given that parametric tests are robust, i.e. they give fairly accurate probability estimates under less optimal conditions (cf. Coolican, 1994), that the significance level is very high and that the results are confirmed by the *post-hoc* test, it is justified to assume that our ANOVA results are valid.

Lactating and non-lactating groups are found to be significantly different ($p<0.001$). The results from the Bonferroni t-test all pairwise comparison can be found in table 3.2. While the index of dispersion does not differ significantly between the two groups for windows of 0.0625 s, 0.125 s, 0.25 s, 0.5 s and 1 s there are significant differences between the indexes of dispersion for windows 2 s, 4 s, 8 s and 16 s ($p<0.05$). The analysis also found a significant difference between the windows after allowing for the effects of the group ($p<0.001$), namely the window size has a significant effect on the index of dispersion.

The pattern of the index of dispersion over all the window sizes is the same for all the stretches from stimulated neurones, as seen in the stretches from before and after stimulation (Figure 3.8 and Figure 3.10). The vertical shift seen between the two can be attributed to the difference in mean firing rate (mean$\pm$sem of 2.36 ± 0.57 and 7.61 ± 1.14 spikes/ s, respectively) which is statistically significant ($p<0.01$, Student's t-test), rather than to differences in intrinsic mechanisms, since the groups consist of stretches from the same neurones recorded only a short time apart.

Consequently, it can be deduced that the difference in the shape between the indexes of dispersion for non-lactating neurones and for lactating neurones presented above indicates differences in the underlying mechanisms, rather than reflecting

superficial differences in the firing as for example firing rates. This is to be expected given the extensive nature of anatomic reorganisation in preparation for lactation (cf. section 1.1.3). Also, given that both suckled and non-suckled lactating neurones display the same pattern in the index of dispersion over different time scales and do not differ statistically, but differ substantially in the pattern to all other groups indicates that the extensive morphological reorganisation in the very last stages of pregnancy and birth are responsible for the difference between lactating and non-lactating groups, rather than the suckling itself.

Altogether these analyses indicate that the spontaneous background activity of oxytocin neurones in different physiological states do not follow a Poisson process, since it fails to fulfil any of the stated criteria: the index of dispersion is not independent of bin-width, randomisation of the events leads to changes in statistical characteristics that should be invariant, and the ISIH cannot be fully described by a single exponential.

3.3.1.3 Mean Firing Rate and Index of Dispersion

In the previous section we suggested that the mean firing rate is intimately linked to some of the effects seen in the analyses, so the next step explores in more detail how the index of dispersion relates to the firing rate. For each recording, the index of dispersion for the smallest time scale was plotted against the corresponding mean firing rate, e.g. index of dispersion for neurone n1 window 0.0625 s – 0.767 – against the corresponding mean firing rate of 5.55 spikes/ s, the index of dispersion for the smallest window for neurone n2 – 0.717 – against firing rate of 4.77 spikes/ s and so on for all neurones individually (cf. Table 3.1). Since the index of dispersion follows a different pattern for the lactating neurones in comparison to the neurones in the other groups, naïve, pregnant and stimulation stretches were analysed together as one group, and lactating neurones were analysed separately.

This analysis reveals a negative correlation, i.e. the higher the mean firing rate of a cell, the lower the index of dispersion, and vice versa for both the lactating and the non-lactating group (non-lactating neurones linear regression slope –0.0381,

lactating neurones slope –0.0461; Figure 3.11). The faster the neurone fires the more ordered the firing appears to be. The slopes for the lactating and the non-lactating groups seem to be very similar in this case – window 0.0625s –, even though both the mean firing rates and the indexes of dispersion between these two groups are significantly different (t-tests, $p<0.01$ and $p<0.05$, respectively).

Exploring the relationship between the firing rate and the index of dispersion further, the analysis was repeated for each group for each window size, i.e. the index of dispersion for the window of 0.0625 s against the mean firing rate for that neurone, index of dispersion for window 0.125 s against the mean firing rate, and so on until the index of dispersion for window size of 16 s against the mean firing rate. A linear regression analysis was carried out for each window size.

As can be seen in Figure 3.12A for the non-lactating group – regardless of time scale – the result suggests the same: the faster the mean firing rate, the smaller the index of dispersion for that neurone, indicating more ordered firing. The slopes remain very similar for all window sizes (–0.055±0.003, mean±sem; range –0.038 to –0.062).

For the lactating group, the linear regression also results in a negative slope (Figure 3.12B). However, with increased window size, the slope for the lactating groups becomes steeper. So, while the slopes for very small window sizes (up to 0.25s) are similar to the equivalent slopes for the non-lactating group, thereafter the slopes become even more negative (Figure 3.12 and Table 3.3). Thus, for the biggest window size investigated – 16 s – the slope for the lactating group is a magnitude steeper than the slope for the non-lactating group (Figure 3.11).

So, for both the non-lactating and the lactating neurones the negative linear regression suggests that the faster the firing the more ordered it is. However, whereas for non-lactating neurones this relationship appears to be constant whatever the time scale, for lactating neurones it becomes gradually more pronounced with increases in the time scale.

The relationship between the mean firing rate and the index of dispersion is as expected: the faster the firing the more ordered it becomes. In theory, in the extreme where the cell is driven to fire near the upper boundary of the firing rate range – although the neurones do not usually fire so fast – the limiting factor is the absolute refractory period and hence the firing is very regular and ordered. Conversely, if the cell fires more slowly there is simply more scope for irregularity.

The results from these analyses complement the outcomes and conclusion described for the index of dispersion analysis (section 3.3.1.2). The vertical shift in the pattern of index of dispersion for recordings before and after hyperosmotic stimulation can be attributed to the shift in the firing rate (2.36±0.57 and 7.61±1.14 spikes/ s mean±sem, respectively) rather than to a change in underlying mechanisms.

However, while this also explains why the indexes of dispersion for suckled neurones are generally very high (the mean firing rates for the groups are 2.07±0.34 spikes/ s for suckled and 2.57±0.59 spikes/ s for non-suckled neurones, or 2.45±0.38 spikes/ s combined, cf. Chapter 2), it does not explain the difference in the pattern of the index of dispersion – where the index of dispersion increases after a window of 2 s – compared to the non-lactating groups. A further indication that there is a fundamental difference between lactating and non-lactating neurones is the disparity in the course of the linear regression over different window sizes (Figure 3.11 and Figure 3.13).

The slope of the linear regression analysis of the mean firing rate and the index of dispersion is – as stated above – the same for non-lactating and lactating groups for the two smallest window sizes, i.e. 0.0625s and 0.125s. However, for window sizes of 0.25s and larger the slope for the non-lactating groups remains constant at approx. –0.06, whereas the slope for the lactating group becomes progressively steeper, until a value of –0.35 for the largest window (16s). While for the non-lactating neurones the inverse relationship between firing rate and index of dispersion remains constant throughout the different time scales, for the lactating groups the relationship becomes stronger with increased window size, i.e. over a

small time scale with increased firing frequency the firing seems to be quite ordered, but over a large time scale this becomes even more pronounced.

This supports the conclusion reached before that the difference in the pattern of the index of dispersion can be attributed to differences in underlying mechanisms between lactating and non-lactating neurones, rather than to differences in firing rates.

3.3.1.4 Summary

To summarise, the main findings from the index of dispersion analyses are as follows:

(a) altogether, the analyses indicate that the spontaneous background activity of oxytocin neurones in different physiological states do not follow a Poisson process.

(b) for non-lactating neurones the general pattern of the index of dispersion shows that the highest values for the index are for small window sizes, decreasing progressively towards larger window sizes. This means that the firing activity appears to be near random when looking at small time scales (0.0625s to 1s), and appears more and more ordered when looking at larger time scales (>1s).

(c) for the lactating group, the index of dispersion displays the same near random values as the non-lactating neurones for small window sizes. However, the values differ significantly for larger window sizes (>1s). So both physiological state and the window size have a significant effect on the index of dispersion.

(d) the difference in the shape of the indexes of dispersion for non-lactating neurones and for lactating neurones suggests that the firing activity of lactating neurones is governed by fundamentally different underlying mechanisms. Furthermore, the result that both suckled and non-suckled lactating neurones display the same pattern in the indexes of dispersion, but differ in the pattern to all other group suggests that the morphological reorganisation in the last stages of pregnancy and birth are responsible for that difference, rather than the suckling itself.

(e) the faster the neurone fires, the more ordered the firing appears to be, regardless of the physiological state of the animal or the window size, indicating that faster firing activity is more ordered. The vertical shift of the same pattern of indexes of dispersion seen between the before and after stimulation neurones can be attributed to the difference in mean firing, rather than to differences in intrinsic mechanisms.

3.4 Autocorrelation and Partial Autocorrelation

3.4.1 Introduction

Since the analyses on the index of dispersion revealed that the arrival of spikes does not follow a Poisson distribution, autocorrelation analyses of the firing rates were performed to further investigate the structure in the firing pattern. *Autocorrelation* refers to the serial dependence of the observations in a stationary time series. Autocorrelation is described by *autocorrelation coefficients*, which measure the correlation between observations at different times apart, or *lags*.

In our case, the observations between which the correlations are calculated are firing rates for a specified period of time, or *window*. To calculate the autocorrelation coefficient of lag 1, the observation at a time t is compared to the observation at time t+1. The observation at a time t is compared to the observation at time t+2 to calculate the autocorrelation coefficient of lag 2. In general, the observation at time t is compared to the observation at time t+n to calculate the autocorrelation coefficient of lag n (for further explanation see Figure 3.14 and Brown & Rothery, 1993).

Partial autocorrelation is a related concept. The partial autocorrelation also measures the correlation between two observations. However, it takes into account the effect of a common correlation. The partial autocorrelation between observations at t and t+2 is an autocorrelation between observations t and t+2 after allowing for the autocorrelation between observations of t and t+1, and the autocorrelation between observations of t+1 and t+2. Both the autocorrelation coefficient and the partial autocorrelation coefficient are dimensionless quantities scaled to take values

in the range of −1 to 1, whereby a value of −1 indicates a perfect negative linear relationship, and a value of 1 indicates a perfect positive relationship. The *autocorrelation function (ACF)* and *partial autocorrelation function (PACF)* are graphs showing the autocorrelation coefficient and partial autocorrelation coefficient of a specified lag plotted against the corresponding lag (Figure 3.15).

What do we expect the ACF to look like? For an infinite series of observations that are independent of each other the autocorrelation would be zero. A series with trends would result in an ACF that would decrease slowly to zero. This possibility should be of no importance in our case since great care has been taken to ensure that the stretches of recordings analysed were stationary, i.e. without trends. For alternating series the ACF will also alternate between negative and positive values. For series that display no trends or systematic variation but show serial dependence and *irregular fluctuations* the ACF will display oscillations that will reflect these irregularities.

3.4.2 Analysis

We calculated ACFs and PACFs using the built-in function in our statistical package, Genstat, up to a specified lag, for different windows. The specified lag was chosen for each window so that a time sequence of approx. 30 s was analysed, as we were looking for signs of a long lasting effect: for a window of 0.0625 s up to lag 500, for a window of 0.125 s up to lag 250, and so on until a window of 16 s up to lag 2. In addition, a 95% confidence interval was calculated. Figure 3.15 shows an example of one complete analysis for one recording.

The ACF and PACF are nearly identical for most lags. They oscillate around zero for most of their length, thus no significant autocorrelation or partial autocorrelation could be found for observations at larger lags. This was to be expected from our data, as it is unlikely that there is a correlation between spikes at long times apart and separated by many intermediate spikes. If any serial dependence should emerge than this should be the case for small lags. To see any serial

dependence on a smaller time scale, i.e. between observations closer together, we looked for significant values amongst the first few lags. We considered the beginning of each ACF for each window and recorded whether a significant positive, a significant negative or no autocorrelation could be detected for that window.

The following pattern emerged for neurones from all physiological groups combined (cf. Table 3.4). For windows of 0.0625 s, 0.125 s, 0.25 s, 0.5 s and 1 s a negative autocorrelation was found for the majority of neurones (n=48, 50, 51, 52, and 46 out of 65, respectively), regardless of their physiological state. For the window of 2 s, 20 out of the 65 neurones showed a negative autocorrelation for the first few lags, while 10 neurones showed a positive autocorrelation. For windows of size 4 s, 8 s, and 16 s a slightly larger number of neurones showed a significant positive autocorrelation (n=15, 13, and 11 out of 65 for window sizes 4 s, 8 s, and 16 s, respectively), than a negative correlation (n=9, 7, and 7 out of 65; Figure 3.16 a-f). Overall, however, at windows of sizes >2 s the majority of neurones showed no significant autocorrelation.

This means that at small time scales of 0.0625 s to 1 s, there is a serial dependence of mean firing rates, with periods of short ISIs likely to be followed by periods with long ISIs, and vice versa. However, when looking at longer time scales of 4 s or above then most likely there is no serial dependence between firing rates. Ignoring the non-significant events, what is interesting about the remaining results is the shift of proportion between the recordings for which a positive autocorrelation and those for which a negative autocorrelation was found: while for small windows the overwhelming majority of autocorrelation is negative, for windows >2 s most significant autocorrelations are positive. Positive autocorrelations indicate that, when comparing large windows a period of short ISIs is more likely to be followed by a further period of short spikes, and vice versa. Thus it seems that on a short and medium time scale the cell possesses a "memory" and balances the activity, whereby short intervals tend to be followed by longer ones, and *vice versa*. However, on long time scales for most cases there is no serial dependence, but for those where a serial dependence was found the effect is of a more homogenous activity. The shift to

positive autocorrelation in larger windows becomes even more evident when excluding the results of the before hyperosmotic stimulation group, which is the only group where the number of negative autocorrelation increases and not decreases. For all the other groups this pattern – negative autocorrelation for small windows, giving way to a majority of no autocorrelations with a few positive autocorrelations for large windows – is remarkably similar (Figure 3.16B-D, F).

The exceptional group – before hyperosmotic stimulation – shows a negative autocorrelation in a little over half of the recordings for small windows, the remaining recordings showing no significant correlation, but all the cells displaying negative autocorrelation for windows of size 2 s and over (Figure 3.16E).

3.4.3 Summary

The main results from the analyses of the autocorrelation and partial autocorrelation of firing rates indicate that

(a) there are no differences between the ACF and the PACF

(b) significant autocorrelations or partial autocorrelations can be found for the first few lags only, whereafter the ACF and PACF oscillate around zero, i.e. relationship between firing rates can only be found between observations close together.

(c) autocorrelation depends on the window size, as for a small time scale (0.0625 s to 1 s) for observations close together there is usually a negative relationship, whereas for larger window it is likely that there is no relationship, but if there is one it is more likely to be positive. The presence of structure in sequences of interspike intervals probably reflects the effects of slow activity-dependent influences on cell excitability. In effect, these influences provide mechanisms by which the current state of activity is recognized and then balanced. The main such mechanism is probably a slow afterhyperpolarisation, observed in experiments *in vitro* after intense activation, but which here was shown to have a significant impact at low (spontaneous) firing rates *in vivo*.

3.5 Discussion

In this chapter we have investigated whether we can detect subtle signs of activity-dependent feedback mechanisms in the firing rates from spontaneous, unexceptional firing activity in oxytocin neurones.

To this means, we started by presenting three criteria that describe random processes, and determined how exactly *in vivo* firing patterns deviate from randomness as discernible by these criteria.

1) If the firing activity of oxytocin neurones adhere to the statistics of Poisson processes, then the interspike interval histogram should be well described by a single negative exponential. We found that a single exponential fits well to the tail of the distribution, however, when extrapolated towards lower values there is a marked deficit of events below the curve in the range from 0-40 ms. This deficit is consistent with the effect of the HAP, where the occurrence of an action potential immediately following an action potential is inhibited by a drastic reduction in excitability. The good fit of the exponential indicates that beyond the effects of the HAP after any given spike the arrival time of the next spike is essentially random. Thus it appears that the activity of oxytocin neurones is dominated by factors affecting the probability of spike occurrence that are independent of previous spike history, like the mean resting potential and the rate of synaptic input, in addition to the effects of the post-spike HAP.

2) If – as indicated by the interspike interval distribution – the firing activity follows a Poisson process, then further randomisation should not result in changes to the statistical characteristics. We found that randomisation of the interspike intervals changes the resulting firing rate distribution in a predictable way: the randomised distributions is consistently more dispersed than the observed firing rate distribution, so the observed firing rate distribution was more uniform than would be expected if there was no serial dependence between interspike intervals. There seems to be weak activity-dependent mechanisms underlying the spontaneous activity of the oxytocin neurones, weak in the sense that their effects are not

readily apparent in the interspike interval distribution, but apparent in the firing rate calculated on a time scale of 1 s.

3) For a Poisson process the index of dispersion should equal 1, should be independent of the mean of the event frequency and should be independent of bin-width. We found that the index of dispersion does not equal 1, and in fact changes with the bin-width over which it is calculated in a characteristic manner: for very small bin-widths the index of dispersion was high, but decreased when the bin-width increased. This suggests that the firing appears to be near random when looking over very small time scales, but becomes more and more ordered when looking over increasingly longer time scales. Also, we found that the mean firing rate influences the index of dispersion in a predictable way, namely the faster the neurone fires, the more ordered its firing seems to be.

Although the analysis of ISIH indicates that the firing is not influenced mechanisms other than the HAP, on closer inspection the firing activity displays subtle signs of structure. We used autocorrelations and partial autocorrelations to investigate the nature of this further. This analysis revealed that for small window sizes (0.0625 to 1s) there is a serial dependence for periods of activity close together, in that periods of short ISIs are followed by periods of longer ISIs, and vice versa. Thus at small time scales periods of relatively high activity are likely to be followed by periods with relatively low average activity, and vice versa. For larger window sizes this relationship disappears. Thus the average firing rate over long period of time is much more regular than would be expected from the local variability in firing rate.

The autocorrelation analyses presented in this chapter are based on firing rates, i.e. they assess temporal dependencies and correlations at fixed intervals of time after events, rather than a fixed number of intervals after the events (see chapter 2). There are different merits to both types of analyses. If we would look at correlations between intervals a fixed time apart we would not know what time dependence is involved: the intermediate intervals might be very short in which case

the time difference is very short, or some of the intermediate intervals might be long, in which case the time difference might be medium or very long. Thus, the two analyses measure different parameters and are complementary ways of assessing time dependence, or as Cox and Isham state:

> *"A complicated form of dependence between successive intervals is a strong indication that a specification not directly based on intervals should be sought."*
> *(Cox & Isham, 1979, page 91)*

A further aim of this chapter was to investigate whether there are consistent difference in the spike patterns of neurones recorded in different physiological states. While generally no major differences between the firing activities from the different physiological groups were apparent, the index of dispersion analysis of the lactating groups suggested they are different in that rather than the firing becoming more ordered over longer windows they become more irregular, indicating heavy clustering. Another subtle difference is in the relationship between mean firing rate and index of dispersion: while for both non-lactating and lactating groups it is true that the faster the cell fires the more ordered the firing appears, this relationship is the same regardless of time scale for non-lactating neurones, it becomes more pronounced with increased time scale for lactating neurones.

The autocorrelation analysis revealed that all the physiological groups behave remarkably similar, the before hyperosmotic stimulation group being the only group following a different pattern. The reason for this not apparent. This group consists of the smallest sample. Also, the mean firing rate is comparatively low, although this cannot be the main cause for the difference, as the mean for the lactating groups is only marginally faster – 2.36 vs. 2.45 – and results for the latter conform to the described pattern (Figure 3.16D). Changes in underlying mechanism seem unlikely, as the same cells after the hyperosmotic stimulation now display positive autocorrelations for larger windows sizes, and no negative autocorrelations for window size of 4 s and larger. The cells for this group were specifically chosen for their 'naturally' slow firing for the purpose of the experiment. Maybe there is a lack

of input that drives the cells to fire at the frequencies usually seen in oxytocin neurones? From the autocorrelation analysis alone no satisfactory explanation for the difference of the before hyperosmotic stimulation group can be given.

Analysis of firing rates is a good starting point to look at longer term patterns in firing activity, as it identifies the strongest influences without requiring too much details. However, the latter can of course be a disadvantage, when more precise information about the nature of these influences is sought. While converting ISIs into firing rates, important information about clustering is lost. The resolution of spikes within a given time interval is not known. A firing rate of 3 Hz does not tell whether the three spikes occurred as a cluster, within say 200 ms, or whether they were spread apart regularly, i.e. 300 ms between each of the spikes. The information about the relationship of one spike to the next is lost. Interpretation of the results can also be more difficult, as results about the relationships between periods of activity do not necessarily reflect the relationship between the underlying individual spikes. This is the focus of the investigations presented in the following chapter.

Figure 3.1 Examples of patterns of activity of a vasopressin neurone (A), an oxytocin neurone (B), and a non-SON neurone (C).

Each of these cells displays a different firing pattern, which results in a different interspike interval distribution (Figure 3.2).
(A) This *in vivo* recording of a vasopressin neurone shows the typical 'phasic' pattern associated with this kind of cells, whereby periods of activity are interspersed with periods of silence.
(B) Oxytocin cells fire in general continuously at between 2 to 6 Hz, with a dramatically different firing pattern during lactation (Figure 1.4 B).
(C) The firing pattern of a cell recorded dorsally of the SON.

Please note that this figure is the same as figure 1.3 in chapter 1, repeated here for the convenience of the reader as the next figure is related, and there are references to it throughout chapter 3.

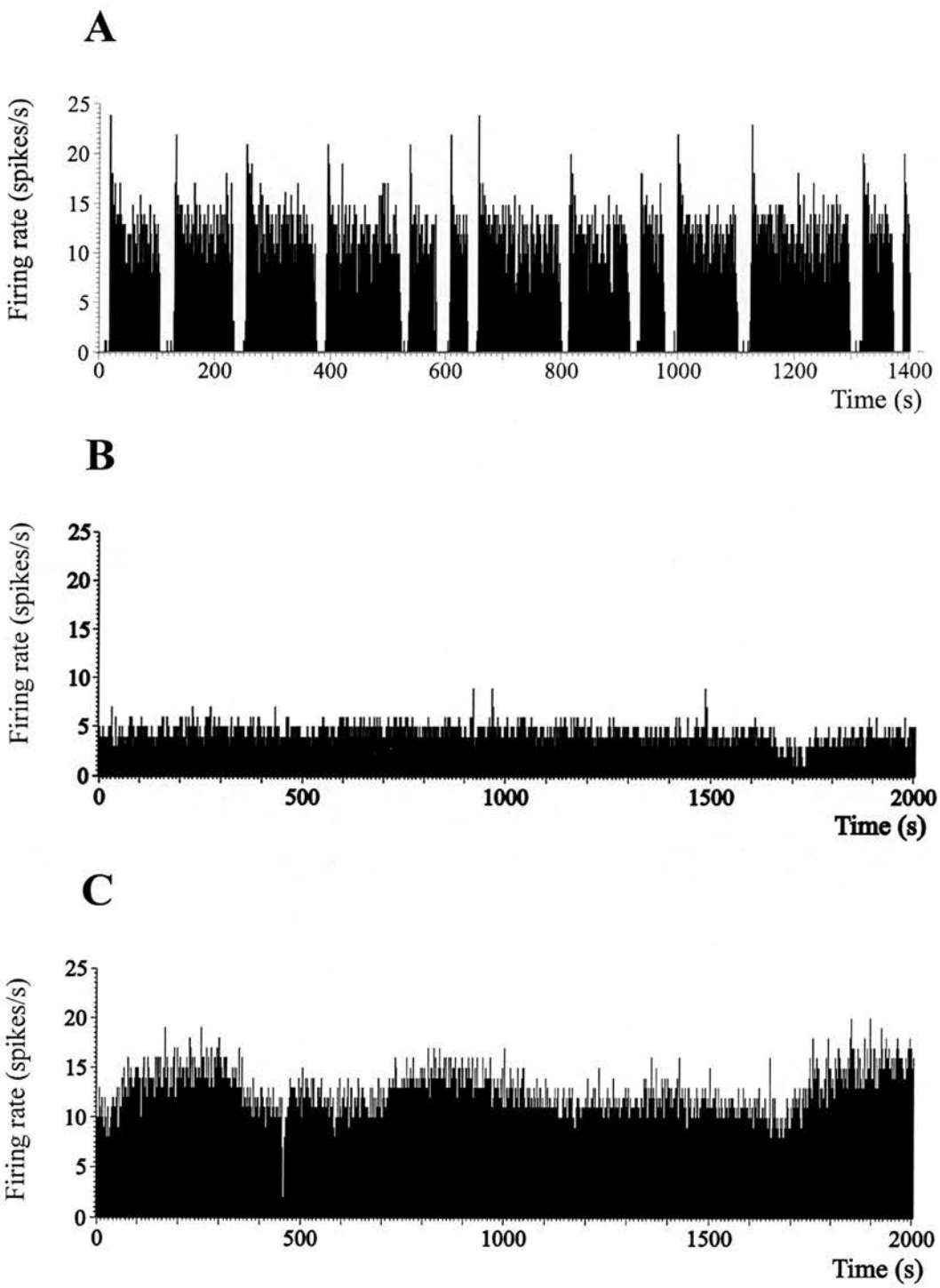
A
Firing rate (spikes/s)
25
20
15
10
5
0
0
200
400
600
800
1000
1200
1400
Time (s)
B
Firing rate (spikes/s)
25
20
15
10
5
0
0
500
1000
1500
2000
Time (s)
C
Firing rate (spikes/s)
25
20
15
10
5
0
0
500
1000
1500
2000
Time (s)

Figure 3.2 Examples for interspike interval histograms for a vasopressin neurone (A), a continuously firing oxytocin neurone (B), and a non-SON cell (C) (based on the examples from Figure 3.1).

The interspike interval histogram in (A) is typical for phasically firing vasopressin cells and differs from the interspike interval distribution of an oxytocin cell (B) in that a greater proportion of intervals occurs close to the mode.
A non-SON cell shows an interspike interval distribution (C), which is clearly different from interval distributions of both types of SON cells.

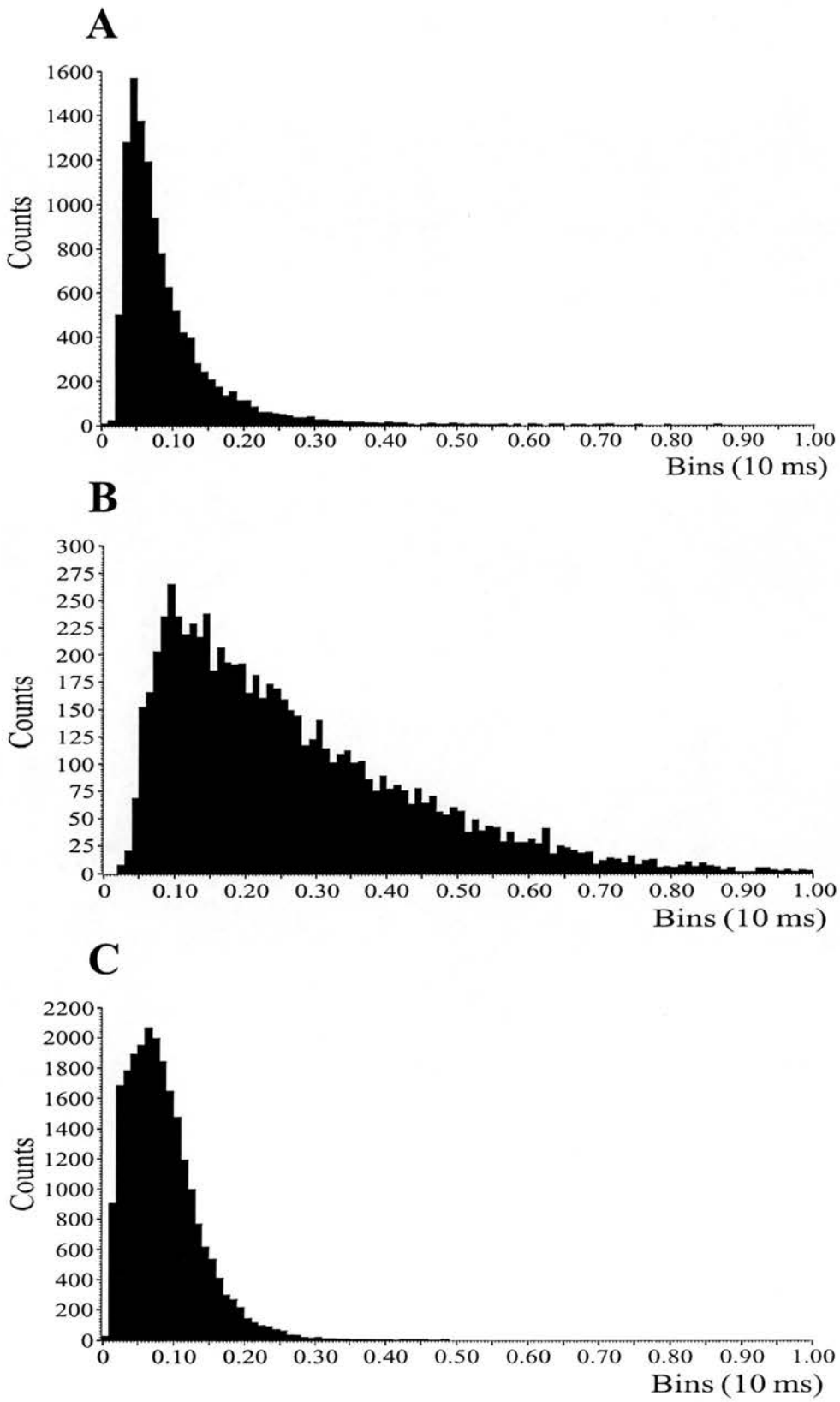
A
Counts
1600
1400
1200
1000
800
600
400
200
0
0 0.10 0.20 0.30 0.40 0.50 0.60 0.70 0.80 0.90 1.00
Bins (10 ms)
B
Counts
300
275
250
225
200
175
150
125
100
75
50
25
0
0 0.10 0.20 0.30 0.40 0.50 0.60 0.70 0.80 0.90 1.00
Bins (10 ms)
C
Counts
2200
2000
1800
1600
1400
1200
1000
800
600
400
200
0
0 0.10 0.20 0.30 0.40 0.50 0.60 0.70 0.80 0.90 1.00
Bins (10 ms)

Figure 3.3 Representative observed (A) and associated log-transformed (B) interspike interval histograms, with curves fitted (red) to the tail of the histogram and extrapolated towards lower values for four oxytocin neurones.

For oxytocin neurones the interspike interval distribution is skewed, with a single mode in the range of 30-80ms and a long tail (A). The tail can be well fitted by a single exponential (red), the extrapolation of which shows a deficit of intervals below the curve in the range of 0-40 ms. This deficit is consistent with the effect of the HAP.
Rather than fitting a single exponential it is better to plot the log-transformed distribution (B). Log-transforming converts the negative exponential into a straight line (red), which can be fitted more robustly.
As can be seen in the examples, for oxytocin neurones the interspike interval distribution can be well described by a single negative exponential.

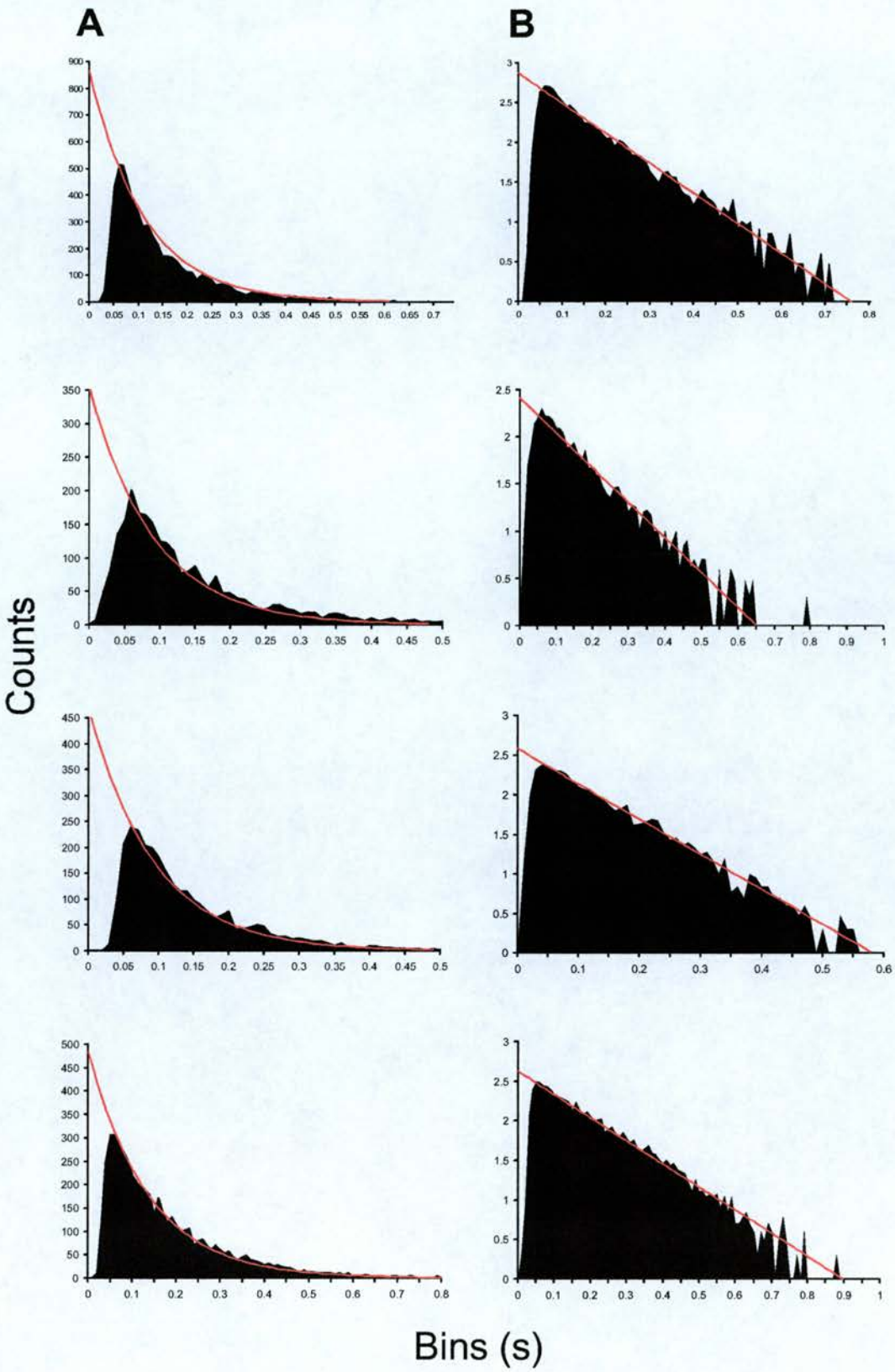
A
B
Counts
Bins (s)

Figure 3.4 Representative observed (A) and associated log-transformed (B) interspike interval histograms, with curves fitted (red) to the tail of the distribution and extrapolated towards lower values for four vasopressin neurones.

For vasopressin neurones the interspike interval distribution is - like for oxytocin neurones - skewed with a single mode in the range of 40-60 ms and a long tail. However, whereas the distribution of a oxytocin neurones is well described by a single exponential (cf. Figure 3.1A), for vasopressin neurones an exponential fitted to the tail of the distribution does not fit well throughout: there is an excess of intervals above the curve in the range 40-100 ms (A). This excess indicates the effects of the DAP, which is expressed little if at all in oxytocin neurones.
The observed distribution (A) was log-transformed and plotted with the exponential (B; red; the exponential becomes a straight line in the log scale) to facilitate comparison with the interspike interval distributions of oxytocin neurones. Whereas the line fits the distribution in oxytocin neurones very well, it cannot be fitted successfully to the interspike interval distribution of vasopressin neurones.

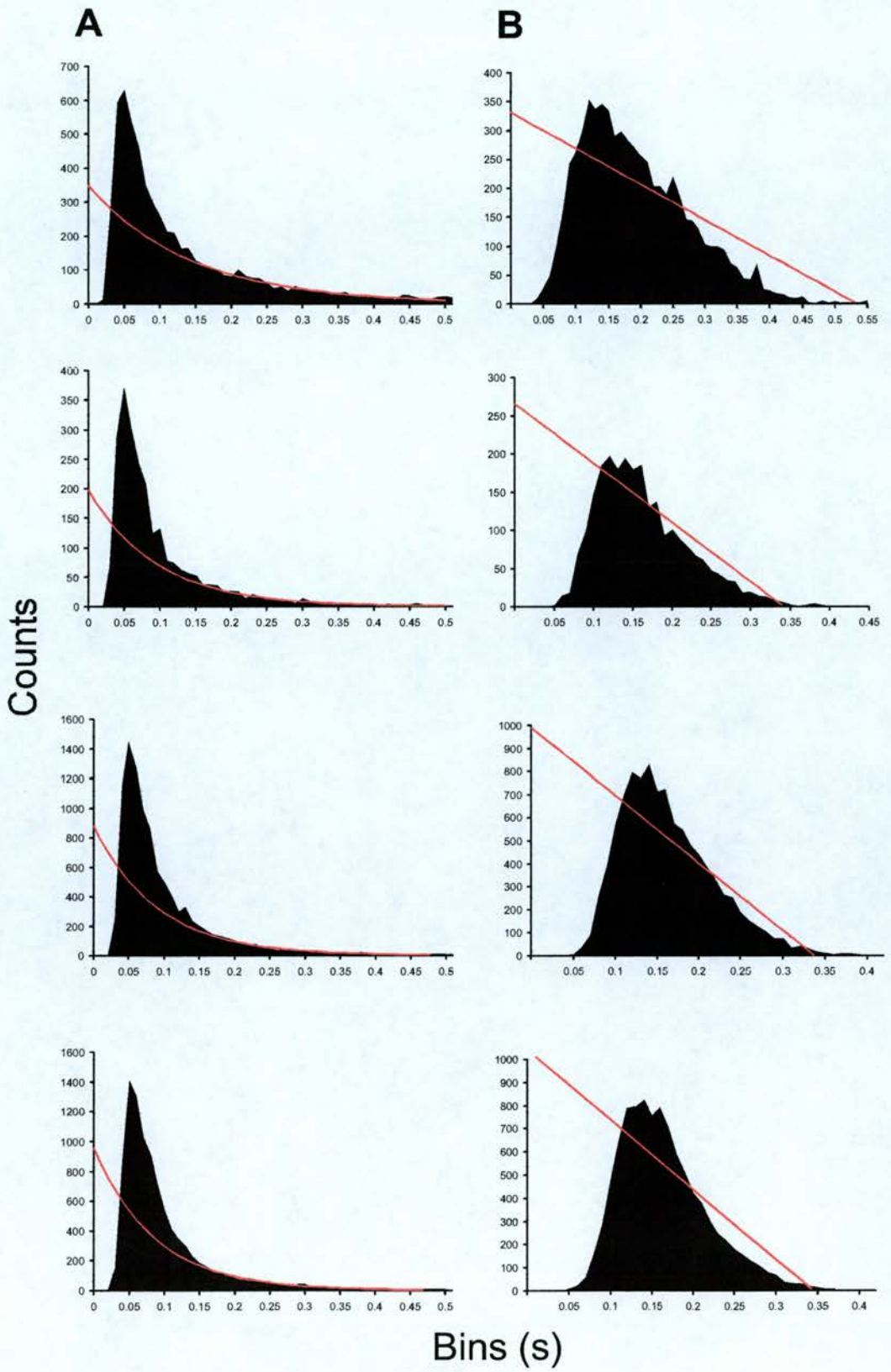
A
B
Counts
Bins (s)

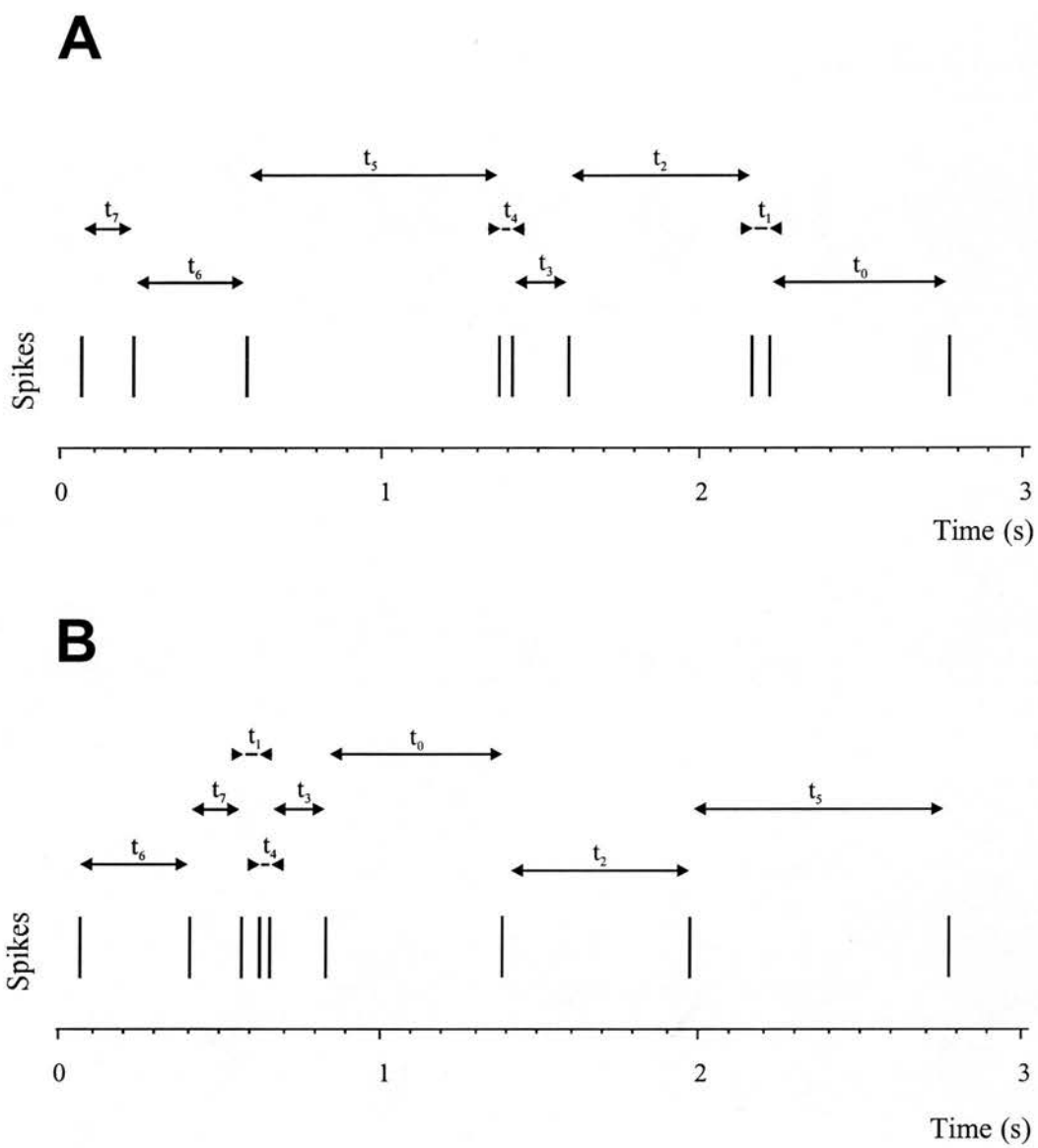

Figure 3.5 Nomenclature used for the statistical analyses.

The analyses are based on the time between one spike and the next, or interspike intervals (ISIs). The current ISI is designated t_0, the ISI immediately preceding is designated t_1, and so on (A). For the firing rate analyses, the number of spikes per second was determined.
For the randomised firing rate distribution the *same* ISIs were randomly shuffled (e.g. from $t_7, t_6, \ldots, t_0$ to $t_6, t_7, t_1, t_4, t_3, t_0, t_2, t_5$), and then the firing rate distribution was calculated as before. For the example given in here this would result in three firing rates of 3 spikes/ s for the original (A), while the randomisation would result in firing rates of 6, 2 and 1spike(s)/ s (B).

Figure 3.6 Observed firing rate distribution (dark area) and randomised firing rate distribution (white area).

The figure shows the analysis of 5 stationary stretches of recordings (length ranging from 170 to 2300 s) taken from different oxytocin neurones with different mean rates of activity. Firing rates were calculated in 1 s bins and the shaded curves show the distributions of firing rates in these 1 s bins. The original ISIs were randomised and from the randomised data new second by second firing rates were calculated (for further details of this procedure cf. Figure 3.3).
The white curves show the distribution of firing rates from the randomised data. The firing rate distribution has a higher peak, but is narrower than the randomised firing rate distribution, indicating that the sample is more uniform than would be expected from a completely random sample. This is true for all the samples analysed, regardless of physiological state of the animal, i.e. whether naïve (A and B), pregnant (C and D), lactating (E), or after a hyperosmotic stimulation (F).
The discrepancy between the two distributions is a first indication for structure in the firing pattern.

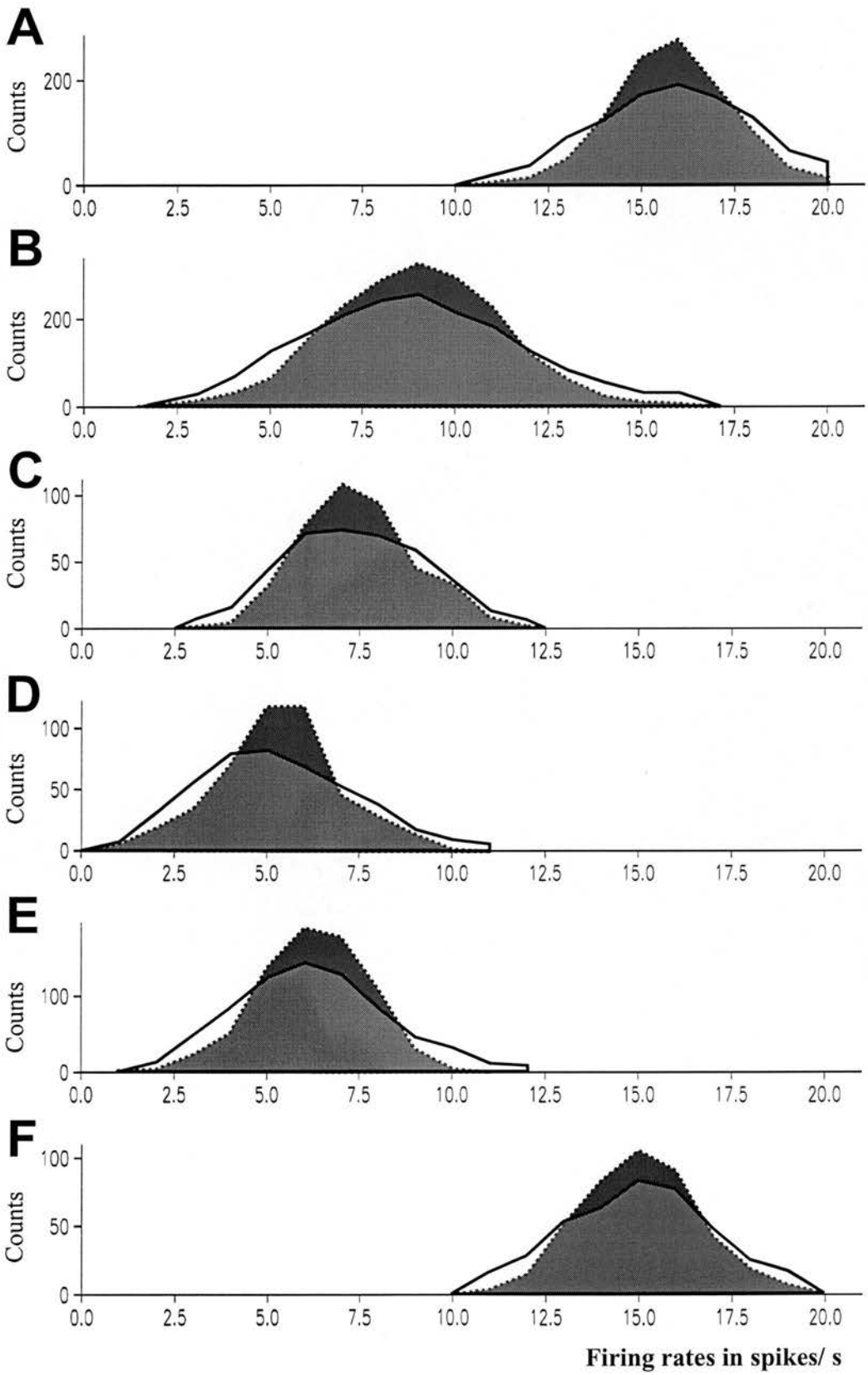
A
B
C
D
E
F
Counts
200
100
50
0
0.0
2.5
5.0
7.5
10.0
12.5
15.0
17.5
20.0
Firing rates in spikes/ s

Figure 3.7 Individual indexes of dispersion for each naïve neurone for each window size and the averaged index of dispersion of the naïve neurones presented including the standard error of means (red).

The index of dispersion for all 13 neurones in the naïve group display all the same characteristic pattern, as summarised by the averaged index of dispersion for this group (red): the index of dispersion was highest for small window sizes, and decreased for progressively larger window sizes until window size of 4 or 8 s, whereafter a slight increase occurred again. This indicates that the firing is near random when looking at a small time scale and becomes more and more ordered for increased time scales.

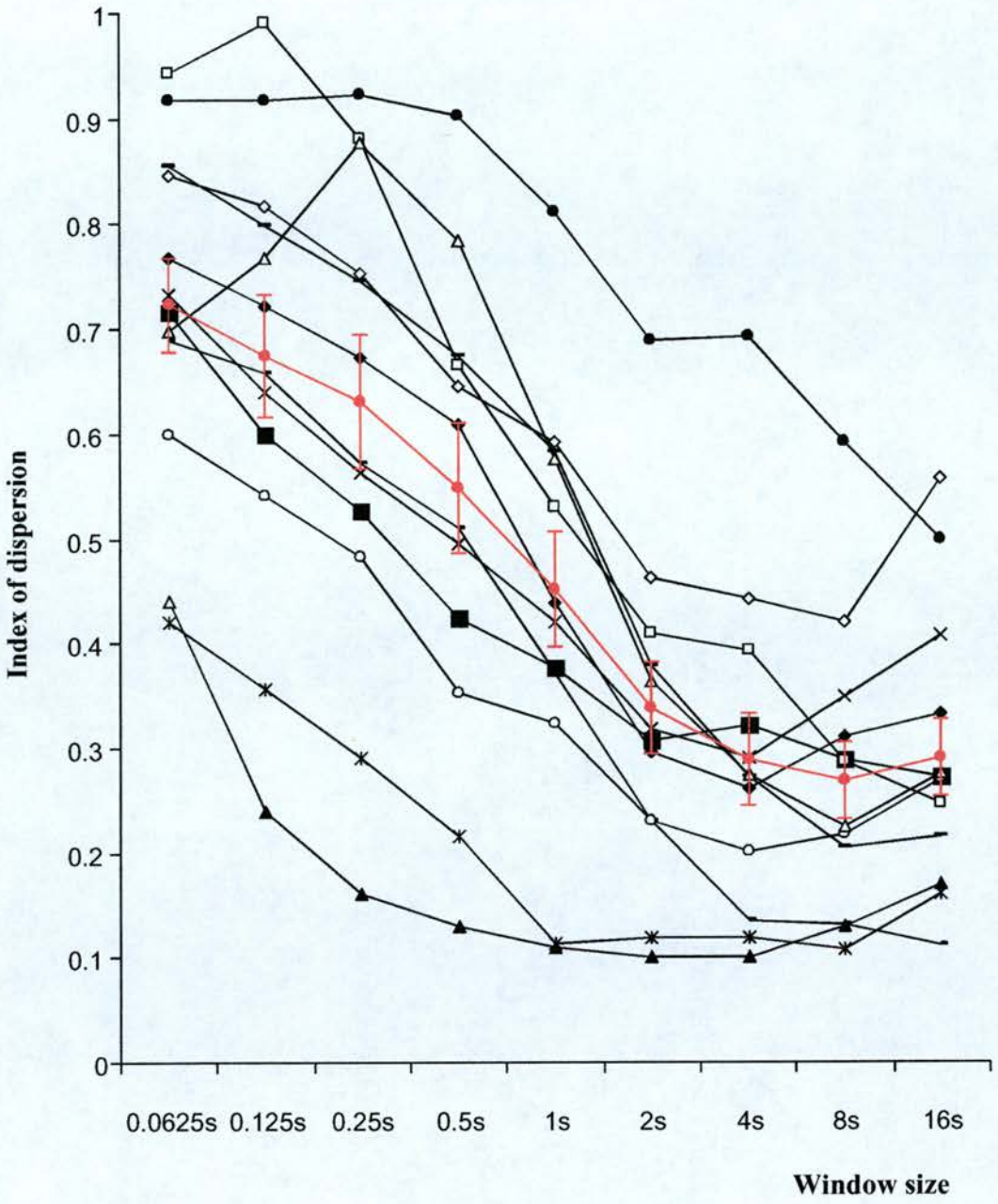
Index of dispersion
1
0.9
0.8
0.7
0.6
0.5
0.4
0.3
0.2
0.1
0
0.0625s
0.125s
0.25s
0.5s
1s
2s
4s
8s
16s
Window size

Figure 3.8 Averaged indexes of dispersion for pregnant, naïve, stimulated (before and after stimulation) and lactating (red, both suckled but non-milkejecting and unsuckled) neurones including standard error of means.

The averaged indexes of dispersion for naïve, pregnant and stimulated neurones all display the same characteristics: from a high index of dispersion for a very small time scale a gradual decrease until a small index of dispersion for a large time scale. The index of dispersion for the lactating group by contrast also starts with a high value for small time scales, but displays only a marginal drop in the medium range before it drastically increases for large time scales.

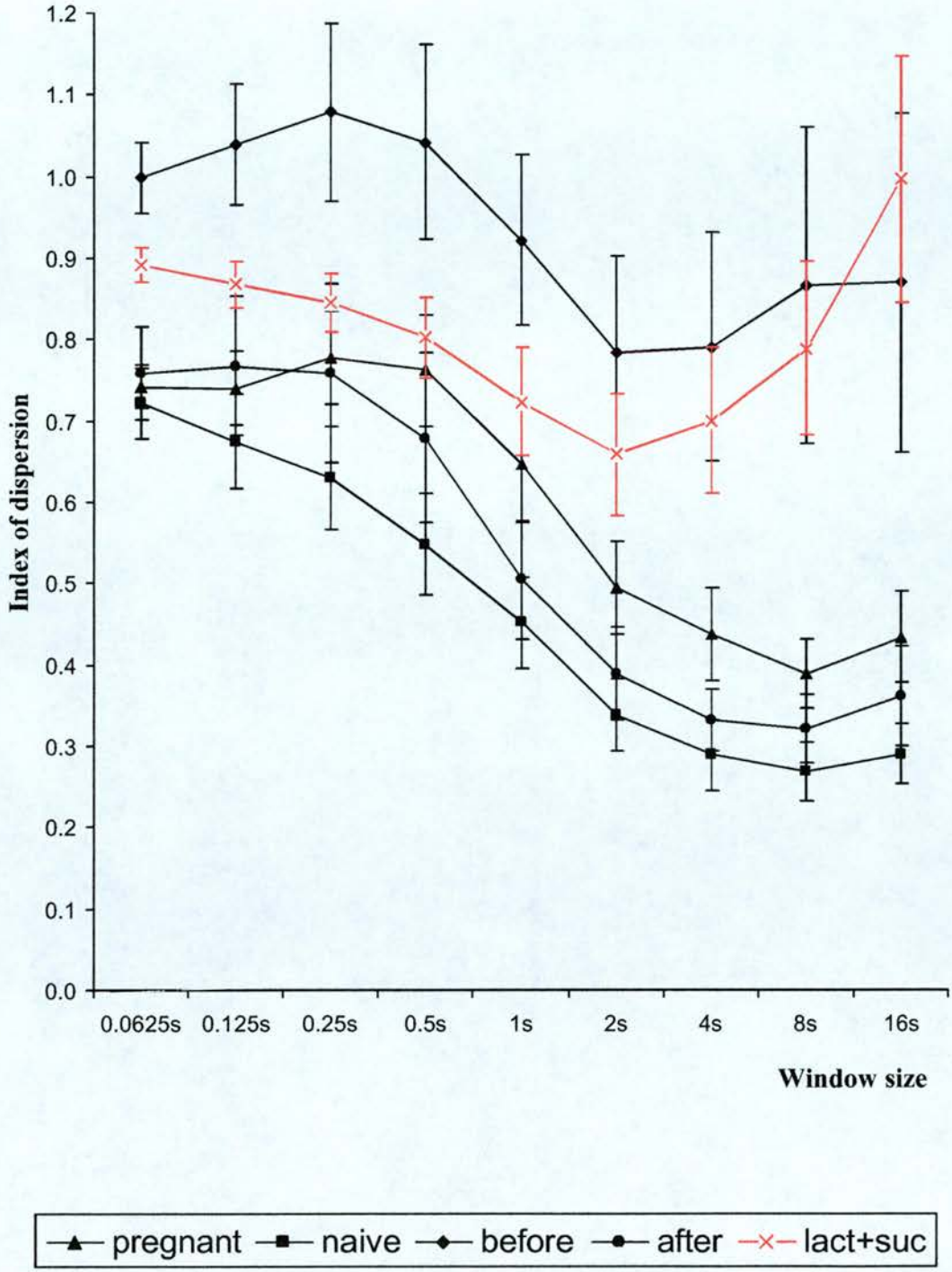
1.2
1.1
1.0
0.9
0.8
0.7
0.6
0.5
0.4
0.3
0.2
0.1
0.0
Index of dispersion
0.0625s
0.125s
0.25s
0.5s
1s
2s
4s
8s
16s
Window size
pregnant
naive
before
after
lact+suc

Figure 3.9 Indexes of dispersion for lactating neurones (suckled and unsuckled) and the averaged indexes of dispersion for all lactating neurones (red) including standard error of means.

Averaged indexes of dispersion for both suckled (but non milk-ejecting) and unsuckled neurones show the same pattern which is dramatically different from the pattern displayed by the indexes of dispersion for the other groups: a very high index of dispersion for a small time scale, a marginal drop thereafter until the 2 s window, after which a big increase occurs.

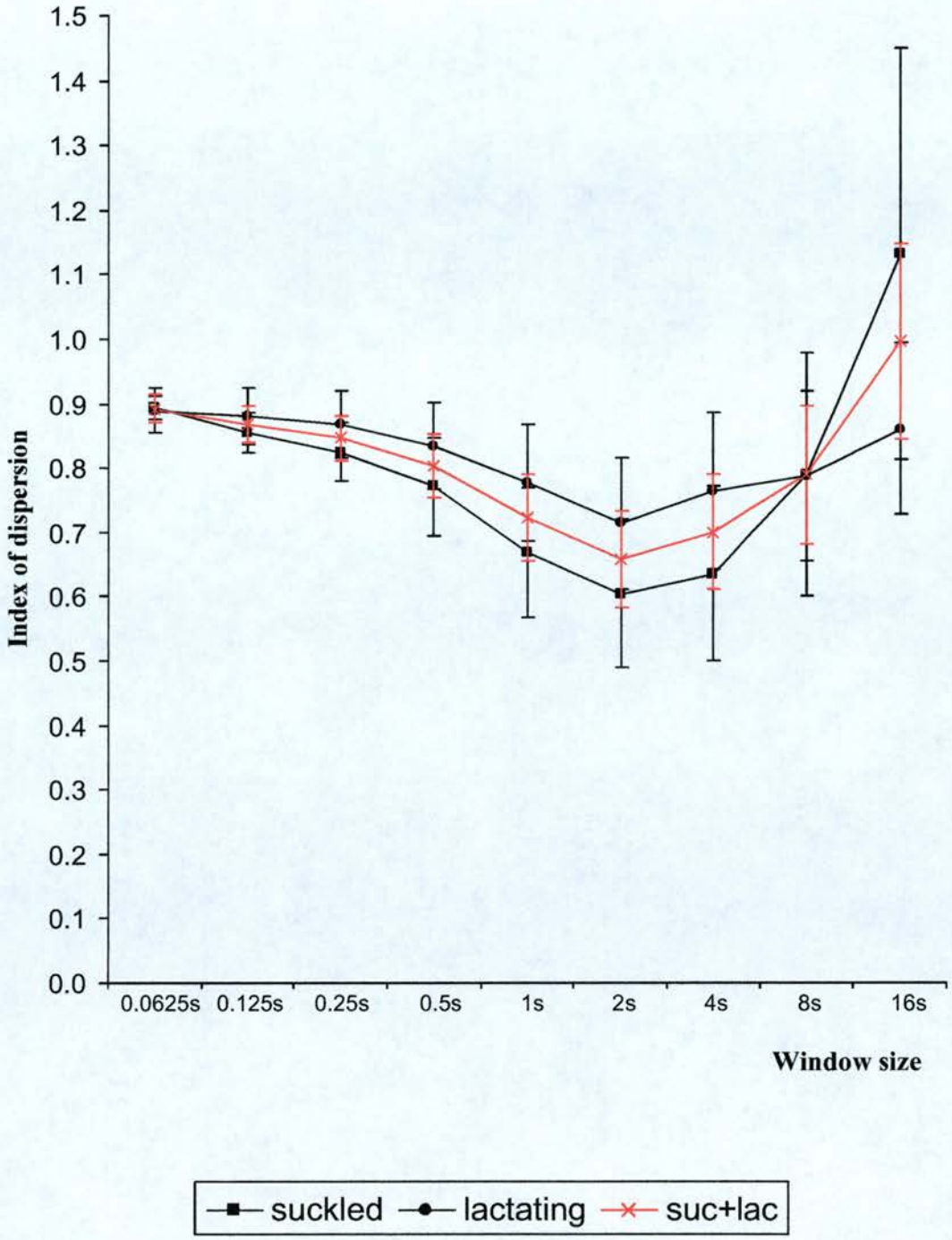
1.5
1.4
1.3
1.2
1.1
1.0
0.9
0.8
0.7
0.6
0.5
0.4
0.3
0.2
0.1
0.0
Index of dispersion
0.0625s
0.125s
0.25s
0.5s
1s
2s
4s
8s
16s
Window size
suckled
lactating
suc+lac

Figure 3.10 Averaged indexes of dispersion for neurones before (open squares) and after (solid squares) hyperosmotic stimulation.

The averaged index of dispersion for the neurones before hyperosmotic stimulation and after hyperosmotic stimulation have a very similar shape. Since the neurones were in the same physiological state bar for the temporary experimentally induced excitation the vertical shift between the two groups can be explained by the rise in firing rate, rather than attributed to a change in intrinsic mechanisms. This is supported by the similarity in shape of the two graphs and the later analysis on the relationship between firing rates and index of dispersion, which shows that the faster the firing rate the lower the index of dispersion tends to be.

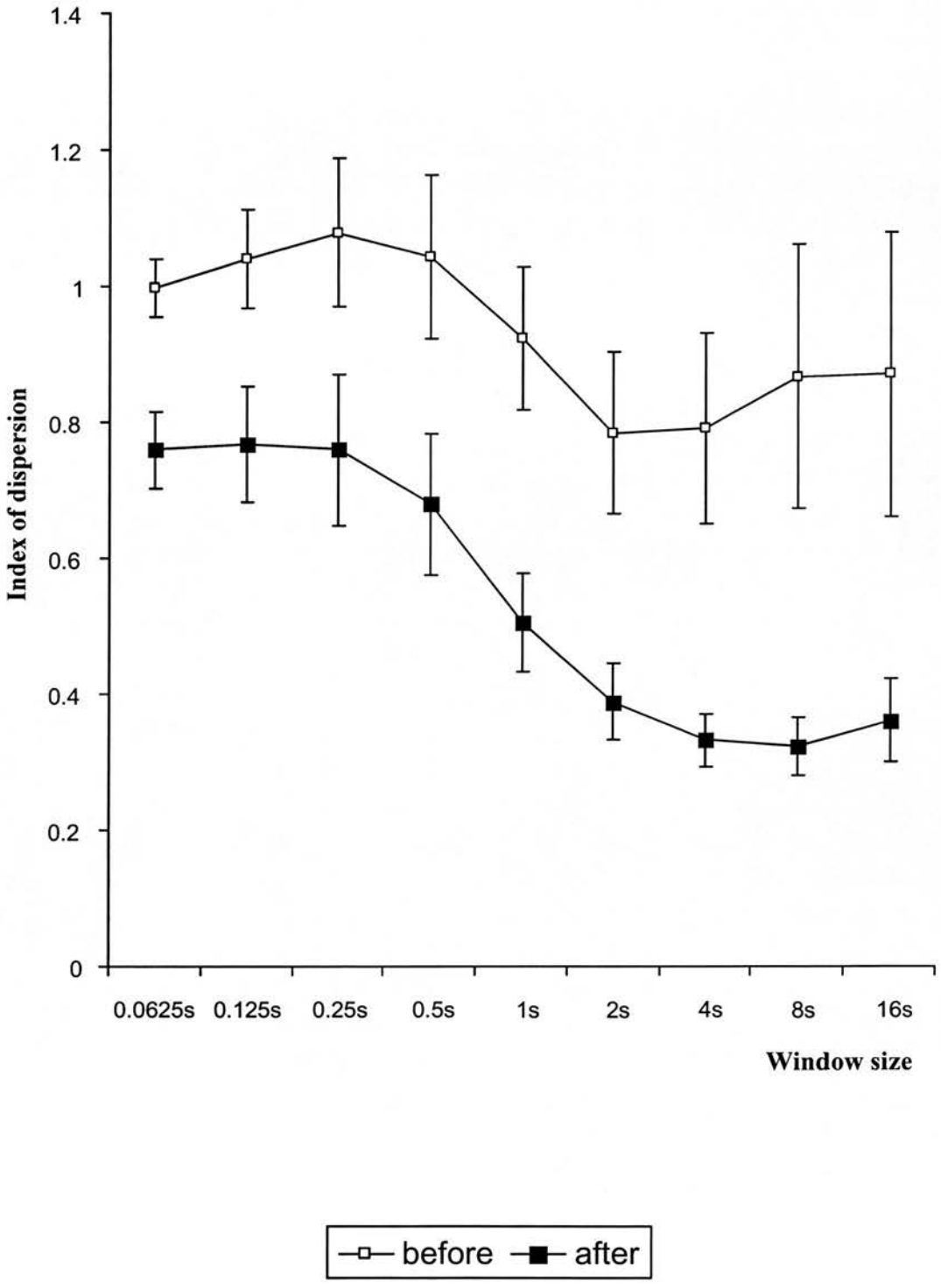
1.4
1.2
1
0.8
0.6
0.4
0.2
0
Index of dispersion
0.0625s
0.125s
0.25s
0.5s
1s
2s
4s
8s
16s
Window size
before
after

Figure 3.11 Linear regressions for index of dispersion vs the mean firing rate for window 0.0625 s for non-lactating (solid black) and lactating (dashed black) neurones, and linear regressions for index of dispersion vs the mean firing rate for window 16 s for non-lacating (solid red) and lactating (dashed red) neurones.

For each individual neurone the index of dispersion for window 0.0625 s was plotted against the corresponding mean firing rate in spikes/ s. A linear regression analysis was performed for the neurones of the non-lactating group, and a separate linear regression for lactating neurones. The same was repeated for window 16 s. For both non-lactating and lactating neurones there is a negative correlation for any window size, i.e. the faster the mean firing rate the more ordered the firing appears to be.
The linear regression slopes for both groups are the same for the window size 0.0625 s (black), but for window 16 s (red) the slope for the lactating group (dashed) is much steeper. While the slope for the non-lactating group (solid) remains the same for both window sizes, for the lactating group (dashed) the slope becomes progressively steeper with increased window size.

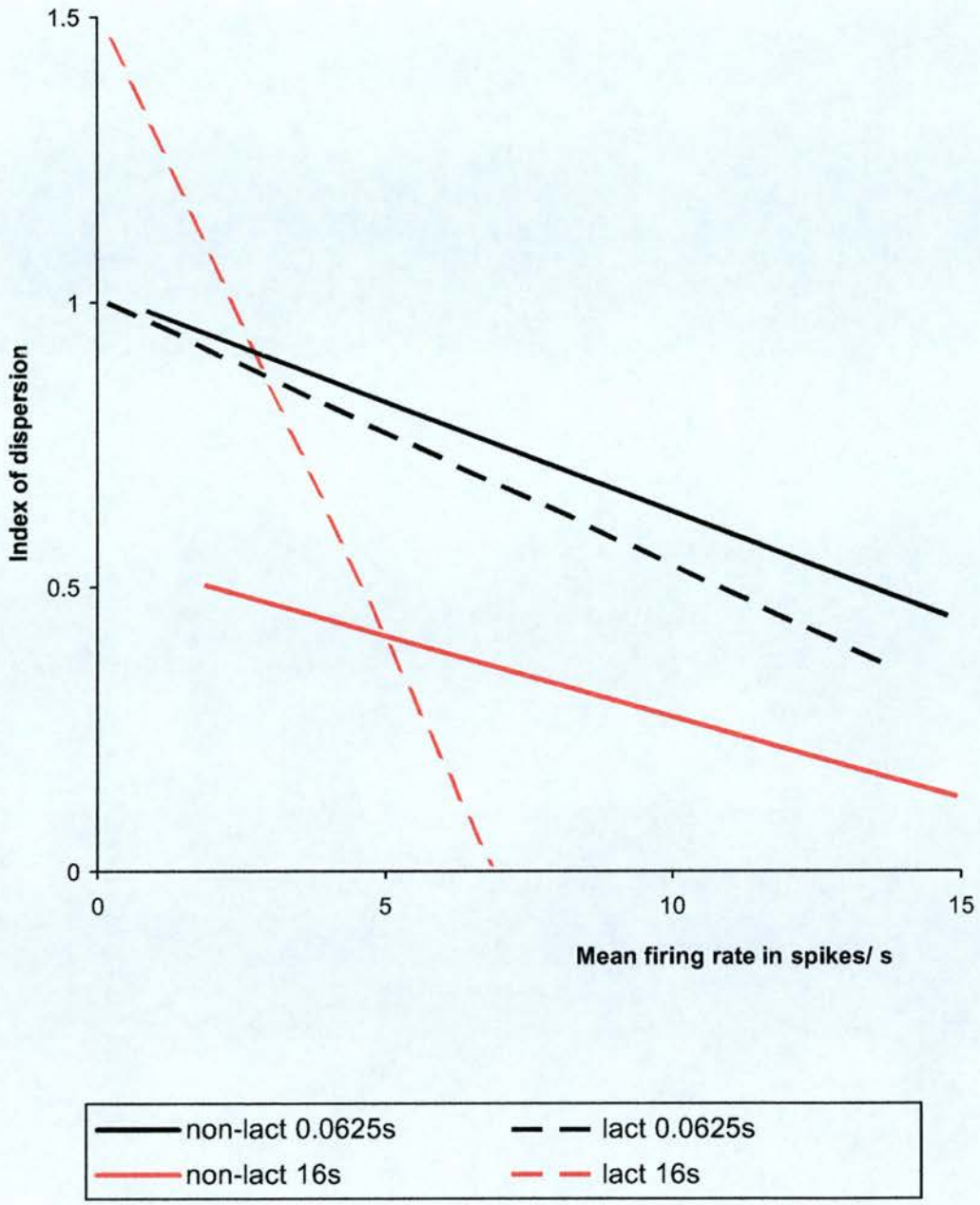
1.5
1
0.5
0
Index of dispersion
0
5
10
15
Mean firing rate in spikes/ s
non-lact 0.0625s
lact 0.0625s
non-lact 16s
lact 16s

Figure 3.12 Indexes of dispersion for all non-lactating (A) and all lactating (B) neurones for all windows plotted against the corresponding firing rate in spikes/ s, and linear regression for each window.

Each individual index of dispersion for every window of every neurone was plotted against the corresponding mean firing rate. Linear regressions were calculated for all values for each window. A negative regression was found in all cases, indicating that the faster the firing rate, the more ordered the firing appears, regardless of window size.
While for both the lactating and the non-lactating group the regression was negative, for non-lactating neurones (A) the slope remained relatively constant throughout the window sizes. For the lactating neurones (B), in contrast, the slope becomes progressively steeper with increases in window size.

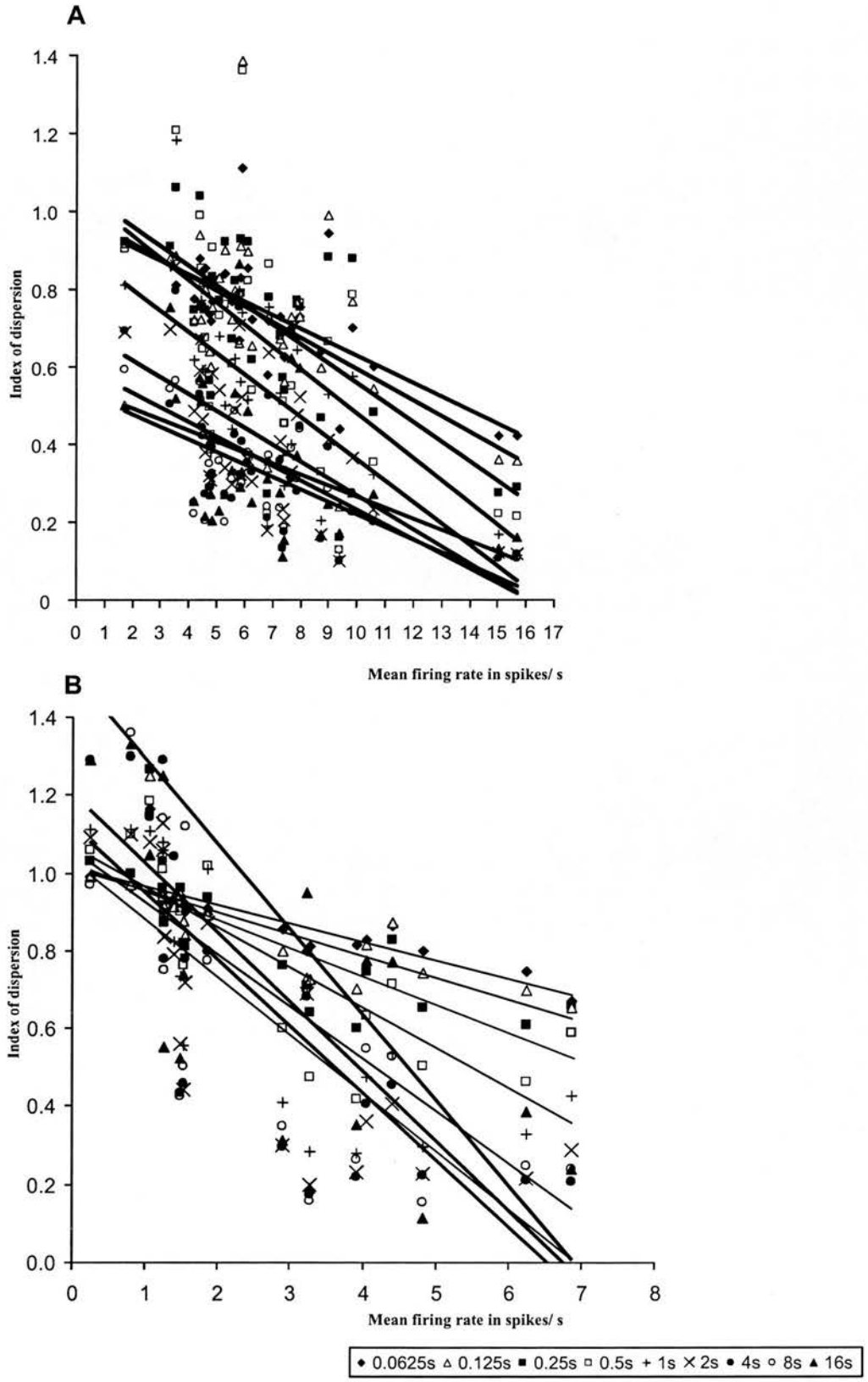
A
Index of dispersion
Mean firing rate in spikes/ s
B
Index of dispersion
Mean firing rate in spikes/ s
◆ 0.0625s △ 0.125s ■ 0.25s □ 0.5s + 1s × 2s ● 4s ○ 8s ▲ 16s

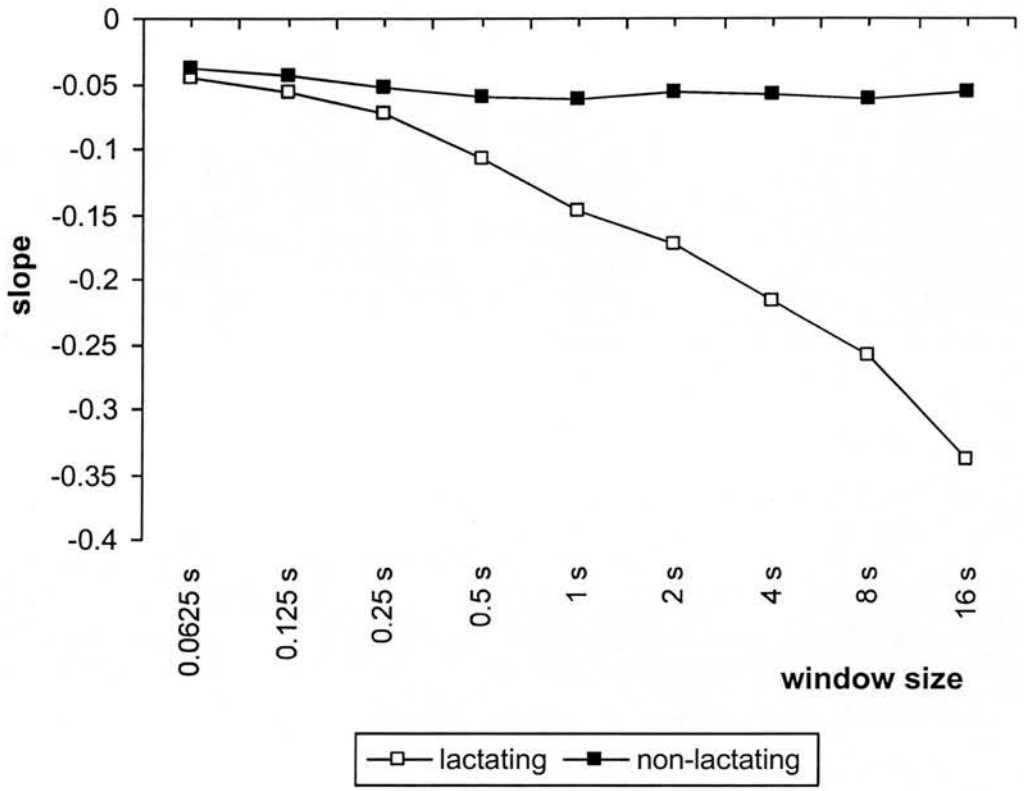

Figure 3.13 Slope of the linear regression analysis between the index of dispersion and the mean firing rate for different window sizes for non-lacating neurones (solid squares) and lactating neurones (open squares).

The slope for both groups is always negative, indicating that the faster the mean firing rate is the more ordered the firing. While the slope for both groups is approx. the same for the 2 smallest window sizes (0.0625 and 0.125 s) they show different behaviour afterwards: the slope for the non-lactating group remains around the same value (-0.06) while the slope for the lactating group becomes significantly steeper (-0.35 for window size of 16s).
This indicates that for non-lactating neurones the relationship between firing rates and the regularity of firing remains constant, but in lactating neurones it becomes more pronounced when looking at a larger time scale.

Figure 3.14 How the autocorrelation and the partial autocorrelation were calculated.

Autocorrelation refers to the serial dependence of the observations in a time series. It is measured by the autocorrelation function (ACF) and the partial autocorrelation function (PACF), which are used for summarising patterns of serial dependence. The pattern of autocorrelation in a time series is described by the autocorrelation coefficients. These measure the correlation between observations at different times apart or lags. To illustrate how we calculated the autocorrelation coefficients consider Figure 3.14.
Figure 3.14a shows the firing rate in spikes/ s. This firing activity is placed in bins with width 1s, or windows of size 1s. These are shown in Figure 3.14b and are the observations between which the autocorrelation is calculated. An autocorrelation between successive observations, e.g. t and t+1 is measured by the autocorrelation coefficient of lag1.
The autocorrelation between t and t+2 is measured by the autocorrelation coefficient of lag 2 and so on. This convention is valid independent of the window size, as can be seen in Figure 3.14c. The autocorrelation coefficient of lag k is calculated according to the following formula:

$$r_k = \frac{\sum_{t=1}^{n-k} (y_t - \bar{y})(y_{t+k} - \bar{y})}{\sum_{t=1}^{n} (y_t - \bar{y})^2}$$

The autocorrelation function (ACF) is a graph showing the autocorrelation coefficient r_k plotted against the lag k (cf. Figure 3.15).
Partial autocorrelation is a related concept. Partial autocorrelation measures the correlation between two observations at different lags. It does, however, take into account the effect of autocorrelation at intermediate lags. So for example, a partial autocorrelation of lag 2 is the autocorrelation between observations at t and observations at t+2 after allowing for the autocorrelation between observations at t and t+1 and the autocorrelation between t+1 and t+2. The general formula to calculate the partial autocorrelation coefficient of lag k is rather complicated, hence we will present here as an example the formula for partial autocorrelation of lag 2 only:

$$r_{2.1} = \frac{r_2 - r_1^2}{1 - r_1^2}$$

where r_1 and r_2 are the autocorrelation coefficients of lag 1 and lag 2, respectively.

The partial autocorrelation coefficient plotted against the corresponding lag is called the partial autocorrelation function (PACF).

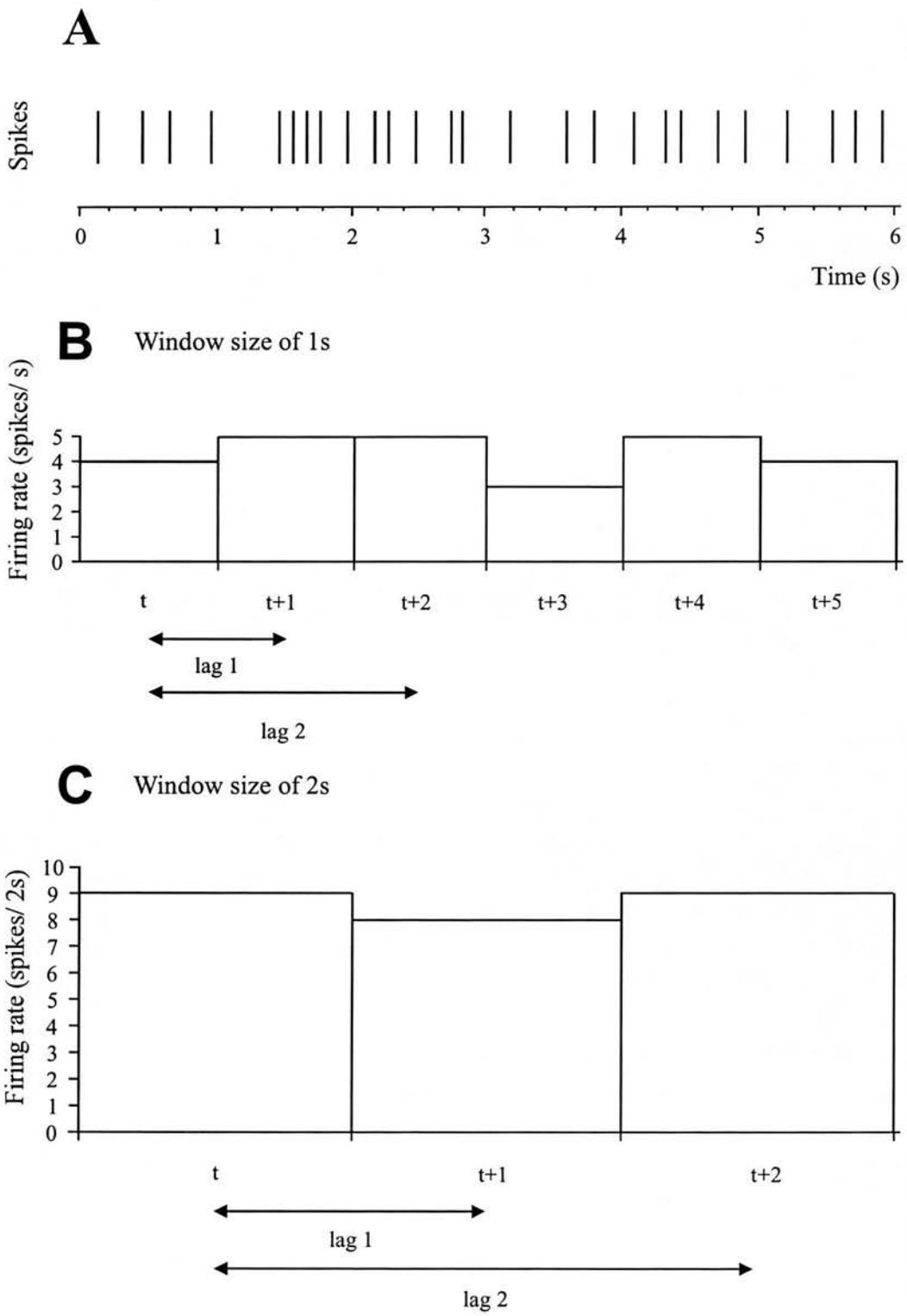
A
Spikes
0
1
2
3
4
5
6
Time (s)
B
Window size of 1s
Firing rate (spikes/ s)
5
4
3
2
1
0
t
t+1
t+2
t+3
t+4
t+5
lag 1
lag 2
C
Window size of 2s
Firing rate (spikes/ 2s)
10
9
8
7
6
5
4
3
2
1
0
t
t+1
t+2
lag 1
lag 2

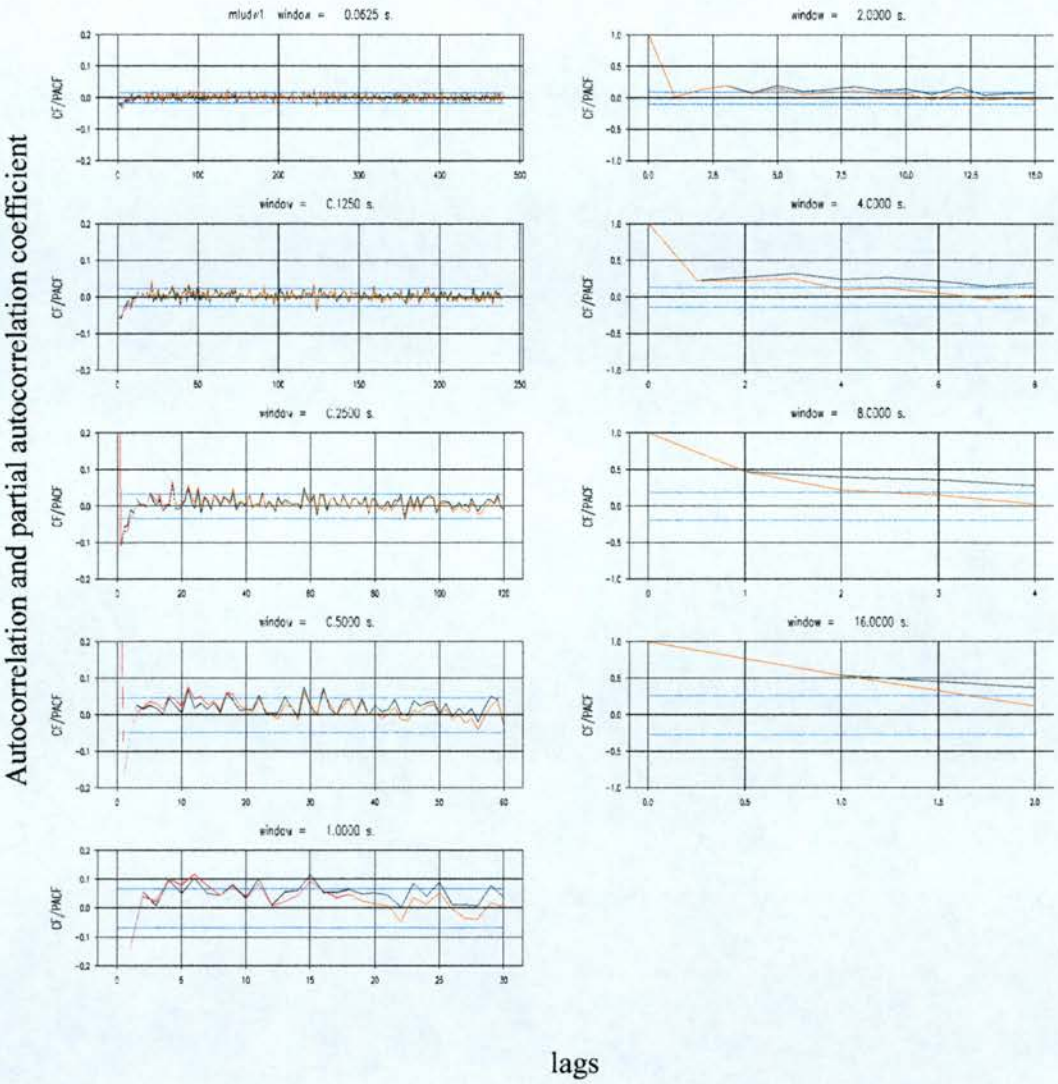

Figure 3.15 Example of a autocorrelation function (ACF, black), and a partial autocorrelation function (PACF, red) for different window sizes for one neurone. 95% confidence interval is plotted as dashed line both sides along zero.

For further explanation cf. Figure 3.14.
There is a significant negative autocorrelation for the first few lags in window size of 0.0625 s, 0.125 s, 0.25 s, 0.5 s and 1 s.
For window size >1 s the autocorrelation is positive for the first lags.

Figure 3.16 Summary of autocorrelations by group.

Each figure shows the number of autocorrelations for the first few lags for window sizes of 0.0625s, 0.125 s, ... and 16 s for
A) all neurones combined
B) naïve neurones
C) pregnant neurones
D) lactating and suckling neurones
E) neurones before hyperosmotic stimulation
F) neurones after hyperosmotic stimulation.

Positive autocorrelations are depicted in black, negative autocorrelations are depicted in red. White depicts the number of recordings for which no significant autocorrelations were found.
As can be seen from these figures, at small window sizes - 0.0625 s to 1 s - a negative autocorrelation was found for the majority of recordings analysed. With increased window size (>1 s) the proportion of negative autocorrelation diminishes, and while a few more positive autocorrelation are now evident, for the majority of recordings no significant correlation can be seen.

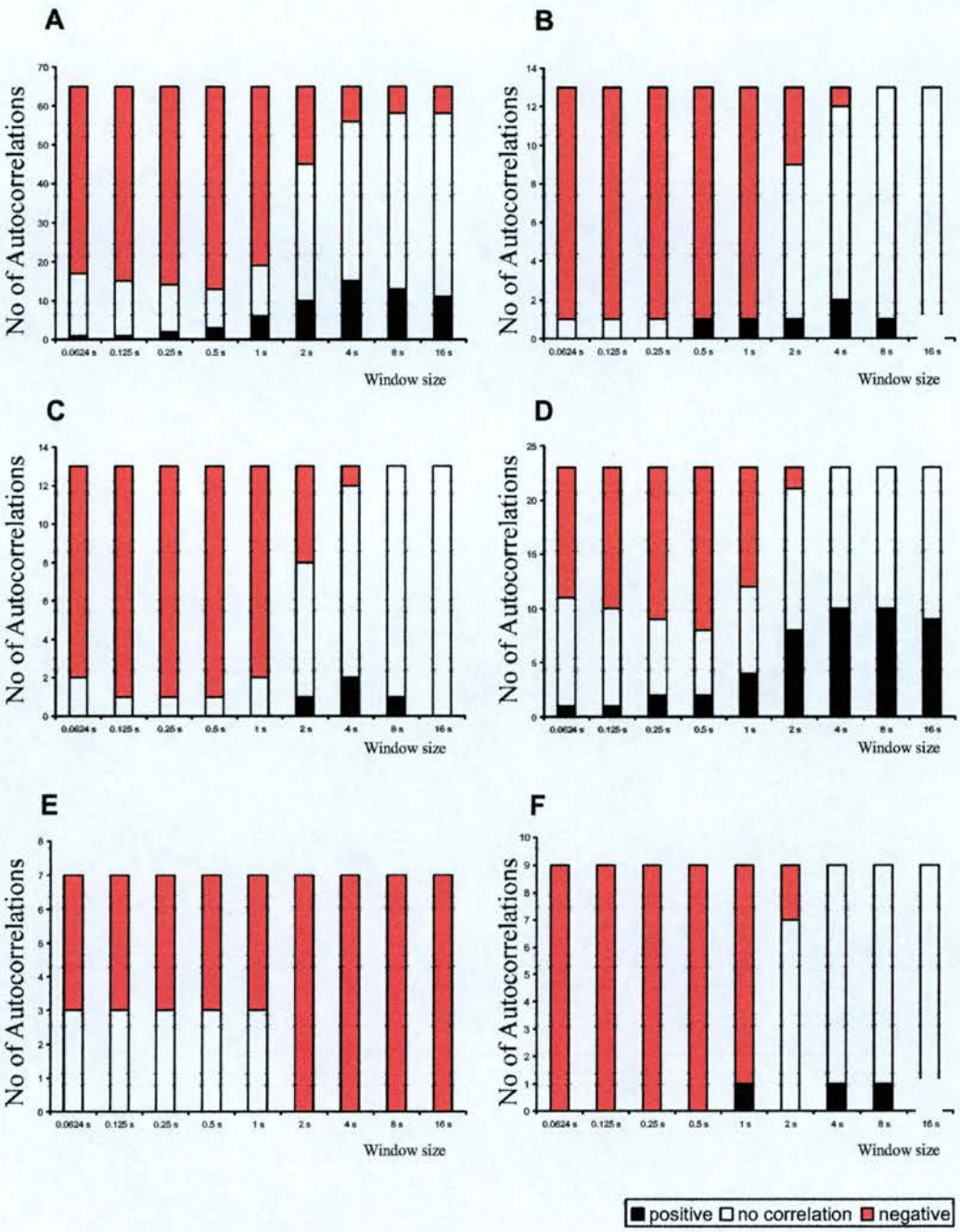
A
B
C
D
E
F
No of Autocorrelations
Window size
0.0624 s
0.125 s
0.25 s
0.5 s
1 s
2 s
4 s
8 s
16 s
positive
no correlation
negative

Cell name	Physiol. state	Mean firing	Index of dispersion 0.0625s	0.125s	0.25s	0.5s	1s	2s	4s	8s	16s
s1	Suckled	1.40	0.932	0.913	0.913	0.911	0.823	0.793	1.042	1.667	2.983
s2	Suckled	1.54	0.918	0.876	0.818	0.761	0.555	0.444	0.458	0.502	0.74
s3	Suckled	1.48	0.942	0.945	0.961	0.901	0.735	0.56	0.434	0.428	0.525
s4	Suckled	3.93	0.814	0.703	0.599	0.418	0.28	0.231	0.219	0.265	0.355
s5	Suckled	3.29	0.81	0.728	0.642	0.476	0.285	0.197	0.173	0.159	0.192
s6	Suckled	2.91	0.856	0.8	0.764	0.6	0.408	0.299	0.298	0.347	0.313
s7	Suckled	1.24	0.93	0.95	0.96	1.04	1.06	1.06	1.03	1.14	1.25
s8	Suckled	1.25	0.95	0.94	0.95	1.01	1.08	1.13	1.29	1.48	1.99
s9	Suckled	1.56	0.9	0.84	0.81	0.82	0.79	0.72	0.78	1.12	1.84
averaged		2.07	0.895	0.855	0.824	0.771	0.668	0.604	0.636	0.790	1.132
	sem	0.34	0.018	0.031	0.045	0.075	0.102	0.115	0.137	0.189	0.320
l1	non-suckled	1.87	0.907	0.893	0.938	1.019	1.012	0.874	0.801	0.776	0.903
l2	non-suckled	0.79	0.96	0.97	1	1.1	1.11	1.1	1.3	1.36	1.33
l3	non-suckled	1.26	0.924	0.914	0.871	0.896	0.895	0.837	0.781	0.752	0.553
l4	non-suckled	0.24	0.99	0.99	1.03	1.06	1.11	1.09	1.29	0.97	1.29
l5*	non-suckled	1.47	0.92	0.94	1.05	1.23	1.52	2.19	3.46	5.92	10.04
l6	non-suckled	6.86	0.668	0.654	0.659	0.587	0.427	0.288	0.208	0.241	0.238
l7	non-suckled	3.24	0.8	0.73	0.71	0.71	0.71	0.69	0.68	0.7	0.95
l8	non-suckled	4.05	0.826	0.815	0.745	0.633	0.473	0.363	0.405	0.547	0.776
l9	non-suckled	4.41	0.863	0.874	0.829	0.715	0.534	0.407	0.455	0.528	0.771
l10	non-suckled	6.24	0.747	0.698	0.609	0.461	0.33	0.215	0.213	0.246	0.384
l11	non-suckled	4.84	0.799	0.744	0.653	0.502	0.298	0.226	0.223	0.153	0.113
l12	non-suckled	1.07	1.164	1.25	1.266	1.184	1.108	1.08	1.144	1.154	1.046
averaged**		2.79	0.889	0.880	0.868	0.834	0.777	0.714	0.765	0.788	0.860
	sem	0.63	0.035	0.044	0.053	0.068	0.090	0.101	0.121	0.132	0.133
	The mean and sem for the lactating group (suckled and unsuckled neurones combined)										
	mean	2.43	0.892	0.868	0.846	0.803	0.723	0.659	0.700	0.789	0.996
	sem	0.40	0.022	0.029	0.036	0.050	0.067	0.075	0.090	0.107	0.151
p1	Pregnant	7.41	0.625	0.561	0.541	0.453	0.293	0.204	0.175	0.186	0.153
p2	Pregnant	7.66	0.7	0.73	0.69	0.55	0.4	0.33	0.31	0.39	0.62
p3	Pregnant	5.85	0.83	0.91	0.93	0.79	0.56	0.32	0.32	0.29	0.29
p4	Pregnant	5.30	0.84	0.9	0.92	0.76	0.5	0.34	0.27	0.2	0.27
p5	Pregnant	4.38	0.88	0.94	1.04	0.99	0.75	0.59	0.53	0.56	0.57
p6	Pregnant	4.43	0.761	0.722	0.758	0.853	0.771	0.672	0.672	0.516	0.509
p7	Pregnant	4.83	0.767	0.754	0.833	0.907	0.821	0.581	0.393	0.324	0.202
p8	Pregnant	6.81	0.58	0.34	0.27	0.22	0.19	0.18	0.21	0.24	0.31
p9	Pregnant	7.88	0.721	0.765	0.773	0.763	0.642	0.475	0.278	0.31	0.373
p10	Pregnant	3.51	0.811	0.885	1.062	1.207	1.182	0.86	0.795	0.563	0.518
p11	Pregnant	5.82	0.667	0.659	0.764	0.783	0.796	0.707	0.753	0.665	0.866
p12	Pregnant	6.85	0.718	0.73	0.777	0.863	0.754	0.637	0.525	0.373	0.357
p13	Pregnant	7.99	0.73	0.729	0.753	0.766	0.755	0.523	0.447	0.439	0.598
averaged		6.06	0.741	0.740	0.778	0.762	0.647	0.494	0.437	0.389	0.434
	sem	0.41	0.024	0.045	0.058	0.068	0.072	0.057	0.057	0.042	0.056
n1	Naïve	5.55	0.767	0.722	0.673	0.608	0.439	0.297	0.261	0.31	0.332
n2	Naïve	4.77	0.717	0.6	0.526	0.425	0.377	0.307	0.322	0.288	0.273
n3	Naïve	4.73	0.734	0.64	0.563	0.496	0.421	0.318	0.29	0.349	0.407
n4	Naïve	1.7	0.918	0.918	0.923	0.904	0.812	0.69	0.693	0.592	0.5
n5	Naïve	4.58	0.855	0.799	0.745	0.674	0.584	0.379	0.272	0.205	0.215
n6	Naïve	4.49	0.847	0.818	0.753	0.646	0.592	0.463	0.443	0.42	0.557
n7	Naïve	9.37	0.44	0.24	0.16	0.13	0.11	0.1	0.1	0.13	0.17
n8	Naïve	8.99	0.944	0.991	0.882	0.665	0.53	0.409	0.393	0.287	0.247
n9	Naïve	7.34	0.69	0.658	0.572	0.51	0.371	0.231	0.135	0.132	0.112
n10	Naïve	10.6	0.599	0.542	0.482	0.353	0.323	0.231	0.201	0.218	0.271
n11	Naïve	9.83	0.699	0.767	0.878	0.784	0.576	0.363	0.275	0.225	0.276
n12	Naïve	15.7	0.42	0.356	0.291	0.216	0.114	0.118	0.119	0.107	0.161
n13	Naïve	4.19	0.776	0.723	0.746	0.715	0.618	0.486	0.249	0.223	0.254
averaged		7.06	0.724	0.675	0.630	0.548	0.451	0.338	0.289	0.268	0.290
	sem	1.03	0.045	0.058	0.064	0.062	0.055	0.044	0.044	0.037	0.036

a1	After stimulation	3.32	0.864	0.877	0.912	0.909	0.859	0.697	0.504	0.543	0.754
a2	After stimulation	5.67	0.78	0.798	0.821	0.78	0.62	0.488	0.426	0.485	0.532
a3	After stimulation	5.90	1.11	1.384	1.566	1.362	0.741	0.522	0.406	0.299	0.327
a4	After stimulation	8.71	0.639	0.595	0.467	0.327	0.202	0.167	0.157	0.157	0.169
a5	After stimulation	15.02	0.421	0.359	0.275	0.222	0.167	0.123	0.107	0.106	0.133
a6	After stimulation	6.28	0.722	0.653	0.618	0.54	0.37	0.303	0.333	0.33	0.251
a7	After stimulation	6.09	0.852	0.898	0.922	0.823	0.515	0.362	0.353	0.38	0.486
a8	After stimulation	12.68	0.647	0.609	0.554	0.417	0.36	0.275	0.27	0.323	0.452
a9	After stimulation	7.26	0.728	0.671	0.681	0.678	0.531	0.407	0.356	0.235	0.275
a10	After stimulation	5.12	0.829	0.828	0.772	0.731	0.678	0.541	0.406	0.358	0.227
averaged		7.61	0.759	0.767	0.759	0.679	0.504	0.389	0.332	0.322	0.361
	sem	1.14	0.057	0.085	0.110	0.104	0.072	0.056	0.039	0.042	0.061

I13	Lactating, before	0.80	0.95	0.92	0.97	0.98	1	0.97	1.32	1.8	1.88
I14	Lactating, before	0.64	0.96	0.99	1	1	1.1	1.14	1.12	1.02	0.95
b1	Before stimulation	3.50	1.22	1.459	1.72	1.671	1.141	0.718	0.659	0.438	0.353
b2	Before stimulation	2.13	0.892	0.831	0.724	0.553	0.399	0.257	0.232	0.254	0.181
b3	Before stimulation	5.17	0.878	0.883	0.854	0.822	0.656	0.47	0.455	0.412	0.542
b4	Before stimulation	0.70	0.983	0.998	1.027	1.024	1.119	1.161	1.226	1.463	1.538
b5	Before stimulation	2.85	0.959	1.006	1.034	0.931	0.715	0.552	0.5	0.574	0.542
b6	Before stimulation	3.07	1.146	1.23	1.3	1.356	1.245	0.997	0.812	0.965	0.971
averaged		2.36	0.999	1.040	1.079	1.042	0.922	0.783	0.791	0.866	0.870
	sem	0.57	0.043	0.073	0.108	0.120	0.105	0.118	0.140	0.194	0.209

*outlier, excluded from analysis
**includes I13 and I14 from the before stimulation group

Table 3.1 Overview of all stretches analysed, their firing rates in spikes/ s and their indexes of dispersion.

groups	lac1	lac2	lac3	lac4	lac5	lac6	lac7	lac8	lac9	non1	non2	non3	non4	non5	non6	non7	non8	non9	groups
lac1		no	no	no	yes	yes	yes	no	no	no	no	no	no	yes	yes	yes	yes	yes	lac1
lac2			no	no	no	yes	no	no	no	no	no	no	no	yes	yes	yes	yes	yes	lac2
lac3				no	no	yes	no	no	no	no	no	no	no	yes	yes	yes	yes	yes	lac3
lac4					no	no	no	no	yes	no	no	no	no	yes	yes	yes	yes	yes	lac4
lac5						no	no	no	yes	no	no	no	no	no	yes	yes	yes	yes	lac5
lac6							no	no	yes	no	no	no	no	no	yes	yes	yes	yes	lac6
lac7								no	yes	no	no	no	no	no	yes	yes	yes	yes	lac7
lac8									yes	no	no	no	no	yes	yes	yes	yes	yes	lac8
lac9										yes	yes	yes	yes	yes	yes	yes	yes	yes	lac9
non1											no	no	no	yes	yes	yes	yes	yes	non1
non2												no	no	yes	yes	yes	yes	yes	non2
non3													no	yes	yes	yes	yes	yes	non3
non4														yes	yes	yes	yes	yes	non4
non5															yes	yes	yes	yes	non5
non6																no	no	no	non6
non7																	no	no	non7
non8																		no	non8
non9																			non9

Tab. 3.2 The results of the post-hoc Bonferroni all pairwise t-test.

Labels are constructed as follows: lac is from the lactating group, non is from the non-lactating group, 1 is window 0.0625 s, 2 is window 0.125 s, 3 is window 0.25 s, ..., 9 is window 16 s.

window	0.0625 s	0.125 s	0.25 s	0.5 s	1 s	2 s	4 s	8 s	16 s
lactating	-0.0461	-0.0559	-0.0733	-0.1079	-0.1469	-0.1735	-0.2159	-0.2585	-0.3374
non-lactating	-0.0381	-0.0445	-0.0534	-0.0603	-0.0615	-0.0561	-0.0578	-0.0623	-0.0567

Table 3.3 Linear regression analysis for each window size for the indicies of dispersion vs mean firing rates, for both lactating and non-lactating neurones.

For each individual neurone within the lactating and separately non-lactating group the index of dispersion for one window was plotted vs the corresponding mean firing rate. This was repeated for every window. A linear regression analysis was performed for all values for each window. The results are shown in the table, the regression function given in the form y=mx+b.

	0.0624 s	0.125 s	0.25 s	0.5 s	1 s	2 s	4 s	8 s	16 s
	suckled								
negative corr	6	6	6	7	5	1	0	0	0
no corr	3	3	2	1	1	4	3	4	4
positive corr	0	0	1	1	3	4	6	5	5
	lactating								
negative corr	6	7	8	8	6	1	0	0	0
no corr	7	6	5	5	7	9	10	9	10
positive corr	1	1	1	1	1	4	4	5	4
	pregnant								
negative corr	11	12	12	12	11	5	1	0	0
no corr	2	1	1	1	2	7	10	12	13
positive corr	0	0	0	0	0	1	2	1	0
	naïve								
negative corr	12	12	12	12	12	4	1	0	0
no corr	1	1	1	0	0	8	10	12	12
positive corr	0	0	0	1	1	1	2	1	1
	after								
negative corr	9	9	9	9	8	2	0	0	0
no corr	0	0	0	0	0	7	8	8	8
positive corr	0	0	0	0	1	0	1	1	1
	before								
negative corr	4	4	4	4	4	7	7	7	7
no corr	3	3	3	3	3	0	0	0	0
positive corr	0	0	0	0	0	0	0	0	0
	combined								
negative corr	48	50	51	52	46	20	9	7	7
no corr	16	14	12	10	13	35	41	45	47
positive corr	1	1	2	3	6	10	15	13	11

Table 3.4 Summary of autocorrelations.

For each group and each window size the number of neurones displaying a negative, positive, or no autocorrelation for small lags is shown, plus the combined total.

CHAPTER FOUR

INTERSPIKE INTERVAL ANALYSES

The advantage of the firing rate analysis is that it is a natural and obvious first step, since it uses the spike data the form in which they are most commonly collected and described. However, it also has its limitations. For instance, a cluster of 5 spikes with ISIs of 50 ms followed by a silent period of 750 ms, which would result in a firing rate of 5 Hz for this 1-s period, but so will 5 spikes with interspike intervals (ISIs) of 200 ms – yet these two patterns clearly are fundamentally different. Therefore, results obtained from firing rate analyses and 'translated' back to the relationship between individual spikes might be misleading.

To investigate the non-randomness in the firing we found with the analyses of firing rates in more detail we consider the relationship between individual successive ISIs, or more specifically how the length of an ISI influences the length of the next ISI.

There are two main types of analyses we could have used to measure the relationship between ISI. To predict a trend in data, or to measure how the value of one variable influences the value of another variable one can fit a straight line through the data and perform a simple linear regression. If the *strength* of the association between two variables is to be measured, the Pearson's Product Moment Correlation (a parametric measure of correlation between two variables, which are of interval or ratio level) can be used instead, but this test does not reveal the causal relationship between variables. The Pearson's Product Moment Correlation does not take into account which variable is dependent and which independent, and whether the relationship between them – if any – takes the form of a straight line. In contrast, regressions predict the value of the dependent variable based on the value of one or more independent variables, and they assume that the relationship between them

takes the form of a straight line (in the case of linear regressions) when plotted in the Cartesian co-ordinate system.

To start with, we decided to use simple linear regressions to predict the length of an ISI from the length of the immediately preceding ISI, or to put it another way, to see how the length of one ISI influences the length of the *next* ISI.

4.1 Investigating the Relationship Between Individual ISIs

Linear regression gives the straight line that most closely describes, or predicts the value of the dependent variable – in our case the succeeding ISI –, given the observed value of the independent variable – the current ISI. Linear regression results consist of an equation for a straight line and a coefficient of determination – the r^2 value – which is a measure of how well the regression model describes the data. The r^2 value can be interpreted as the proportion of the variance in the dependent variable attributable to the variance in the independent variable (in contrast to the r value – the correlation coefficient – which takes values in the range of –1 to +1 and measures the degree of linear association between two variates). It takes values in the range of 0 to +1 and measures the closeness of fit of the scattergraph to its regression line – the closer r^2 values are to 1 the better the line describes the data: When r^2 equals 0 the independent variable does not allow any prediction of the dependent variable, while when r^2 equals 1 the dependent variable can be predicted perfectly from the independent variable. However, it should be remembered that r^2 is dependent on the amount of data over which the linear regression is fitted, with an increase in data making it less likely that a simple line describes all of the points. To put it bluntly, a line fitted to two points will fit perfectly, while with each additional point a perfect fit becomes less likely. Therefore, the r^2 value is used for indicating how much of the data is 'explained' by a dependent relationship between two variables (as opposed to stochastic variation). However, it does not say anything about the strength of the relationship, nor does it say whether the relationship is statistically significant – a low r^2 value may be

associated with a highly significant correlation, and vice versa. For this reasons the r^2 values in our analyses are of little importance to us and we will concentrate on the equations that describe the dependent variable given the independent variable.

4.1.1 Methods

ISIs were calculated from spontaneous extracellular *in vivo* recordings of oxytocin neurones (cf. Chapter 2 for methods for data gathering and sample description). As oxytocin neurones will not display ISIs shorter than 40 ms during background activity, and even during bursting display ISIs in the range of 8-14 ms (Dyball & Leng, 1986) ISIs shorter than 7 ms were presumed to be noise. In order to ensure that we analysed only true ISIs events occurring after an ISI of less then 7 ms were deleted and the ISIs were recalculated. It should be stressed that the recordings had only very few of these events – indeed many had none at all, but as the effects we were looking for could be expected to be of particular influence on very short ISIs it was of paramount importance to perform the analyses only on genuine action potentials. More recently a novel way of spike discrimination – based on digital shape evaluation – has been suggested (Dyball & Bhumbra, 2003). However, this method is still in its infancy and requires the additional tracing of action potential shapes (in addition to recording spike arrival times), which was not available for our data. This method appears to be promising for recordings containing a lot of noise, but in view of the quality of our recordings digital shape evaluation the effort-to-gain-ratio does not justify its use.

ISIs were left in the order derived from the recording and placed in a list. ISIs were 'coupled' or linked with the immediately succeeding ISIs, i.e. t_1 was coupled with t_0, t_2 with t_1, and so on (recall the nomenclature given in Figure 3.5). This ensured that throughout the next steps of the analysis the relationship between successive intervals is preserved. Hereafter, t_1 is treated as the *current* ISI and designated to be the dependent variable for the regression analysis, as it makes more sense in this case to look at how the length of one ISI influences the length of the next ISI, rather than look at what an ISI can tell about the previous ISI. The whole

procedure resulted in two lists, one being for the current ISIs and one for the immediately succeeding ISIs, which form the bases of all further steps.

The pairs of coupled ISIs were sorted in ascending order of t_1, so the ISIs are sorted from the shortest to the longest, while the succeeding ISIs are not sorted by their own length but by the *length of the ISIs they are coupled to*. If we were to perform a regression analysis at this point and plot the current against the succeeding ISIs this would result in a 'cloud' of data, which makes it impossible to see a trend (even though the regression equation would still be correct; Figure 4.1). In order to make trends more visible the data was averaged before further examination. Thus, from the new order the current and the succeeding ISIs were averaged in group-sizes that depended on the overall amount of data available for analysis, e.g. for lists of around 1000 ISIs or more the averages were derived for groups of 200 ISIs, while lists of more than 3000 ISIs were averaged in groups of 500. This was done for the sake of clarity, as this uncovers the main trends in the data amongst hugely variable individual points. The standard error of means for t_1 was also calculated.

Our oxytocin data is not normally distributed. In order to achieve a normal distribution for the analysis we log transformed the succeeding ISIs, the standard way to treat data that is exponentially distributed. Obviously, this method is only applicable to exponentially distributed data. We then proceeded again as above, sorting the pairs according to t_1 and averaging the log-transformed succeeding ISIs, and calculating the standard error of means. The resulting averaged values for the log transformed t_0 were exponentiated – or inverse log transformed – to return them to the original scale. The standard error of means are asymmetrical in the log scale and we wanted to preserve this asymmetry. In the log scale, the upper limit was determined by adding the absolute value of the standard error to the corresponding log t_0, i.e. the position of the upper end of the error as plotted on the Cartesian co-ordinate system, and the lower limit by subtracting the standard error from log t_0, i.e. the lower end of the error as plotted on the Cartesian co-ordinate system. These values in turn were exponentiated, and in the original scale the corresponding t_0 was subtracted from the upper limit and the lower limit was subtracted from the

corresponding t_0, thus deriving at an asymmetrical standard error of means in the original scale. Each ISI was then plotted against the succeeding ISI, i.e. t_1 against t_0 together with the corresponding standard error of means (Figures 4.2 and 4.3) and a linear regression analysis was performed.

4.1.2 Results

Scattergrams from several recordings indicated that the short ISIs (length varying between recordings, but usually in the range of up to ~100 ms, see below) follow a different trend to the rest of the ISIs. For these, the above-described procedure was repeated, but this time the short ISIs were averaged in smaller group-size to avoid 'diluting' effects in this range by the counter-balancing effects of intervals with relatively higher t_0 values. A linear regression analysis was performed for the short ISIs in addition to the linear regression analysis for the rest of the values (Figures 4.4 and 4.5).

Altogether, the linear regression analyses shows that from 65 stretches of recordings analysed only 15 (or 23%) have a positive slope, the remainder display a negative slope. The positive slopes are distributed between the different physiological groups as follows (Table 4.1):

- no positive slopes for the 9 lactating-suckled recordings
- 2 positive slopes out of 14 lactating non-suckled recordings (or 14%)
- 6 positive slopes out of 13 pregnant recordings (or 46%)
- 2 positive slopes out of 13 naïve recordings (or 15%)
- 2 positive slopes out of 8 before recordings (or 25%)
- 4 positive slopes out of 10 after recordings (or 40%)

The mean slope for each group was –0.199±0.031 (mean±standard error of means), –0.091±0.025, 0.018±0.02, –0.048±0.022, –0.1±0.046 and –0.023±0.015 for suckled, non-suckled, pregnant, naïve, before and after hyperosmotic stimulation recordings, respectively. Please note, only the averaged slope from pregnant recordings is positive.

One-way ANOVA show the slopes of the groups to be significantly ($p<0.001$) different. A post-hoc all pairwise multiple comparison procedure (Tukey test) reveals significant differences ($p<0.05$ as the significance level) between the mean slopes of (a) [suckled] *and* [non-suckled, pregnant, naïve and after hyperosmotic stimulation] groups, (b) non-suckled *and* pregnant groups, and (c) pregnant *and* before hyperosmotic stimulation groups. Together these analyses indicate that the slopes of the linear regression analyses for the suckled group are significantly more negative then all but one other group (before hyperosmotic stimulation), and the slopes of the pregnant group are significantly different from all but the after hyperosmotic stimulation group – not surprisingly, since this is the only group with a positive average slope.

4.1.3 Effects in the Range of Very Short ISIs

In addition, the linear regression analyses of short ISIs showed that 27 (or 42%) of the 65 recordings display a different trend in the range of short ISIs compared to the remaining ISIs. The difficulty here is to define 'short' precisely, because it has to be seen in context, compared to the lengths of the remaining ISIs for the same recording. Recordings for which the linear regression analyses do not reveal a different trend for 'short' ISIs also display ISI lengths in the same, short ISI range, so no absolute value for the range or threshold of ISI lengths that we can call 'short' can be given. Further exploration of this issue is given below.

The majority of these results have a positive slope, only two displaying a negative slope. The occurrence of an additional effect for short ISI is similar for the different groups: 4 (or 44%), 5 (or 36%), 5 (or 38%), 6 (or 46%), 3 (or 38%), and 4 (or 40%) recordings for suckled, non-suckled, pregnant, naïve, before and after groups, respectively (Table 4.1). To compare the slopes of the linear regression for short ISIs, slopes from the regression analyses of all the ISIs are included for the cases where no additional effect could be detected, as these slopes are calculated over the whole range of ISI lengths – including very short ones. A one-way analysis

of variance (ANOVA) shows no significant differences between mean slopes of all the groups.

These results indicate that in the majority of cases analysed the length of a ISI is inversely related to the length of the immediately succeeding ISI, i.e. a short ISI is likely to be followed by a longer ISI, and vice versa. Also, for approx. 40% of all the recordings for very short ISI (see above) the reverse is true: a positive regression indicates that a very short ISI is followed by another very short ISI. This positive regression appears in approx. the same proportion in each group – namely around 40%. Thus its occurrence cannot be attributed to any particular physiological state of the animal.

As mentioned before, the difficulty is to find a precise definition of 'very short' ISIs that is valid for all of the recordings, since the average length of ISIs up to which the effect is apparent is 70 ms, with a wide range of 20 to 200 ms. Also, small ISIs are apparent in both recordings that do and recordings that do not display a separate linear regression slope in the range of very small ISIs. Further exploration of this issue involves a linear regression analysis between the slopes for the very small ISIs – positive or otherwise – and the index of dispersion. The result shows a positive slope: for small indexes the slopes tend to also be small, indicating that for ordered firing the relationship between successive very small ISIs disappears. No regression was found when we repeated this analysis for relatively longer ISIs.

Intuitively, this outcome makes sense: for ordered, regular firing there are presumably few very short ISIs, and when they occur they occur not in clusters – i.e. followed by further short ISIs – but in isolation – followed by slightly longer ISIs. Hence, very short ISIs are seldom neighbouring but usually spaced further apart and no influence between them is possible.

A Pearson's Product Moment Correlation for the firing rate and the slopes of very small ISIs shows no significant relationship between the two, thus confirming that a faster firing rate does not automatically produce (very) *short* ISIs – although of course average ISIs during fast firing activity will be *shorter* than average ISIs for slow activity (cf. Table 2.1 and 3.1). A further Pearson's Product Moment

Correlation analysis between the indexes of dispersion for different window sizes (as determined and discussed in the previous chapter; cf. section 3.3.1) and the slopes for very small ISIs –whether positive or otherwise – revealed a significant positive correlation, but only for windows sizes smaller than 1 s: $r=0.32$, $p<0.05$; $r=0.35$, $p<0.01$; $r=0.36$, $p<0.01$; $r=0.3$, $p<0.05$ for window sizes of 0.0625 s, 0.125 s, 0.25 s and 0.5 s, respectively. The analyses for larger window sizes are not significant. This indicates that, when the firing appears to be irregular on a short time scale (as indicated by a large index of dispersion) then there is the tendency for the slope to be large. The explanation is that irregular firing has more scope for clustered firing, where very small ISIs are followed by further very short ISIs. These could produce favourable conditions for the appearance of an additional positive effect in the range of very small ISIs.

4.2 Investigating the Influence of the History of Previous ISIs

The firing rate analysis considered the relationship between periods of activity in oxytocin cells, while the individual interspike interval analysis has only considered the relationship between successive intervals. How does a *period* of activity influence the *individual* interspike interval? How long exactly is the duration of the underlying mechanism, i.e. what is the time scale of the effect that exerts an influence on the individual interval?

Also, for the analysis of periods of activity, firing rates were calculated for fixed bins, e.g. 1 s, regardless of the number of spikes occurring. In this analysis we look at the influence of a fixed number of preceding spikes, independent of the amount of time which they require. Thus, this analysis is independent of any arbitrarily chosen time constraints, as e.g. 100 spikes at a firing frequency of 2 Hz occur within 50 s, while the same number of spikes at a frequency of 5 Hz occur within 20 s.

In order to look at the relationship between the periods of activity and individual spikes and determine how long the underlying effect lasts during spontaneous electrical activity we calculated – similar to the analysis above – t_0

against t_1, t_0 against t_1+t_2, t_0 against $t_1+t_2+t_3$, and so on until t_0 against $t_1+\ldots+t_n$, with varying n.

4.2.1 Methods

The analysis started with a list of all ISIs. Next, the sums of the length of 2, 3, 4, 5, 6, 7, 8, 9, 10, 15, 20, 50, 100 and (subject to sufficient data) 200 preceding ISIs were calculated. The ISI and the sum of the lengths of the preceding intervals were coupled and sorted in ascending order according to the length of the sum. Both the sums and the associated intervals were averaged in group sizes dictated by the amount of data available. Also, the standard errors of means were calculated. The averaged ISIs were plotted against the associated averaged sum of preceding ISIs.

For each recording the analysis was repeated for the whole range of sums, i.e. 2 to 200 previous ISIs were summated. A linear regression analysis was performed for each of the plots of ISI against sum of preceding ISIs. The resulting slopes were compared for all the sums for each recording, between the recordings in each group of recordings, and for the averages between the groups (Figure 4.6).

4.2.2 Results

Of the 65 recordings analysed in this way, only 5 display positive slopes for one of the sums of the previous intervals. All the remaining slopes are negative (cf. Table 4.2).

Generally, the slope of the regression analyses is steepest for the sum of the last 2 to 6 ISIs. For each additional ISI integrated in the sum the slope decreases slowly towards zero. However, there are differences between the groups (Figure 4.7).

For all but the two lactating groups the slope is steeper for the sum of several previous ISIs than for only the last, individual ISI. This is of great importance as it indicates that the effects of the underlying mechanism summate and become stronger after several spikes. However, while for both lactating groups the slopes decrease continuously from the very beginning, and for the naïve recordings the slopes

decrease from the steepest one for the previous sums of the previous 2 interval, for the before, after and pregnant recordings the steepest slopes occur for the sums of the previous 4, 5 and 6 intervals, respectively.

The lactating groups – both suckled and non-suckled – also display a slightly different pattern to the other groups: while the slopes for the non-suckled recordings are similar to the non-lactating groups for the sums of up to the 5 preceding intervals, the slopes for the suckled recordings are much steeper than the slopes from other groups for the sums for up to the 3 preceding sums. For the sums of the 6 to 20 preceding sums, however, for both these groups the slopes decrease much faster and are much flatter than any of the other groups. This indicates that the underlying mechanism is not very long lasting in these groups, and hence summates only over relatively few spikes.

4.2.3 Long-Term Effects of Previous Activity, Excluding Short-Term Influences

One striking observation in the above described analysis is that – contrary to expectations – in many cases (approx. 55%) the slope decreases, but does not reach zero – even for the sums of the previous 100 or 200 ISIs (Figure 4.8; analyses of sums for even larger numbers of intervals would have been difficult due to availability of sufficient data and were deemed unnecessary). The negative linear regression between the length of several intervals and the succeeding interval indicates that several spikes which occur within a short time will be followed by a spike after a relatively long interval, while spikes trains with relative long interspike intervals will be followed by a spike after a short interval. Due to this, we would expect that over enough ISIs this pattern of alternating lengths would even out and hence no influence of long stretches of spikes on further spike occurrence should be apparent. Further – as mentioned before – we expect the effect to be strongest for around 1 second, which – depending on the firing rate – will mean after 3 to7 spikes. However, 100 ISIs at an average firing rate of 5 Hz would mean the effect lasts 20 s. Clearly, this is physiologically unfeasible. To investigate why there appears to be an

influence of very long stretches of activity on the timing of individual spikes, an additional analysis was performed on a selection of recordings.

One possible explanation could be that the amount of error in the prediction of the ISIs – measured by the standard error of means – increases with each additional interval in the sum until the error is so large as to make the whole prediction invalid. This scenario seems unlikely based on the large number of analyses showing this trend. After inspecting the differences in the standard errors of means between the analyses of different sums in several recordings this possibility can be excluded: the standard error of means does not differ significantly (one way ANOVA, $p=0.99$) between the analyses for sums for different amounts of ISIs (Figure 4.9 and Table 4.3).

Another simple explanation is that since each sum incorporates all the preceding sums, any effect seen for the 'small' sums would be carried forward and be noticeable in the 'larger' sums, too. Hence, the negative linear regression between the sum of the previous 2 to 10 intervals and the succeeding interval would still show in the relationship between the sum of the last 100 or more intervals and the succeeding interval, albeit in a weaker form. To test this hypothesis it was decided to look how the exclusion of the immediately preceding 10 or 20 ISIs from the sum of the preceding 100 ISIs and the next interval influences the linear regression.

For this purpose, the sums of the preceding 100 but 10 (and also preceding 100 but 20) ISIs were calculated and coupled to the associated individual ISIs. The pairs were sorted according to the sum of the interval lengths and then averaged in appropriate group sizes. The standard error of means was calculated. The sums were plotted against the associated ISIs, and the linear regression was calculated. The results for the sum of the preceeding 100 intervals was compared to the sums of the last 100 but 10, and the last 100 but 20 ISIs.

As can be seen in Figure 4.10 the exclusion of the last 10 or 20 ISIs from the sum of the preceding 100 ISIs results in the slope of the linear regression decreasing towards zero. We can therefore conclude that the sum of the last 10 intervals has the strongest influence on the length of the succeeding intervals, and that the effect seen

in sums of more ISIs present an artefact of that relationship. Thus there is no contradiction to our original assumption and interpretation of the underlying influences.

4.3 Relationship Between ISIs in Cells Displaying Milk-Ejection Bursts

Of particular interest is the behaviour of oxytocin neurones during lactation. Explanation of the milk-ejection bursts – the synchronised high frequency discharges associated with the bolus release of oxytocin responsible for milk let-down – has so far proved elusive to experimental methods. Now that we are able to characterise the relationship between individual ISIs we turn our attention to the ISIs recorded in animals 'successfully' lactating, i.e. displaying milk-ejection bursts, and compare the underlying mechanism in the different physiological groups.

4.3.1 Methods

In a first step ISIs were calculated for recordings of the milk-ejecting animals. Periods of manipulation such as high frequency stimulation and any noise were removed by deleting each event after an ISI less than 7 ms long. 7 ms was chosen as a cut-off point as Dyball and Leng (1986) reported that during bursting oxytocin neurones can display ISIs in the range of 8-14 ms. Again, only very few of these instances occurred and the decisions were usually clear cut – i.e. intervals of less than 3 ms, and no occurrences of ISIs in the range of 3 to 10 ms allowed for easy and confident identification of 'real' as opposed to artificial events. It is important for the validity of the results that the analysis is conducted only on spontaneous ISIs. This is particularly essential in the range of very small ISIs, as we were looking for effects that are expected to be of particular relevance in this range.

These 'cleaned' recordings were divided into separate data samples (selection procedure described below in detail): a 5 s period from 15 to 10 s before a burst, a 5 s period from 10 to 5 s before a burst, the 5 s period immediately prior to a burst, and the burst. All ISIs not falling into one of the above four samples were summarised as the 'background' activity.

Bursts display a characteristic profile, whereby the peak frequency of up to 80 Hz is reached within a few initial spikes and maintained for a short period, then decreasing and ending in several hundreds of milliseconds up to seconds of electrical quiescence (Leng & Brown, 1997). High frequency discharges throughout each recording were identified and extracted in the form of ISIs starting with the first very short interval to the last interval before the pause in firing activity. All ISIs extracted from all the bursts within one recording were lined up one after the other, thus creating a sample of ISIs large enough for statistical analysis (referred to as the 'burst' sample). The analysis is based on intervals and not spike arrival times, which has the advantage that it makes it possible to group periods taken from different time points of the recording while preserving the information carried by the relationship between spikes since ISIs are disengaged from their temporal context.

Once the bursts have been extracted from the recording all ISIs in the 5 s periods leading up to the bursts were selected and gathered in a separate sample. This was repeated for the ISIs in the 5 s periods starting 10 s, and the 5 s periods starting 15 s before each burst. Thus, we derived 3 separate samples of ISIs from the 15 s before each burst for analysis, hereafter referred to as the '15 s', the '10 s' and the '5 s' sample, respectively. The ISIs which were not used for one of the above mentioned samples were gathered together to form a last sample, the period far away from the bursts or 'background' activity. It should be mentioned that attempts were made to analyse the activity after each burst. However, the variation in the length of the quiescence period and the low firing rate following a burst prevented the acquisition of sufficient data to allow an analysis.

With these samples of ISIs from the recordings of lactating and milk-ejecting animals prepared in this way the analyses were performed in the same way as described above for non-lactating animals (section 4.1) to find linear regression between one ISI and the succeeding ISI.

4.3.2 Results

Unfortunately, one of the cells displayed a very low firing rate between bursts, so that not enough ISIs were available for analysis. For the remaining 7 recordings, the averaged slopes are –0.133±0.021 (mean±sem), –0.082±0.033 and –0.015±0.048 for the 15 s, 10 s and 5 s samples, respectively (see Table 4.4 for details). Only 2 analyses (out of 7) for the 15 s samples and 3 analyses from the 5 s samples displayed a positive slope for very small ISIs. In contrast, all 8 background samples display both a negative slope (–0.067±0.022) and a positive slope for very small ISI (2.286±0.752), and also all 8 of the burst samples display a positive slope only (0.609±0.084) (Figure 4.11).

The negative slope of the background sample falls into the range of slopes obtained in the analysis of the non-milk-ejecting recordings, being closest to the slopes of lactating non-suckled and before hyperosmotic stimulation samples (see above). The negative slope in the linear regression indicates that short ISIs are followed by longer ISIs, and vice versa. The positive slope in contrast indicates that very short ISIs tend to be followed by further short ISIs. This indicates a tendency for clustering: several very short ISIs in succession followed by a short break in activity, which allows to balance the activity out again and accounts for the negative slope seen for the background activity.

For the linear regression analysis for the ISIs during a burst, nothing else but a positive slope could be expected. Within a few spikes at the beginning of each burst the maximal frequency is reached, and thereafter the ISIs get progressively longer again, i.e. at the beginning each ISI is followed by a shorter one, and then each ISI is followed by a longer one all throughout the burst. Hence, when analysing how the length of one ISI influences the next one then this pattern of rather strictly ascending or descending order of the ISIs should result in a positive linear regression slope.

The most difficult to interpret are the analysis of the 'before the burst' samples. What pattern would we expect to see in this sample? As mentioned in the introduction (section 1.6.2), Brown *et al.* (2000) demonstrated that the occurrence of bursting and the intensity of the bursting pattern in oxytocin neurones is most

strongly correlated with increased irregularity – as measured by the standard deviation of firing rate and the index of dispersion – of the firing activity just before the burst. When the bursting was experimentally restrained the variability was decreased, too, i.e. the firing was more regular. Conversely, under conditions that facilitate bursting in oxytocin neurones the variability is increased. In preparation for a burst the firing becomes increasingly irregular and clustered. Thus, we expect to see a negative slope indicating the intrinsic 'balancing' mechanisms of the neurones which stabilises the firing and prevents the activity to 'run away'. Also, as it is presumed (Kirkpatrick & Bourque, 1996) that the temporary deactivation of the mechanism allows the neurone to fire at the high frequencies seen during the burst its influence should become weaker closer to the burst. Therefore, if there are changes in firing pattern from 15 s prior to a burst, to 10 s prior to a burst to the last 5 s before a burst – and these differences are strong enough – then over these three samples we would expect the negative slope to become gradually less steep. Very small ISIs – which should become more numerous as the clustering in the activity increases – might result in a positive slope in this range, as in clusters several very short intervals follow each other.

We have found negative slopes for all three samples. Although the differences between the samples are statistically not significant (one-way ANOVA, $p=0.093$), a trend can be seen (cf. Table 4.4), whereby the averages of the slopes for the 7 cells decrease with increases in proximity of the sample to the burst (-0.133 ± 0.021, -0.082 ± 0.033, -0.015 ± 0.048, mean±sem for the 15 s, 10 s and 5 s samples, respectively). Thus, for the cells analysed, the mean slope becomes less negative between the samples 15 s and 5 s before the burst, consistent with our hypothesis (Figure 4.11). Furthermore, only a minority of recordings shows a positive slope for very small ISIs (2 out of 7 for the 15 s sample, none for the 10 s sample and 3 for the 5 s sample). However, the result of this analysis is very uncertain for any single cell, since for any given recording it is based on relatively few ISIs (384±100 spikes mean±sem; cf. Table 2.5).

Overall, the small size of our sample does not allow us to draw firm conclusions, but the results suggest a trend in keeping with the prediction about the changes in the intrinsic mechanisms which we can make based on previous *in vitro* work. Therefore we can conclude that our results support the notion that the intrinsic mechanisms – which balance the spontaneous activity in non-milk-ejecting neurones and the background activity in milk-ejecting neurones – become progressively weaker prior to a burst in preparation for high frequency firing.

4.3.3 Summary for the Analyses of Milk-Ejection Recordings

In summary, the main results from the analysis of milk-ejecting recordings are as follows:

(a) all slopes for the 'burst' samples are positive

(b) the analysis shows both a negative slope and a positive slope for small ISIs for all of the 'background' samples

(c) for all the 'before' periods there is a negative slope, which on average decreases in steepness the nearer to the burst the sample is; there is a steep positive slope for some, but not all samples

The main results of the analyses performed on recordings from milk-ejecting neurones indicate that the characteristics of the background activity (the activity far away from a burst) are the same for milk-ejecting neurones as non-milk-ejecting oxytocin neurones. The activity within a burst is inherently non-stationary i.e. it displays a strong systematic trend: once the peak frequency is reached the ISIs become progressively longer. Due to this progressive increase in the lengths the positive linear regression we found was expected and did not add any new insights. Most interestingly, however – although no firm conclusions can be drawn due to the small size of the available ISI sample – the results of the activity leading up to the burst supports the hypothesis that the intrinsic balancing mechanism becomes progressively deactivated in the run up to the burst. This observation is in agreement

with previous reports about the role of the AHP in high frequency bursts in oxytocin neurones during lactation (Kirkpatrick & Bourque, 1996).

4.4 Conclusion

In this chapter we have expanded on the results obtained from the firing rate analyses and explored the non-randomness in the firing of oxytocin neurones by investigating the influences between individual ISIs.

Linear regression analyses performed on individual ISIs from lactating, naïve and hyperosmotic stimulation groups show a negative slope, i.e. a short ISI is more likely to be followed by a longer ISI, and vice versa. Only the analysis for the pregnant group reveals a positive slope, indicating that a short ISI is likely to be followed by a further short ISI. In addition to this major effect, in approx. 40% of all recordings – regardless of the physiological state of the animal – a further effect was found in the range of very small ISI lengths ('very short' meaning different ranges for each recording): a positive slope in the linear regression analysis suggests that a very short ISI is likely to be followed by another very short ISI.

Investigating how a period of activity influences the individual ISI led us to perform linear regression analyses between the sum of several ISIs and the successive interval. Again, we found a negative slope, however the gradient varies with the amount of ISIs in the sum in a predictable manner: for non-lactating groups the slope is steeper for the sum of several previous ISIs than it was for only the last ISI, being the steepest for the sum of 4 to 6 intervals. For the lactating groups, in contrast, the gradient decreases much faster and is flatter than in the other groups. If large enough amounts of previous ISIs are included in the sums the slope decreases to zero, but only if the effect of immediately preceding ISIs (i.e. approx. the last 10 before the succeeding ISI) is excluded.

The linear regression analyses are an extension to the investigations of serial dependence presented in Chapter 3. Again, the results for both approaches – considering how the length of a given interval depends on both the preceding ISI, and also on the history of previous ISIs as represented by the sum of preceding

intervals – show a balancing effect. An inverse relationship between the length of an ISI and the lengths of the previous ISIs might be small, but the constancy of this phenomenon throughout all physiological groups, paired with an increase to its maximum effect for around the last 6 ISIs and its disappearance for sums exceeding 20 argues that this is the influence of a activity-dependent inhibitory mechanism slow enough to summate over several spikes in 1-2 s.

We then turned to the exploration of recordings from milk-ejecting neurones. To this means each recording was divided into different samples: the burst itself, three periods before each burst, and the period far away from a burst, i.e. the background activity. The analyses performed on these samples were the same as the ones for non-milk-ejecting recordings. The results indicate that the background activity is comparable to the activity in non-milk-ejecting neurones. All the burst samples show positive slopes in the linear regression analysis, as expected due to their inherent non-stationarity. While the ISIs samples for the before the burst periods are very small and hence only allow us to draw tentative conclusions, the trend displayed is in agreement with the predictions based on previous work: the slopes of the linear regression decreases with increased proximity of the sample to the burst.

Figure 4.1 Example of linear regression analysis between one ISI and the immediately succeeding ISI shown for A) original and B) for averaged data.

Plotting the length of one ISI against the length of the immediately succeeding ISI results in a 'cloud' of data (A), which makes the detection of a trend difficult if not impossible. Therefore, we have averaged the data in group sizes appropriate to the amount of data (B), to present the regressions found in a way more accessible to the reader.
As can be seen from the trendlines and the equations from the linear regression analysis the slope and intercept in both cases are essentially the same, but for the r^2 values. These take values in the range of 0 to +1 and measures the closeness of fit of the scattergraph to its regression line: the closer r^2 values are to 1 the better the line describes the data. However, as r^2 is dependent on the amount of data over which the linear regression is fitted an increase in the amount of data makes it less likely that a simple line describes all of the points.

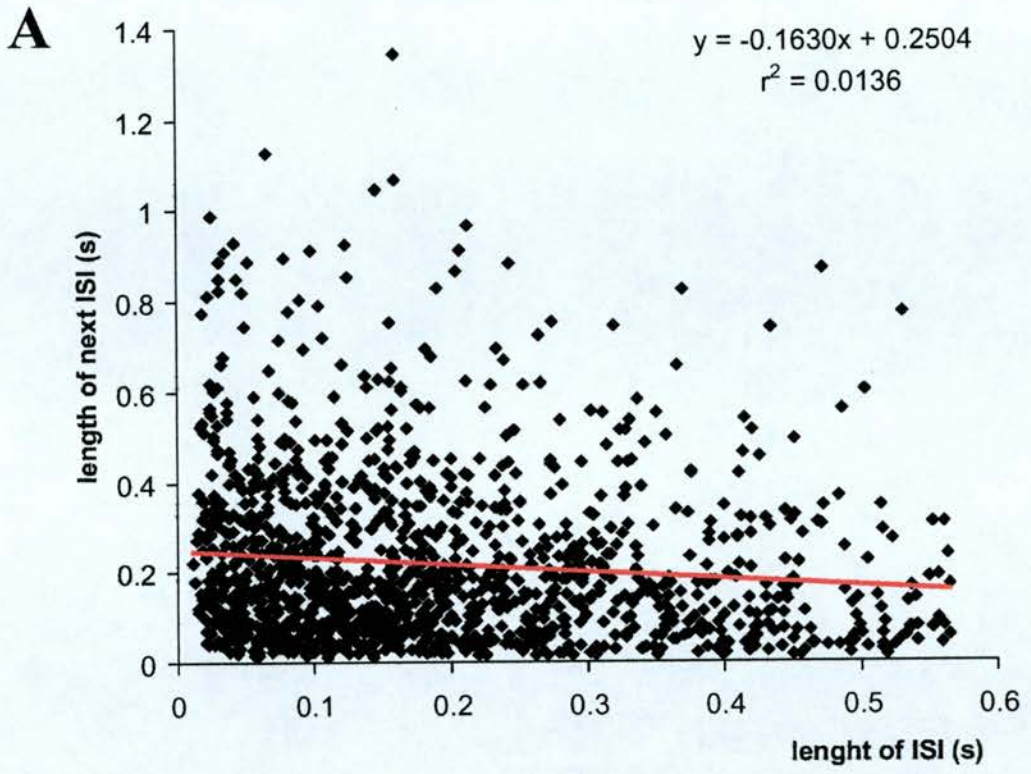
A
y = -0.1630x + 0.2504
r2 = 0.0136
length of next ISI (s)
lenght of ISI (s)
0
0.2
0.4
0.6
0.8
1
1.2
1.4
0.1
0.3
0.5

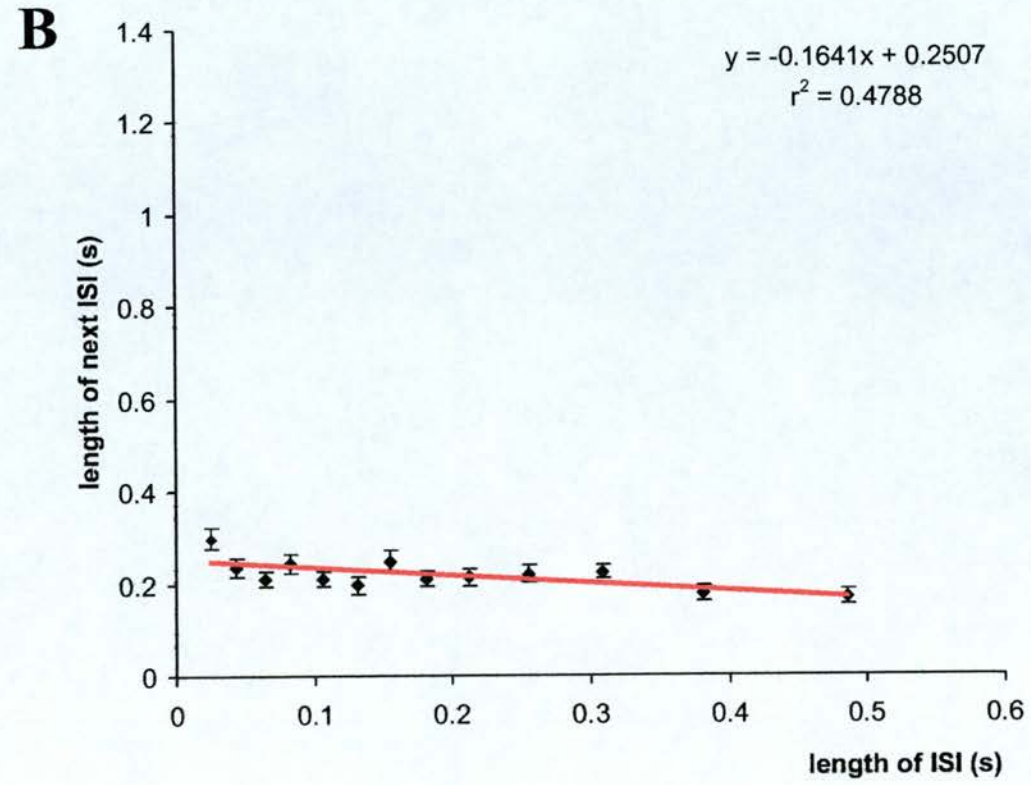
B
y = -0.1641x + 0.2507
r2 = 0.4788
length of next ISI (s)
length of ISI (s)
0
0.2
0.4
0.6
0.8
1
1.2
1.4
0.1
0.3
0.5

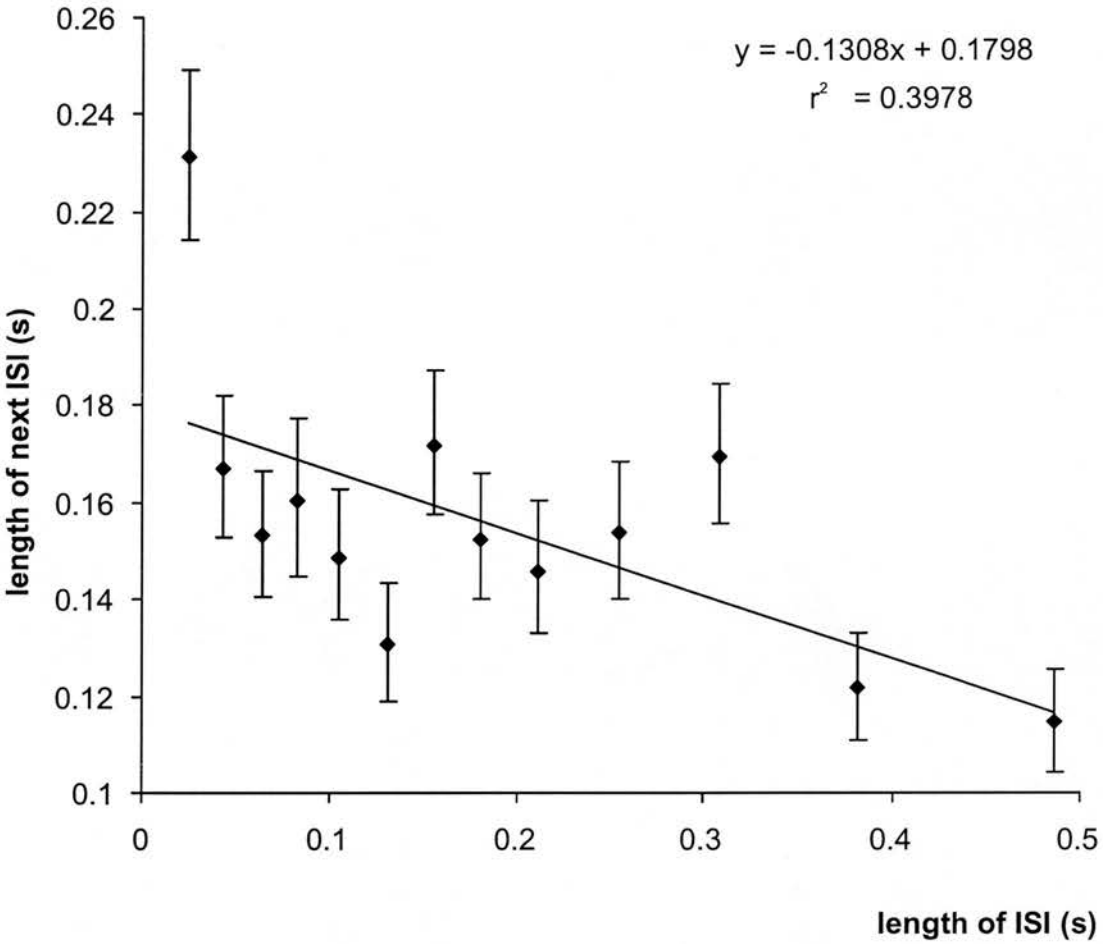

Figure 4.2 Example of linear regression analysis between one ISI and the immediately succeeding ISI.

A linear regression analysis with the length of an ISI as the independent variable and the length of the immediately succeeding ISI as the dependent variable for one recording. Each point represents an averaged length of ISIs of similar length and the averaged length of their immediately succeeding ISI. Standard means of error are indicated. The equation for the trendline is given in the linear regression equation in the left corner, as well as the r^2 value.
The regression between one ISI and the immediately succeeding ISI is negative, indicating that a short ISI is followed by a longer ISI, and vice versa.

Figure 4.3 Examples of a linear regression analyses of recordings from the different groups A) lactating and suckled, but non milk-ejecting animal B) lactating, but unsuckled animal C) pregnant animal D) naïve animal E) after hyperosmotic stimulation and F) before hyperosmotic stimulation.

As in Figure 4.2, averaged ISIs and associated succeeding averaged ISIs, standard error of means, linear regression equations and r^2 values. Please note that the figures are all in different scales.
For the majority (cf. Table 4.1) of recordings, regardless of the physiological state of the animal the linear regressions are negative, meaning that a short ISI is followed by a longer ISI, and vice versa.

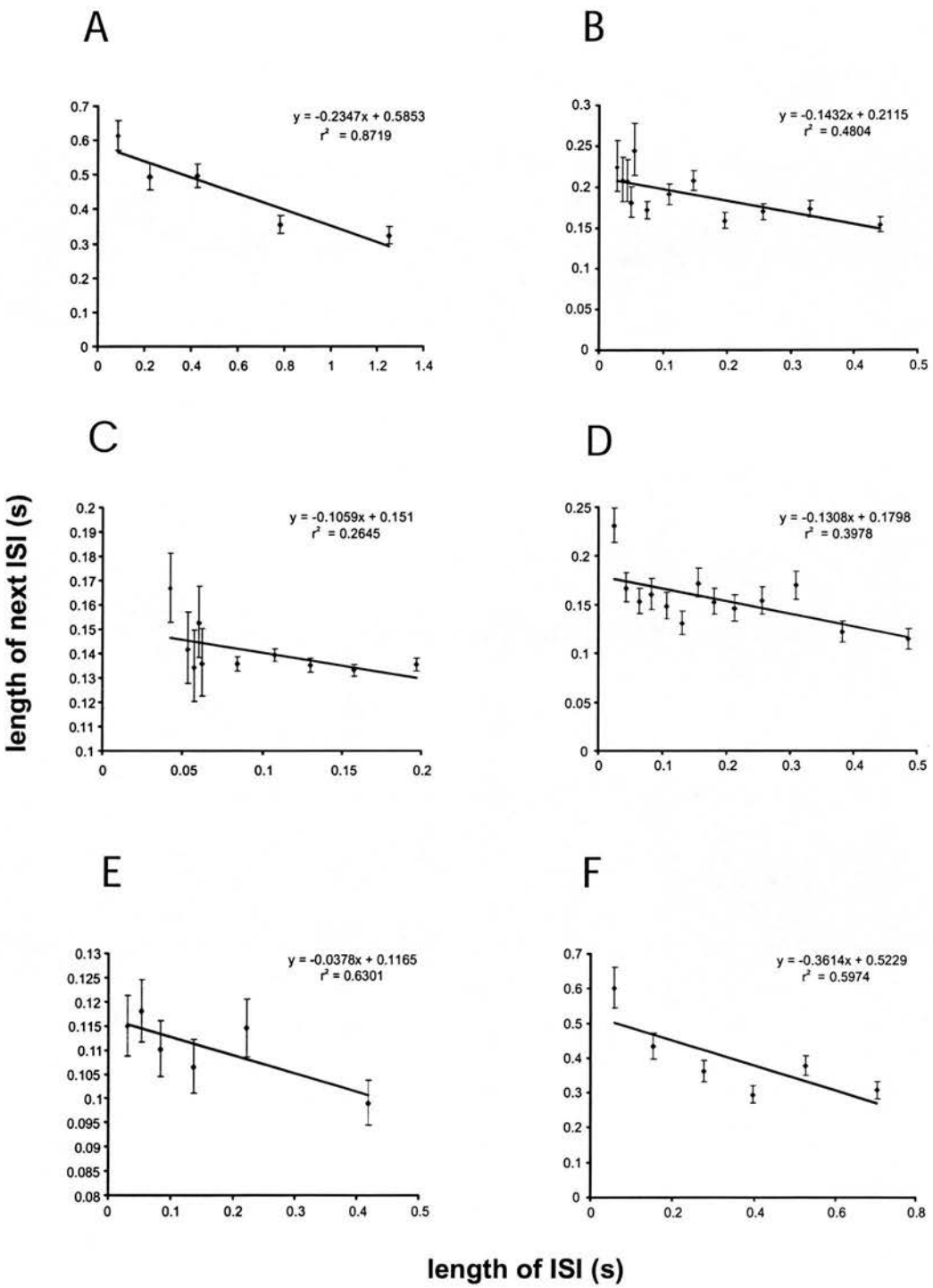
A
y = -0.2347x + 0.5853
r² = 0.8719
B
y = -0.1432x + 0.2115
r² = 0.4804
C
y = -0.1059x + 0.151
r² = 0.2645
D
y = -0.1308x + 0.1798
r² = 0.3978
E
y = -0.0378x + 0.1165
r² = 0.6301
F
y = -0.3614x + 0.5229
r² = 0.5974
length of next ISI (s)
length of ISI (s)

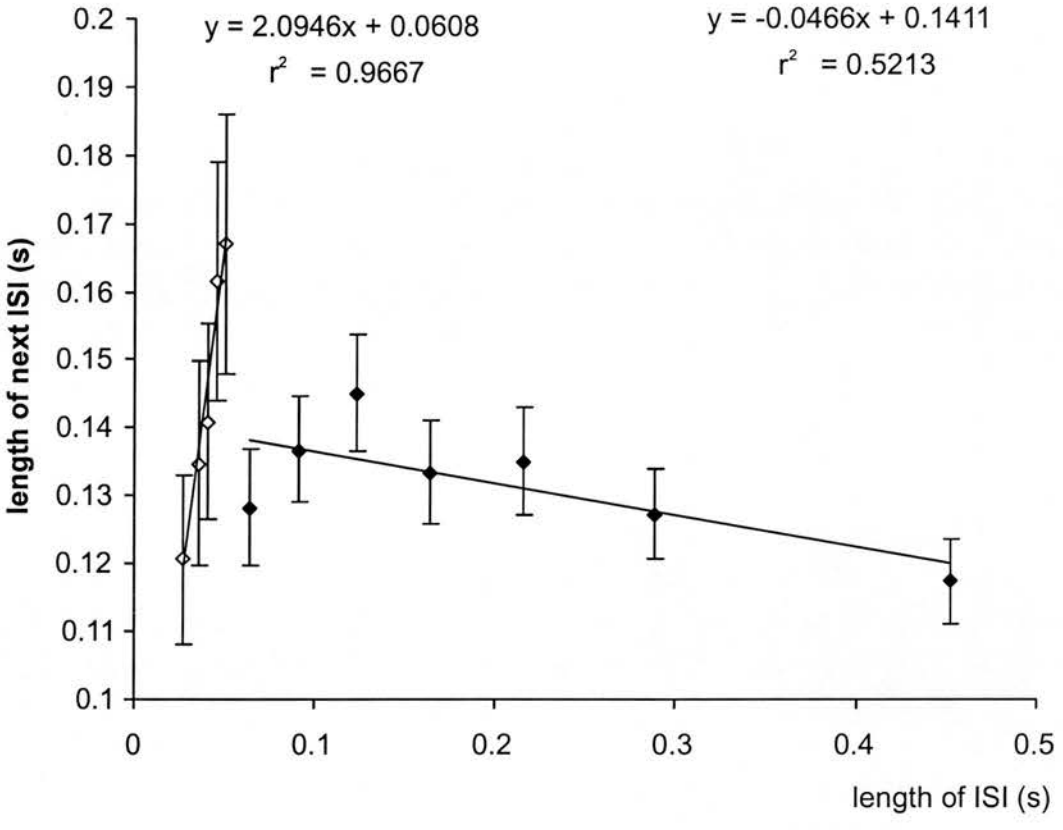

Figure 4.4 Example of a linear regression analysis between one ISI and the immediately succeeding ISI, displaying a different trend for small ISIs than for the remaining ISIs.

As in Figure 4.2., each point represents an averaged length of similar sized ISIs and their associated averaged succeeding ISIs, and their standard error of means is indicated. As a different trend emerged for small ISIs, two separate linear regression analyses where performed. The linear equation on the left is for the small ISIs, while the one on the right is for the remaining ISIs.
While the regression for the remaining ISIs shows the same trend as described in Figures 4.2 and 4.3 - namely that short ISIs are followed by longer ISIs - the trend for the small ISIs is the opposite: a positive regression indicates that a very short ISI is followed by another short interval.

Figure 4.5 Examples of linear regression analyses of ISIs of recordings from different physiological conditions, where the very short ISIs follow a different trend to the remaining ISIs: A) lactating and suckled, but non milk-ejecting animal B) lactating, but unsuckled animal C) pregnant animal D) naïve animal E) after hyperosmotic stimulation and F) before hyperosmotic stimulation.

As in Figure 4.4, two separate linear regression analyses were performed for each recording, one for short ISIs and another for the remaining ISIs. Each point indicates an average of ISIs from a certain range and their associated immediately succeeding averaged ISIs, and their standard errors of means is indicated. Please note that the averages for short ISIs (empty symbols) are for a smaller number of ISIs than the averages for the remaining ISIs (solid symbols). The linear regression equation and r^2 value in the left hand corner are for the analyses of very short ISIs, and the ones in the right hand corner are for the analyses of the remaining ISIs.
Again, in nearly all the analyses performed a negative linear regression is apparent, indicating that a short ISI is followed by a longer ISI. In addition, in 42% of all cases a different trend becomes apparent for very short ISIs: the linear regression is positive, indicating that a very short ISI is followed by a short ISI again. This trend can be observed for recordings from all the physiological groups.
The insets show a close up of the positive linear regression and are included where appropriate for the sake of clarity, i.e. where the scale of the figure does not make the slope visible.
Please note that the scale of the axes is different between the figures.

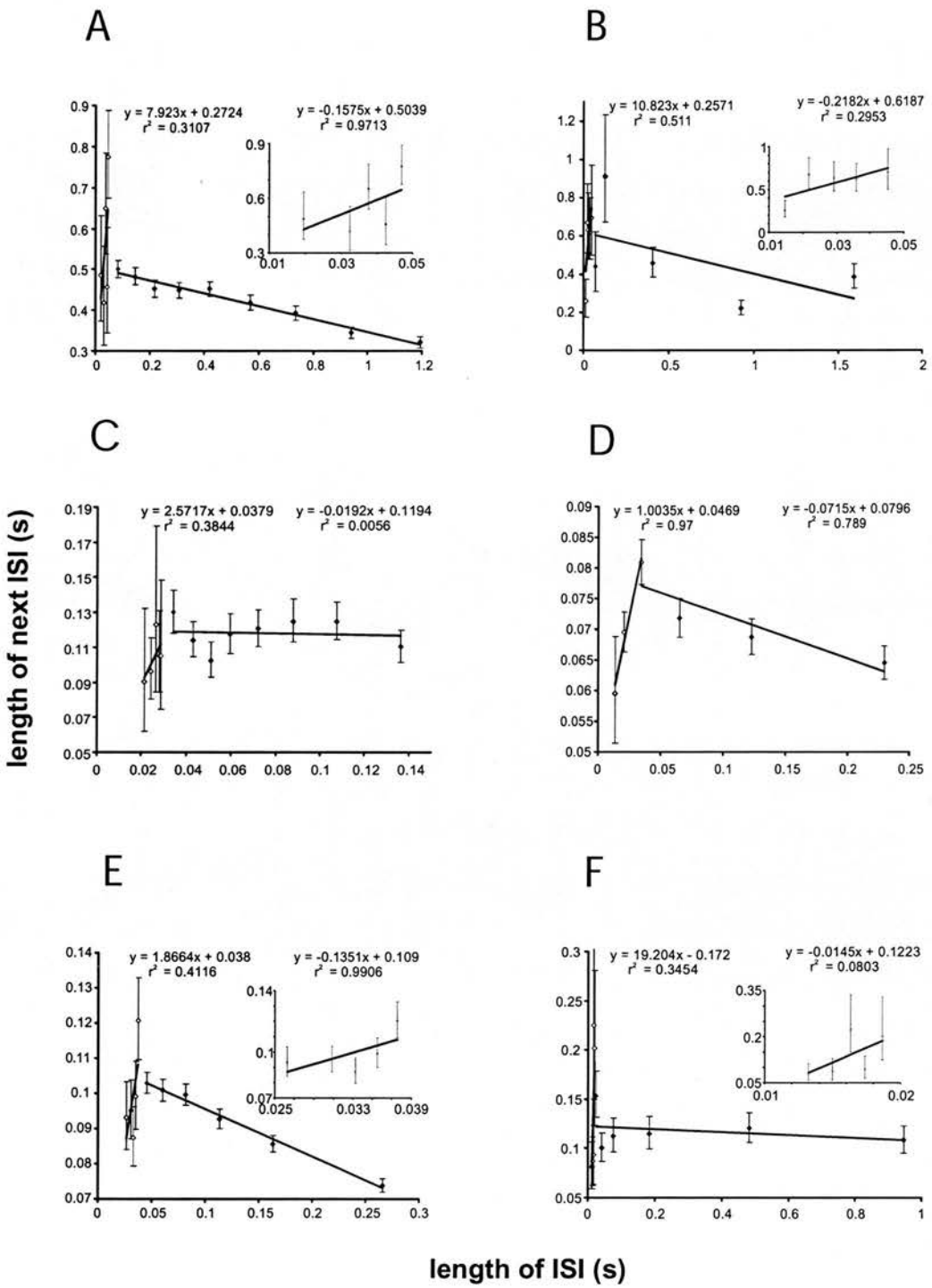
A
y = 7.923x + 0.2724
r² = 0.3107
y = -0.1575x + 0.5039
r² = 0.9713
B
y = 10.823x + 0.2571
r² = 0.511
y = -0.2182x + 0.6187
r² = 0.2953
C
y = 2.5717x + 0.0379
r² = 0.3844
y = -0.0192x + 0.1194
r² = 0.0056
D
y = 1.0035x + 0.0469
r² = 0.97
y = -0.0715x + 0.0796
r² = 0.789
E
y = 1.8664x + 0.038
r² = 0.4116
y = -0.1351x + 0.109
r² = 0.9906
F
y = 19.204x - 0.172
r² = 0.3454
y = -0.0145x + 0.1223
r² = 0.0803
length of next ISI (s)
length of ISI (s)

Figure 4.6 Example of a linear regression analyses of the sum of the lengths of n (n=1, 2, ..., 15) preceding ISIs and the current ISI.

For each recording the sums of the lengths of n ISIs were calculated (n=1, 2, 3, ..., 9, 10, 15, 20, 50, 100, 200) and coupled to the associated current ISI. Each sum was plotted against the ISI, and for each pair a linear regression analysis was performed. (A) shows the plots of the sums of the lengths of ISIs vs the current ISI, as well as their standard error of means. (B) shows exactly the same analyses, but expressed as regression lines for emphasis. Please note that in both instances only a selection of the range of sums has been presented for the sake of clarity (for all the results cf. Table 4.2). There is a negative slope for the regression analyses for t_0 against t_1, which becomes progressively steeper for each sum until t_0 vs the sum of $(t_1+..+t_5)$. For sums of larger n the slope decreases progressively. This indicates that the effects of the underlying mechanism summate and become stronger after several action potentials.

(C) shows one particular regression analysis from the aforementioned range (namely n=8, open symbols) and compares it to the outcome of the identical analyses performed on exactly the same ISIs *after they have been randomly shuffled* (solid symbols), thus destroying any serial dependency between successive ISIs (cf. Chapter 3 section 3.3). As can be seen from the linear regression analysis performed on the shuffled ISIs no relationship can be found between a period of activity and the succeeding ISI once the order of the ISI is removed.

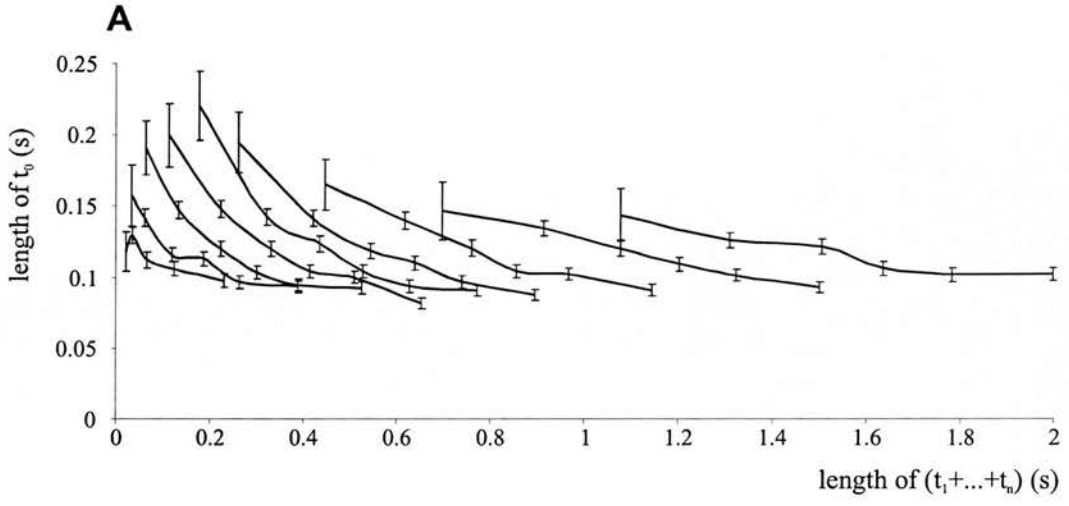
A
length of t_0 (s)
0.25
0.2
0.15
0.1
0.05
0
0 0.2 0.4 0.6 0.8 1 1.2 1.4 1.6 1.8 2
length of $(t_1+...+t_n)$ (s)

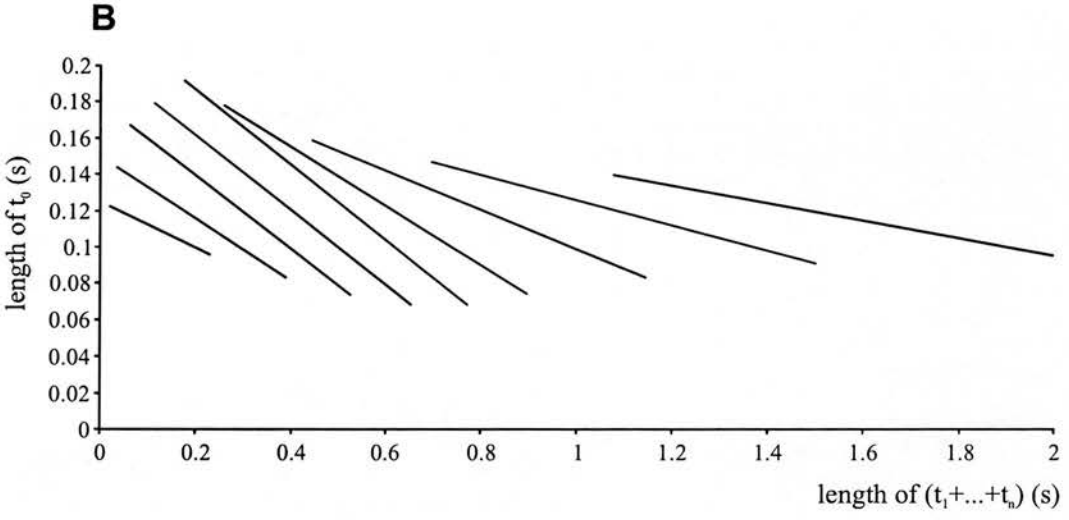
B
length of t_0 (s)
0.2
0.18
0.16
0.14
0.12
0.1
0.08
0.06
0.04
0.02
0
0 0.2 0.4 0.6 0.8 1 1.2 1.4 1.6 1.8 2
length of $(t_1+...+t_n)$ (s)

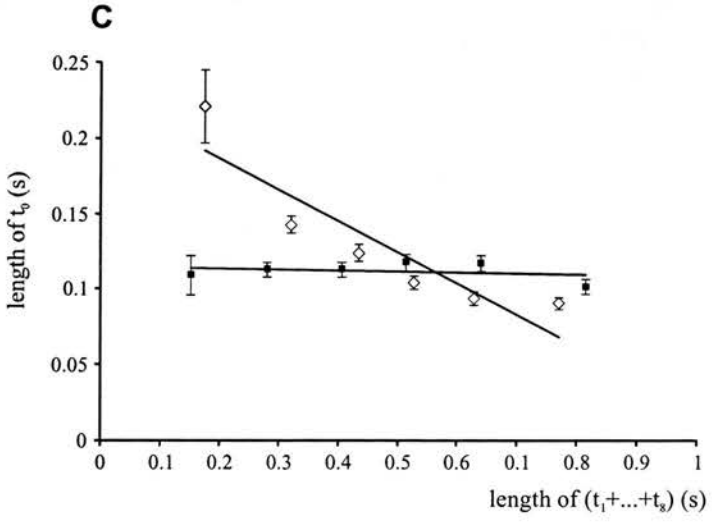
C
length of t_0 (s)
0.25
0.2
0.15
0.1
0.05
0
0 0.1 0.2 0.3 0.4 0.5 0.6 0.1 0.8 0.9 1
length of $(t_1+...+t_8)$ (s)

Figure 4.7 The slopes of the linear regression analyses between the length of t_0 and the length of the sums of n previous intervals, shown for n=1,2, ..., 9, 10, 15, 20, 50, 100, 200 by each group (lactating-suckled, lactating-unsuckled, naïve, pregnant, before and after hyperosmotic stimulation, and the total average in red).

Averaged slopes for the naïve, pregnant, and before and after hyperosmotic stimulation groups become progressively steeper over the first few n, and decrease thereafter slowly towards zero. This indicates that the effects of the underlying mechanism summate over several action potentials and are strongest after approx. 5 intervals.
The slopes for the suckled neurones are much bigger than any of the other groups for n=1, 2, and 3, but do decrease rapidly. Also, for both the suckled and the lactating neurones the slopes do not increase first before decreasing towards zero, and are much shallower than the non-lactating groups in the range of n=6 to 15 (see arrow). This is possibly due to the underlying mechanism being weaker during lactation in preparation for milk-ejection.

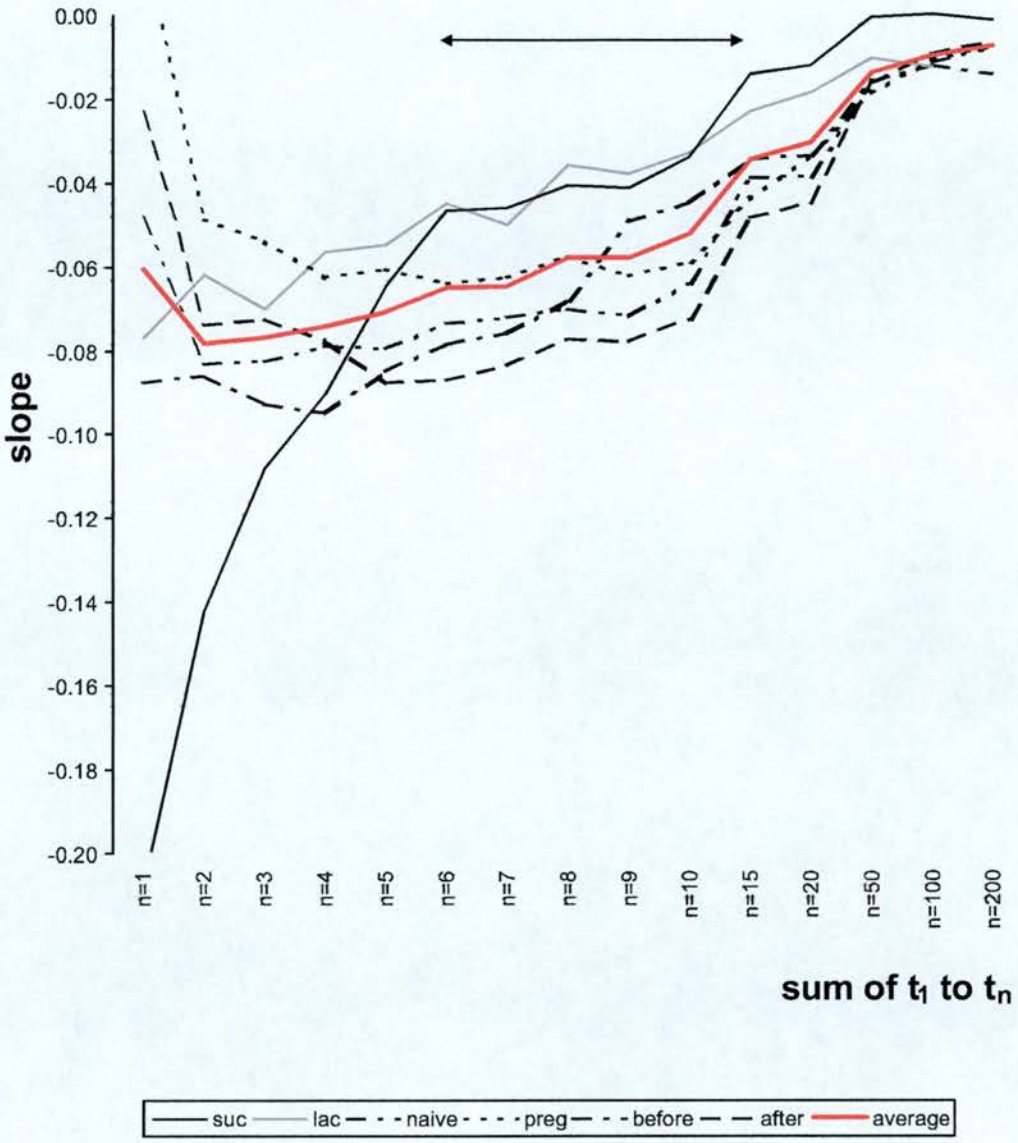
0.00
-0.02
-0.04
-0.06
-0.08
-0.10
-0.12
-0.14
-0.16
-0.18
-0.20
slope
n=1
n=2
n=3
n=4
n=5
n=6
n=7
n=8
n=9
n=10
n=15
n=20
n=50
n=100
n=200
sum of t_1 to t_n
suc
lac
naive
preg
before
after
average

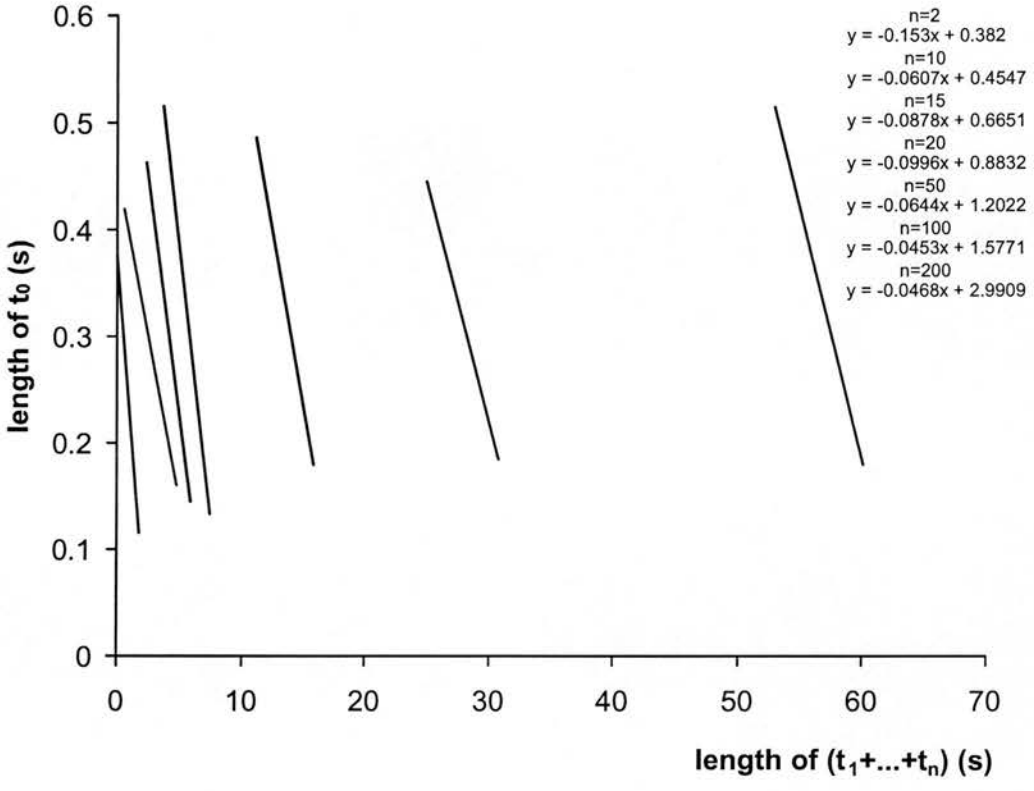

Figure 4.8 An example of a linear regression analysis of t_0 against the sum of n preceding ISIs (n=2, 10, 15, 20, 50, 100, 200) where the slope decreases, but does not reach zero.

The negative linear regression between the current interval and the sum of preceding intervals indicates that several short intervals will be followed by a relatively long interval, and vice versa. Over relatively large samples of ISIs, however, the activity should be balanced out and therefore the slope should decrease to zero. As can be seen in this example this is not always the case even for samples of 100 intervals or more.

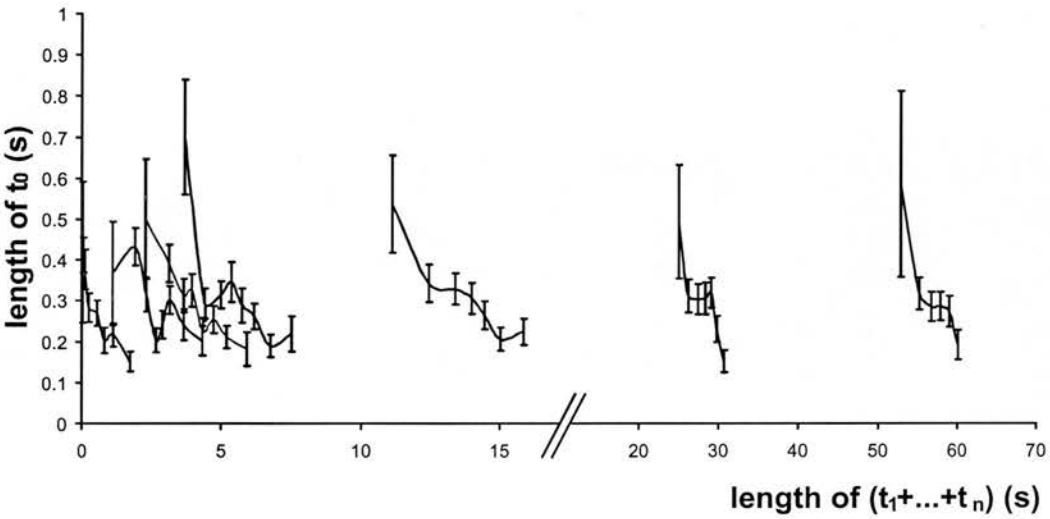

Figure 4.9 An example of a linear regression analysis for t_0 and the sum of n preceding intervals (n=2, 10, 15, 20, 50, 100, 200), shown with standard errors of mean.

The negative correlation between the current interval and the sum of previous intervals indicates that action potentials that occur within a short time of each other are likely to be followed by an action potential after a longer interspike interval, and vice versa. As can be seen in this example, this relationship seems to be true even for a large sample of action potentials. However, 100 or more spikes at an ordinary background activity firing rate would amount to more than 20s, which is physiologically unlikely.
One explanation could be that with each addition ISI added to the sum the error in the prediction increases it is so great as to make the whole predication meaningless. Looking at the standard errors of mean for the different sums above, it becomes clear that this is not the case: the standard errors of means for sums of large n are not significantly greater than sums for small n, and do not overlap in the prediction (please note, the standard error of means for the first point of each sum is relatively greater as it is averaged over a smaller sample than the rest). Thus, this hypothesis can be rejected.

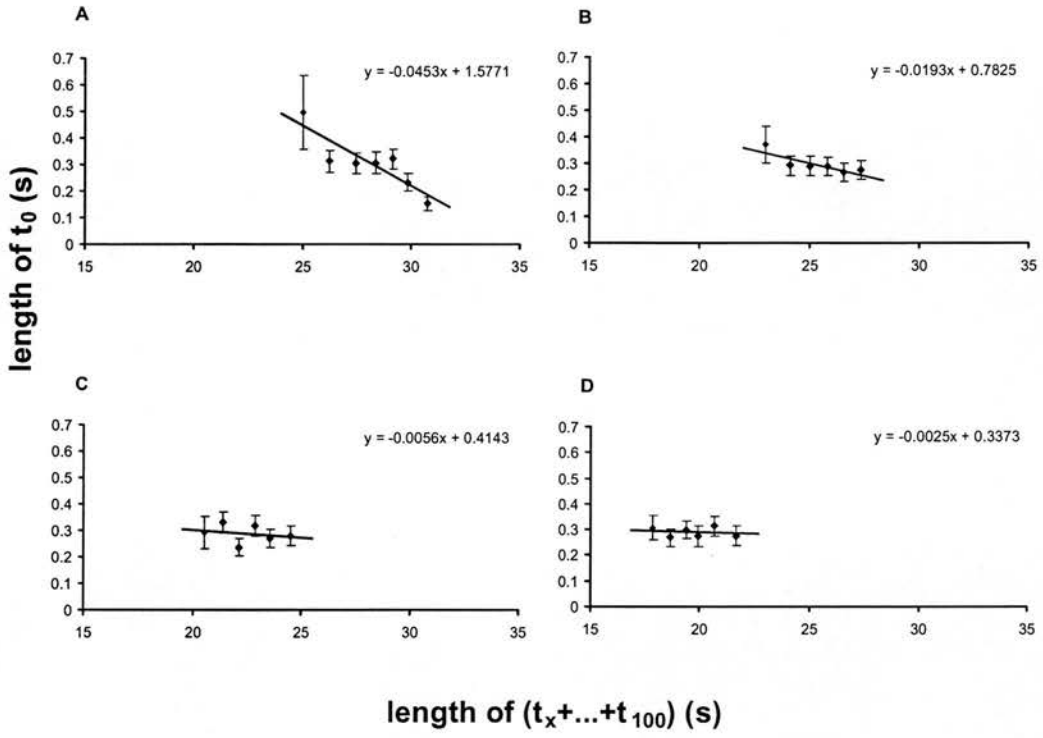

Figure 4.10 Excluding the first 10 (B), 20 (C), and 30 (D) ISIs from the 100 preceding ISIs from the linear regression analysis between t_0 and the 100 (A) preceding intervals results in a proportionately decreased slope.

(A) shows an example of a linear regression analysis between t_0 and the sum of the 100 preceding intervals. The negative regression indicates that 100 ISIs that add up to a relatively small sum are likely to be followed by a relatively long ISI, and vice versa. This appears to be physiologically unlikely, as 100 ISIs at a background firing rate of e.g. 5 Hz translate to a duration of 20s.
One possible explanation is that the strong effect between the current and a few immediately preceding ISIs is still apparent in the sums of larger samples. To examine this possibility the analysis was repeated, excluding a number of immediately preceding ISIs.
(B) shows a linear regression analysis performed on the same data as before, but this time between t_0 and $(t_{10}+...+t_{100})$. (C) shows the analysis between t_0 and $(t_{20}+...+t_{100})$, and (D) between t_0 and $(t_{30}+...+t_{100})$. As can be seen from the graphs and the linear equations, with the exclusion of the immediately preceding ISIs from the analysis the relationship between the current and the sum of the last 100 ISIs diminishes gradually. Therefore we conclude that the strong effect of the immediately preceding intervals influences the results for larger samples.

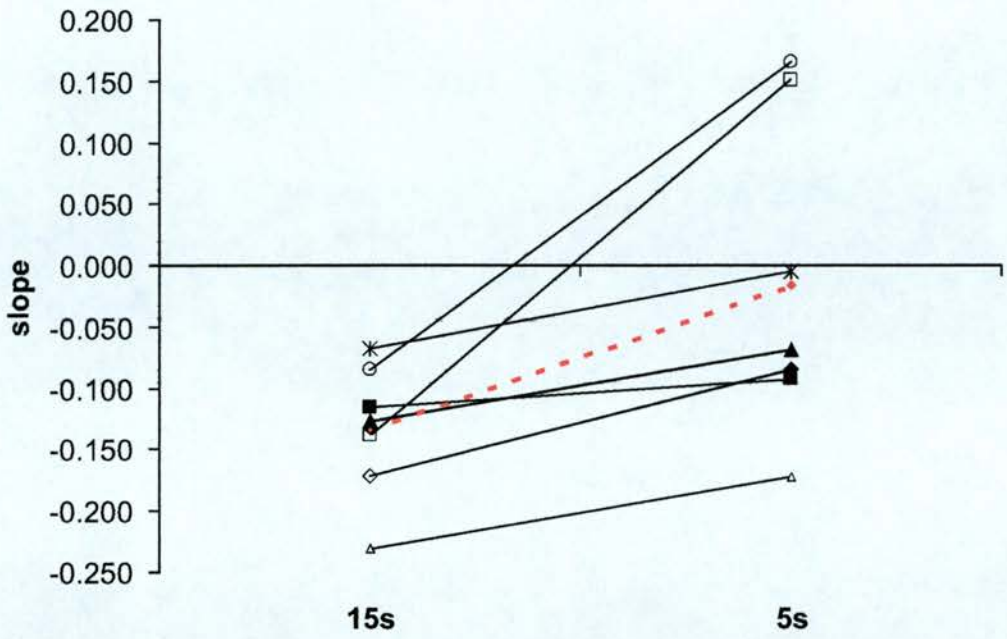

Figure 4.11 The slopes for the linear regression analyses between t_0 and t_1 for 5s ISI samples starting 15s and 5s before a burst for the 7 cells analysed and their average (red).

The slopes from the linear regression analyses in all 7 cells analysed are steeper for the 15s sample compared to the 5s sample, indicating that the effect of the underlying mechanism decreases closer to the burst, allowing oxytocin cells to reach the high firing frequencies they display during a milk-ejection burst.

Cell name	Physiol. state	Number of ISI in recording	slope for small ISI	slope
s1	Suckled	5052	7.923	-0.158
s2	Suckled	500	-0.210	-0.210
s3	Suckled	1000	-0.235	-0.235
s4	Suckled	4745	2.450	-0.334
s5	Suckled	1397	0.717	-0.301
s6	Suckled	1385	1.560	-0.237
s7	Suckled	671	-0.040	-0.040
s8	Suckled	1205	-0.092	-0.092
s9	Suckled	1400	-0.184	-0.184
n=9		1928	1.321	-0.199
		572	0.883	0.031
l1	non-suckled	1836	2.238	-0.057
l2	non-suckled	200	-0.120	-0.120
l3	non-suckled	703	-0.116	-0.116
l4	non-suckled	93	-0.059	-0.059
l5	non-suckled	1200	0.140	0.140
l6	non-suckled	6260	2.604	-0.032
l7	non-suckled	1395	0.368	-0.066
l8	non-suckled	1838	-0.143	-0.143
l9	non-suckled	1269	-0.086	-0.086
l10	non-suckled	4478	2.583	-0.091
l11	non-suckled	1358	-0.177	-0.177
l12	non-suckled	494	10.823	-0.218
l13	non-suckled	75	-0.185	-0.185
l14	non-suckled	315	0.027	0.027
n=14		1439	1.181	-0.091
		467	0.766	0.025
n=23		1623	1.233	-0.132
(whole lactating group)		357	0.569	0.022
p1	Pregnant	2931	-0.039	-0.039
p2	Pregnant	2446	2.009	-0.007
p3	Pregnant	1340	2.572	-0.019
p4	Pregnant	2387	-0.026	-0.026
p5	Pregnant	3502	0.216	-0.034
p6	Pregnant	2403	0.066	0.066
p7	Pregnant	1975	0.174	0.174
p8	Pregnant	2248	-0.106	-0.106
p9	Pregnant	1315	0.044	0.044
p10	Pregnant	933	0.951	-0.013
p11	Pregnant	1101	0.020	0.020
p12	Pregnant	2367	0.123	0.123
p13	Pregnant	1598	0.048	0.048
n=13		2042	0.465	0.018
		209	0.238	0.020

n1	Naïve	1663	2.095	-0.047
n2	Naïve	1431	-0.082	-0.082
n3	Naïve	1795	-0.073	-0.073
n4	Naïve	858	0.677	-0.031
n5	Naïve	1374	-0.131	-0.131
n6	Naïve	1347	-0.127	-0.127
n7	Naïve	7077	0.667	-0.085
n8	Naïve	2694	1.004	-0.072
n9	Naïve	2199	0.078	-0.109
n10	Naïve	3177	0.915	-0.054
n11	Naïve	2950	0.167	0.167
n12	Naïve	4713	0.030	0.030
n13	Naïve	1174	-0.014	-0.014
n=13		2496	0.400	-0.048
		481	0.181	0.022

l13	Lactating, before	75	-0.185	-0.185
l14	Lactating, before	315	0.027	0.027
b1	Before stimulation	657	19.204	-0.015
b2	Before stimulation	640	-0.361	-0.361
b3	Before stimulation	1185	-9.574	0.018
b4	Before stimulation	669	-0.040	-0.040
b5	Before stimulation	820	5.378	-0.099
b6	Before stimulation	1004	-0.144	-0.144
n=8		671	1.788	-0.100
		125	2.878	0.046

a1	After stimulation	2658	-0.047	-0.047
a2	After stimulation	3557	0.007	0.007
a3	After stimulation	2053	-1.931	0.016
a4	After stimulation	3249	1.866	-0.135
a5	After stimulation	6272	-0.007	-0.007
a6	After stimulation	1249	0.954	-0.038
a7	After stimulation	1800	-0.038	-0.038
a8	After stimulation	3000	0.013	0.013
a9	After stimulation	2517	0.024	0.024
a10	After stimulation	1710	3.596	-0.026
n=10		2807	0.444	-0.023
		449	0.461	0.015

Total

n=65	2014	0.922	-0.065
	188	0.405	0.013

Table 4.1 Overview of all linear regression analyses results

cell	n=1	n=2	n=3	n=4	n=5	n=6	n=7	n=8	n=9	n=10	n=15	n=20	n=50	n=100	n=200
a1	-0.047	-0.072	-0.067	-0.073	-0.079	-0.081	-0.073	-0.065	-0.064	-0.057	-0.039	-0.022	0.000	0.002	0.002
a2	0.007	-0.045	-0.021	-0.014	-0.061	-0.061	-0.075	-0.073	-0.068	-0.055	-0.039	-0.026	-0.020	-0.004	-0.001
a3	0.016	-0.084	-0.094	-0.121	-0.152	-0.163	-0.163	-0.179	-0.190	-0.166	-0.111	-0.099	-0.038	-0.022	-0.017
a4	-0.135	-0.187	-0.178	-0.171	-0.168	-0.159	-0.148	-0.140	-0.122	-0.115	-0.064	-0.056	-0.021	-0.013	-0.006
a5	-0.007	-0.041	-0.047	-0.053	-0.060	-0.056	-0.061	-0.052	-0.054	-0.049	-0.036	-0.037	-0.013	-0.006	-0.002
a6	-0.038	-0.078	-0.079	-0.097	-0.103	-0.079	-0.069	-0.059	-0.055	-0.056	-0.034	-0.032	-0.005	-0.010	-0.007
a7	-0.038	-0.098	-0.092	-0.090	-0.113	-0.114	-0.118	-0.072	-0.094	-0.080	-0.040	-0.070	-0.023	-0.018	-0.010
a8	0.013	-0.046	-0.042	-0.032	-0.038	-0.045	-0.041	-0.046	-0.041	-0.046	-0.039	-0.027	-0.008	-0.006	-0.002
a9	0.024	-0.016	-0.052	-0.056	-0.049	-0.048	-0.028	-0.034	-0.034	-0.045	-0.049	-0.029	-0.013	-0.003	-0.004
a10	-0.026	-0.073	-0.053	-0.068	-0.055	-0.064	-0.057	-0.051	-0.057	-0.055	-0.033	-0.048	-0.021	-0.012	-0.012
	-0.023	-0.074	-0.072	-0.077	-0.088	-0.087	-0.083	-0.077	-0.078	-0.072	-0.048	-0.045	-0.016	-0.009	-0.006
	0.015	0.015	0.014	0.014	0.014	0.014	0.014	0.014	0.015	0.012	0.008	0.008	0.003	0.002	0.002
b1	-0.015	-0.153	-0.113	-0.154	-0.195	-0.170	-0.176	-0.142	-0.098	-0.061	-0.088	-0.100	-0.064	-0.045	-0.047
b2	-0.361	-0.233	-0.243	-0.152	-0.140	-0.122	-0.069	-0.077	-0.053	-0.058	-0.040	-0.027	-0.014	-0.008	-0.007
b3	0.018	-0.069	-0.088	-0.084	-0.086	-0.101	-0.104	-0.084	-0.075	-0.077	-0.037	-0.034	-0.012	-0.004	0.000
b4	-0.040	-0.015	0.039	0.033	0.024	0.046	0.047	0.025	0.012	0.025	0.009	0.008	0.002	-0.002	0.000
b5	-0.099	-0.059	-0.087	-0.127	-0.066	-0.079	-0.099	-0.069	-0.043	-0.049	-0.022	-0.028	-0.004	-0.001	-0.004
b6	-0.144	-0.110	-0.133	-0.139	-0.125	-0.123	-0.107	-0.117	-0.081	-0.083	-0.051	-0.040	-0.013	-0.003	-0.006
l14	0.027	0.037	-0.023	-0.040	-0.006	0.000	-0.024	-0.012	-0.007	-0.009	-0.012	-0.011	-0.007	-0.019	-0.032
	-0.088	-0.086	-0.093	-0.095	-0.085	-0.078	-0.076	-0.068	-0.049	-0.045	-0.034	-0.033	-0.016	-0.012	-0.014
	0.051	0.034	0.033	0.026	0.029	0.029	0.027	0.022	0.015	0.015	0.012	0.013	0.008	0.006	0.007

cell	n=1	n=2	n=3	n=4	n=5	n=6	n=7	n=8	n=9	n=10	n=15	n=20	n=50	n=100	n=200
l1	-0.057	-0.052	-0.050	-0.044	-0.043	-0.043	-0.037	-0.021	-0.031	-0.020	-0.014	-0.001	0.005	0.003	0.001
l2	-0.120	-0.094	-0.089	-0.074	-0.151	-0.057	-0.012	-0.012	-0.014	-0.044	-0.008	-0.016	-0.001	-0.091	ned
l3	-0.116	-0.037	-0.035	-0.004	-0.012	-0.018	-0.030	-0.029	-0.025	-0.029	-0.016	-0.014	-0.034	-0.009	-0.016
l4	-0.059	-0.133	-0.043	0.000	0.006	-0.007	0.023	0.012	-0.017	0.024	0.024	-0.010	-0.026	ned	ned
l5	0.140	0.201	0.105	0.165	0.153	0.130	0.031	0.098	0.080	0.074	0.055	0.041	0.017	0.006	0.003
l6	-0.032	-0.062	-0.101	-0.092	-0.075	-0.093	-0.112	-0.067	-0.061	-0.056	-0.067	-0.050	-0.016	-0.010	-0.004
l7	-0.066	-0.035	-0.045	-0.041	-0.028	-0.027	-0.031	-0.030	-0.025	-0.027	-0.022	-0.009	-0.004	-0.002	0.001
l8	-0.143	-0.098	-0.112	-0.090	-0.082	-0.059	-0.053	-0.042	-0.068	-0.051	-0.015	-0.010	0.001	0.004	0.002
l9	-0.086	-0.149	-0.181	-0.110	-0.129	-0.125	-0.100	-0.089	-0.103	-0.065	-0.049	-0.035	-0.003	-0.001	0.002
l10	-0.091	-0.140	-0.136	-0.136	-0.141	-0.139	-0.132	-0.125	-0.114	-0.099	-0.057	-0.049	-0.011	-0.001	0.001
l11	-0.177	-0.211	-0.182	-0.189	-0.168	-0.144	-0.149	-0.134	-0.128	-0.104	-0.109	-0.070	-0.039	-0.019	-0.027
l12	-0.218	-0.031	-0.016	-0.080	-0.031	-0.001	-0.023	-0.014	0.022	-0.015	-0.006	-0.005	-0.014	-0.006	0.001
l13	recording too short														
l14	0.027	0.037	-0.023	-0.040	-0.006	0.000	-0.024	-0.012	-0.007	-0.009	-0.012	-0.011	-0.007	-0.019	-0.032
	-0.077	-0.062	-0.070	-0.056	-0.055	-0.045	-0.050	-0.036	-0.038	-0.032	-0.023	-0.018	-0.010	-0.012	-0.006
	0.025	0.028	0.021	0.023	0.024	0.020	0.016	0.017	0.016	0.013	0.011	0.008	0.004	0.008	0.004
s1	recording too short														
s2	-0.210	-0.180	-0.088	-0.076	-0.041	-0.024	-0.013	0.016	-0.004	0.012	0.020	0.021	0.008	0.006	-0.009
s3	-0.235	-0.164	-0.177	-0.062	-0.051	-0.055	-0.027	-0.015	-0.033	-0.020	-0.023	-0.012	-0.002	-0.002	-0.001
s4	-0.334	-0.255	-0.234	-0.194	-0.175	-0.117	-0.105	-0.091	-0.081	-0.075	-0.039	-0.031	-0.006	-0.002	0.001
s5	-0.301	-0.239	-0.276	-0.206	-0.137	-0.068	-0.147	-0.179	-0.145	-0.147	-0.072	-0.087	-0.024	-0.007	-0.008
s6	-0.237	-0.258	-0.207	-0.137	-0.123	-0.114	-0.109	-0.091	-0.091	-0.069	-0.030	-0.032	-0.004	0.001	-0.001
s7	-0.040	-0.004	-0.007	-0.025	-0.012	-0.020	0.003	-0.017	-0.020	-0.017	-0.011	0.005	0.005	-0.003	0.004
s8	-0.092	0.018	0.004	0.010	0.022	0.017	0.017	0.027	0.021	0.019	0.016	0.016	0.007	0.004	0.003
s9	-0.184	-0.057	0.120	-0.034	0.000	0.008	0.013	0.028	0.023	0.028	0.029	0.024	0.012	0.007	0.003
	-0.204	-0.142	-0.108	-0.090	-0.065	-0.047	-0.046	-0.040	-0.041	-0.034	-0.014	-0.012	0.000	0.000	-0.001
	0.035	0.040	0.049	0.028	0.025	0.018	0.023	0.026	0.021	0.021	0.012	0.013	0.004	0.002	0.002

cell	n=1	n=2	n=3	n=4	n=5	n=6	n=7	n=8	n=9	n=10	n=15	n=20	n=50	n=100	n=200
n1	-0.047	-0.077	-0.084	-0.125	-0.115	-0.077	-0.056	-0.057	-0.056	-0.060	-0.024	-0.020	-0.010	-0.003	-0.004
n2	-0.082	-0.088	-0.080	-0.062	-0.059	-0.050	-0.047	-0.032	-0.066	-0.055	-0.015	-0.016	-0.006	-0.007	-0.004
n3	-0.073	-0.098	-0.092	-0.069	-0.055	-0.062	-0.066	-0.061	-0.054	-0.066	-0.011	-0.011	-0.007	-0.005	-0.001
n4	-0.031	-0.092	-0.085	-0.047	-0.040	-0.077	-0.044	-0.086	-0.065	0.004	-0.024	-0.012	-0.005	-0.006	-0.010
n5	-0.131	-0.169	-0.113	-0.101	-0.107	-0.098	-0.116	-0.122	-0.119	-0.092	-0.097	-0.055	-0.032	-0.032	-0.028
n6	-0.127	-0.111	-0.093	-0.086	-0.072	-0.058	-0.073	-0.035	-0.052	-0.053	-0.018	-0.019	-0.008	-0.008	-0.001
n7	-0.085	-0.042	-0.025	-0.017	-0.004	-0.002	-0.001	0.001	-0.005	-0.001	0.002	-0.006	0.003	0.002	0.001
n8	-0.072	-0.171	-0.202	-0.205	-0.207	-0.163	-0.127	-0.108	-0.102	-0.085	-0.048	-0.070	-0.024	-0.011	-0.009
n9	-0.109	-0.048	-0.055	-0.077	-0.104	-0.108	-0.122	-0.116	-0.121	-0.128	-0.063	-0.068	-0.035	-0.023	-0.013
n10	-0.054	-0.093	-0.104	-0.099	-0.074	-0.056	-0.083	-0.068	-0.052	-0.048	-0.023	-0.037	-0.021	-0.005	-0.005
n11	0.167	0.048	0.016	-0.008	-0.017	-0.024	-0.035	-0.082	-0.073	-0.071	-0.068	-0.077	-0.034	-0.013	-0.010
n12	0.030	-0.045	-0.067	-0.072	-0.079	-0.097	-0.090	-0.079	-0.095	-0.091	-0.045	-0.049	-0.014	-0.010	-0.007
n13	-0.014	-0.094	-0.087	-0.057	-0.098	-0.085	-0.074	-0.062	-0.075	-0.083	-0.068	-0.060	-0.020	-0.025	-0.013
	-0.048	-0.083	-0.083	-0.079	-0.079	-0.073	-0.072	-0.070	-0.072	-0.064	-0.039	-0.038	-0.016	-0.011	-0.008
	0.022	0.016	0.014	0.014	0.014	0.011	0.010	0.010	0.009	0.010	0.008	0.007	0.003	0.003	0.002
p1	-0.039	-0.061	-0.071	-0.068	-0.083	-0.087	-0.090	-0.079	-0.092	-0.074	-0.057	-0.055	-0.024	-0.017	-0.011
p2	-0.007	-0.087	-0.113	-0.122	-0.097	-0.081	-0.090	-0.085	-0.081	-0.082	-0.058	-0.039	-0.012	-0.002	0.000
p3	-0.019	-0.106	-0.097	-0.141	-0.143	-0.149	-0.139	-0.132	-0.129	-0.134	-0.100	-0.084	-0.038	-0.021	-0.013
p4	-0.026	-0.112	-0.130	-0.153	-0.129	-0.129	-0.133	-0.120	-0.123	-0.117	-0.084	-0.067	-0.032	-0.013	-0.008
p5	-0.034	-0.099	-0.127	-0.120	-0.120	-0.107	-0.086	-0.088	-0.076	-0.071	-0.043	-0.033	-0.022	-0.015	-0.008
p6	0.066	-0.031	-0.035	-0.033	-0.038	-0.031	-0.030	-0.031	-0.038	-0.041	-0.025	-0.015	-0.014	0.001	-0.006
p7	0.174	0.003	-0.015	-0.041	-0.034	-0.049	-0.042	-0.035	-0.051	-0.035	-0.055	-0.027	-0.017	-0.006	-0.007
p8	-0.106	-0.019	0.003	-0.008	-0.002	-0.010	-0.015	-0.025	-0.017	-0.014	0.003	0.007	0.008	0.002	0.001
p9	0.044	-0.018	-0.032	-0.027	-0.040	-0.049	-0.049	-0.060	-0.056	-0.054	-0.040	-0.026	-0.015	-0.015	-0.006
p10	-0.013	-0.049	-0.027	-0.048	-0.047	-0.052	-0.050	-0.074	-0.075	-0.065	-0.041	-0.030	-0.026	-0.033	-0.016
p11	0.020	-0.031	-0.029	-0.028	-0.024	-0.029	-0.025	-0.015	-0.014	-0.020	-0.012	-0.008	-0.020	-0.004	-0.008
p12	0.123	-0.011	-0.018	-0.017	-0.023	-0.024	-0.026	-0.031	-0.027	-0.027	-0.031	-0.024	-0.016	-0.012	-0.012
p13	0.048	-0.011	-0.006	-0.006	-0.008	-0.033	-0.039	0.030	-0.029	-0.032	-0.031	-0.034	-0.015	-0.004	-0.004
	0.018	-0.049	-0.054	-0.062	-0.061	-0.064	-0.063	-0.057	-0.062	-0.059	-0.044	-0.033	-0.019	-0.011	-0.007
	0.020	0.011	0.013	0.015	0.013	0.012	0.011	0.012	0.011	0.010	0.008	0.007	0.003	0.003	0.001

Total	-0.061	-0.078	-0.077	-0.074	-0.071	-0.065	-0.065	-0.058	-0.058	-0.052	-0.034	-0.030	-0.013	-0.009	-0.007
	0.013	0.010	0.009	0.008	0.008	0.007	0.006	0.007	0.006	0.005	0.004	0.004	0.002	0.002	0.001

Table 4.2 Slopes from the linear regression analysis between t_0 and $(t_1+...+t_n)$ for n=1, 2, ...9, 10, 15, 20, 50, 100, 200 for each individual recording.

n=2	n=3	n=4	n=5	n=6	n=7	n=8	n=9	n=10	n=15	n=20	n=50	n=100	n=200
0.173	0.101	0.194	0.191	0.231	0.239	0.168	0.173	0.127	0.145	0.140	0.119	0.140	0.228
0.043	0.045	0.046	0.045	0.047	0.045	0.047	0.044	0.046	0.046	0.037	0.045	0.041	0.039
0.049	0.047	0.045	0.046	0.038	0.039	0.039	0.038	0.040	0.040	0.034	0.038	0.037	0.037
0.035	0.031	0.031	0.035	0.035	0.037	0.038	0.042	0.029	0.040	0.049	0.038	0.039	0.035
0.032	0.032	0.030	0.034	0.034	0.033	0.040	0.024	0.034	0.034	0.041	0.035	0.038	0.037
0.030	0.037	0.036	0.029	0.038	0.034	0.024	0.039	0.034	0.033	0.031	0.028	0.033	0.036
0.028	0.027	0.024	0.028	0.021	0.024	0.028	0.030	0.039	0.028	0.028	0.032	0.027	
0.024	0.028	0.032	0.023	0.027	0.025	0.039	0.042	0.036	0.042	0.044			

Table 4.3 Comparison of standard errors of mean of linear regression analyses between t0 and (t1+...+tn) for one cell.

cell	burst slope	15s slope (small ISI)	15s slope	10s slope	5s slope (small ISI)	5s slope	rest slope (small ISI)	rest slope
me1	0.945	not enough data for analysis					3.825	-0.017
me2	0.959	0.898	-0.171	-0.079	1.897	-0.085	2.278	-0.040
me3	0.599		-0.115	-0.041		-0.092	1.963	-0.170
me4	0.334		-0.127	-0.231	2.557	-0.069	0.272	-0.094
me5	0.412		-0.067	-0.043		-0.005	6.443	-0.056
me6	0.585	3.866	-0.230	0.020	1.775	-0.172	0.611	-0.137
me7	0.642		-0.085	-0.030		0.165	1.764	0.021
me8	0.400		-0.138	-0.166		0.150	1.130	-0.046
average	0.609		-0.133	-0.082	2.166	-0.015	2.286	-0.067
sem	0.084		0.021	0.033	0.319	0.048	0.710	0.022

Table 4.4 Slopes of linear regression analysis t_0 vs t_1 for the samples of ISIs for the burst, the 5s starting 15s, 10s, and 5s before a burst, and the remaining ISIs for all milk-ejecting cells.
Small ISI slope is shown where a different trend was detected for very small ISIs.

CHAPTER 5

GENERAL DISCUSSION

Computational models of single neurones that take into account all intrinsic mechanisms will be extremely complex, and hence building large-scale models of neurone networks will be computationally intense, if not infeasible. In order to develop simple models which still reflect realistically the intrinsic properties of the neurone we first need to know which of the many identified mechanisms are the most important for its function. But how do we decide which features or properties are the most important? The selection criterion that we believe to be the most straightforward and intuitive is what influences the behaviour most, i.e. the firing of the cell.

5.1 Background and Motivation

5.1.1 Model System

Oxytocin neurones were chosen as the model system for several reasons. The somata of oxytocin neurones are located mainly in the paired supraoptic and paraventricular nuclei, where they synthesise the hormone oxytocin. The SON is easily accessible from the ventral surface of the rat brain. In addition, the vast majority of cells within the SON are magnocellular neurosecretory neurones, or in other words, the nuclei are very homogenous. Together, these characteristics of the SON make it very convenient for experimental manipulation. In addition, the axons of oxytocin neurones – along which the action potential generated at the soma is conducted to the terminals in the posterior pituitary gland – pass through the hypophysial stalk. Thus, the neurones can be unequivocally identified, as they are excitable by antidromic stimulation of the stalk. Also, the hormones released from the terminals into the circulation are analogous to neurotransmitter release from conventional neurones, but in contrast to the transmitter release occur in such large quantities that they can be readily measured. Due to the ease of manipulation the magnocellular neurosecretory system has been a model system for a wide range of

investigations, and has been studied extensively using both *in vitro* and *in vivo* techniques. Thus, the intrinsic cell properties of these neurones have been well characterised, as have their responses to a variety of stimuli. Accordingly, they are one of the few groups of central neurones of which we know the behaviour in specific physiological circumstances, and of which we know the precise outcome in response to their behaviour, i.e. hormone output in relation to changes in activity pattern.

Since the electrical activity of these neurones is readily recorded and their secretory output can be measured directly, these cells provide the opportunity for developing models that can be evaluated against a much wider variety of experimental controls. Oxytocin and vasopressin neurones share many intrinsic properties. However, while the hyperpolarising afterpotentials are identical in both, vasopressin neurones additionally display depolarising afterpotentials. Also, vasopressin neurones have an additional firing mode, 'phasic' firing. This firing pattern is non-stationary, and hence unsuitable for many of our statistical examinations. Therefore, we decided that oxytocin neurones are the better choice for a proof of principle investigation.

5.1.2 Aim and Purpose

In the magnocellular neurosecretory system, the rate and pattern of action potentials are intimately linked to the amount and pattern of the hormone release into the bloodstream (Poulain & Wakerley, 1982). The firing patterns depend on both the intrinsic properties of the neurones and the synaptic inputs they receive. Therefore, whatever properties or mechanisms influence the firing pattern of the neurones most can be assumed to be of chief importance for their function. Certainly, although each cell has a multitude of membrane properties, channels, input, connections with other neurones, and other intracellular properties that influence its function, not all of these exert an equal influence over the firing activity at all times. Which of these influence the firing patterns most, and which ones can – at least for the moment – be neglected?

While *in vivo* techniques provide a way to study the neurones in the living organism, i.e. in their natural state, with connections intact, relatively undisturbed by experimental manipulation and receiving input, this approach is unfortunately not suitable to examine all parameters. The conventional approach to investigate intrinsic membrane properties and their role in single neurones is to conduct detailed experiments on individual isolated cells *in vitro*. With the knowledge gained, one then speculates about how individual channel properties might contribute to the functioning of the neurones *in vivo*. However, *in vitro* experiments consider the neurone in a highly artificial situation, in which connections are interrupted, and thus the afferent input altered or eliminated. It is difficult to estimate just how much the preparations for the procedure alter the properties of the neurone, and therefore impossible to judge just how close the results obtained *in vitro* represent the function of the neurone *in vivo*.

In this thesis we have described a novel, radically different and a rather more direct way of investigation. We take spontaneous, unexceptional firing activity recorded *in vivo* as the starting point of our analyses. In this way, we avoid interventions that fundamentally disturb or distort cell properties, and are able to take into account the influence of afferent input. The purpose of this work is to examine ordinary discharge patterns of oxytocin neurones using statistical methods in order to determine the key features involved in their regulation, and consider possible explanations in terms of known intrinsic properties. A further, secondary objective was to investigate whether there are any consistent, characteristic differences in the firing pattern of oxytocin neurones recorded under a variety of physiological conditions.

The results of our statistical analysis show that the most important parameters to determine the firing of oxytocin neurones (for a given synaptic input) are the post-spike HAP and the post-train AHP. The HAP sets a firm upper limit on the discharge frequency of oxytocin neurones, and this is exceeded only during the burst discharge observed during parturition and suckling. By inference the mechanisms underlying the HAP must be altered to allow bursting to occur. The AHP 'regularises' the

discharge activity of oxytocin neurones, making the mean second-by-second variability in discharge rate much less than would otherwise be the case.

5.2 Main Results

We started by seeking *in vivo* recordings of oxytocin neurone activity that would provide the basic pool of data for rigorous statistical analysis. Electrical activity was recorded from naïve (n=13), pregnant (n=13), lactating-unsuckled (n=9), lactating-suckled (but not displaying milk-ejection bursts; n=14), milk-ejecting (n=8), before (n=8) and after (n=10) hyperosmotic stimulation rats under urethane anaesthesia, using both single and paired cell recording techniques. Stretches of recordings were selected according to pre-specified criteria regarding stationarity and lack of noise to ensure that the analyses were performed only on true spontaneous activity, free of trends or rhythmic variations that might invalidate the results.

Starting with these selected stretches of spontaneous, unexceptional electrical activity we investigated whether we could detect subtle signs of activity-dependent feedback mechanisms in the firing patterns of oxytocin neurones. The analyses described in this thesis can be broadly divided into three categories: (a) the relation between periods of activity, (b) the relation between individual ISIs, and (c) the relation between a period of activity and an individual ISI. Each of these approaches has its advantages and disadvantages.

Periods of activity as represented by firing rates in spikes per time unit – especially spikes/ 1s – is a natural measure. It is easy to calculate, and hence widely used to collect and examine data, which is therefore readily available in this form. Further, because it is common, results obtained using this type of measure are readily understood by experimental scientists. However, because the boundaries are set arbitrarily, i.e. without consideration of the natural time scales, an effect that is shorter or longer lasting might be missed. Firing rates measured per second are not intrinsically more meaningful than rates measured per minute or per 10 minutes, but the features of activity vary, as shown here, with the time scale of measurement.

The analysis of individual ISIs, in contrast, eliminates artificial time constraints. An ISI preserves the relationship between two neighbouring spikes, regardless of the absolute time scale of their occurrence. Hence it is independent of the firing frequency, and we can also consider it independently of its temporal context. However, effects that encompass several spikes are not easily recognised.

Analysing periods of activity as measured by a predestined number of ISIs represents a compromise between the other two approaches. An investigation of this kind is more complicated to set up, and its results are less straightforward to interpret. However, because it is based on ISIs the time scales are again independent of the firing frequency. Since the number of the ISIs is pre-specified we can avoid temporal constraints, although this can be either an advantage or a disadvantage, depending on what is investigated. Further, this method allows us to examine influences that last for longer periods and encompass several ISIs.

The initial ISIH analysis showed clearly that spontaneous firing in oxytocin neurones is dominated by the effects of the HAP. Further, it indicates that beyond the effects of the HAP the activity is dominated by activity-independent factors, i.e. that outside the time course of the HAP the activity is essentially random. However, subsequent randomisation of ISIs, and analyses of the firing rate distributions based on these randomisation provide a first indication that there is a weak activity-dependent mechanism that influences the firing pattern in oxytocin neurones. This was confirmed by the examination of the indexes of dispersion, which indicate that there are some 'regulatory' effects, such that over longer time scales – 2 to 8 s – the activity is more ordered than it should be based on its features seen on a short time scale, i.e. 0.0625 or 0.125 s.

The autocorrelation analysis of firing rates showed that on a small time scale periods of relatively high activity are likely to be followed by periods with relatively low average activity, and vice versa, while for long time scales this relationship

disappears. Of the known intrinsic mechanisms the AHP effects the firing activity in a way compatible with these firing characteristics. In periods of intense activity the AHP quickly summates to its maximum size and thus the inhibition on the generation of further spikes is large. Because of this inhibition the following period of activity will be comparatively low. Conversely, during periods of low activity the AHP can decay between spikes, and thus there is no post-spike inhibition other than the HAP to space successive action potentials. This allows for a few short ISIs, or in other words localised fast firing. Overall however, the effect is that the activity is balanced and maintained at an appropriate and steady average level, which is why no association can be detected at larger time scales. Indeed, what is clear from this analytical approach is that the AHP has a large effect even at low spontaneous firing rates. Conventionally, the AHP has been observed in response to brief intense activation *in vitro* – where it is readily detectable. This has led to the belief that the AHP may be responsible for the silent periods following the milk-ejection burst for instance, but may play a negligible effect otherwise because of its small magnitude at low firing rates. However, as shown here, the effect of the AHP is clearly discernible on discharge patterns and must equally have a strong effect on discharge frequency. Our results therefore support *in vitro* findings by Kirkpatrick and Bourque (1996), reporting the occurrence of the AHP at firing rates as low as 1 Hz.

The principle described for firing rates can be extended to the serial dependence of ISI lengths. If action potentials occur close together, i.e. if the ISI is short, then their AHPs summate. Since the spike inhibition is now larger the generation of a further spike requires stronger depolarisation, and the probability of another spike occurring is diminished. Thus, if one ISI is quite short, then the summated AHP makes a further spike less likely, spacing it further apart and resulting in the next ISI to be relatively longer. Conversely, if one ISI is long, then the AHP decays, and as the post-spike inhibition is minimal the next action potential can occur after a shorter period. This is reflected in the negative linear regression between one ISI and the next. As overall the activity is balanced, i.e. on a long time scale the firing is quite homogenous, the association seen on a short time scale between firing rates vanishes for long time scales.

In addition to the negative linear regression between ISIs in 40% of all analysed neurones there is a positive linear regression in the range of very short ISIs. 'Very short' in this context is relative for each cell, as a short interval length in one recording falls into a medium length range in another, hence no absolute values can be given. The occurrence of this separate trend for small ISIs is independent of the firing rate, but on the other hand depends on the orderliness of the firing. The relationship between firing rate, orderliness of the activity and the occurrence of small ISIs is not immediately obvious.

Intuitively, the relationship between the firing rate and the orderliness of the firing activity seems to be straightforward: the faster a neurone fires the more regular we expect the firing to be. This is only partially valid. Consider the extreme situation when the neurone is driven by strong synaptic input to fire near the upper limit of the firing rate. Under these circumstances the activity is continuous, and action potentials are spaced by the post-spike absolute refractory period and the AHP. The latter summates, and during fast firing has no time to decay substantially, hence remains near its maximum size. Therefore, the depolarising input has to be very strong to overcome this inhibition. However, the strong input and the AHP can keep a 'balance', whereby a new spike is generated as soon as the AHP can be overcome. As the inhibiting mechanisms remain at a consistent strength in this extreme and rare situation the firing is fast and very regular. In contrast, at firing rates that are fast but not extremely so, i.e. when there is time for the post-spike inhibitions to decay – partially if not completely – then there is scope for some variability. We can see one example of the dichotomy between mean firing rate and irregularity of the activity in physiologically relevant circumstances in the work of Brown *et al.* (2000). They report that experimental manipulations affecting bursting behaviour in lactating rats also influence the properties of the background activity in characteristic ways: i.c.v. applications of oxytocin result in both increases in mean firing rate, and also in the irregularity of firing as measured by both the standard deviation of firing rate and the index of dispersion; i.p. injections of hypertonic saline also increase the mean firing rate, but in contrast the irregularity of the firing activity is reduced in these circumstances. Thus, the firing pattern does usually, but not necessarily become

more regular when the firing frequency increases, indicating again that irregularity of the firing is an important feature for the function of the neurone, and showing that mechanisms that control irregularity have a pivotal role in the control of neuronal output (as discussed in section 5.4.1).

Overall, during rather fast firing there is less scope for variability and so the firing will be relatively more regular. More regular firing will also result in – on average – shorter ISIs. However, *faster* firing does not necessarily facilitate *very* short ISIs, the occurrence of which on the other hand will be helped by very *irregular* spiking activity.

Again, consider the case of extremely fast firing. As described above, the ISI lengths will be defined by the combination of synaptic input and the post-spike inhibitions, the absolute refractory period and the AHP. The contribution of the AHP – which in these specific circumstances is at or near its maximum size – helps to maintain a certain minimum ISI length, thus placing a limit on the maximum possible firing rate.

On the other hand, at lower firing rates the absolute refractory period remains unchanged. In contrast, the AHP will be more variable in size and hence its inhibitory effect on spike generation will vary: after several short ISIs the AHP will be relatively large and hence the next spike will be delayed. Conversely, a period of relatively low firing frequency allows the AHP to decay substantially – or even fully – between spikes, and a further spike can occur after the time it takes for the HAP to decay. Thus, as the additional inhibition is less strong this makes isolated cases of exceptionally short ISIs possible. This explanation is supported by our observation that for all recordings the length of their shortest ISI is remarkably similar, even though the differences in the mean lengths and the firing rates are vast.

Summarising, a faster firing rate will usually result in more regular firing and overall relatively shorter, more uniform lengths of ISIs. A low firing rate can be more variable, and the ISI lengths will be more dispersed. While the ISIs in fast firing neurones will on average be much shorter than the majority of 'relatively'

short ISIs in neurones with lower firing rates, 'extremely' short ISIs are possible in these neurones due to the decay of the AHP.

Turning our attention back to the positive linear regressions, if the synaptic input does not drive the cell to fire at high frequencies the AHP can decay between spikes, and thus is quite small, or even absent at times. Hence a very short ISI is possible, and – as the AHP is still relatively small and its inhibition minimal – a further short ISI can occur. Only if a few spikes occur close together does the AHP summate again and inhibits further spikes, preventing the activity to 'run away', and at a long time scale maintaining a stable firing rate. Thus, while the firing activity is irregular on a small time scale, the clusters of very small ISIs are responsible for the expression of the positive linear regression. Further, as the cluster results in a large AHP there will be an inhibition on further activity, thus resulting in the negative autocorrelation between neighbouring firing rates on a small time scale described above. Of course, because overall the activity is balanced there should be no dependencies between firing rates calculated for longer time scale. This is why in our analysis the negative autocorrelation between firing rates seen on a short time scale disappears for longer time scales.

It should be mentioned that in contrast to a negative linear regression, which can only be explained by non-random influences on the firing activity, a positive linear regression could be explained by non-stationarity, i.e. short-term trends. However, since the recordings were specifically selected for being stable and stationary, and the positive regression can be seen consistently in nearly half of neurones across all the groups it is more likely that it represents a real phenomenon, rather than being an delusion.

As can be seen above, while the two approaches of statistical analysis – association between periods of activity, and association between individual ISIs – are similar in concept they do not simply duplicate findings, but cover different aspects,

thus contributing to a rounded picture. We decided to follow up on these results by combining the two approaches. Their synthesis is the investigation of how an individual ISI is influenced by the preceding activity, varying in duration from the last couple to several tens of ISIs. While the linear regression slopes are again negative, they are steeper for the linear regressions between *several* ISIs and the succeeding ISI, compared to the slope between only a *single* ISI and the succeeding ISI. The steepest slope is for the regression with 2 to 6 preceding ISIs – depending on the physiological group – thereafter with each additional ISI decreasing towards zero.

Again, the negative regression slope is the indication of the AHP, whereby after several spikes close together the AHP is summated and therefore the next spike is likely to be delayed. Equally, several spikes at longer intervals allow the AHP to decay – at least partially – and the succeeding spike can occur sooner.

Further, the increase in the slope for a number of ISIs is consistent with the effects of the summation of the AHP over several ISIs. With the summated AHP being more pronounced after a period of faster activity, its increased balancing effect is evident in the steeper slope. When looking at periods of activity longer than 6 ISI it is more and more balanced, i.e. longer periods are increasingly averaged out, therefore at long time scales the considered ISIs will sum up to approximately the same length. Thus, no assumption can be made about the length of the succeeding ISI on the basis of the length of the previous ISIs, and the linear regression decreases to zero.

Thus, each of the three different but related approaches revealed evidence of the AHP in the spontaneous firing activity of oxytocin neurones. Their results indicate that the AHP works as a kind of 'memory', whereby the current state of activity is recognised and balanced, thus maintaining a steady – and sustainable – firing rate and accordingly a steady hormone output.

5.3 Further Results

A further aim of our work was to investigate whether there are consistent differences in the spike patterns of neurones recorded in different physiological states.

Importantly, no significant differences in the characteristics of the firing pattern of neurones before and after hyperosmotic stimulation can be seen. The activity of the before hyperosmotic stimulation is – according to the results of the index of dispersion analysis – more variable than the after hyperosmotic stimulation activity, but this is a function of the lower mean firing rate. Further, the activity of these two samples does not differ from the firing activity of naïve neurones. This was anticipated, as the changes in the firing are induced externally, and in keeping with natural stimuli. Thus, assuming the hyperosmotic stimulation influences only the rate of synaptic input and induces a direct steady depolarisation, but does not – directly or indirectly – affect intrinsic properties of the cells otherwise it appears unlikely that the intrinsic mechanisms would change in such a short time in such a fundamental way that we can detect the signs in the firing activity of the neurone.

In contrast, the characteristics of the activity of the two lactating groups are subtly different in several ways from all other but the before hyperosmotic group: the mean firing rate is lower, and while the shortest ISI length is comparable to the other groups, the longest ISI – and consequently the mean and median ISI length – are much longer than in the other groups.

In addition, the index of dispersion analysis of the lactating groups suggests that there are differences. Unlike the non-lactating groups, which become *more ordered*, the firing of the lactating groups becomes *more irregular* for longer time scales, i.e. the activity of lactating neurones is irregular for all time scales. The importance of this cannot be stressed enough, as the irregularity of the firing during lactation seems to be an essential feature for successful milk let-down. Brown *et al.* (2000) showed that regularisation of firing activity in lactating neurones is not

compatible with the full expression of milk-ejection bursts, while experimental manipulation that increases irregularity of the firing is associated with a more proficient bursting pattern. Thus, the analyses of the index of dispersion provide a first indication about the functions involved in the regulation of irregularity in lactation, namely that the activity-dependent balancing mechanism is lacking, and that beyond the effects of the HAP the activity of lactating neurones is essentially random.

A further subtle difference lies in the relationship between mean firing rate and the index of dispersion: while for both non-lactating and lactating groups it is true that the faster the cell fires the more ordered the firing appears, this association is constant regardless of time scale for non-lactating neurones. In contrast, this association becomes more pronounced with increases in time scale for lactating neurones. As discussed above, the dependence of orderliness on firing frequency is plausible. However, why should this effect in lactating neurones differ to non-lactating neurones? The index of dispersion shows that for long time scales the activity of lactating neurones is very variable. This might be a function of the firing rate, which is much lower in lactating neurones when compared to non-lactating neurones (2.3 Hz to 6.9 Hz). Thus, it seems that for these neurones the firing needs to be relatively fast to be ordered, and hence orderliness is particularly dependent on the firing rate, as reflected in the increased slopes for larger time scales.

The other major point in which the lactating groups differ from the non-lactating groups becomes apparent in the results of the linear regression analysis between periods of activity and individual ISIs. The regression slopes for these groups are negative, as for the other groups, but the slopes are steepest for the analysis between *individual* ISIs, whereas for all the other groups the steepest slope was found for *several* ISIs and the succeeding ISI. In fact, the slope for the individual ISIs for the lactating-suckled neurones is much steeper than for any other group, and the lactating-non-suckled slope is steeper than any non-lactating group bar the before hyperosmotic stimulation. However, slopes for both lactating groups decrease rapidly and are much flatter than for non-lactating groups for regressions between more than

6 ISIs and the succeeding ISI. The pronounced slope at the beginning indicates that the activity-dependent mechanism is stronger during lactation. In contrast, the rapidly decreasing slope suggests that the mechanism is short-lasting and decays much faster in lactating neurones than in non-lactating neurones.

This suggestion supports our earlier findings, which indicate that the firing activity in lactation lacks the balancing mechanism: in non-lactating neurones the firing is irregular on a small time scale, but on a long time scale the AHP balances the activity which thus becomes more ordered. In contrast, if the AHP decays faster during lactation then it cannot balance the activity effectively, and while its increased size might help to keep the firing from 'running away', the activity remains heavily clustered.

Recently, Teruyama and Armstrong (2002) have published *in vitro* work that is in agreement with this conclusion. Using hypothalamic explants from virgin, late pregnant, and lactating rats the response to depolarising pulses was recorded intracellularly. They found that for identified oxytocin neurones the amplitude and decay of the AHP following spike trains was significantly larger and faster in lactating rats, compared to virgin rats. Thus, we can see the effects of an AHP adapted in lactation in the analyses of oxytocin firing activity *in vivo*.

However, Teruyama and Armstrong also report a larger amplitude and a faster decay of the AHP in late pregnant rats. In our analysis the pregnant group showed the same behaviour as the non-lactating groups, namely a steeper slope for several ISIs, with the steepest slope between six ISIs and the succeeding ISI, thereafter gradually decreasing towards zero. The disagreement between these two results cannot be explained by timing in pregnancy as the experiments in both our and the *in vitro* study were performed on day 21-22 pregnant animals. How can we explain this discrepancy? In order to answer this question let us first look at all the analyses for pregnant neurones in more detail.

It is worth recalling at this point that the pregnant group did also differ from the lactating groups – and displayed the same characteristics as the other non-lactating groups – in the index of dispersion analysis. Curiously, the pregnant group differed in its result only in one investigation, the linear regression analysis between neighbouring ISIs, where it is the only group – from all lactating or non-lactating groups – to display a *positive* slope. The positive linear regression slope indicates that a short ISI is more likely to be followed by another short ISI, and a long ISI is more likely to be followed by another long ISI. This would indicate a lack of activity-dependent negative feedback mechanism. However, as explained above, the results for both the periods of activity investigations and the periods of activity and individual ISIs investigations do not differ from the results of the non-lactating groups, and these clearly show the effects of a balancing mechanism.

As mentioned before, a positive linear regression could be the expression of some inherent non-stationarity. However, if this were the case for our recordings then the non-stationarity should be seen in the results of the other analyses, which are all very sensitive to short-term trends. What is the reason for the difference between the negative slopes for the analysis of the relationship between neighbouring periods of activity, and for the relationship between periods of activity and the succeeding ISI, and the positive slope seen for the analysis between individual ISIs?

From the index of dispersion analysis, and both analyses involving periods of activity – autocorrelations between firing rates and linear regression between several ISIs and the succeeding individual ISI – we conclude that there is a balancing mechanism, maintaining the activity at a steady level. However, the positive linear regression slope between neighbouring ISIs implies that there is no balancing effect from one interval to the next. Is it possible that the AHP is weak and short lasting in the last stages of pregnancy, and therefore has little effect from one spike to the next, but over a period of firing has enough presence to keep the activity balanced? Thus overall the behaviour of pregnant neurones is comparable to other non-lactating neurones.

Returning to Teruyama and Armstrong's results, the *in vitro* work suggests that pregnant neurones have the same characteristics as lactating neurones. In contrast, our results suggest that pregnant neurones behave more like non-lactating neurones. This would suggest that the rearrangements in preparation for lactation are not yet in place in late pregnancy, and are only completed with the start of lactation. However, intuitively is seems more logical that the anatomical and intrinsic restructuring should be completed in late pregnancy, as indeed it has been suggested by previous work (Montagnese *et al.*, 1987; Stern & Armstrong, 1996).

The one possible explanation is that while the anatomical restructuring and the intrinsic properties are completely rearranged late in pregnancy – as visible in dissociated data – other mechanisms, such as synaptic input, prevents these changes to take influence on the firing until after parturition, say through network connections which weigh input differently. This could also be an explanation why we found that the AHP was strongest but shortest in suckling rats in *lactating*-suckled – though not milk-ejecting – animals, which is slightly different to the lactating *non*-suckled animals. If only intrinsic membrane properties were responsible for the results seen – as proposed by Teruyama and Armstrong's results – then surely there should not be a difference between these two groups. Since our results do show a slight difference between lactating-suckled and lactating non-suckled neurones, and a fundamental difference between the lactating groups and the pregnant group, we conclude that both the intrinsic cell properties and the synaptic input received are important for the expression of the AHP. Further work is necessary to establish the exact cause of this irregularity in the behaviour of oxytocin neurones during late pregnancy which were uncovered by our statistical analyses. However, these results show that statistical analyses generate additional information not accessible by experimental work, and thus are able to make a substantial contribution to research efforts.

A particularly interesting, if very complicated event is the milk-ejection burst during lactation. Although much studied, so far not much is know about the mechanisms leading to this phenomenon. It has, however, been suggested

(Kirkpatrick & Bourque, 1996) that a weakening or a temporary deactivation of the AHP allows the oxytocin neurones to escape the normal limitations on their firing rates and fire at the high frequencies seen during the burst in response to suckling. We have presented evidence indicating that the AHP is bigger in amplitude but decays faster during lactation. What signs of the AHP can we see in the firing of oxytocin neurones during milk-ejection?

Unfortunately, the nature of the activity during milk-ejection makes statistical analyses of the kind described for non-milk-ejecting neurones difficult, in fact, the inherent non-stationarity makes the investigation of each recording in its entirety impossible. For this reason each recording was divided into three samples – with one being further divided into a three sub-categories – each of which was analysed separately. Since the investigations involving periods of activity were most susceptible to non-stationarity, it was decided that the linear regression analysis between individual ISIs was the most suitable for the data.

The results for the sample of background activity – the activity between bursts – are very similar to the results for non-milk-ejecting recordings, in that a negative slope – falling within the range of slopes seen in non-milk-ejecting recording – can be seen, as well as a positive slope for very small ISIs. This is an important point as it suggests that the changes in intrinsic properties and structural rearrangements are not the sole influence on the background activity in milk-ejecting animals. The high proportion of neurones displaying a positive regression slope in the range of very small ISIs – when considered in conjunction with the results for non-milk-ejecting neurones – suggest that the firing is highly irregular and clustered, which is in agreement with previous work (Brown *et al.*, 2000).

A steep positive slope was found for the burst samples. This was what we expected to find, given that – after the quick rise up to the peak in firing rate – the ISIs within a burst become progressively longer, thus ensuring that each ISIs is followed by a longer ISI. Therefore, no new insights can be gained from this finding.

Brown *et al.* (2000) report that irregular firing is a pre-requisite for milk-ejection burst: in condition where bursting was experimentally restrained the

variability of the firing was decreased, while conversely under conditions that facilitate milk-ejection bursts the variability is increased, too. Thus, we would expect to see a negative slope as the indicator of the intrinsic 'balancing' mechanisms that stabilise the firing activity. Further, it has been suggested that the temporary deactivation of these mechanisms – disengaging the "stabiliser" – allows oxytocin neurones to escape this limitations into the high firing frequencies seen during the milk-ejection burst (Kirkpatrick & Bourque, 1996). As the mechanism becomes progressively weaker towards the burst, this should be reflected by a less steep slope for the samples closer to the burst.

It is worth pointing out that our data samples are too small to allow us to draw any firm conclusion, and simply to reject or accept the hypothesis. The crux is that the emerging trend is in keeping with our predictions based on earlier findings and supports previously reported *in vitro* work.

Clearly, oxytocin neurones have an activity-dependent negative-feedback mechanism that ensures that overall the activity is consistent and uniform.

5.4 Physiological Relevance

5.4.1 Relevance of Orderliness

In oxytocin neurones, it has been shown that the rate and pattern of action potentials are intimately linked to the amount and pattern of hormone released into the circulation (Poulain & Wakerley, 1982). Thus, changes in the firing pattern have important consequences for the neurosecretion of the cell. Oxytocin neurones are remarkable in that they fulfil two completely different but important functions simultaneously, namely the regulation of milk let-down, and sodium excretion from the kidneys. They are able to combine these two roles because the output requirements to fulfil each are dramatically different, and hence there are different demands on the firing pattern.

Long term, the emphasis of the firing pattern is on balance and stability. The biological message encoded by a single oxytocin neurone is only a small contribution to the output of the entire oxytocin population. The overall hormone release has an enormous physiological significance, as it is closely related to the secretion of the appropriate amount of hormone required for regulating natriuresis. Therefore, it is imperative that over prolonged periods the firing rate remains at a stable average level in response to hormone demand.

In contrast, short-term variability in the firing of an individual neurone is of lesser physiological significance for the organism, except when such changes are synchronised throughout the entire oxytocin population. This situation occurs during parturition and lactation. Here, the requirement is very specific and quite different to the continuous, level hormone output needed to regulate natriuresis: a short exposure to a large amount of the hormone, which is met by a bolus release of oxytocin. The burst is followed by a short period of silence, and the interburst interval of 5-10 min allows the hormone to clear from the system, thus preventing a desensitisation of the target tissue.

Evidence for the significance of local variability in the firing activity of oxytocin neurones during lactation is accumulating. Analysing the activity between milk-ejection bursts, Brown *et al.* (2000) report a correlation between the irregularity of this background activity and bursting behaviour. Experimental manipulations that are associated with an inhibition of the bursting pattern also induce more regularity of the firing. In contrast, experimental manipulations that facilitate bursting also increase the irregularity of the background activity. This suggests that variability of the activity prior to a milk-ejection burst is an essential accompaniment of a marked bursting pattern. Why should this be so?

One possible explanation maintains that the increased variability of the background activity facilitates bursting by helping the cell to be receptive to inputs at the appropriate time. A neurone is maximally receptive to excitatory inputs when it is in a non-refractory state. Due to the AHP that summates to a substantial size after a period of intense activity oxytocin neurones become refractory for a short while. This

brief rest is necessary so that the neurone can become again maximally responsive to inputs from other cells. The alternations between intense activity and silence, i.e. high variability of the firing, therefore, help to keep the cell in the most receptive state to receive signals that lead to bursts.

Another argument focuses on the association between increased randomness of input and the increased variability of the firing. The signal for the onset of a burst might be local (see below), in which case the mechanism involved could entail strengthening of the interactions between neurones. One way to accomplish this is to increase the effectiveness of signal transmission by random noise. An appropriate amount of random noise improves the ability of a neurone to detect subthreshold periodic signals (Pei *et al.*, 1996), and also the performance of a neuronal control signal. Thus, stochastic resonance – where an optimal level of random noise maximises the fidelity of a neurone's response to a subthreshold input – may be an important mechanism by which information transmission efficiency in oxytocin neurones is facilitated, leading to enhanced interactions that may be necessary for a burst. Increased randomness of the input could lead to the enhancement of local variability in the firing activity.

The mechanism involved in increasing variability could be dendritically released oxytocin itself. As seen in the study described above i.c.v. application of oxytocin is associated with an increase in irregularity of the background activity and a marked facilitation of bursting behaviour (Brown *et al.*, 2000). Commonly, we refer to the different compartments of the neurone as if each had a single, strictly delineated purpose, i.e. that dendrites convey incoming information to the soma, and that the neurone's product is released from axons. This notion is of course simplistic. In particular, there is now considerable evidence that some neurones – and amongst them oxytocin neurones – are releasing their products not only from their axons, but also from their soma and dendrites (for a discussion see Ludwig, 1998). Furthermore, evidence is mounting that dendritic release is not simply a by-process of axonal release, but happens in a independent manner and is a rather active procedure. For instance, it has been shown that some stimuli that trigger systemic release of

vasopressin and oxytocin also trigger hormone release within the SON. In the latter not only is the release delayed but it also occurs over a much longer time course (Ludwig *et al.*, 1994). More dramatically, Moos *et al.* (1989) have shown that the release of oxytocin within the SON is increased several minutes *prior* to the milk-ejection reflex, i.e. independent of the bolus release of hormone. Oxytocin is one of the peptides known to be able to trigger dendritic release of oxytocin, or to put it another way dendritic release of oxytocin is a self-perpetuating process. This could be a mechanism – indicated above – by which the interactions between the neurones are strengthened, as it changes the functional connectivity between them by enabling dendro-dendritic interactions. It is worth pointing out that during parturition and lactation intranuclear release of oxytocin increases 2.5-4 -fold (Neuman *et al.*, 1993), thus further supporting the argument that intranuclear oxytocin release is essential for bursting activity in oxytocin neurones. While oxytocin itself is only weakly depolarising (Yamashita *et al.*, 1987) even a weak mutual excitatory interaction might be beneficial for triggering bursting activity. Thus, intranuclear oxytocin in its autoregulatory role could facilitate clustering in the firing activity, and thus underlie the generation of milk-ejection bursts during lactation. It should be noted however, that oxytocin does not induce bursting if the suckling stimulus is not present, thus while intranuclear oxytocin seems to facilitate bursting behaviour, it does not on its own explain bursting, which is dependent on the appropriate input.

However, the significance of local variability in efficient hormone release outside the specialised situation of lactation should not be underestimated. Cazalis *et al.* (1985) have explored in a series of experiment *in vitro* the role of fine temporal structure in the activity of vasopressin neurones. They report that a stimulation consisting of a single burst of pulses with an intraburst frequency of 13 Hz resulted in a greater amount of hormone released than the same number of pulses delivered at a constant frequency of 13 Hz. The amount could be enhanced further with a silent period of at least 21 s between stimulating bursts, indicating that electrical quiescence between periods of activity provide time necessary for recovery from spike failure and secretory fatigue, supporting efficient hormone secretion induced by subsequent bursts. These relatively crude patterns have already a marked effect on

hormonal output. In addition, release is enhanced markedly when the pattern of stimulating pulses within the bursts mimics the natural sequence of spikes, such as interspersing clusters of four spikes at a rate of 60 Hz with silent periods, rather than maintaining a constant rate of 4 Hz. These results prove that not only is the basic firing pattern correlated to hormone release, but that the fine temporal structure within this 'coarse' pattern has a further enhancing function. As vasopressin and oxytocin neurones are closely related we can safely assume that the same principles apply to both cell types.

Short-term variability of the firing activity therefore is of physiological relevance. However, it might be more important in some circumstances than in others. In the regulation of natriuresis the most important thing for oxytocin neurones is to maintain the correct plasma oxytocin levels. In order to accomplish this the long-term orderliness in the firing activity is imperative. Clearly, for oxytocin neurones it is important to have an activity-dependent negative feedback mechanism that helps to maintain the long-term stability of a steady firing rate, and thus to ensure a constant release of the hormone.

A constant, steady firing rate might also be important for another reason. For vasopressin neurones, Moos *et al.* (1998) report that dendritically released vasopressin favours the expression of an activity pattern known to optimise hormone output, i.e. a phasic pattern where the neurone is active and silent in approximately the same proportions. Interestingly, the action of vasopressin upon the individual cell depends on the initial level of activity of that cell: neurones active at the high end of the range were inhibited, neurones at the lower end of the range were excited, and neurones in the mid-range were unaffected. So whatever the activity of the neurone is to begin with, the effect of vasopressin is to bring it into the mid-range of activity. Over the whole population of vasopressin neurones, therefore, intranuclear vasopressin homogenises the activity pattern around a medium level of activity. These effects – prevention of sustained inefficient activation through the inhibition, and recruitment of a larger pool of neurones into moderate activity through excitation – fit with the high and sustained demand of systemic vasopressin, distributing the

load of hormone production over a wide number of neurones and thus ensuring an adequate supply over long time periods while protecting each individual neurone from the strain of fast firing.

It seems likely that a similar principle operates for oxytocin neurones. Fast firing places a strain on the neurone, and while oxytocin neurones can fire at frequencies approaching 100 Hz for a short time – as seen during milk-ejection bursts – sustaining high firing rates over longer periods would lead to damage and cell death. Intranuclear oxytocin might help to activate slower firing cells (as discussed above). Activity-dependent negative feedback would regularise fast firing cells. Thus, the load of hormone output would be equalised amongst the population of oxytocin neurones by bringing the majority of the population into a mid-range, steady activity level, protecting those firing very fast from the consequences of the strain this might cause, while simultaneously ensuring adequate long-term hormone output.

5.4.2 Relevance of AHP

What is the physiological relevance of the AHP, the most important consequences for the neurone that expresses the underlying currents? Two possibilities emerge, as suggested by previous work and seen from our analyses of the action of the AHP on the activity patterning. As discussed before, the AHP follows spike trains, at frequencies as low as 1 Hz. It can summate if the spikes are sufficiently close together, so has the largest amplitude during high frequency firing. The AHP inhibits the generation of further action potential, the inhibiting action being in proportion to its size, i.e. the inhibition is strongest for very high frequencies. Therefore, in one capacity the AHP prevents the firing activity from 'running-away', placing a limit on the maximum firing rate possible, and so protecting the cell from damage or even cell death caused by the strain of fast firing. Clearly, as the possible consequences are so catastrophic this is an extremely important function. However, another mechanism that places a firm upper limit on the firing rate exists already: the large but relatively short-lasting HAP. In addition,

nitric oxide within the SON may work as an inhibitory feedback regulator, protecting neurones from excessive excitation. Is it that important to prevent the consequences of excessive fast firing that several mechanisms were deemed necessary, in case one fails? An alternative explanation is that this effect of the AHP – as a 'delimiter' – is secondary to the other role implied by the results of our analyses.

Consider again the influence of the AHP on firing activity. Even after a spike train few relatively short ISIs the AHP summates and inhibits further activity. Vice versa, during a period of slow firing the AHP can decay between spikes, and thus the inhibition on further spikes decreases. Overall, therefore, the AHP functions as a 'balancer', regularising the activity and keeping it more ordered. The regularity – and irregularity – of the firing is important in terms of hormone release, i.e. the function of the neurone, as is the long-term stability of activity. While situations which would demand the AHP in its role as 'delimiter' occur rather rarely, the regulation of natriuresis – and with this the need for steady and sustained hormone output as generated by a balanced and constant firing activity – is a prevailing and continuous requirement. The omnipresence of this demand and the importance of regularity for the organism argue in favour of the latter explanation: that regularisation is the primary role of the AHP, while the role of placing a limit on the firing rate occurs as a side effect.

Is it important to establish which of the two roles of the roles of the AHP in oxytocin neurones is the main one, which a side effect, or even whether they are of equal significance? For the time being we have no way of clarifying this point, and it is of little relevance to our work.

Another question that requires consideration is the significance of the AHP for the firing activity in the changed circumstances during lactation. Comparing the results for the different physiological groups the most striking observation is that they are remarkably similar. Given the anatomical and intrinsic restructuring during late pregnancy and lactation reported in previous work (cf. Stern & Armstrong, 1996; 1998), as well as the additional or different input due to suckling one would expect

radically different behaviour in these cells. However, the differences we found were rather subtle and hence we can speculate that restructuring and different input do not have such a big impact on the function of oxytocin neurones as previously thought. If so, the changes in the AHP – higher amplitude but shorter lasting – could be representing changes in intrinsic mechanisms.

Alternatively, changes in structure, intrinsic properties and input could have substantial consequences, but these could interact in such a way that they cancel each other out, such that the activity governed by all these factors remains the same not because of, but despite these changes. If this were true then the role of the changed AHP could be to aid maintaining the status quo of firing behaviour.

Either way, this discrepancy between expectations raised by *in vitro* results and observations made *in vivo* highlights the benefit of the statistical methods presented in this thesis as a tool for investigating intrinsic mechanisms underlying the function of the neurone in its natural context. Thus, the statistical approach can further our understanding when neither of the experimental techniques can provide clear answers.

5.5 Outlook and Conclusion

In this thesis we have examined spontaneous, unmanipulated discharge patterns of oxytocin neurones recorded under different physiological conditions *in vivo* using statistical methods in order to determine the key features involved in their regulation, and consider possible explanations in terms of known intrinsic properties. We have shown that the most important parameters involved in the regulation of firing patterns (for a given synaptic input) are the two components of the hyperpolarisation: the post-spike hyperpolarising afterpotential (HAP), which is large but short-lasting (approx. 30 ms), and the post-train afterhyperpolarisation (AHP), which is small but much longer lasting (up to several s). The HAP sets a firm upper limit on the discharge frequency – which is exceeded only during high frequency discharges seen during parturition and lactation –, while the AHP 'smoothes' firing

activity of oxytocin neurones, a feature that is of particular importance for the role oxytocin plays in the regulation of natriuresis. Further, we confirmed earlier reports that the AHP has a discernible effect at firing rates as low as 1.5 Hz.

The most striking results of comparing firing activity characteristics for the different physiological groups was how little they differed from each other, in contrast to the expectations raised by previous reports about extensive anatomical, intrinsic and network restructuring. Our results were in agreement with *in vitro* work reporting that in lactation the AHP is larger in amplitude but decays faster, thus having less of a regularising effect on the activity than prior to lactation. However, disagreement arises on account of the AHP in late pregnancy, as the *in vitro* results suggest that these neurones behave as those during lactation, while our results suggest their behaviour is more similar to neurones recorded in naïve animals. Further work is needed to establish the cause of this discrepancy, such as whether the disturbance or elimination of synaptic connections or other network properties in dissociated cells prevent the expression of firing activity in the same way as neurones *in vivo*.

Unfortunately, limited availability of appropriate data samples prevented us to obtain unequivocal results from the analyses of data from neurones displaying milk-ejection bursts. However, as these synchronised discharges at firing rates escaping the frequency limitations that govern the activity outside parturition and lactation are of particular importance – and have so far proven to be elusive to investigations using experimental methods – this point certainly deserves further scrutiny.

The main results presented in this thesis – the key components needed to describe the firing activity of oxytocin neurones with reasonable accuracy are the HAP and the AHP – show that sufficient information is available from spontaneous discharge activity to develop concise computational models. Further, this will simplify the task of building a physiologically realistic but computationally viable computational model of oxytocin neurones. Such a model would closely mimic cell behaviour dictated by the key features that describe the impact of intrinsic mechanisms, and by design would be well matched to experimental data. Moreover,

the model would be capable of generating fresh insights into cell properties, testing the coherence and feasibility of biological hypothesis, and aid in generating novel and counter-intuitive predictions, in turn giving rise to experimental work designed to examine them.

The oxytocin cell is an output neurone, with few axonal collaterals to make any recurrent connection with other neurones in the central nervous system, and hence activity-dependent influences on the firing primarily reflect intrinsic cell properties in normal circumstances. Therefore, it might be argued that the approach demonstrated here is of little relevance for neurones with elaborated connectivity. Nevertheless, it is potentially equally appropriate for analysing the behaviour of neurones where activity-dependent influences are mediated by interaction with other neurones, because as far as the analytical approach it is concerned it makes no difference whether activity-dependent influences reflect intrinsic properties or external feedback. Thus, the proof or principle work presented here can be transferred and extended to other neurones.

REFERENCE LIST

Acher, R., Chauvet, J., & Rouille, Y. (1997). Adaptive evolution of water homeostasis regulation in amphibians: vasotocin and hydrins. *Biol.Cell* **89**, 283-291.

Andrew, R. D. & Dudek, F. E. (1983). Burst discharge in mammalian neuroendocrine cells involves an intrinsic regenerative mechanism. *Science* **221**, 1050-1052.

Andrew, R. D. & Dudek, F. E. (1984b). Analysis of intracellularly recorded phasic bursting by mammalian neuroendocrine cells. *J.Neurophysiol.* **51**, 552-566.

Andrew, R. D. & Dudek, F. E. (1984a). Intrinsic inhibition in magnocellular neuroendocrine cells of rat hypothalamus. *J.Physiol (Lond)* **353**, 171-185.

Andrew, R. D. & Dudek, F. E. (1985). Spike broadening in magnocellular neuroendocrine cells of rat hypothalamic slices. *Brain Res.* **334**, 176-179.

Arletti, R., Benelli, A., & Bertolini, A. (1992). Oxytocin involvement in male and female sexual behavior. *Ann.N.Y.Acad.Sci.* **652**, 180-193.

Armstrong, W. E. (1995). Morphological and electrophysiological classification of hypothalamic supraoptic neurons. *Prog.Neurobiol.* **47**, 291-339.

Armstrong, W. E. & Hatton, G. I. (1980). The localization of projection neurons in the rat hypothalamic paraventricular nucleus following vascular and neurohypophysial injections of HRP. *Brain Res.Bull.* **5**, 473-477.

Armstrong, W. E., Scholer, J., & McNeill, T. H. (1982). Immunocytochemical, Golgi and electron microscopic characterization of putative dendrites in the ventral glial lamina of the rat supraoptic nucleus. *Neuroscience* **7**, 679-694.

Armstrong, W. E., Smith, B. N., & Tian, M. (1994). Electrophysiological characteristics of immunochemically identified rat oxytocin and vasopressin neurones in vitro. *J.Physiol* **475**, 115-128.

Armstrong, W. E. & Stern, J. E. (1998). Electrophysiological distinctions between oxytocin and vasopressin neurons in the supraoptic nucleus. *Adv.Exp.Med.Biol.* **449**, 67-77.

Armstrong, W. E., Warach, S., Hatton, G. I., & McNeill, T. H. (1980). Subnuclei in the rat hypothalamic paraventricular nucleus: a cytoarchitectural, horseradish peroxidase and immunocytochemical analysis. *Neuroscience* **5**, 1931-1958.

Baimbridge, K. G., Celio, M. R., & Rogers, J. H. (1992). Calcium-binding proteins in the nervous system. *Trends Neurosci.* **15**, 303-308.

Balment, R. J., Brimble, M. J., Forsling, M. L., Kelly, L. P., & Musabayane, C. T. (1986). A synergistic effect of oxytocin and vasopressin on sodium excretion in the neurohypophysectomized rat. *J.Physiol* **381**, 453-464.

Bargmann, W., & Scharrer, E.. (1951). The site of origin of the hormones of the posterior pituitary. *American Scientist* **39**, 255-259.

Belin, V. & Moos, F. (1986). Paired recordings from supraoptic and paraventricular oxytocin cells in suckled rats: recruitment and synchronization. *J.Physiol (Lond)* **377**, 369-390.

Belin, V., Moos, F., & Richard, P. (1984). Synchronization of oxytocin cells in the hypothalamic paraventricular and supraoptic nuclei in suckled rats: direct proof with paired extracellular recordings. *Exp.Brain Res.* **57**, 201-203.

Berridge, M. J, Bootman, M.D., & Lipp, P. (1998). Calcium – a life and death signal. *Nature* **395**, 645-648.

Berridge, M. J., Lipp, P., & Bootman, M.D. (2000a). The versatility and universality of calcium signaling. *Nat Rev Mol Cell Biol.* **1**, 11-21.

Berridge, M. J., Lipp, P., & Bootman, M.D. (2000b). Signal transduction. The calcium entry pas de deux. *Science* **287**, 1604-5.

Bicknell, R. J., Brown, D., Chapman, C., Hancock, P. D., & Leng, G. (1984). Reversible fatigue of stimulus-secretion coupling in the rat neurohypophysis. *J.Physiol* **348**, 601-613.

Bourque, C. W. (1986). Calcium-dependent spike after-current induces burst firing in magnocellular neurosecretory cells. *Neurosci.Lett.* **70**, 204-209.

Bourque, C. W. (1988). Transient calcium-dependent potassium current in magnocellular neurosecretory cells of the rat supraoptic nucleus. *J.Physiol* **397**, 331-347.

Bourque, C. W. (1989). Ionic basis for the intrinsic activation of rat supraoptic neurones by hyperosmotic stimuli. *J.Physiol* **417**, 263-277.

Bourque, C. W., Brown, D. A., & Renaud, L. P. (1986). Barium ions induce prolonged plateau depolarizations in neurosecretory neurones of the adult rat supraoptic nucleus. *J.Physiol* **375**, 573-586.

Bourque, C. W., Oliet, S. H., Kirkpatrick, K., Richard, D., & Fisher, T. E. (1993). Extrinsic and intrinsic modulatory mechanisms involved in regulating the electrical activity of supraoptic neurons. *Ann.N.Y.Acad.Sci.* **689**, 512-519.

Bourque, C. W., Randle, J. C., & Renaud, L. P. (1985). Calcium-dependent potassium conductance in rat supraoptic nucleus neurosecretory neurons. *J.Neurophysiol.* **54**, 1375-1382.

Bourque, C. W. & Renaud, L. P. (1985). Activity dependence of action potential duration in rat supraoptic neurosecretory neurones recorded in vitro. *J.Physiol (Lond)* **363**, 429-439.

Bourque, C. W. & Renaud, L. P. (1991). Membrane properties of rat magnocellular neuroendocrine cells in vivo. *Brain Res.* **540**, 349-352.

Bredt, D.S., Hwang, P.M., & Snyder, S. H. (1990). Localisation of nitric oxide synthase indicating a neural role for nitric oxide. *Nature.* **347**, 768-770.

Brimble, M. J. & Dyball, R. E. (1977). Characterization of the responses of oxytocin- and vasopressin- secreting neurones in the supraoptic nucleus to osmotic stimulation. *J.Physiol* **271**, 253-271.

Brown, D., Fontanaud, P., & Moos, F. C. (2000). The variability of basal action potential firing is positively correlated with bursting in hypothalamic oxytocin neurones. *J.Neuroendocrinol.* **12**, 506-520.

Brown, D., & Moos, F. C. (1997). Onset of bursting in oxytocin cells in suckled rats. *J.Physiol.* **503(3)**, 625-634.

Brown, D., & Rothery, P. (1993). *Models in Biology: Mathematics, Statistics and Computing*. John Wiley and Sons Ltd, Chichester.

Brownstein, M. J., Russell, J. T., & Gainer, H. (1980). Synthesis, transport, and release of posterior pituitary hormones. *Science* **207**, 373-378.

Caldwell, J. D., Barakat, A. S., Smith, D. D., Hruby, V. J., & Pedersen, C. A. (1990). A uterotonic antagonist blocks the oxytocin-induced facilitation of female sexual receptivity. *Brain Res.* **512**, 291-296.

Cazalis, M., Dayanithi, G., & Nordmann, J. J. (1985). The role of patterned burst and interburst interval on the excitation- coupling mechanism in the isolated rat neural lobe. *J.Physiol* **369**, 45-60.

Chan, W. Y., Wo, N. C., & Manning, M. (1996). The role of oxytocin receptors and vasopressin V1a receptors in uterine contractions in rats: implications for tocolytic therapy with oxytocin antagonists. *Am.J.Obstet.Gynecol.* **175**, 1331-1335.

Chiodera, P., Volpi, R., & Coiro, V. (1994). Inhibitory control of nitric oxide on the arginine-vasopressin and oxytocin response to hypoglycaemia in normal men. *Neuroreport.* **5(14)**, 1822-4.

Coolican, H. (1994). *Research Methods and Statistics in Psychology.* Hodder & Stoughton, London.

Cooke, B. A., Choi, M. C., Dirami, G., Lopez-Ruiz, M. P., & West, A. P. (1992). Control of steroidogenesis in Leydig cells. *J.Steroid Biochem.Mol.Biol.* **43**, 445-449.

Cox, D.R. & Isham, V. (1979). *Point Processes.* Monographs on Statistics and Applied Probability Series 12. Chapman & Hall, London.

Cunningham, E. T., Jr. & Sawchenko, P. E. (1991). Reflex control of magnocellular vasopressin and oxytocin secretion. *Trends Neurosci.* **14**, 406-411.

Dayanithi, G., Sabatier, N., & Widmer, H. (2000). Intracellular calcium signalling in magnocellular neurones of the rat supraoptic nucleus: understanding the autoregulatory mechanisms. *Exp.Physiol* **85 Spec No**, 75S-84S.

Dreifuss, J. J., Harris, M. C., & Tribollet, E. (1976). Excitation of phasically firing hypothalamic supraoptic neurones by carotid occlusion in rats. *J.Physiol* **257**, 337-354.

Dreifuss, J. J., Kalnins, I., Kelly, J. S., & Ruf, K. B. (1971). Action potentials and release of neurohypophysial hormones in vitro. *J.Physiol* **215**, 805-817.

Dubois-Dauphin, M., Armstrong, W. E., Tribollet, E., & Dreifuss, J. J. (1985). Somatosensory systems and the milk-ejection reflex in the rat. II. The effects of lesions in the ventroposterior thalamic complex, dorsal columns and lateral cervical nucleus-dorsolateral funiculus. *Neuroscience* **15**, 1131-1140.

Dunn, F. L., Brennan, T. J., Nelson, A. E., & Robertson, G. L. (1973). The role of blood osmolality and volume in regulating vasopressin secretion in the rat. *J.Clin.Invest* **52**, 3212-3219.

Dutton, A. & Dyball, R. E. (1979). Phasic firing enhances vasopressin release from the rat neurohypophysis. *J.Physiol* **290**, 433-440.

Dyball, R. E. J. & Bhumbra, G. S. (2003). Digital spike discrimination combining size and shape elements. *Proceedings of the Physiological Society*, University College London, Oral Communication, 547P D9.

Dyball, R. E. & Kemplay, S. K. (1982). Dendritic trees of neurones in the rat supraoptic nucleus. *Neuroscience* **7**, 223-230.

Dyball, R. E. & Leng, G. (1986). Regulation of the milk ejection reflex in the rat. *J.Physiol* **380**, 239-256.

Ecelbarger, C. A., Nielsen, S., Olson, B. R., Murase, T., Baker, E. A., Knepper, M. A., & Verbalis, J. G. (1997). Role of renal aquaporins in escape from vasopressin-induced antidiuresis in rat. *J.Clin.Invest* **99**, 1852-1863.

Fisher, A. W., Price, P. G., Burford, G. D., & Lederis, K. (1979). A 3-dimensional reconstruction of the hypothalamo-neurohypophysial system of the rat. The neurons projecting to the neuro/intermediate lobe and those containing vasopressin and somatostatin. *Cell Tissue Res.* **204**, 343-354.

Fisher, T. E. & Bourque, C. W. (1995). Voltage-gated calcium currents in the magnocellular neurosecretory cells of the rat supraoptic nucleus. *J.Physiol* **486 (Pt 3)**, 571-580.

Fisher, T. E. & Bourque, C. W. (1996). Calcium-channel subtypes in the somata and axon terminals of magnocellular neurosecretory cells. *Trends Neurosci.* **19**, 440-444.

Foehring, R.C. & Armstrong, W.E. (1996). Pharmacological dissection of high-voltage-activated Ca^{2+} current types in acutely dissociated rat supraoptic magnocellular neurons. *J.Neurophysiol* **76(2)**, 977-983.

Freund-Mercier, M. J. & Richard, P. (1984). Electrophysiological evidence for facilitatory control of oxytocin neurones by oxytocin during suckling in the rat. *J.Physiol* **352**, 447-466.

Ghamari-Langroudi, M. & Bourque, C. W. (1998). Caesium blocks depolarizing after-potentials and phasic firing in rat supraoptic neurones. *J.Physiol (Lond)* **510 (Pt 1)**, 165-175.

Ghamari-Langroudi, M. & Bourque, C. W. (2000). Excitatory role of the hyperpolarization-activated inward current in phasic and tonic firing of rat supraoptic neurons. *J.Neurosci.* **20**, 4855-4863.

Gouzenes, L., Desarmenien, M. G., Hussy, N., Richard, P., & Moos, F. C. (1998). Vasopressin regularizes the phasic firing pattern of rat hypothalamic magnocellular vasopressin neurons. *J.Neurosci.* **18**, 1879-1885.

Greffrath, W., Martin, E., Reuss, S., & Boehmer, G. (1998). Components of after-hyperpolarization in magnocellular neurones of the rat supraoptic nucleus in vitro. *J.Physiol* **513 (Pt 2)**, 493-506.

Harris, M. C., Dreifuss, J. J., & Legros, J. J. (1975). Excitation of phasically firing supraoptic neurones during vasopressin release. *Nature* **258**, 80-82.

Hatton, G. I. (1990). Emerging concepts of structure-function dynamics in adult brain: the hypothalamo-neurohypophysial system. *Progress in Neurobio.* **43**, 437-504.

Hatton, G. I. & Tweedle, C. D. (1982). Magnocellular neuropeptidergic neurons in hypothalamus: increases in membrane apposition and number of specialized synapses from pregnancy to lactation. *Brain Res.Bull.* **8**, 197-204.

Hatton, G. I. & Yang, Q. Z. (1994). Incidence of neuronal coupling in supraoptic nuclei of virgin and lactating rats: estimation by neurobiotin and lucifer yellow. *Brain Res.* **650** , 63-69.

Higuchi, T., Honda, K., Fukuoka, T., Negoro, H., Hosono, Y., & Nishida, E. (1983). Pulsatile secretion of prolactin and oxytocin during nursing in the lactating rat. *Endocrinol.Jpn.* **30**, 353-359.

Hille, B. (1991). Potassium Channels and Chloride Channels. In *Ionic Channls of Excitable Membranes* pp. 115-139. Sinauer Associates Inc., Sunderland, Mass.

Hugues, M., Romey, G., Duval, D., Vincent, J. P., & Lazdunski, M. (1982). Apamin as a selective blocker of the calcium-dependent potassium channel in neuroblastoma cells: voltage-clamp and biochemical characterization of the toxin receptor. *Proc.Natl.Acad.Sci.U.S.A* **79**, 1308-1312.

Inenaga, K., & Yamashita, H. (1986). Excitation of neurones in the rat paraventricular nucleus *in vitro* by vasopressin and oxytocin. *J.Physiol* **370**, 165-180.

Jackson, M. B., Konnerth, A., & Augustine, G. J. (1991). Action potential broadening and frequency-dependent facilitation of calcium signals in pituitary nerve terminals. *Proc.Natl.Acad.Sci.U.S.A* **88**, 380-384.

Jard, S. (1983). Vasopressin: mechanisms of receptor activation. *Prog.Brain Res.* **60**, 383-394.

Kadekaro, M., Liu, H., Terrell, M.L., Gestl, S., Bui, V., & Summy-Long, J.Y. (1997). Role of NO on vasopressin and oxytocin release and blood pressure responses during osmotic stimulation in rats. *Am J Physiol.* **273(3 Pt 2)**, R1024-30.

Kadowaki, K., Kishimoto, J., Leng, G., & Emson, P.C. (1994). Up-regulation of nitric oxide synthase (NOS) gene expression together with NOS activity in the rat hypothalamo-hypophysial system after chronic salt loading: evidence of a neuromodulatory role of nitric oxide in argenine vasopressin and oxytocin secretion. *Endocrinology* **134**, 1011-1017.

Kirkpatrick, K. & Bourque, C. W. (1996). Activity dependence and functional role of the apamin-sensitive K+ current in rat supraoptic neurones in vitro. *J.Physiol (Lond)* **494 (Pt 2)**, 389-398.

Lambert, R. C., Dayanithi, G., Moos, F. C., & Richard, P. (1994). A rise in the intracellular Ca2+ concentration of isolated rat supraoptic cells in response to oxytocin. *J.Physiol* **478 (Pt 2)**, 275-287.

Leng, G. (1981). The effects of neural stalk stimulation upon firing patterns in rat supraoptic neurones. *Exp.Brain Res.* **41**, 135-145.

Leng, G., Brown, C.H., Bull, P.M., Brown, D., Scullion, S., Currie, J., Blackburn-Munro, R.E., Feng, J., Onaka, T., Verbalis, J.G., Russell, J.A., & Ludwig, M. (2001). Responses of magnocellular neurons to osmotic stimulation involves coactivation of excitatory and inhibitory input: an experimental and theoretical analysis. *J Neurosci.* **21(17),** 6967-77.

Leng, G. & Brown, D. (1997). The origins and significance of pulsatility in hormone secretion from the pituitary. *J.Neuroendocrinol.* **9**, 493-513.

Leng, G. & Mason, W. T. (1982). Influence of vasopressin upon firing patterns of supraoptic neurons: a comparison of normal and Brattleboro rats. *Ann.N.Y.Acad.Sci.* **394**, 153-158.

Leng, G., Reiff-Marganiec, A., Ludwig, M., & Sabatier, N. (in press). Generating quantitatively accurate, but computationally concise, models of single neurons. To appear in: *Computational Neuroscience: A Comprehensive Approach*. J.F. Feng (Ed.). Chapman & Hall/ CRC Press, Boca Raton.

Li, Z., Decavel, C., & Hatton, G. I. (1995). Calbindin-D28k: role in determining intrinsically generated firing patterns in rat supraoptic neurones. *J.Physiol* **488 (Pt 3)**, 601-608.

Li, Z. & Hatton, G. I. (1997b). Ca2+ release from internal stores: role in generating depolarizing after-potentials in rat supraoptic neurones. *J.Physiol* **498 (Pt 2)**, 339-350.

Li, Z. & Hatton, G. I. (1997a). Reduced outward K+ conductances generate depolarizing after-potentials in rat supraoptic nucleus neurones. *J.Physiol* **505 (Pt 1)**, 95-106.

Lincoln, D. W. & Wakerley, J. B. (1974). Electrophysiological evidence for the activation of supraoptic neurones during the release of oxytocin. *J.Physiol* **242**, 533-554.

Ludwig, M., Callahan, M.F., Neumann, I., Landgraf, R., & Morris, M. (1994). Systemic osmotic stimulation increases vasopressin and oxytocin release within the supraoptic nucleus. *J.Neuroendocrinol* **6**, 369-373.

Ludwig, M., Sabatier, N., Bull, P. M., Landgraf, R., Dayanithi, G., & Leng, G. (2002). Intracellular calcium stores regulate activity-dependent neuropeptide release from dendrites. *Nature* **418**, 85-89.

Ludwig, M. (1998). Dendritic release of vasopressin and oxytocin. *J.Neuroendocrinol.* **10**, 881-895.

Mezey, E., & Kiss, J.Z. (1991). Coexpression of vasopressin and oxytocin in hypothalamic supraoptic neurons of lactating rats. *Endocrinology* **129**, 1814-1820.

Miller, C., Moczydlowski, E., Latorre, R., & Phillips, M. (1985). Charybdotoxin, a protein inhibitor of single Ca2+-activated K+ channels from mammalian skeletal muscle. *Nature* **313**, 316-318.

Miyata, S., Khan, A. M., & Hatton, G. I. (1998). Colocalization of calretinin and calbindin-D28k with oxytocin and vasopressin in rat supraoptic nucleus neurons: a quantitative study. *Brain Res.* **785**, 178-182.

Montagnese, C. M., Poulain, D. A., Vincent, J. D., & Theodosis, D. T. (1987). Structural plasticity in the rat supraoptic nucleus during gestation, post-partum lactation and suckling-induced pseudogestation and lactation. *J.Endocrinol.* **115**, 97-105.

Moos, F., Gouzenes, L., Brown, D., Dayanithi, G., Sabatier, N., Boissin, L., Rabie, A., & Richard, P. (1998). New aspects of firing pattern autocontrol in oxytocin and vasopressin neurones. *Adv.Exp.Med.Biol.* **449**, 153-162.

Moos, F. C. & Ingram, C. D. (1995). Electrical recordings of magnocellular supraoptic and paraventricular neurons displaying both oxytocin- and vasopressin-related activity. *Brain Res.* **669**, 309-314.

Moos, F., Poulain, D.A., Rodriguez, F., Guerne, Y., Vincent, J.D., & Richard, P. (1989). Release of oxytocin within the supraoptic nucleus during the milk ejection reflex in rats. *Exp. Brain Res.* **76**, 593-602.

Morris, J. F. & Pow, D. V. (1991). Widespread release of peptides in the central nervous system: quantitation of tannic acid-captured exocytoses. *Anat.Rec.* **231**, 437-445.

Neumann, I., Russell, J.A., & Landgraf, R. (1993). Oxytocin and vasopressin release within the supraoptic and paraventricular nuclei of pregnant, parturient and lactating rats: a microdialysis study. *Neuroscience* **53**, 65-75.

Nordmann, J. J. (1977). Ultrastructural morphometry of the rat neurohypophysis. *J.Anat.* **123**, 213-218.

Panksepp, J. (1992). Oxytocin effects on emotional processes: separation distress, social bonding, and relationships to psychiatric disorders. *Ann.N.Y.Acad.Sci.* **652**, 243-252.

Pei, X., Wilkens, L. & Moss, F. (1996). Noise-mediated spike timing precision from aperiodic stimuli in an array of Hodgkin-Huxley-type neurons. *Physic Rev Lett* **77**, 4679-4682.

Poulain, D. A., Brown, D. & Wakerley, J. (1988). Statistical analysis of patterns of electrical activity in vasopressin and oxytocin secreting neurones. In *Pulsatility in Neuroendocrine Systems*, ed. Leng, G., pp. 119-154. CRC Press, Florida.

Poulain, D. A. & Wakerley, J. B. (1982). Electrophysiology of hypothalamic magnocellular neurones secreting oxytocin and vasopressin. *Neuroscience* **7**, 773-808.

Poulain, D. A., Wakerley, J. B., & Dyball, R. E. (1977). Electrophysiological differentiation of oxytocin- and vasopressin- secreting neurones. *Proc.R.Soc.Lond B Biol.Sci.* **196** , 367-384.

Randle, J. C., Bourque, C. W., & Renaud, L. P. (1986). Serial reconstruction of Lucifer yellow-labeled supraoptic nucleus neurons in perfused rat hypothalamic explants. *Neuroscience* **17**, 453-467.

Renaud, L. P., Tang, M., McCann, M. J., Stricker, E. M., & Verbalis, J. G. (1987). Cholecystokinin and gastric distension activate oxytocinergic cells in rat hypothalamus. *Am.J.Physiol* **253**, R661-R665.

Rho, J. H. & Swanson, L. W. (1989). A morphometric analysis of functionally defined subpopulations of neurons in the paraventricular nucleus of the rat with observations on the effects of colchicine. *J.Neurosci.* **9**, 1375-1388.

Russell, J. A. & Leng, G. (1998). Sex, parturition and motherhood without oxytocin? *J.Endocrinol.* **157**, 343-359.

Sabatier, N., Richard, P., & Dayanithi, G. (1998). Activation of multiple intracellular transduction signals by vasopressin in vasopressin-sensitive neurones of the rat supraoptic nucleus. *J.Physiol* **513 (Pt 3)**, 699-710.

Sah, P. & McLachlan, E. M. (1991). Ca(2+)-activated K+ currents underlying the afterhyperpolarization in guinea pig vagal neurons: a role for Ca(2+)-activated Ca2+ release. *Neuron* **7**, 257-264.

Sawyer, W. H. (1977). Evolution of neurohypophyseal hormones and their receptors. *Fed.Proc.* **36**, 1842-1847.

Sherlock, D. A., Field, P. M., & Raisman, G. (1975). Retrograde transport of horseradish peroxidase in the magnocellular neurosecretory system of the rat. *Brain Res.* **88**, 403-414.

Smithson, K. G., Weiss, M. L., & Hatton, G. I. (1989). Supraoptic nucleus afferents from the main olfactory bulb--I. Anatomical evidence from anterograde and retrograde tracers in rat. *Neuroscience* **31**, 277-287.

Sofroniew, M. V. & Schrell, U. (1980). Hypothalamic neurons projecting to the rat caudal medulla oblongata, examined by immunoperoxidase staining of retrogradely transported horseradish peroxidase. *Neurosci.Lett.* **19**, 257-263.

Srisawat, R., Ludwig, M., Bull, P.M., Douglas, A.J., Russell, J.A., & Leng, G. (2000). Nitric oxide and the oxytocin system in pregnancy. *J Neurosci.* **20(17)**, 6721-7.

Stern, J. E. & Armstrong, W. E. (1995). Electrophysiological differences between oxytocin and vasopressin neurones recorded from female rats in vitro. *J.Physiol* **488 (Pt 3)**, 701-708.

Stern, J. E. & Armstrong, W. E. (1996). Changes in the electrical properties of supraoptic nucleus oxytocin and vasopressin neurons during lactation. *J.Neurosci.* **16**, 4861-4871.

Stern, J. E. & Armstrong, W. E. (1998). Reorganization of the dendritic trees of oxytocin and vasopressin neurons of the rat supraoptic nucleus during lactation. *J.Neurosci.* **18**, 841-853.

Stricker, E. M. & Verbalis, J. G. (1986). Interaction of osmotic and volume stimuli in regulation of neurohypophyseal secretion in rats. *Am.J.Physiol* **250**, R267-R275.

Studenmund, A. H. (2001). *Using Econometrics: A Practical Guide* (4th Edition). Addison Wesley Longman, Boston.

Summerlee, A. J. & Lincoln, D. W. (1981). Electrophysiological recordings from oxytocinergic neurones during suckling in the unanaesthetized lactating rat. *J.Endocrinol.* **90**, 255-265.

Swaab, D. F., Pool, C. W., & Nijveldt, F. (1975). Immunofluorescence of vasopressin and oxytocin in the rat hypothalamo- neurohypophypopseal system. *J.Neural Transm.* **36**, 195-215.

Teruyama, R., & Armstrong, E. (2002). Changes in the active membrane properties of rat supraoptic neurones during pregnancy and lactation. *J. Neuroendocrin.* **14**, 933-944.

Theodosis, D. T., Poulain, D. A., & Vincent, J. D. (1981). Possible morphological bases for synchronisation of neuronal firing in the rat supraoptic nucleus during lactation. *Neuroscience* **6**, 919-929.

Thomson, A. M. (1984). Supraoptic neurons sustain high frequency firing when extracellular Ca2+ is replaced with other divalent cations in rat brain slices. *Neuroscience* **12**, 495-502.

Tweedle, C. D., Smithson, K. G., & Hatton, G. I. (1989). Neurosecretory endings in the rat neurohypophysis are en passant. *Exp.Neurol.* **106**, 20-26.

Ueta, Y., Levy, A., Lightman, S.L., Hara, Y., & Brown, D. (1978). Comparison of firing patterns in oxytocin- and vasopressin-releasing neurones during progressive dehydration. *Brain Res.* **148**, 425-440.

Ueta, Y., Levy, A., Lightman, S.L., Hara, Y., Serino, R., Nomura, M., Shibuya, I., Hattori, Y., & Yamashita, H. (1998). Hypovolemia upregulates the expression of neuronal nitric oxide synthase gene in the paraventricular and supraoptic nuclei of rats. *Brain Res.* **790(1-2)**, 25-32.

Verbalis, J. G., McCann, M. J., McHale, C. M., & Stricker, E. M. (1986). Oxytocin secretion in response to cholecystokinin and food: differentiation of nausea from satiety. *Science* **232**, 1417-1419.

Wakerley, J. B., Poulain, D. A., & Brown, D. (1978). Comparison of firing patterns in oxytocin- and vasopressin-releasing neurones during progressive dehydration. *Brain Res.* **148**, 425-440.

Xi, D., Kusano, K., & Gainer, H. (1999). Quantitative analysis of oxytocin and vasopressin messenger ribonucleic acids in single magnocellular neurons isolated from supraoptic nucleus of rat hypothalamus. *Endocrinology* **140**, 4677-4682.

Yamashita, H. (1987). Oxytocin predominantly excites putative oxytocin neurons in the rat supraoptic nucleus *in vitro*. *Brain Res* **416**, 364-368.

Yoshizaki, K., Hoshino, T., Sato, M., Koyano, H., Nohmi, M., Hua, S. Y., & Kuba, K. (1995). Ca(2+)-induced Ca2+ release and its activation in response to a single action potential in rabbit otic ganglion cells. *J.Physiol* **486 (Pt 1)**, 177-187.

Young, W. S., III, Shepard, E., Amico, J., Hennighausen, L., Wagner, K. U., LaMarca, M. E., McKinney, C., & Ginns, E. I. (1996). Deficiency in mouse oxytocin prevents milk ejection, but not fertility or parturition. *J.Neuroendocrinol.* **8**, 847-853.

Publications

Generating quantitatively accurate, but computationally concise, models of single neurons

Gareth Leng, Arleta Reiff-Marganiec, Mike Ludwig and Nancy Sabatier

College of Medical and Veterinary Sciences

University of Edinburgh. EH9 8XD, UK

Address correspondence to:

Professor Gareth Leng

Division of Biomedical Sciences

College of Medical and Veterinary Sciences

University of Edinburgh

Hugh Robson Bldg, George Square

Edinburgh EH9 8 XD, UK

e-mail gareth.leng@ed.ac.uk

Introduction

Information in the brain is carried by the temporal pattern of action potentials (spikes) generated by neurons. The patterns of spike discharge are determined by intrinsic properties of each neuron and the synaptic inputs it receives; modulation of either of these parameters changes the output of the neurons, and, through this, the behavior or physiology of the organism. Computational models of brain function have principally focussed on how patterns of connectivity contribute to information processing, but most models largely neglect the different intrinsic properties of different neuronal phenotypes.

The scale of the problem

Computational models of single neurons that realistically reflect intrinsic membrane properties can be extremely complex, and hence building large-scale realistic models of neuronal networks is computationally intense. A typical neuron may make 10,000 synaptic contacts with other neurons, and receive a similar number of inputs. Each neuron expresses a large number of channels that contribute to its membrane excitability - including several different classes of Ca^{2+}, K^+ and Na^+ channels, and each neuronal phenotype differs in its exact composition of membrane channels. Neurons also differ from each other morphologically, in the distribution of channel types in different cellular compartments, and in intracellular properties that influence channel function. A model of a single neuron incorporating all these factors will have a very large number of parameters that must be estimated with reasonable precision from experimental observations, but many of which must be guessed for particular cell types, as the detailed information is not available. Moreover, experimental observations of biophysical parameters are typically made *in vitro* in conditions that are different from *in vivo* conditions. The relative scarcity of afferent input in *in vitro* preparations must always be taken into account, but beyond this, biophysical measurements often require interventions that fundamentally disturb cell properties. For example, measurements of membrane potential often derive from patch-clamp recordings, which may involve dialysis of the neuronal cytoplasm, altering the composition of the intracellular fluid, changing ion gradients and diluting second messenger systems. Measurements of intracellular Ca^{2+} involve introducing fluorophores into the cell that effectively function as additional Ca^{2+} buffers. Thus measurements of many variables require consideration of the context in which they are measured.

How many neurons must be included in a realistic network model is far from clear. The human brain is commonly estimated to contain about 2×10^{10} neurons, but a rat gets by with perhaps 10^7 neurons; the major source of this discrepancy is of course in the size of the neocortex. The neocortex, however, is one of the parts of the brain about which we understand least, substantially because the functions that we think it is principally involved in are, in general, not very amenable to reductionist experimental testing at the single cell level. In the rat brain, probably around 10^6 neurons are in the hypothalamus, and this region controls a wide diversity of clearly definable functions that are much more amenable to experimental investigation. Different neuronal groups in the hypothalamus control the release of different hormones from the pituitary gland – oxytocin; vasopressin; prolactin; growth hormone; the gonadotrophic hormones; adrenocorticotrophic hormone (that in turn controls

steroid secretion from the adrenal glands); thyroid stimulating hormone (that controls the functions of the thyroid gland); and melanocyte-stimulating hormone. The hypothalamus also controls thirst, feeding behavior (including specific appetites such as sodium appetite), body composition, blood pressure, thermoregulation, and much instinctive or reflex behavior including male and female sexual behavior and maternal behavior. These functions involve highly specialised cells with specific properties; cells for instance that have receptors or intrinsic properties that enable them to respond to glucose concentration, or the osmotic pressure of extracellular fluid, or to detect specific blood-borne signals released from peripheral tissues, such as leptin from fat cells, angiotensin from the kidney, and ghrelin from the stomach. Many of these cells in turn signal to other neurons using distinct chemical messengers: neurotransmitters, neuromodulators and neurohormones but also other types of signalling molecule, that are transduced by specific receptors that can occur in multiple forms even for one given signalling molecule.

Estimating the number of distinguishable neuronal phenotypes in the rat hypothalamus is imprecise, but there seem likely to be up to 1,000, each of which may be represented by about 1,000-10,000 individual neurons. This may seem a high estimate of diversity, but let's consider. The ventro-rostral extent of the hypothalamus is bounded by the organum vasculosum of the lamina terminalis (OVLT). This region is highly specialised in lacking a blood-brain barrier; how many cell types it contains we do not know for sure, but they include a highly specialised population of osmoreceptive neurons (1). Another area lacking a blood-brain barrier marks the dorso-rostral extent of the hypothalamus – this is the subfornical organ and it contains amongst its neurons (there seem to be at least six types) a population of specialised angiotensin- processing neurons. Between these, the preoptic region of the hypothalamus contains several identified nuclei and many different neuronal populations; one small but interesting population comprises about 700 luteinising-hormone releasing hormone (LHRH) neurons; these are remarkable cells, they are born in the nasal placode and migrate into the brain late in development, and are essential for controlling pituitary gonadotrophic secretion and thereby are essential for spermatogenesis in males and ovarian function in females (2). Though very scattered throughout the preoptic area they nonetheless discharge bursts of electrical activity in synchrony to elicit pulsatile secretion of gonadotrophic hormones from the pituitary. Most of these project to the median eminence, the site of blood vessels that enter the pituitary, but some LHRH neurons project to the OVLT – why, we don't know. The preoptic region also includes a sexually dimorphic nucleus – larger in males than in females. In the midline periventricular nucleus are neurosecretory somatostatin neurons that provide inhibitory regulation of growth hormone secretion, alongside growth-hormone releasing- hormone neurons of the arcuate nucleus. Caudal to the periventricular nucleus is the paraventricular nucleus; this contains thyrotropin-releasing hormone neurons that indirectly regulate the thyroid gland; corticotrophin-releasing hormone neurons that indirectly control the adrenal gland, magnocellular vasopressin neurons that control the kidney and magnocellular oxytocin neurons that are responsible for controlling parturition and lactation; in addition, smaller, centrally projecting oxytocin neurons regulate gastric function, and centrally projecting vasopressin neurons that regulate body temperature and blood pressure, some of which project into the spinal cord (as do some oxytocin neurons, a subpopulation that seems to be involved in

penile erection). Below this, the suprachiasmatic nucleus is the body's principal circadian pacemaker, one population of neurons here makes vasoactive intestinal peptide, another makes vasopressin; these cells are governed by "clock genes" that confer 24-h cyclicity on their behavior. Behind the suprachiasmatic nucleus is the arcuate nucleus, that in addition to growth-hormone releasing-hormone neurons contains leptin-sensitive neuropeptide Y neurons that regulate feeding, dopamine neurons that regulate the secretion of prolactin, opioid (β-endorphin) neurons that impact on many neuronal systems through extensive central projections, and a large population of centrally projecting somatostatin neurons of unknown function. Above this, the ventromedial nucleus contains specialised glucoreceptive neurons, and alongside it the lateral hypothalamus contains orexin neurons; orexin is linked to sleep and wakefulness, and orexin knock-out results in narcolepsy.

We haven't gone far in the hypothalamus yet, and we have described only some of the best-known populations, and neglected subpopulations of interneurons and many distinctive subnuclei. In addition, the individual cells vary even within a given population: these "homogeneous populations" are far from clones. Moreover, individuals in one population interact to differing extents with individuals of many other populations, and these interactions differ from cell to cell even within a population.

The populations are not fully interconnected– but neither are they as separable as we would like. Take for instance the magnocellular oxytocin neurons of the hypothalamus – and we probably know as much or more about these than about any cells in the brain (see 3). These are simple neurons in many respects; there are about 3,000 of them in the rat brain, and each has a single axon that projects to the neural lobe of the pituitary gland. Oxytocin, released from the nerve endings in the pituitary, controls milk let-down in response to suckling, and it controls the progress of parturition by its actions on the uterus. But in the rat, oxytocin also controls the excretion of sodium at the kidney. Moreover, centrally released oxytocin is involved in maternal behavior, sexual behavior, and affiliative behaviors generally, and stress responsiveness, and the magnocellular oxytocin system is involved in these behaviors through secretion of oxytocin from its dendrites rather than from classical nerve endings. Dendritic secretion unfortunately does not parallel secretion from axonal endings – the mechanisms underlying dendritic secretion differ in important ways from those that govern axonal secretion. The diversity of roles played by oxytocin shows both that the oxytocin neurons receive very functionally diverse inputs, and also that they influence many other neuronal populations, including some to which they are not synaptically connected, even indirectly. It would be dangerous to think that oxytocin neurons are exceptionally complicated, just because we know more about them than other neurons; in fact, from what we do know of other neurons, oxytocin neurons are if anything rather simple.

Thus models of any function or part of the brain must take due account of the diversity of neuronal phenotypes. In particular, models that seek to understand information processing must take account of the diversity of electrophysiological phenotypes exhibited within interconnected populations. The number of distinct electrophysiological phenotypes may be less than the number of chemically definable phenotypes alluded to, but the degree of difference between phenotypes can be striking. For example, magnocellular vasopressin neurons discharge spikes in a distinctive "phasic"

pattern, alternating between periods of silence and periods of stable spike discharge, and these cells function as true bistable oscillators. Other cells, such as those in the suprachiasmatic nucleus, exhibit highly regular discharge activity, whereas the spontaneous activity of oxytocin neurons appears quasi-random. Other cells display intrinsically oscillatory discharge activity, or display a propensity to discharge in brief rapidly adapting bursts. Each of these radically different electrophysiological phenotypes has significant consequences for information processing within the networks of which they are a part (see 4).

Strategies for developing computationally concise models

The number of parameters involved in modelling any single neuron to biophysical accuracy is large, at least 100 parameters would seem necessary; to build a realistic network model, these must be estimated for each cell type in the network. Even with the huge computational power available now, the computational task involved in systematically assessing models of such complexity is daunting, if this is to involve a rigorous assessment of the robustness of model performance for variable parameter values. The uncertainties and inaccuracies in estimating individual parameters are so large as to make the utility of the effort questionable. The purpose of any model is to understand a system by simplifying it, reveal the key, important variables. It makes little sense to try to build a model of the brain that is as complex as the brain. Clearly, we need to develop computationally simple models of neurons that preserve essential properties and discard those which have no major impact upon their information processing functions. However, it is not always clear which properties of a neuron are important and must be included in any model, and those which, for the moment, can be neglected.

The conventional approach to understanding the role of intrinsic membrane properties in neurons has been to study channel properties in detail through experiments on isolated cells *in vitro*, and then to speculate about how these might contribute to spike patterning or neuronal responses *in vivo*. However, rather than look at membrane properties and speculate about how they might influence firing patterns, it is also possible to look at spontaneous firing patterns to see how they can be modelled most simply, and then look for explanations in terms of the known intrinsic properties (5). What we describe here is an illustration of this approach. We are not seeking to build a complex model of an oxytocin cell by attempting to incorporate all known features of these cells. Instead, we seek a minimalist, computationally concise representation of its information-processing functions in a way that is both biologically referable in its parameters and quantitatively accurate in its match to experimental data, while being also founded on explicit assumptions in a manner that gives it true predictive and explanatory power.

The Hypothalamo-Hypophysial System

The magnocellular neurosecretory neurons of the hypothalamus are concentrated in the supraoptic and paraventricular nuclei; axons from these cells project to the posterior pituitary gland (also known as the neural lobe, or neurohypophysis) where the hormones that they synthesize, oxytocin and vasopressin, are released into the circulation. These hormones are released in response to spikes that are generated at the cell bodies and conducted along the axons; hormone release from these

neurosecretory terminals is analogous to neurotransmitter release from conventional neurons, but unlike transmitter release, hormone release occurs in such large amounts that it can be measured very easily. The soma and axons of the magnocellular neurons are readily identifiable and accessible for experimental manipulation through a wide variety of *in vivo* and *in vitro* experimental approaches. Thus, they are one of the few groups of central neurons in which changes in activity pattern can be related to the physiological stimulus and the precise neuronal response to the stimulus, the state of the organism and the hormonal secretion, respectively (see 5-9 for reviews).

Through its role as the antidiuretic hormone, vasopressin is primarily concerned with body fluid homeostasis. Vasopressin is released in response to increased plasma osmotic pressure, and in response to reduced plasma volume, and it acts on the kidney to promote conservation of water by concentrating the urine, and to restrict plasma volume by vasopressor actions on blood vessels. The classical roles of oxytocin are in lactation and parturition. At parturition, oxytocin stimulates uterine contractions to promote parturition. During lactation, oxytocin is released in response to suckling in a pulsatile manner, and promotes milk let-down from the mammary gland. Oxytocin is also released in response to increased osmotic pressure, hypovolemia, and gastric distension, reflecting a secondary role at the kidney to stimulate sodium excretion in response to increased sodium intake. Oxytocin and vasopressin also have intriguing behavioral actions. These are intriguing first because oxytocin and vasopressin released into the blood does not re-enter the brain, which is protected by a blood-brain barrier; so these behavioral effects are mediated by central release of vasopressin and oxytocin. The oxytocin and vasopressin cells have few axonal endings within the brain, but they can release very large amounts of these peptides from their dendrites. The behavioral actions seem remarkable apposite to the peripheral roles of the hormones. Oxytocin for instance promotes maternal behavior after parturition, seen in rats as nest building and retrieval of young. These behavioral actions are typical of the effects of central injection of peptides endogenous to the hypothalamus in being complex behaviors expressed over a prolonged period after brief central exposure to the peptide. Interestingly, these behavioral effects appear to be exerted via neuronal receptors expressed in regions where there is little or no innervation by oxytocin-containing fibres, suggesting that neurohormonal-like secretion from dendrites may be the important modulator of behavior.

Firing patterns of vasopressin neurons

When vasopressin cells are activated by a rise in osmotic pressure, their spike discharge activity consists of alternating periods of activity and silence lasting tens of seconds each, so called *phasic* firing (Fig. 1). Vasopressin cells fire phasically when their mean discharge rate exceeds 3 Hz; at lower firing rates no clear pattern is discernible. Phasic firing is important in vasopressin cells, but not because of the apparently obvious temporal patterning. Different vasopressin cells discharge asynchronously, so while the output of individual cells is pulsatile, the net output of the whole population is continuous. Phasic patterning optimises *the efficiency of secretion from nerve terminals.* In response to trains of electrical stimuli, vasopressin release from nerve endings is facilitated as the frequency of stimulation increases, but "fatigues" as the duration is extended. The frequency-facilitation of release is ascribed to a facilitation of Ca^{2+} entry at the nerve terminals, resulting in part from a

broadening of spike duration at high frequencies of stimulation, in part from depolarisation caused by accumulation of K^+ in the extracellular clefts, and in part from a progressively more complete invasion of the arborised terminal field of an axon during repetitive stimulation, resulting finally in a greater Ca^{2+} influx through voltage-gated channels to trigger enhanced exocytosis. The facilitation of secretion is transient; stimulation sustained for longer than about 20s results in a steep decline in hormone release, which probably reflects inactivation of Ca^{2+} entry into the terminals. This "fatigue" is readily reversed, and a 20s rest period will allow a new stimulus again to evoke efficient release. Phasic firing appears to make optimal use of the properties of the terminal membranes to enable hormone release to occur with minimal expenditure of energy on spike generation.

Phasic firing is the result of intrinsic membrane properties. The bursts are not not passive responses to a phasically patterned input, nor do they reflect spontaneous oscillations of membrane potential. Instead, the bursts are regenerative, in that the first few spikes of a burst trigger prolonged activity. The bursting depends on intracellular Ca^{2+}; blockade of Ca^{2+} entry or chelation of intracellular Ca^{2+} will block phasic firing. At the start of a burst, a small but long-lasting depolarising after-potential (DAP) follows each spike, and these DAP's summate, bringing the membrane potential close to the spike threshold. After the first few spikes, a depolarising plateau, reflecting a persistent inward current, sustains a burst. The plateau can be viewed as an alternative state of the resting potential. When depolarised by about 10 mV from its normal resting potential of about -70mV, a vasopressin cell will tend to settle at a new, more depolarised resting (plateau) potential, which is sustained by a constant depolarising current, and which is close enough to the spike threshold for EPSP's to frequently trigger spikes. The DAP after each spike brings the membrane potential back into the range for activating the low threshold, non-inactivating currents, so plateau potentials normally are triggered by, and maintained by, spike activity. The vasopressin cell is *bistable,* in exhibiting two alternative stable states: the "normal" resting potential, and the plateau potential; it is either active in a burst, or it is silent - and it repeatedly oscillates between these states.

An essential component of phasic activity is activity-dependent inactivation of the plateau, which allows the vasopressin cell to fall silent after a burst until DAP conductances are activable again. This makes the cell a *bistable oscillator*: it will tend not to stay in either stable state indefinitely, but will alternate between the two. Bursts evoked by current injection or by antidromic stimulation are followed by an activity-dependent after-hyperpolarisation resulting from a slow, Ca^{2+}-dependent K^+-conductance which functions as a feedback inhibitor of spike activity; this channel type can be identified by use of the toxin apamin; in the presence of apamin, the afterhyperpolarisation (but not the HAP) is blocked; as a result, bursts are more intense but phasic firing is still present, so this after-hyperpolarising mechanism does not alone account for burst termination.

Implications of membrane bistability for responsiveness to afferent input

The membrane properties of vasopressin cells are reflected in distinctive features of their behavior. Electrical stimuli applied to the axons evoke spikes that are propagated antidromically to

the cell bodies. Just as spontaneous spikes are followed by a DAP, so are antidromic spikes, and brief trains of antidromic spikes can trigger full bursts of activity in vasopressin cells. Interestingly, trains of antidromic spikes can also *stop* established bursts, through exaggerating the activity-dependent inactivation of the plateau potential. Low-frequency antidromic spikes on the other hand produces the interesting effect that cells appear to compensate for the additional evoked spikes by a matching reduction in spontaneous discharge. Vasopressin cells thus "defend" their firing rate against perturbations, probably via an intrinsic after-hyperpolarisation (AHP), which acts as a feedback inhibitor of spike activity. Antidromic activation mimics particular effects of synaptic excitation - consequences of spike activity *per se* follow whether the spikes are induced by synaptic input or by direct stimulation. Thus excitatory inputs may trigger a burst if a vasopressin cell is silent, or may stop a burst if a cell is active, or may have no effect if it is weak enough to allow the cell to defend its firing rate effectively. Similar paradoxical effects are observed with inhibitory stimuli.

So vasopressin cells fire in bursts, and bursts release vasopressin efficiently. Bursting reflects an intrinsic membrane bistability, and this property causes vasopressin cells to respond to inputs in a complex manner. Vasopressin cells require tonic synaptic input in order to function normally, but are individually relatively insensitive to changes in the level of input, except that small changes can, rather unpredictably, trigger transitions between activity and silence. One role of synaptic input is thus to permit the expression of patterns of activity in vasopressin cells - without synaptic "noise", this behavior cannot be displayed.

Signals and noise are often thought of as mutually incompatible. However, the reliability of information transfer can, in some systems, be paradoxically enhanced by noise, a phenomenon referred to as *stochastic resonance*. Background activity in neurons in the absence of an identifiable signal associated with that activity, what we might call neural noise, may not merely reflect activity in neurons poised at the threshold of responsiveness, but may play a role in fashioning the behavior and signal sensitivity of target neurons. One implication of this is that when removal of an input impairs the response of a neuron to a stimulus, we cannot infer, from this observation alone, that the input encodes any information about the stimulus. Some neurons may play an important role even if they carry no identifiable information, and their output is unaffected by physiological stimuli, if their activity provides a level of synaptic noise which is important to support key dynamical behavior, either in neuronal networks or in single cells.

Firing patterns of oxytocin cells

Unlike vasopressin neurons, oxytocin neurons never discharge phasically. Under most circumstances they discharge continuously, at between 0 and 12Hz, but an important exception to this is seen during lactation, when, in response to suckling, in addition to the background activity that resembles that seen in non-lactating animals, oxytocin cells display occasional high frequency discharges of spikes at up to 100Hz for 2 –4s (Fig 1). In the rat, these "milk-ejection bursts" occur every 5-10min, for as long as the suckling continues, and occur synchronously between all oxytocin cells in the hypothalamus. At all other times, no correlation is apparent between the discharge activities of neighbouring oxytocin cells. Thus, normally, oxytocin cells appear to behave autonomously, but in

some circumstances they discharge in a manner reflecting positive-feedback interaction amongst the population. At present, it is believed that this interaction reflects a labile dendro-dendritic interaction between oxytocin cells that provides a variable level of weak mutual excitatory interaction. Dendritic release of oxytocin is activity dependent, but it is also modulated by intracellular signalling mechanisms. Importantly, the amount of activity-dependent oxytocin release is determined largely by extrinsic priming factors.

Intrinsic Properties

Magnocellular neurons have a resting membrane potential of between –55 and –70mV, an input resistance of between 50 and 250MO, and membrane time constants ranging between 9 and 18ms. Single electrode voltage-clamp recordings measured steady-state current-voltage (I-V) relations that were nearly linear between –100 and –60mV when performed from a holding potential near –60mV. Varying the holding potential and the application of various channel blockers, resulting in changes in the I-V relationship, show a variety of Ca^{2+} and K^{+} currents. In particular, whole-cell patch-clamp recordings have revealed at least five different components in the voltage-dependent Ca^{2+} currents in magnocellular neurons: a T-type current with a low threshold of activation (-60mV), rapid inactivation at peak amplitudes (~40ms), high sensitivity to Ni^{2+}; a low threshold L-type channel with a threshold of around –50mV, slowly inactivating (~1300ms), and sensitive to nifedipine; a R-type current, threshold of –50mV, inactivation of ~200ms, and insensitive to toxins; a P-type current, non-inactivating, and blocked by ? -agatoxin IVA; and an N-type-current, slowly inactivating (~1800ms), blocked by ? –conotoxin GVIA.

In both oxytocin cells and vasopressin cells, every spike is followed by a hyperpolarising afterpotential (HAP), which lasts between 50-100ms, and results from a rapidly activated Ca^{2+}-dependent K^{+} conductance, similar to the current termed I_a, in other cells. The I_a can be activated when a cell is depolarised following a period of hyperpolarisation, and it serves as a "damper" to space successive spikes. Accordingly, the HAP sets an upper limit on the maximal firing rate which can be achieved during a depolarising stimulus, and in the case of magnocellular neurons the HAP is large and long lasting, and this upper limit is accordingly quite low. Under most circumstances oxytocin and vasopressin cells will not sustain a discharge rate exceeding 15Hz for more than a few seconds, and the minimum interval between successive spikes is very rarely less than about 30ms. Oxytocin cells adhere to this limit under all circumstances but one: during milk-ejection bursts they dramatically escape this limit. The outward current underlying the HAP is evoked by a depolarising voltage current pulse from a threshold of –75mV, reaches the peak within 7ms and subsequently decays monotonically with a time constant of 30ms. Steady-state inactivation is complete at potentials positive to –55mV, and the inactivation is removed following tens of milliseconds at hyperpolarised voltages. Further, the I_{to} is strongly dependent on extracellular Ca^{2+}, whereby its influx during a spike may contribute to the repolarisation, as well as to the peak and initial phase of the HAP. Indeed, its amplitude appears to be directly proportional to the external concentration of Ca^{2+}.

In contrast to the HAP, which is evoked by single spike, trains of spikes are followed by a prominent afterhyperpolarisation (AHP). The magnitude of the AHP is proportional to the number of

spikes during the preceding spike train, with an exponentially progressing onset and a maximum after the first 15-20 spikes, regardless of the frequency at which spikes were evoked. The steady-state amplitude increases logarithmically between 1 and 20Hz. The AHP lasts hundreds of ms, and its duration also depends on the duration and frequency of the spike train. The AHP is associated with a 20-60% decrease in input resistance, shows little voltage dependence in the range –70 to –120mV, and is proportional to the extracellular Ca^{2+} concentration. These observations led to the conclusion that the AHP results from the activation of a slow, voltage-independent Ca^{2+} -dependent K^+ conductance, the I_{AHP}. The distinction between the I_{AHP} and the I_{to} (and correspondingly between the post-train AHP and the post-spike HAP) is made since the ionic currents are pharmacologically distinct. The I_{to} is less sensitive to tetraethyl ammonium, but is reduced by 4-aminopyridine and dendrotoxin. In contrast, I_{AHP} is blocked by apamin, with the effect of a threefold increase in the mean firing rate of spontaneously active neurons. Pharmacologically, the AHP appears to have a fast component and a slow component; the fast AHP is blocked by apamin, while the slow AHP is blocked by charybdotoxin, and is affected by low concentrations of tetraethyl ammonium. Apamin generally blocks small-conductance (SK) Ca^{2+} dependent K^+ channels, while charybdotoxin blocks big-conductance (BK) Ca^{2+} dependent K^+ channels, as well as some other K^+ channels.

Intracellular Ca2+ concentration

In response to any spike activity, there is a large Ca^{2+} entry into oxytocin cells and vasopressin cells via several different voltage-gated Ca^{2+} channels. In addition, intracellular Ca^{2+} stores can be mobilised via second messenger pathways to give very large increases in intracellular Ca^{2+} concentration ($[Ca^{2+}]_i$) (see 10-13). The dynamics of Ca^{2+} change differ between the cell types, as they differently express Ca^{2+} binding protein calbindin (14). Oxytocin cells contain more calbindin than vasopressin cells, allowing them a higher Ca^{2+} buffering capacity, which prevents generation of DAP's and therefore phasic firing. DAP's and phasic firing can be evoked in oxytocin cells by neutralising calbindin or by increasing $[Ca^{2+}]_i$. Conversely, phasic firing neurons can be switched to continuous firing by introduction of exogenous calbindin or by chelation of intracellular Ca^{2+}. The amplitude of DAPs depends on Ca^{2+} influx through voltage-dependent Ca^{2+} channels of L- and N-types, but also on Ca^{2+} release from intracellular Ca^{2+} stores, notably thapsigargin-sensitive stores, located in the endoplasmic reticulum.

Both vasopressin and oxytocin cells have thapsigargin-sensitive intracellular Ca^{2+} stores. In oxytocin cells, oxytocin itself induces an increase in $[Ca^{2+}]_i$ by activating IP_3 pathway-coupled oxytocin receptors, which results in the release of Ca^{2+} from thapsigargin-sensitive stores. Oxytocin apparently does so without any strong accompanying depolarisation. In vasopressin cells, vasopressin also induces a Ca^{2+} response, but in a more complex way. Vasopressin-induced $[Ca^{2+}]_i$ increase mainly involves an influx of Ca^{2+} via voltage-dependent Ca^{2+} channels of L-, N- and T-types, as it can be reduced by specific blockers of these channel types. In addition to Ca^{2+} coming from the extracellular medium, part of the response to vasopressin is also due to release of Ca^{2+} from thapsigargin-sensitive intracellular stores. The complexity of vasopressin actions probably results from activation of several types of receptors coupled to different intracellular messenger pathways. Vasopressin receptors

(described so far) comprise V_{1a} and V_{1b} type receptors, which are coupled to phospholipase C (PLC), and V_2-type receptors, which are coupled to adenylyl cyclase. Agonists of both V_{1a}- and V_2- receptor types can induce a $[Ca^{2+}]_i$ increase in vasopressin cells. In addition, inhibitors of PLC and adenylyl cyclase pathways, by blocking the production of intracellular messengers IP_3 and cAMP, decrease the Ca^{2+} response to vasopressin. Vasopressin clearly can depolarise vasopressin cells to induce Ca^{2+} entry via voltage-gated channels, but also induces some liberation of Ca^{2+} from intracellular stores, and can also probably hyperpolarise vasopressin cells via Ca^{2+} -activation of Ca^{2+} -dependent K^+ channels; in practice, it seems that the actions of vasopressin on vasopressin cells are state-dependent; when applied on vasopressin cells *in vivo*, vasopressin tends to excite silent or slow firing cells but it tends to decrease the firing rate in active cells.

Implications

To build a realistic biophysical model of an oxytocin cell or a vasopressin cell from the "bottom up", there are in principle a very large number of basic membrane properties to be incorporated. Apart from the Na^+ and K^+ conductances that underlie the generation of the spike, there are a large number of Ca^{2+} conductances and K^+ conductances that appear to play specific, potentially important roles, and since several of the latter are Ca^{2+} -dependent, the intracellular Ca^{2+} dynamics, involving buffering and mobilisation of intracellular Ca^{2+} stores also need to be included. The disposition of these conductances in different cellular compartments is poorly understood, and other conductances, in particular to chloride, and non-specific cation conductances, are also important, as may be the precise cellular topology. To build a network model it would also be necessary to incorporate elements reflecting the nature of stimulus-secretion coupling and the different underlying mechanisms at dendrites and nerve endings; vasopressin cells for instance express different populations of Ca^{2+} channels at the soma and nerve terminals.

On the other hand, we might take an approach that is consciously simplistic, incorporating progressively only those features of cells that are essential to explain particular behaviors, and incorporating these in a minimalist way. We need to set a verifiable objective: to develop computational models that mimic cells so closely, that for specific defined attributes, they are essentially indistinguishable in their behavior from real cells. In the example shown hereon, we look at the normal discharge patterning of oxytocin cells and seek a minimalist quantitatively accurate model of this. To be a good model, the spike output of the model cell must be indistinguishable from outputs of real cells by any statistical analysis that is applied.

Statistical methods to investigate the intrinsic mechanisms underlying spike patterning

Selecting recordings for analysis

Before starting the analysis of the firing activity, we must select suitable recordings. Stationarity is an essential prerequisite for the analysis to be meaningful. A series is stationary if there are no systematic trends or "rhythmic" variations. We started with stable, long recordings (up to 3h) of spontaneous activity from identified rat oxytocin cells *in vivo*, and from these, stationary recordings, or

long stationary stretches from recordings that were not stationary throughout, were chosen. Stationarity was checked with the help of "bicubic splines", a series of smooth cubic curves fitted over short stretches of activity, then joined with the same slope at the joints to form one continuous curve. One way of looking at temporal patterns is by looking at the time between consecutive spikes ("interspike intervals"). Interspike intervals provide information about the relationship between spikes in a way easily accessible for statistical scrutiny. The interspike interval histogram is a graphical representation of the distribution of the occurrence of intervals of a variable length. The distribution allows a first indication about spike patterning in an individual neuron.

Interspike interval distributions

For both oxytocin cells and vasopressin cells, the interspike interval distribution is skewed, with a single mode and a long tail (Fig. 2). For vasopressin cells, modes are in the range 40-60ms, and for oxytocin cells, in the range 30-80ms. The tail of each distribution (> 200ms) can be well fitted by a single exponential, and extrapolation of this exponential shows a deficit of intervals below the curve in the range 0-40ms, consistent with the effect of a HAP. For vasopressin cells, there is an excess of intervals above the curve in the range 40-100ms, consistent with the effect of a DAP. No such excess is observed in oxytocin cells, indicating that oxytocin cells display little or no DAP when normally active *in vivo*. The good exponential fits for oxytocin cells indicate that, to a first approximation, beyond about 80 ms after any given spike the arrival time of the next spike is essentially random. Thus the activity of oxytocin cells is dominated by factors affecting the probability of spike occurrence that are independent of previous spike history– i.e. the mean resting potential and the rate of synaptic input; and a reduction in excitability following each spike that decays over 40-80ms, consistent with the expected effects of a post-spike HAP. This inference is more clearly apparent from the construction of hazard functions (Fig. 3): these describe cell excitability as a function of time elapsed since an spike, by calculating the probability of cell firing per unit elapsed time from the interspike interval data. For oxytocin cells the hazard function shows a low probability of firing (reflecting the HAP) for about 50ms, and a constant hazard thereafter; vasopressin cells show a sequence of low probability followed by high probability before return to constant hazard.

Modelling

To test this inference, we (15) modelled oxytocin cells and vasopressin cells by a modified "leaky integrate and fire model" (16). EPSP's and IPSP's generated randomly and independently at mean rates R_E and R_I produce perturbations of membrane potential that decay exponentially. These summate to produce a fluctuating "membrane potential". When a fluctuation crosses a spike threshold, T, a spike is generated, followed by a HAP, modelled as an abrupt, exponentially decaying increase in $T = T_0(1+ke^{-\lambda t})$ where t is the time since the last spike, T_0 is the spike threshold at rest, and k and λ are constants. Intracellular recordings from oxytocin cells reveal EPSP's and IPSP's of 2-5mV that last for 5-10ms; we assumed that EPSP's and IPSP's at rest were of equal and opposite magnitude (at T_0) with identical half-lives. Oxytocin and vasopressin cells have resting potentials of about -62mV with a spike threshold of about -50mV, and are depolarised in direct response to hyperosmotic stimulation following shrinkage, resulting in inactivation of specialised non-adapting stretch-sensitive K^+ channels

(17). *In vivo,* the peak activation (at ≈12Hz) is attained after osmotic stimulation has raised extracellular [Na^+] by ~ 10mM, producing a direct depolarisation of ≈3-5mV. The equilibrium value for T, T_0, was thus set at 12mV for the simulations shown, and simulations were conducted over 1mV below to 5mV above this level. We conducted simulations with parameter values systematically spanning the ranges above, restricted to output ranges (0-16Hz) consistent with the behavior of oxytocin cells.

Simulating oxytocin cell activity.

We found that the inter-spike interval distribution from each oxytocin cell could be closely matched by a model cell with a resting potential (T_0) of 12mV below spike threshold subject to random EPSP's of 4mV amplitude and 7.5ms half-life (Fig. 3). Each cell could be closely fitted by varying just λ and I_E. The fits were not unique; good fits could be achieved for different values of EPSP size (2-5mV) or half-life (3-20ms), or for different values for T_0 by changes in R_E, or for different values of k by adjusting λ. Similarly, the shape of the distribution is little affected if the model is challenged not with EPSP's alone but with a mixture of EPSP's and IPSP's. However, for a chosen value of k, every distribution could be characterised by a unique λ, and by T_0, R_E and R_I, which affect the output rate but have little other effect on the shape of the distribution in the relevant range.

For vasopressin cells, inter-spike interval distribution could be well fitted by the output of a similar model cell with the addition of a component to mimic the effect of a slow DAP, modelled as an abrupt, exponentially decaying *increase* in $T = T_0(1+ke^{-\lambda t})$ where t is the time since the last spike (Fig. 3). Adding this to the oxytocin model produces a sequence of fast HAP followed by a slow DAP. Of course this simple model does not reproduce phasic firing, only the characteristic distribution of inter-spike intervals. Essentially, phasic firing does not occur in this simple model because it incorporates no mechanism for burst termination or burst refractoriness, hence once a burst is triggered it may continue indefinitely, or once stopped nay be retriggered immediately.

But leaving aside the vasopressin cell model for the present, the good fit of a simple model to oxytocin cell data enabled us to test the hypothesis that the oxytocin cell response to osmotic stimulation arises from an increase in synaptic input combined with a direct depolarisation, with no change in the intrinsic mechanisms that govern post-spike excitability. If so, then it should be possible to fit inter-spike interval histograms from any one oxytocin cell at different levels of activity with a common λ. This proved true for each cell tested (Fig 4). We then studied how the firing (output) rate of model cells changes with the synaptic input rate, and with increasing depolarisation.

Experimental testing of the model

In a healthy adult, above a fixed threshold, vasopressin release varies linearly with osmotic pressure over a wide dynamic range. The relationship between the plasma concentration of vasopressin (v) and osmotic pressure (x) fits the equation $v = ax + b$, where b is the "threshold" osmotic pressure or "set point", and a is the "slope" of the osmoregulatory mechanism. When the behavior of individual vasopressin cells and oxytocin cells is studied, it is strikingly apparent that individual neurons also show a linear increase in firing rate in response to increased osmotic pressure, that this linearity is

apparent throughout the normal dynamic range of their spike activity, and that the slope of the response is relatively constant between cells even when their spontaneous firing rates differ markedly (Fig. 5).

However, in the absence of IPSP's, an increase in EPSP rate produces a non-linear increase in output (over the physiological output range), and this is true broadly regardless of the parameter values within the ranges as described above. Elaborating the model to incorporate a reversal potential for EPSP's (of –38mV) does not significantly alter this conclusion. The effective dynamic range of oxytocin cells is from about 0.5Hz (lower range of spontaneous rates) to about 10Hz (peak sustained rates). This range was spanned in the model cells by a narrow range of R_E –typically by a change in R_E from 110/s to 180/s. Osmotic stimulation is accompanied by a direct depolarisation of 3-5mV (17), and an equivalent change in T_0 leads to a compression of the range of R_E needed. This suggests that tonically active cells subject to EPSP input alone will respond strongly to osmotic stimuli as a result of the direct osmotic depolarisation, even with no change in synaptic input. Furthermore, similar changes in R_E from a different initial rate, but accompanied by the same osmotic depolarisation, result in very different amplitudes of responses. This suggests that oxytocin cells that differ in initial firing rate as a result of differing initial EPSP rates will respond in a divergent manner to a subsequent identical stimulus (Fig. 5).

Although these inferences are broadly independent of assumptions about EPSP size, half-life, and resting potential, they are not consistent with experimentally observed behavior. Osmotic stimulation is accompanied by large increases in the activity of afferent neurons. Moreover, the inference of divergent responsiveness of cells with different initial firing rates is not consistent with the consistency and linearity of the neuronal responses observed *in vivo*.

However, in model cells, the relationship between output rate and input rate becomes shallower as the ratio of IPSP's to EPSP's is increased, and this is true both for models that assume that EPSP and IPSP size are independent of voltage, and for models that incorporate appropriate reversal potentials for both. Comparing simulation results of models with and without reversal potentials, it is apparent that while the latter are less sensitive to synaptic input, it is equally true for both models that a high proportion of IPSP's produces a linearisation of the input-output relationship (18). We therefore conducted simulations combining a direct depolarisation with an increase in *balanced* input, comprising equal average numbers of EPSP's and IPSP's (Fig. 3). Under these conditions, model cells that differ in initial output rate as a result of differing initial input rates respond similarly to a given stimulus.

The simple oxytocin cell model described here indicates that an increase in IPSP frequency that accompanies either an increase in EPSP frequency or a steady depolarising influence, will moderate the rate of increase in firing rate, will linearise the input-output relationship, will extend the effective dynamic range of the output neuron, and will tend to make the response of a neuron to a given input independent of the initial firing rate. The theoretical analysis thus indicated that a high proportional activation of inhibitory input confers appropriate characteristics upon the responses of magnocellular neurons to osmotic inputs. Thus this model produced the highly counter-intuitive prediction that when magnocellular neurons are excited in response to an increase in osmotic pressure, that increase reflects not only an increase in excitatory input but also an increase, of equal or greater

magnitude, in inhibitory input. This counter-intuitive prediction was then tested, and supported first by direct measurement of a large increase in the release of the inhibitory neurotransmitter GABA in the supraoptic nucleus during osmotic stimulation, and second by studies of the effects of blocking GABA neurotransmission on the responses of oxytocin cells to osmotic stimulation.

Firing rate analysis

As can be seen above, we might conclude from the shape of the interspike interval distribution that spontaneous firing of an oxytocin cell is a renewal process – effectively Poissonian except for the effect of the HAP. However, weak, slow activity-dependent influences might not be apparent from the interspike interval histogram, as to exert a significant influence, they would require summation of the effects of several spikes occurring in a short period. Since we are interested in periods of activity as opposed to individual spikes, we can take one of two approaches: we can analyse serial dependence between average firing rate measured in successive short time intervals; or we can look at serial dependence of instantaneous interspike interval length on the past discharge activity.

What would we expect if spikes were generated wholly independently of the previous incidence of spikes? For a renewal process, the probability of an event occurring at any given time is independent of the timing of preceding events. In particular:

i) The tail of the inter-spike interval distribution should be well described by a single negative exponential (i.e. except where the refractory period of the cell prevents firing).

ii) Data should show invariant statistical characteristics when shuffled randomly.

iii) As the variance of the event frequency (σ^2) equals the mean of the event frequency (μ) for a Poisson process, the **index of dispersion** (σ^2 / μ) should be close to 1 (if the relative refractory period is relatively small), and should be independent of binwidth.

We analysed recordings from oxytocin cells to investigate how they deviate from randomness by each of these criteria. For each cell, the sampled firing rates (sampled in successive short time intervals, e.g. 1-s bins) were expressed as a distribution, showing the relative frequency of the occurrence of particular firing rates. These distributions are typically bell-shaped, with the peak around the mean firing rate, and a rather symmetrical spread. In the next step the interspike intervals were shuffled randomly creating a new "recording". We recalculated the firing rates - again for 1-s bins -, and compared the new distribution of firing rates to the original distribution. If the original distribution is based on randomly occurring intervals, than further randomisation should have no effect. However, in the overwhelming majority of cases, the distribution of randomised firing rates was wider than the distribution of observed firing rates (Fig. 6). In other words, the observed firing rate distribution was more uniform than would be expected if there were no serial dependence between interspike intervals.

If randomisation did not consistently affect the shape of the distribution we might have reasonably concluded that there were no activity-dependent influences that had a significant influence on spike patterning beyond those that influence the interspike interval distribution. Since it does, we can conclude that activity-dependent mechanisms underlie the spontaneous activity of oxytocin cells. The mechanisms are weak in the sense that their effects are not readily apparent in the interspike

interval distribution, but are apparent on a time scale of 1-s. In other words, variations in average activity of the order observed from second to second are enough to produce discernible feedback effects on spike activity.

Index of dispersion

We stated above what we expect from the index of dispersion if spike arrival would be generated independently of previous spikes. The index of dispersion is the ratio of the variance of firing rate to the mean firing rate. For a Poisson distribution, the variance of the event frequency equals the mean, and the index of dispersion = 1, and is independent of bin width. The closer to 0 the index of dispersion, the more ordered the underlying series. An index of dispersion above 1 suggests that the series is more irregular than a Poisson process, and could be an indication of heavy clustering. We calculated the index of dispersion for oxytocin cells, using different bin sizes; the index of dispersion differed with varied bin widths in a characteristic way: for very small bins the index of dispersion was high, (average value 0.7 ± 0.05), but decreases when the bin width increases. Thus, when looking at the recording at a very short time scale such as 0.06s, firing appears to be near random, but, when looking at increasingly longer periods (up to 2s), the firing appears to be more and more ordered. The firing appears to be most ordered when looking at a time scale of 4 to 8s, where the index of dispersion is the smallest (0.27 ± 0.4). Since the index of dispersion depends on bin size, the generation of spikes is not independent of previous activity.

Autocorrelation analysis

Autocorrelation refers to the serial dependence of observations in a stationary time series; autocorrelation coefficients measure the correlation between observations at different lag times. In our case, the observations are firing rates for a specified period of time, or window, and to calculate the autocorrelation coefficient of lag n, the observation at time t is compared to the observation at time t+n. For small windows (0.06 to 1s), a negative autocorrelation was found for most oxytocin cells, but for larger window sizes, this negative autocorrelation disappears. Thus, at small time scales (0.06 s to 1s), periods of relatively high activity are likely to be followed by periods with relatively low average activity, and vice versa. Thus the average firing rate over long periods of time is much more regular than would be expected from the local variability in firing rate.

This type of analysis can be logically extended to serial dependence of interval length. The simplest approach is to consider how the length of a given interval t_1 depends upon the history of previous spike activity – the preceding intervals t_1, t_2, t_3, t_4, t_5 ..... When oxytocin cell recordings are analysed in this way, there is a negative relationship between t_1 and $t_2+....+ t_n$, the slope of which is typically maximal for n between 5 and 10, and which approaches 0 as n exceeds about 20. This indicates that for oxytocin cells firing at typical background rates, there is a negative effect of discharge rate upon spike activity through mechanisms slow enough to summate over 5-10 spikes in 1-2 s (Fig.7)

It should be remembered that the biological message encoded by a single oxytocin cell is only the contribution that that cell makes to the secretion from the oxytocin population as a whole. The

overall secretion rate has considerable biological significance, and the rate must be maintained at an appropriate and steady average level for prolonged periods when necessary for regulating sodium excretion (natriuresis), but local second-by second variability in the secretory rate of individual neurons is of no biological significance unless such changes occur synchronously throughout the population (as during reflex milk ejection). For oxytocin cells therefore, what is important for natriuresis is only that they accurately maintain an average steady state activity when measured over long periods. Oxytocin cells clearly have activity-dependent negative-feedback mechanisms that ensure long term stability of average firing rate.

Summary and Conclusions

Although the interspike interval distributions of oxytocin cells seem to suggest that spike arrival times (during spontaneous activity) are largely independent of previous firing activity (except for the refractory period), closer analysis shows otherwise. Firing rate analysis demonstrated that the index of dispersion did not equal 1and was not independent of bin width. Further, while the activity appears to be nearly random at a small time scale, over a scale of several seconds it appears much more ordered. The analysis of serial dependence showed that on a small time scale the activity is clustered, but on a larger time scale the activity is more homogenous. Thus on a short and medium time scale the cell possesses a "memory" and balances the activity, whereby periods of short intervals tend to be followed by periods with longer ones, and *vice versa*. However, on a long time scale the activity is rather homogenous. These results demonstrate structure in sequences of interspike intervals, and from its characteristics we may conclude it to be the effect of the AHP.

Thus sufficient information seems to be available from the characteristics of spontaneous discharge activity to produce concise computational models that can mimic this behavior closely when they incorporate features that appropriately describe the impact of intrinsic, activity-dependent mechanisms. Such models are unique descriptors of a particular neuronal phenotype, and are by design well-matched to experimental data, but are also capable of generating fresh insight into cell properties, testing the coherence and feasibility of biological hypotheses, and capable of generating novel and counter-intuitive predictions.

We have concentrated on demonstrating this approach for an example neuron with limited network connectivity. The oxytocin cell is an output neuron, with few axonal collaterals to make any recurrent connection with other neurons in the CNS, hence activity-dependent influences in activity primarily reflect intrinsic cell properties in normal circumstances. However this approach is potentially particularly appropriate for analysing the behavior of neurons where activity-dependent influences are mediated by interactions with other neurons. As far as the analytical approach is concerned, this is indifferent to whether activity-dependent influences reflect intrinsic properties or external feedbacks, and concise models can be equally indifferent to this where it helps to collapse mini-neuronal networks into single elements.

As considered above, oxytocin neurons normally function autonomously, but during suckling in lactating rats, oxytocin cells show dramatically different behavior that reflects weak pulse coupling through dendro-dendritic interactions (19,20). These weak, mutually excitatory interactions have been extensively studied experimentally. The underlying mechanisms are complex: oxytocin is released from the dendrites in response to a rise in intracellular Ca^{2+}, but little oxytocin release normally results from spike activity. However agents that liberate Ca^{2+} from intracellular stores also cause a large mobilisation of dendritic stores of oxytocin into readily-releasable stores that are subsequently available for activity-dependent release. One such agent is oxytocin itself, which triggers Ca^{2+}mobilisation from thapsigargin-sensitive stores in the endoplasmic reticulum after binding to specific oxytocin receptors on oxytocin cells. Thus dendritic oxytocin can enable subsequent activity-dependent oxytocin release. Oxytocin released around the dendrites has multiple other effects, in particular inhibiting glutamate release from afferent excitatory synapses and attenuating the effect of synaptically-released GABA by post-synaptic actions. Oxytocin is released in very high concentrations around the dendrites and in CSF has a long half-life, making it a neurohormonal like messenger within the brain that can potentially act at distant sites and over a prolonged time scale, though local expression of peptidases may protect some sites of potential action.

Dendritic release of signalling molecules is far from unique to the oxytocin cells; dendritic release has been demonstrated in a number of systems and for a variety of molecules including vasopressin and dopamine, and may be a wholly general phenomenon, at least for peptidergic transmitters. The capacity of peptides to act at a distance through their long half-life in the brain, their ability to act at low concentrations through G-protein coupled receptors linked to a diversity of neuromodulatory actions, and the remarkable ability of peptides to selectively induce the expression of coherent behaviors, makes it important to integrate their effects into models of brain function. To model dendritic influences within biophysical frameworks is of course possible, but it may be as revealing and helpful to analyse and model their impact, rather than the underlying mechanisms.

The impact of activity-dependent positive feedback on the normal spontaneous activity of oxytocin cells should be apparent from the above-described statistical analyses; but there is no visible impact, or any impact overlaps with and is fully occluded by activity-dependent negative feedback (mediated by the AHP). To look at the *potential* for activity-dependent positive feedback in the network we can however look at how the structure of discharge activity is altered in defined experimental conditions. First, we can look at the effect on the activity of an oxytocin cell of synchronised activation of its neighbours through the technique of constant-collision stimulation. This reveals the existence of a rapid and transient mutual excitation that is normally masked by the HAP except when synchronous activation of neurons enhances this effect. Second we can look at the consequences of priming the releasable pool of oxytocin in the dendrites by treatment with the intracellular Ca2+ mobilising agent thapsigargin. Thapsigargin, like constant-collision stimulation, reveals weak mutual excitation, though whereas constant-collision stimulation amplifies this effect by the artificial synchronisation of electrical discharge, thapsigargin does so by amplifying the releasable pool of oxytocin in the dendrites. As these actions are independent, they can be combined with additive

or synergistic effect, giving rise to a clear and strong appearance of positive-feedback excitation, and with that, clustered firing, including occasional intense bursts of activity (Fig. 8)

In oxytocin cells, priming of dendritic release switches the behavior of oxytocin cells from being a population of autonomous neurons whose individual activity is governed by their synaptic inputs independently of their neighbours, to being a loosely-coupled population in which synchronous bursts of activity erupt through mutual excitatory excitation, while at the same time, external influences on activity are suppressed. This capacity for functional re-wiring of neuronal networks provides a possible explanation for how peptides can initiate long-lasting, coherent behavioral responses.

To summarise: neurons exhibit a wide diversity of electrophysiological phenotypes that have important consequences for how they process information. Neurons have several modes of communication with other neurons, as well as fast transmitter-mediated interactions via conventional synapses, neurons can release peptides and other substances from dendrites that have a neurohormonal-like action over a wide target area, the specific targets being defined by their expression of specific receptors. Neurohormonal actions have limited target specificity compared to neurotransmitters, where the target is restricted to the particular synapses. Neurohormonal actions also have limited temporal specificity, requiring integrated release over extended periods of time. The actions of neurohormones however can include organisational influences on networks, changing the strength of interactions by priming releasable reserves. While we have shown this for the releasable pools of oxytocin in dendrites, similar mechanisms may apply generally, perhaps including priming of release from synapses.

To model such a functional architecture we need concise models of individual neurons that accurately encapsulate their electrophysiological phenotype. For a model, the phenotype of a neuron may express not merely its intrinsic properties but also those properties conferred upon its behavior that are intrinsic to the network; models must be concerned with activity-dependent influences on a cell's behavior, but need not be concerned whether those influences result from a cell's intrinsic membrane properties or from recurrent network connections. However, the electrophysiological phenotype may be functionally plastic under the influence of certain types of signal, including in particular neurohormonal signals.

This chapter has discussed in particular examples of hypothalamic neurons. We have argued that the diversity of neuronal phenotypes is great, and we need models to understand the functional implications of the differences. We have argued that for this we do not necessarily need complex biophysical models, but we do need quantitatively accurate, computationally concise representations of the electrophysiological phenotypes. It may be questioned whether there is not some difference between the hypothalamus and other regions of the brain, such as the neocortex. Of course there are differences. Most importantly, we know some of the things that the hypothalamus does; sometimes in great detail, including *why*, and what we don't know is generally amenable to hypothesis and testing.

We also know that what the hypothalamus does is important. But we need strong conceptual frameworks, with predictive power, to build our understanding.

Fig. 1 Electrical activity in supraoptic nucleus oxytocin and vasopressin neurones recorded *in vivo* in urethane-anesthetized rat (**A**) Typical example of firing pattern in an oxytocin cell, identified by its activation in response to i.v. injection of 20 μg/kg of CCK. During suckling of pups, brief and high frequency bursts of spikes are superimposed upon the slow and irregular background activity. These bursts occur synchronously amongst all oxytocin cells in the hypothalamus.
(**B**) Typical example of phasic discharge pattern in a vasopressin neuron characterised by succession of silent periods and active periods. Mean burst duration varies considerably between vasopressin cells, and the bursts occur asynchronously amongst the population of vasopressin cells.
(C) Intracellular recording from a vasopressin cell *in vitro*. Spikes arise in these cells when EPSPs summate to bring the membrane potential above spike threshold. Phasic bursts occur because a sustained plateau potential, depolarising the vasopressin cell by typically about 7 mV, produces a sustained increase in excitability. The plateau is however itself activity dependent.

Fig. 2 Representative inter-spike interval distributions from an oxytocin cell (**A**) and a vasopressin cell (**B**) showing exponential curves fitted to the tails of the distributions and extrapolated to lower interval values. Both vasopressin cells and vasopressin cells show a deficit of intervals below the fitted curve in the region 0-30 ms, reflecting the presence in both cells of a strong post spike hyperpolarisation (the HAP). For vasopressin cells, but not for oxytocin cells, such extrapolations revealed a large excess of intervals above the fitted curve in the range 30-150ms, reflecting the presence in vasopressin cells only of a depolarising afterpotential (DAP) following the HAP.

Fig. 3 Left panels: inter-spike interval distributions from two oxytocin cells (top) and two vasopressin cells (bottom), each of which is modelled by a modified leaky-integrate-and-fire model neuron (see text). The histograms from the model cells are superimposed on the original cell data.
Right panels; hazard functions plotted from the same data for each cell and each model neuron superimposed.
The interspike interval distributions of oxytocin cells and vasopressin cells can be fit remarkably well with relatively simple models, that in the case of oxytocin cells mimic the effects of a HAP only, and for vasopressin cells that mimic the effects of a HAP and subsequent DAP.

Fig. 4 Comparison between model inter-spike interval distributions (lines) at different levels of synaptic input, and distributions observed in an oxytocin cell at different times during infusion of hypertonic saline (points). Oxytocin cell inter-spike interval distributions were constructed over 1000s, model cell distributions over a simulated 25000s, normalised for comparison. Oxytocin cell distributions correspond to mean firing rates of 12.8Hz, 9.3Hz 4.8Hz and 2.5Hz. Model cell

distributions were constructed for equal average numbers of EPSP's and IPSP's, over a range of PSP frequencies that matched the range in firing rates observed during the period of recording analysed, producing output rates close to the average firing rates of oxytocin cells. A single value of λ (0.08) produces good fits for this cell at all levels of activity.

Fig. 5

(**A**) Response of a typical oxytocin cell to a linear increase in plasma osmotic pressure, induced by an slow intravenous infusion of hypertonic saline administered in the period marked by the double headed arrow. This recording also shows the transient excitation induced by intravenous injection of CCK. Note the striking linearity of the increase in firing rate.

(**B**) Relationship between the output rate of a model oxytocin cell and EPSP rate R_E. The different lines show the effect of adding IPSPs in proportion to the EPSPs. For a balanced input, comprising equal average numbers of EPSPs and IPSPs, the input-output relationship is shallower and more linear than for EPSPs alone.

(**C**) Relationship between output rate and R_E, for values of resting potential varying in 0.4mV steps from the standard value (62mV), The double headed arrows connect points corresponding to an output rate of 1Hz at the initial resting potential to points corresponding to 10Hz at a membrane potential depolarised by 4mV. This line thus indicates the apparent dynamic range of oxytocin cells in response to osmotic stimulation *in vivo*. (**C**) shows simulations for a cell stimulated by EPSP's alone, (**D**) shows simulations for a cell stimulated by an equal number of EPSP's and IPSP's. From Leng et al (16).

Fig. 6 Observed firing rate distribution (dark area) and randomised firing rate distribution (white area). The figure shows the analysis of a stationary stretch of a recording of the activity of an oxytocin neurone. Firing rates were calculated in 1 s bins and the shaded curve shows the distribution of firing rates in these 1 s bins. The original interspike intervals were randomised and from the randomised data new second by second firing rates were calculated. The white curve shows the distribution of firing rates from the randomised data. The firing rate distribution has a higher peak, but is narrower than the randomised firing rate distribution, indicating that the sample is more uniform than would be expected from a completely random sample. The discrepancy between the two distributions is a first indication for structure in the firing pattern.

Fig. 7 The effects of constant-collision stimulation (CCS) and thapsigargin on oxytocin neurons

(**A**) Schematic diagram illustrating the technique of constant-collision stimulation (CCS). Spontaneous extracellular spikes are recorded from a supraoptic neuron. Each spontaneous spike triggers the application of an electrical stimulus pulse to the neural stalk, which initiates an antidromic spike in the axon of every supraoptic neuron, since all supraoptic neurons project to the pituitary via the neural stalk. The antidromic spike evoked in the axon of the recorded neuron is extinguished by collision but other antidromic spikes persist to invade the cell bodies of most neighbouring neurons, and thence activates intranuclear connections and dendritic release of oxytocin. (19)

(**B**) Every interspike interval (t_1) in a selected recording period was paired with its predecessor (t_2) and preceding intervals t_3, t_4.... to study the dependence of current activity upon preceding activity- B shows the analysis of a representative oxytocin neuron, the mean t_1 (± standard error) is plotted against t_2 before (left upper panel) and after (right upper panel) CCS, and the corresponding interspike interval distributions before and after CCS (bottom panel). CCS stimulation induces an increase in the proportion of short intervals, as seen in the interspike interval histograms, and an increase in clustered firing, as shown by the positive relationship between t_1 and t_2

(**C**) Example of the mean t_1 (± standard error) against t_2, or $t_2 + t_3$, or $t_2 + t_3 + t_4 + t_5$ (with linear or polynomial trend lines) for a representative neuron in control conditions (upper panels), during CCS (middle panels), and during CCS + thapsigargin (bottom panels). From the top left panel in C it seems there is little influence of t_2 upon t_1, there is a negative regression, but with a very shallow slope. However this weak influence is long-lasting and so summates with successive spikes, because in looking at t_1 vs. $t_2+...+t_5$, there is now a strong inverse correlation. During CCS this negative relationship is still present but is preceded by a positive relationship, indicating a short-lasting positive feedback action superimposed upon the normal slow negative feedback.

Reference List

1. McKinley MJ, Bicknell RJ, Hards D, McAllen RM, Vivas L (1992) Efferent neural pathways of the lamina terminalis subserving osmoregulation. Prog Brain Res 91: 395-402.
2. Wray S (2001) development of luteinising hormone releasing hormone neurones. J Neuroendocrinol 13: 3-12.
3. Douglas AJ, Leng G, Ludwig M, Russell JA (2000) (Editors) "Oxytocin and Vasopressin – from molecules to function" Special Edition of Exp Physiol (Volume 85S)
4. Leng G (1988) *Pulsatile release of hormones and bursting activity in neuroendocrine cells* CRC Press; Boca Raton, Florida. 261pp
5. Leng G , Brown D (1997) The origins and significance of pulsatility in hormone secretion from the pituitary. J Neuroendocrinol 9: 493-513
6. Leng G, Brown CH, Russell JA (1999) Physiological pathways regulating the activity of magnocellular neurosecretory cells. Prog Neurobiol 57: 625-655
7. Bourque CW, Renaud LP (1990) Electrophysiology of mammalian magnocellular vasopressin and oxytocin neurosecretory neurons. Front Neuroendocrinol 11: 183-212.
8. Armstrong WE (1995) Morphological and electrophysiological classification of hypothalamic supraoptic neurons. Prog Neurobiol 47: 291-339.
9. Bourque CW, Oliet SH, Richard D (1994) Osmoreceptors, osmoreception, and osmoregulation. Front Neuroendocrinol 15: 231-274.
10. Lambert R, Dayanithi G, Moos F, Richard P (1994) A rise in intracellular Ca2+ concentration of isolated rat supraoptic cells in response to oxytocin. J Physiol 478: 275-288.
11. Dayanithi G, Widmer H, Richard P (1996) Vasopressin-induced intracellular Ca2+ increase in isolated rat supraoptic cells. J Physiol 490: 713-727
12. Sabatier N, Richard P, Dayanithi G (1998) Activation of multiple intracellular transduction signals by vasopressin in vasopressin-sensitive neurones of the rat supraoptic nucleus. J Physiol 513: 699-710.
13. Li Z, Hatton G (1997) Ca^{2+} release from internal stores: role in generating depolarising after-potentials in rat supraoptic neurones. J Physiol 498: 339-350.
14. Li Z, Decavel C, Hatton G (1995) Calbindin-D28k: role in determining intrinsically generated firing patterns in rat supraoptic neurones. J Physiol 488: 601-608.
15. Leng G, Brown CH, Bull PM, Brown D, Scullion S, , Currie J, Blackburn-Munro RE, Feng J, Onaka T, Verbalis JG, Russell JA, Ludwig M (2001) Responses of magnocellular neurons to osmotic stimulation involves coactivation of excitatory and inhibitory input: an experimental and theoretical analysis. J Neurosci 21: 6967-6977

16. Tuckwell HC (1988) Introduction to Theoretical Neurobiology, Vol. 2, Cambridge UK, Cambridge University Press.
17. Oliet SH, Bourque CW (1993) Mechanosensitive channels transduce osmosensitivity in supraoptic neurons. Nature 364: 341-343.
18. Feng J, Brown B (1999) Coefficient of variation of interspike intervals greater than 0.5. How and when? Biol Cybern 80:291-297.
19. Ludwig M, Sabatier N, Bull PM, Landgraf R, Dayanithi G, Leng G (2002) Intracellular calcium stores regulate activity-dependent neuropeptide release from dendrites. Nature 418: 85-89
20. Ludwig M (1998) Dendritic release of vasopressin and oxytocin J Neuroendocrinol 10: 881-895.

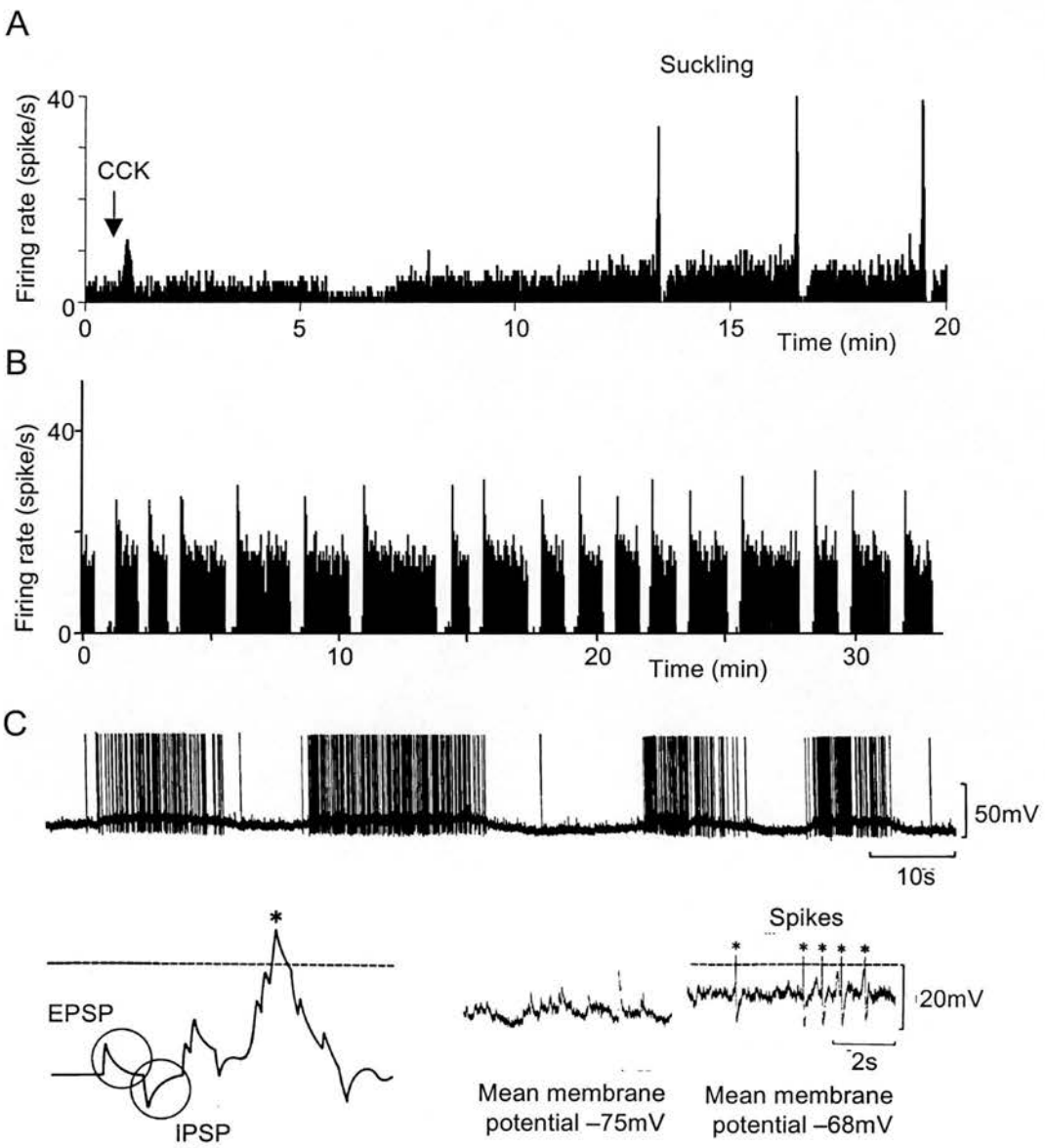

Leng et al., Fig. 1

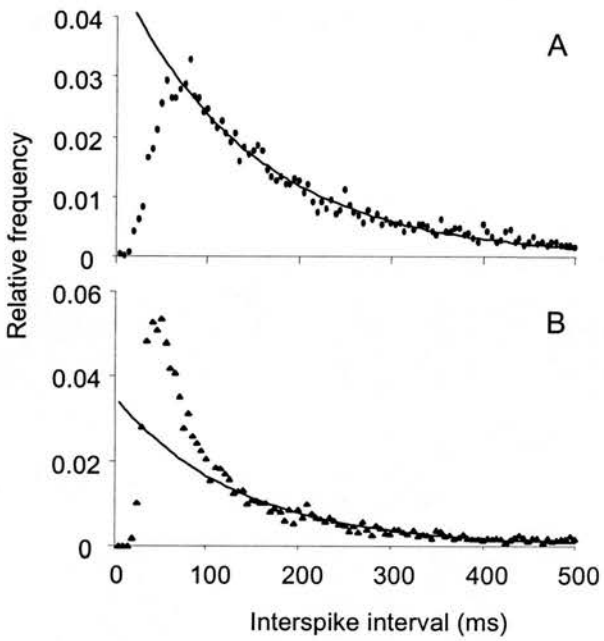

Leng et al., Fig. 2

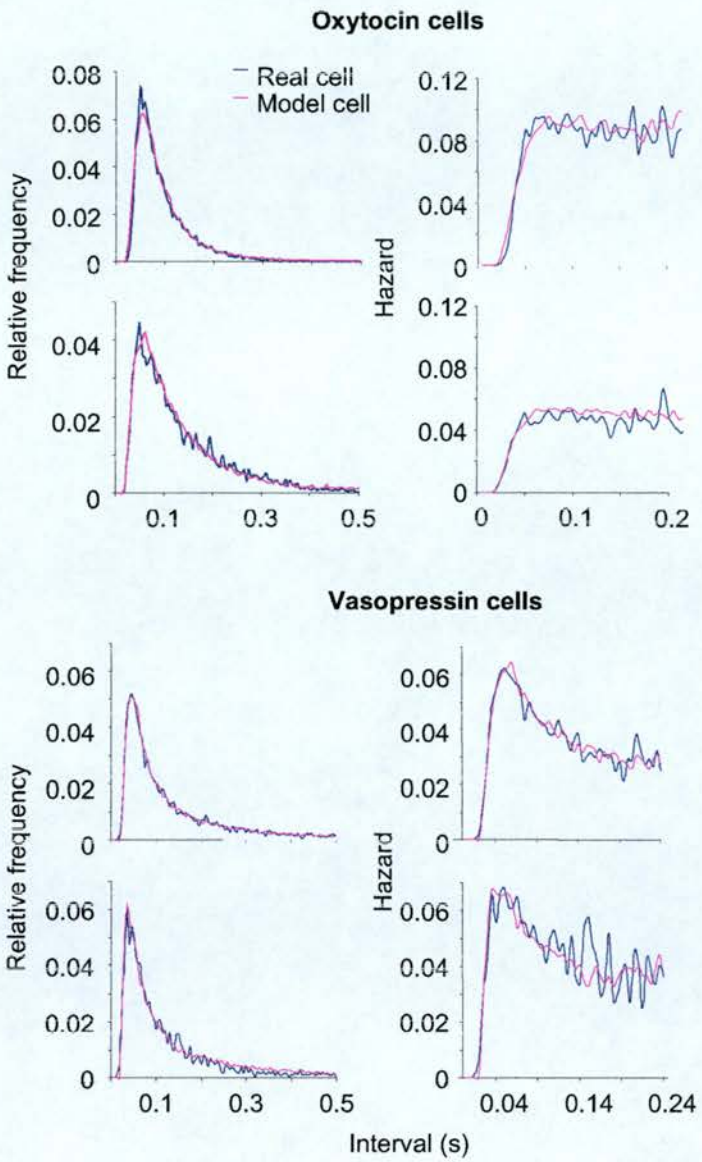

Leng et al., Fig. 3

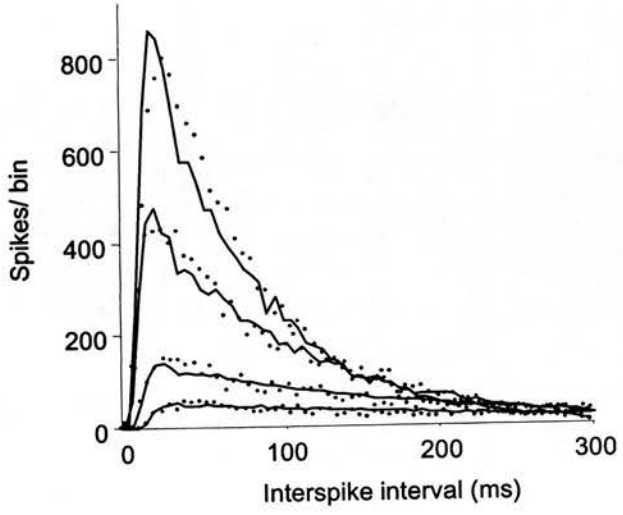

Leng et al., Fig. 4

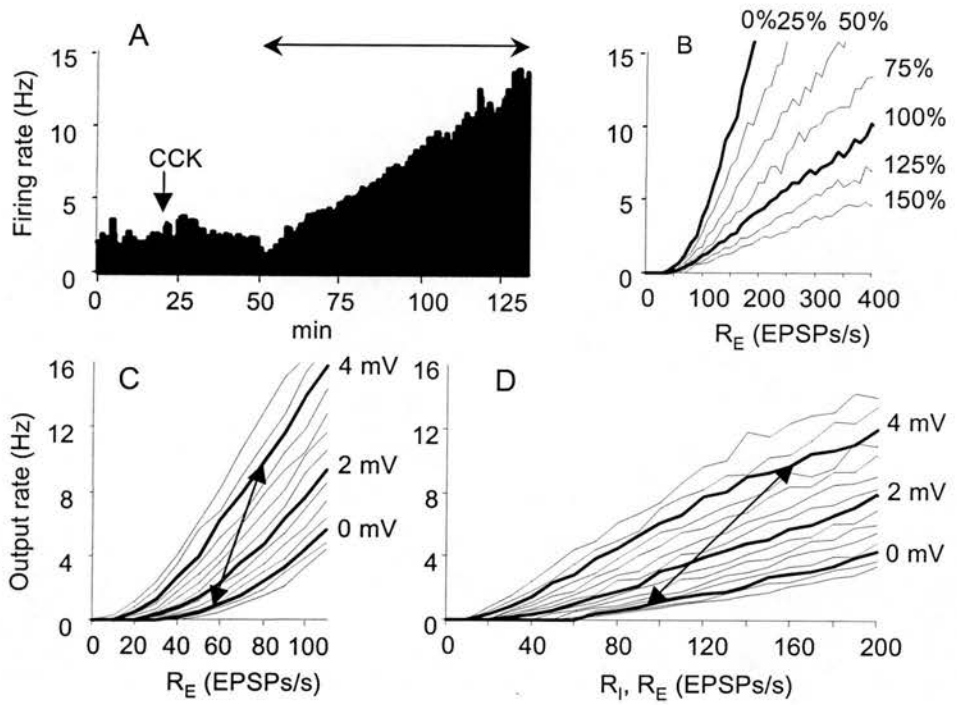

Leng et al., Fig. 5

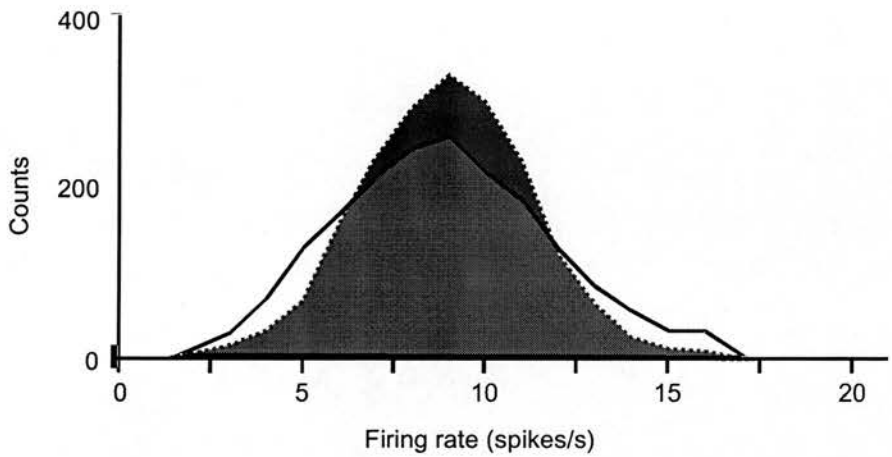

Leng et al., Fig. 6

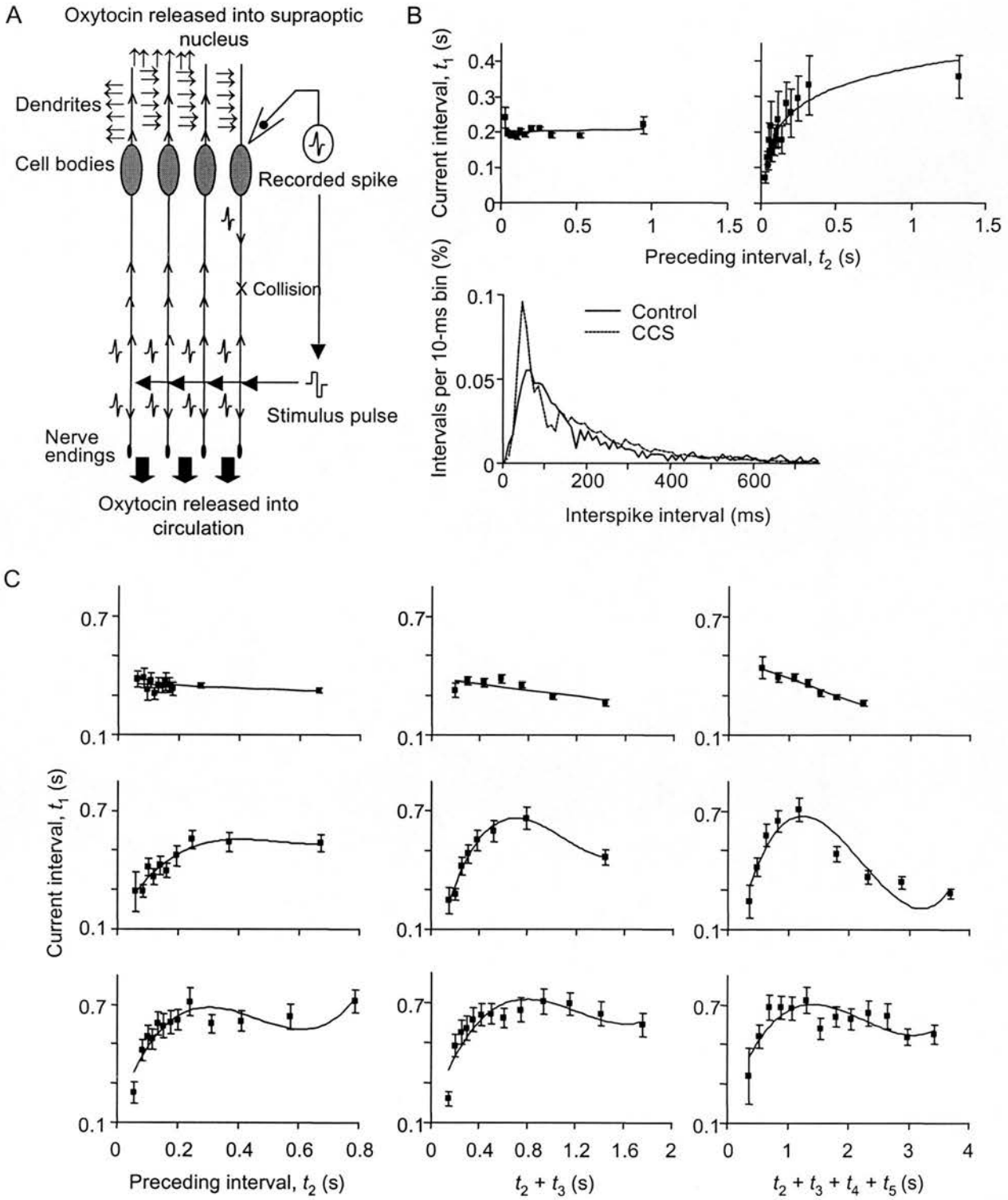

Leng et al., Fig. 7

Statistical Analysis of Oxytocin Cell Discharge Patterns

Reiff-Marganiec Arleta,[1] Brown David, Leng Gareth.
Department of Biomedical Sciences, University Medical School, Edinburgh EH8 9AG and [1]Department of Computational Neuroscience, Babraham Institute, Cambridge, CB2 4AT, UK.

The electrical activity of oxytocin cells changes with increased osmotic stimulation from electrical silence, to a slow irregular, to a fast continuous pattern in non-lactating rats, with a dramatically different pattern during lactation. The current analysis was designed to look at the fine structure of spike activity in oxytocin cells in non-lactating rats, to look for features that reflect either membrane properties of singe cells or network properties.
A statistical computer package (Genstat) was used to analyse 21 recordings of the background activity of oxytocin cells in non-lactating rats, recorded under urethane anaesthesia. Firing rate distributions, calculated over different lengths of interval, were examined, together with distributions of interspike intervals and sequences of interspike intervals, and a dispersion index was calculated for each cell for the firing rate per 4, 2, 1, ½, ¼. 1/8, and 1/16 seconds. It became apparent that, when firing rates were calculated for relatively long intervals, the rates were much less variable than would be expected from the variability apparent between short intervals. For a regression analysis, each interspike interval was correlated against the interspike interval before, the last two intervals, the last three… up to the last 50 intervals. The correlation coefficient was significant and negative for most cells, thought it differed for how many intervals it was significant. Summarising, the cells exhibit, in their spontaneous activity, a surprisingly long 'memory' of preceding spike activity – a mechanism by which the current state of activity is recognised and then balanced. Such a memory is likely to reflect activity-dependent negative feedback.

Presented at:

1999 World Congress on Neurohypophysial Hormones
Edinburgh, Scotland

STATISTICAL ANALYSIS OF OXYTOCIN NEURON DISCHARGE ACTIVITY

A. Reiff-Marganiec, D. Brown[1] and G. Leng*. Dept. Biomedical Sciences, Univ Med Sch , Teviot Place, Edinburgh EH8 9AG, UK and [1]Dept Computational Neuroscience, Babraham Institute, Cambridge, CB2 4AT, UK.

Intrinsic mechanisms governing the excitability of oxytocin (OT) neurons are assumed to be important for discharge patterns that are efficient for hormone secretion. If so, it should be possible to infer their impact from statistical analysis of discharge activity. Recordings of rat OT cells were analysed during episodes of stationary activity. The tails of interspike interval histograms could be well fitted by a single exponential, except for intervals < the mode, consistent with discharge activity dominated by random EPSPs and IPSPs, and by the impact of a post-spike hyperpolarising afterpotential. To look for the impact of slower mechanisms, distributions of firing rates (spikes/period) were plotted for different period lengths, together with distributions of randomly shuffled intervals. The distributions were bell shaped with a peak at the mean firing rate and a symmetrical spread. However, randomised distributions had a wider spread, i.e. the observed activity had a more regular structure than expected from randomly shuffled intervals. The dispersion index (variability of firing rate/mean, indicating how far a distribution is from Poisson, 1 being perfect Poisson, 0 perfectly ordered) was calculated for periods of 16s, 8s, 4s.. to 1/16s. With reducing period size, the dispersion index rises from relatively ordered to near Poisson. Autocorrelations and partial autocorrelations were calculated to investigate serial dependence over the same range of period sizes. OT cells showed significant negative correlations at lag 1 for periods of 1/16, 1/8, ¼, ½ and 1s. To investigate serial dependencies between interspike intervals, partial autocorrelations were calculated. Significant negative correlations were observed in all cells, although the number of previous intervals that were significant, differed between cells. Thus OT cells display a mechanism by which the current state of activity is recognised and then balanced. This probably reflects the slow afterhyperpolarisation, readily demonstrated after intense activation, but which seems to have a significant impact at low firing rates also.

Supported by the E.C. Bio4-98-0135

Presented at:

30th Annual Meeting of the Society for Neuroscience
New Orleans, La., 2000

EVIDENCE FOR AFTERHYPERPOLARISATION (AHP) IN RAT OXYTOCIN CELLS *IN VIVO*: STATISTICAL APPROACH

Arleta Reiff-Marganiec, David Brown[1], Francoise Moos[2], & Gareth Leng
Biomedical Sciences, University Medical School, Edinburgh, [1]Babraham Institute, Cambridge and [2]CNRS UPR-9055, Biologie des Neurones Endocrines, Montpellier

In magnocellular neurosecretory cells (MNC's) of the supraoptic nuclei (SON) trains of high frequency discharge (20-50 Hz) are followed by an afterhyperpolarisation (AHP), which last around 1 sec and is generated by the activation of a calcium dependent potassium channel. It has been suggested that the *I*AHP is a voltage-independent calcium activated potassium current that is important in the regulation of continuous and phasic firing in SON cells. Further, through its inhibition there might be a possible mechanism by which MNC's could fire at the high frequencies that occur during milk-ejection bursts. However, all studies to date have been performed *in vitro*. Here we employ statistical methods to determine the presence of the AHP and its effects in *in vivo* recordings of oxytocin neurons. We report the presence of a distinctive structure in the sequence of interspike intervals, whereby on a time scale of ~ 1sec a short interval is more likely to be followed by a long interval, and vice versa. This work compares results from the statistical analysis of *in vivo* recordings of naïve animals and *in vivo* recordings in lactating animals. We hypothesise that the observed pattern in the interspike intervals probably reflects the AHP.

Presented at:

16th national meeting of the British Neuroscience Association
Harrogate, UK, 2001

THE EFFECTS OF THE AFTERHYPERPOLARISATION ON FIRING PATTERN *IN VIVO*: A STATISTICAL APPROACH

Arleta Reiff-Marganiec, Francoise C. Moos* & Gareth Leng
Division of Biomedical Sciences, Medical School, University of Edinburgh, UK and *Biologie des Neurones Endocrines, CNRS UMR5101, Montpellier, France

In vitro studies in magnocellular neurosecretory cells (MNC's) of the supraoptic nuclei (SON) showed that trains of high frequency discharge (20-50 Hz) are followed by an afterhyperpolarisation (AHP), which lasts around 1s and is generated by the activation of a calcium dependent potassium channel. It has been suggested that the AHP is of importance in the regulation of continuous and phasic firing in SON cells, and its inactivation may be necessary to enable MNC's to fire at the high frequencies that occur during milk-ejection bursts. However, since *in vitro* experiments include the injection of a depolarising current and hence create an artificial situation the physiological role of the AHP *in vivo* remained unclear. To investigate whether the AHP has a role in the *in vivo* activity of oxytocin neurones, the present study employed statistical methods to analyse *in vivo* extracellular recordings of virgin and lactating rat. We investigated the relationship between successive interspike intervals (ISI's) of long recordings of continuous firing cells and the background activity of cell displaying high frequency discharges associated with milk-ejection burst. We report a non-random distribution of spikes, whereby a short interval is more likely to be followed by a long interval, and vice versa. If the AHP has an impact at spontaneous firing rates *in vivo*, we would expect to find a balancing effect, i.e. a period of slower activity should follow after a period of more intense activity. This hypothesis is consistent with our observations of *in vivo* firing patterns.

Presented at:

2001 World Congress on Neurohypophysial Hormones
Bordeaux, France

Feedback influences on the patterning of electrical activity of oxytocin neurones

A. Reiff-Marganiec & G. Leng
DBCLS, University of Edinburgh, Edinburgh, UK.

The excitability of magnocellular neurosecretory cells of the supraoptic nuclei is governed by a range of intrinsic mechanisms that are believed to be important in controlling their firing activity, and thus contributing to the regulation of efficient hormone discharge. These mechanisms are thought to include activity-dependent feedback. If so, then we might expect to find signs of the same mechanisms operating at all times, under different physiological conditions.

We have used statistical methods to look at the temporal patterning of spontaneous activity in rat oxytocin neurones (n=65). Cells were recorded *in vivo* in naïve, pregnant, and lactating rats, and before and after hyperosmotic stimulation.

We analysed the distributions of firing rates for each recording, indexes of dispersion and autocorrelations for different bin sizes for firing rates, as well as linear regressions between individual interspike intervals. In general, during spontaneous activity, clusters of spikes are followed by periods of relative inactivity. Thus there is a negative correlation between the current firing rate and the subsequent firing rate when measured in different ways. Firing appears to be very variable when seen on a small scale (0.125 to 0.25s), but averaged over a longer period (4 to 8s) it appears to be more regular than would be expected from the high local variability.

This activity-dependent negative feedback can be found in the activity of all oxytocin neurones, regardless of physiological state. However, while the main characteristics of spontaneous firing are the same under different physiological states, characteristics of activity from lactating (but not milk-ejecting) rats are shown to differ in subtle ways. Activity in lactating rats is more variable when averaged over long periods than in non-lactating rats, and the index of dispersion does not show the pattern of decline seen in other groups, indicating changes in intrinsic feedback mechanisms.

Presented at:

The 5th International Congress of Neuroendocrinology
Bristol, Uk, 2002